

**Synthesis and solid state characterization of actinide cyanometallates and  
actinide benzimidazole compounds**

by

Branson A. Maynard

A dissertation submitted to the Graduate Faculty of  
Auburn University  
in partial fulfillment of the  
requirements for the Degree of  
Doctor of Philosophy

Auburn, Alabama  
May 4, 2014

Copyright 2014 by Branson Allen Maynard

Approved by

Anne Gorden, Chair, Associate Professor, Department of Chemistry and Biochemistry  
David Stanbury, J. Milton Harris Professor, Department of Chemistry and Biochemistry  
Michael McKee, Professor, Department of Chemistry and Biochemistry  
Curtiss Shannon, Andrew T. Hunt Professor, Department of Chemistry and Biochemistry

## Abstract

The square-planar cyanometallate anions allow for the unique columnar structural feature in the solid state, termed in the literature as pseudo 1-D  $M\cdots M$  interactions in the Pt analogs. The distance between metal sites has been coined,  $R$ , and can be tuned by many physical and chemical processes. While the alkali and alkaline earth metal tetracyanoplatinates have been known for two centuries, few compounds have been reported in the actinide square planar cyanometallate class of compounds,  $An_x[M(CN)_4]_y$ . Utilizing this structural feature provides a new means for probing the chemistry of the  $5f$  elements. Described here is the synthesis, emission spectroscopy, Raman spectroscopy, computation analysis, and structural characterization using small molecule X-ray single crystal diffraction of the recently reported actinide cyanometallates, general formula  $An_x[M(CN)_4]_y$ .

## Acknowledgements

First, I will make the acknowledgement that I will forget to mention someone, or funding agency, that has provided support for this work. My parents, Mark and Sharon, played the principal role in facilitating an environment where pursuit of higher education was important. Along these lines, the research I performed under the supervision of Dr. Richard Sykora at the University of South Alabama was paramount to starting a path in structural elucidation of solid state *f*-block coordination compounds.

Further, I have been lucky enough to receive several outside funding sources that provided learning opportunities that were not possible on the campus of Auburn University. These include a trip to Oak Ridge National Laboratory to learn neutron diffraction techniques (Funding: Oak Ridge National Laboratory and Argonne National Laboratory) and a summer fellowship to Los Alamos National Laboratory to learn computational analysis (Funding: Seaborg Institute). Also the local section of the American Chemical Society and the Auburn University Graduate School have provided funding to disseminate my research at local and national meetings. Research assistance has been provided through DTRA.

Certainly other names should be included as during one point or another of this graduate study I received valuable insight into a problem: John Gorden, Mohan Bharara, Brian Little,

Kushan Weeirasairi, Mike Devore, Walter Casper, Nick Klann, Phong Ngo and the many other graduate and undergraduate students.

Undoubtedly I would be remiss if I did not acknowledge Dr. Anne Gorden. During my time at Auburn University she has provided advice, leadership, and mentoring in the proper doses. I will be forever grateful that Dr. Gorden was my primary investigator. Additionally I would like to thank Dr. Gorden and Dr. Ortiz for continuing my funding during the time I was in the hospital and recovering. Also I would like to thank my committee members for proofreading this text.

Last but, certainly not least; I will forever be indebted to my wife, Amanda Maynard, for her support through the toughest times of this doctoral work. The reason why this text exists is, in large part, due to her understanding that it may not ever be written, or I would not be able to write it. Amanda provided this understanding at the time I needed it most and it helped serve as motivation to make sure it was written.

## Table of Contents

Abstract .....	ii
Acknowledgments.....	iii
List of Tables .....	vii
List of Illustrations.....	viii
List of Abbreviations .....	xi
Chapter 1 Introduction .....	1
A Brief History of a 5f Element, Uranium.....	1
5f Coordination Compounds .....	6
References Cited .....	24
Chapter 2 Solid State Structural Elucidation of the Th <sup>IV</sup> , UO <sub>2</sub> <sup>VI</sup> , and U <sup>IV</sup> Cyanometallates ....	27
5f-Cyanometallate Coordination Complexes .....	33
Crystallographic Overview .....	53
References Cited .....	56
Chapter 3 Emission and Raman Spectroscopy of the Actinide Tetracyanometallates .....	59
Excitation and Emission .....	60
Raman Spectroscopy.....	66

DFT analysis .....	71
Discussion .....	74
Conclusions .....	80
References Cited .....	86
Chapter 4 Synergistic Thorium Mediated Synthesis of 2,3-Diaminophenazine.....	89
Conclusions .....	94
References Cited .....	98
Chapter 5 Synthesis, Isolation, Structural Characterization and Emission Spectroscopy of Salzine Compounds .....	99
X-ray diffraction .....	102
CRAIC Microspectrophotometer.....	105
References Cited .....	110
Chapter 6 Conclusions and Future Work .....	111
Future Work .....	112
Appendix 1: Crystallographic Tables .....	119

## List of Tables

Table 1 ORTEP projections of solid state actinide complexed ligands.....	5
Table 2 Crystallographic information for Th1, Th2, and U3.....	50
Table 3 Crystallographic information for U4, Th5, and U6 .....	51
Table 4 Crystallographic information for Th7 and Th8.....	52
Table 5 Cyanide vibrational stretches of the cyanometallate salts .....	67
Table 6 Single point energy calculations performed .....	72
Table 7 Cyanide vibrational stretches of Th1, Th2, U3, U4, Th5, and U6.....	76
Table 8 Vibrational modes calculated by the unrestricted B3LYP functional .....	80
Table 9 Tabulated results from the oxidation of OPD.....	96

## List of Illustrations

Figure 1 Thermal ellipsoid projection of $[\text{UO}_2(\text{N,N-bis(2-hydroxy-3,5-dimethylbenzyl)-4-amino-1-butanol})]$ .....	6
Figure 2 Thermal ellipsoid projection of $[\text{UO}_2(\text{N',N'-bis(2-hydroxy-3-methoxy-5-(propen-2-yl)benzyl-N-(2-aminoethyl)morpholine})_2] \cdot 2\text{CH}_3\text{CN}$ .....	8
Figure 3 Thermal ellipsoid projection of $\{\text{UO}_2(\mu_2-\text{ReO}_4)(\text{ReO}_4)(\text{TBPO})_2\}_2$ .....	9
Figure 4 Thermal ellipsoid projection of $[\text{UO}_2(3-(2-\text{Hydroxybenzylideneamino})\text{propane}-1,2-\text{diol})_2 \cdot \text{C}_3\text{H}_7\text{NO}$ .....	11
Figure 5 Thermal ellipsoid projection of $\text{UO}_2(2\text{-quinoxilinol})$ .....	12
Figure 6 Thermal ellipsoid projection of $[\text{Cyclo}[6]\text{pyrrole}(\text{UO}_2)]$ .....	15
Figure 7 The ball and stick projection of $[\text{NpO}_2([18]\text{crown-6})]^+$ .....	17
Figure 8 Projection of $[\text{Pu}(5\text{LIO(Me-3,2-HOPO)}_2)]$ .....	19
Figure 9 Projection of $\text{PuI}_2(\text{Aracnac})_2$ .....	22
Figure 10 Asymmetric unit of $\text{Th}(\text{H}_2\text{O})_7[\text{Pt}(\text{CN})_4]_2 \cdot 10\text{H}_2\text{O}$ (Th1) .....	33
Figure 11 Packing diagram of $\text{Th}(\text{H}_2\text{O})_7[\text{Pt}(\text{CN})_4]_2 \cdot 10\text{H}_2\text{O}$ (Th1) .....	34
Figure 12 Projection of $\text{Th}_2(\text{H}_2\text{O})_{10}(\text{OH})_2[\text{Pt}(\text{CN})_4]_3 \cdot 5\text{H}_2\text{O}$ (Th2) .....	35
Figure 13 Packing diagram of $\text{Th}_2(\text{H}_2\text{O})_{10}(\text{OH})_2[\text{Pt}(\text{CN})_4]_3 \cdot 5\text{H}_2\text{O}$ (Th2) .....	36
Figure 14 Packing diagram of $\text{K}_3[(\text{UO}_2)_2(\text{OH})(\text{Pt}(\text{CN})_4)_2]_2 \cdot \text{NO}_3 \cdot 1.5\text{H}_2\text{O}$ (U3) .....	37

Figure 15 Projection of $\{\text{U}_2(\text{H}_2\text{O})_{10}(\text{O})[\text{Pt}(\text{CN})_4]_3\} \cdot 4\text{H}_2\text{O}$ (U3) .....	40
Figure 16 Packing diagram of $\{\text{U}_2(\text{H}_2\text{O})_{10}(\text{O})[\text{Pt}(\text{CN})_4]_3\} \cdot 4\text{H}_2\text{O}$ (U4) .....	42
Figure 17 Projection of $\{\text{Th}_2(\text{H}_2\text{O})_{10}(\text{OH})_2[\text{Pd}(\text{CN})_4]_3\} \cdot 8\text{H}_2\text{O}$ (Th5) .....	43
Figure 18 Extension of the one-dimensional structure of $\{(\text{UO}_2)_2(\text{DMSO})_4(\text{OH})_2[\text{Ni}(\text{CN})_4]\}$ .....	45
Figure 19 Projection of the ionic structure of $[\text{Th}(\text{C}_2\text{H}_6\text{SO})_9][\text{Pt}(\text{CN})_4]_2 \cdot 4\text{H}_2\text{O}$ (Th7) .....	47
Figure 20 Projection of the structure of $[\text{Th}(\text{C}_2\text{H}_6\text{SO})_8][\text{Fe}(\text{CN})_6] \cdot \text{NO}_3$ (Th8) .....	48
Figure 21 Single crystal sample of $\text{Th}(\text{H}_2\text{O})_7[\text{Pt}(\text{CN})_4]_2 \cdot \text{H}_2\text{O}$ (TH1).....	60
Figure 22 Emission spectra of starting materials, Th1, Th2 and U3 .....	61
Figure 23 Excitation spectrum of $\text{Th}(\text{H}_2\text{O})_7[\text{Pt}(\text{CN})_4]_2 \cdot 10\text{H}_2\text{O}$ (TH1).....	63
Figure 24 Excitation spectrum of $\text{Th}_2(\text{H}_2\text{O})_{10}(\text{OH})_2[\text{Pt}(\text{CN})_4]_3 \cdot 5\text{H}_2\text{O}$ (Th2) .....	64
Figure 25 Emission spectra of the $\text{K}^+$ salts of the $d^8$ tetracyanometallates.....	65
Figure 26 Raman spectra of the $\text{K}^+$ salts of the $d^8$ tetracyanometallates .....	66
Figure 27 Raman data of Th1 and Th2 .....	68
Figure 28 Raman spectra of Th5.....	69
Figure 29 Raman spectrum of U4 .....	70
Figure 30 Projections of the atom positions from jobs run in Gaussian .....	74
Scheme 1 Oxidation of ortho-phenylenediamine to 2,3-diaminobenzene.....	89
Figure 31 Scatter plot depicting the data from OPD oxidation reactions .....	90
Figure 32 Projection of the asymmetric unit of $(\text{C}_{12}\text{H}_{10}\text{N}_4)_2 \cdot 7\text{H}_2\text{O}$ .....	93
Figure 33 Projection of the 2-quinoxolinol salen molecule.....	99
Figure 34 Projection of the asymmetric unit of the salzine molecule.....	103
Scheme 2 Proposed reaction scheme for the salzine synthesis.....	102

Figure 35 Projection of the asymmetric unit of tbut-salzine.....	103
Figure 36 Projection of the asymmetric unit of salzine-UO <sub>2</sub> .....	104
Figure 37 Transmission and emission spectra of the salzine compound.....	105
Figure 38 Transmission and emission spectra of the salzine-UO <sub>2</sub> complex.....	106
Figure 39 Transmission and emission spectra of the tbut-salzine .....	107
Figure 40 Transmission and emission spectra of 2-quinoxalinol salen .....	108
Scheme 3 Reaction of 2,3-diaminophenazine with glycine to form the phenazineimidazole product .....	115
Scheme 4 Starting with the phenazineimidazole starting material. ....	116
Figure 41 Possible 2:1 salzine metal complex.....	117
Figure 42 Possible 1:1 phenezeneimidazole metal complex. ....	117

## List of Abbreviations

BTBP	Bis-triazinyl bipyridine
CIF	Crystallographic Information file
Cp	Cyclopentadienyl ligand
CP*	Pentamethylcyclopentadienyl ligand
DAP	2,3-diaminophenazine
DFE	Desferrioxamine E
DMA	Dimethylacetamide
DMF	Dimethylformamide
DMSO	Dimethylsulfoxide
mWe	million watts of electric capacity
OPD	<i>ortho</i> -phenylenediamine
SMMs	Single molecule magnets
TBP	Tributyl Phosphate
TCNi	Tetracyanonickelate
TCPd	Tetracyanopalladate
TCPt	Tetracyanoplatinate

TPTZ      Tripyridyl triazine

UV          Ultraviolet

XRD        X-ray diffraction

Reference format follows the format of the Journal of the American Chemical Society

Crystallographic projections were generated in Olex2.1

Figures or tables are made by Microsoft Word or Microsoft Excel

Portions of this dissertation are from published articles:

### **Chapter 1: Introduction**

Gorden, A. E. V.; DeVore, M. A.; Maynard, B. A. *Inorganic Chemistry* **2013**, 52, 3445.

### **Chapter 2**

Maynard, B. A.; Sykora, R. E.; Mague, J. T.; Gorden, A. E. V. *Chemical Communications* **2010**, 46, 4944.

Maynard, B. A.; Lynn, K. S.; Sykora, R. E.; Gorden, A. E. V. *Journal of Radioanalytical and Nuclear Chemistry* **2013**, 296, 453.

Maynard, B. A.; Lynn, K. S.; Sykora, R. E.; Gorden, A. E. V. *Inorganic Chemistry* **2013**, 52, 4880.

### **Chapter 3**

Maynard, B. A.; Lynn, K. S.; Sykora, R. E.; Gorden, A. E. V. *Inorganic Chemistry* **2013**, 52, 4880.

# **Chapter 1: Introduction**

The existence of the *5f* actinide elements, thorium and uranium, has been known for roughly 200 years (185 and 225 years respectively).<sup>1</sup> Uranium is important from a historical standpoint, as it is one of two elements that stopped World War II by the detonation of nuclear fission bombs over the cities of Hiroshima and Nagasaki. The history of uranium is important to mention in the context of how and why it has been released into the environment. Following the brief historical recap of uranium is an overview of the last decade of actinide-containing solid state structures. This highlights the structure-function relationship and the importance of establishing bonding parameters in the *5f* series. This leads the way for the main text, which discusses the solid state structural elucidation and properties of two new classes of actinide containing compounds: actinide cyanometallates and actinide benzimidazoles.

## **A Brief History of a *5f* Element, Uranium**

Martin Heinrich Klaproth is credited to first identifying the element uranium, found in a heterogeneous oxide ore commonly known as pitchblende, in 1789.<sup>1</sup> Enrico Fermi first reported the bombarding of uranium with neutrons and incorrectly concluded the nuclear absorption of the neutron and subsequent nuclear decay yielded elements with 93 and 94 protons, essentially claiming the discovery of the elements that would later be

named neptunium and plutonium.<sup>2</sup> Ida Noddack may have been the first, publicly, to suggest that the uranium nucleus may break up into several large fragments when bombarded by a neutron.<sup>3</sup> We know this now to be induced nuclear fission, but the term fission was only used in reference to the process in cell biology at the time. Her description of the process "*it is conceivable that the nucleus breaks up into several large fragments, which would of course be isotopes of known elements, but would not be neighbors of the irradiated element.*" Otto Frisch and Lise Meitner were both more famously credited with discovering fission during an excursion; Frisch was skiing and Meitner was walking, and reportedly keeping pace with Frisch, through the countryside. Their conversation centered on a letter Otto Hahn had sent Meitner describing that the neutron bombardment product of uranium contains barium. Frisch and Meitner worked out the calculations on a fallen tree trunk. Their idea was that the incoming/bombarding neutron perturbed the nucleus enough to produce two large fragments, explaining the appearance of barium.<sup>4</sup>

This is understood more easily, if the nucleus is considered as a liquid drop. Two forces are present; the weak force can be understood as surface tension and the electromagnetic force, which is due to the positively charged protons repelling themselves.<sup>4</sup> If the number of neutrons and protons in the nucleus is sufficiently high, then the surface tension of the liquid drop is just enough to counterbalance the repulsive force of the protons. If a bombarding neutron finds the liquid drop nucleus of  $^{235}\text{U}$ , it can rupture the liquid drop into two more stable fragments. The now excess nuclear binding energy of the two fragments is released and the amount of energy can be found if the

daughter products are known from Einstein's  $E=mc^2$ .<sup>4,5</sup> From these early observations, it could be deduced that large sums of energy could be realized from a fission incident.

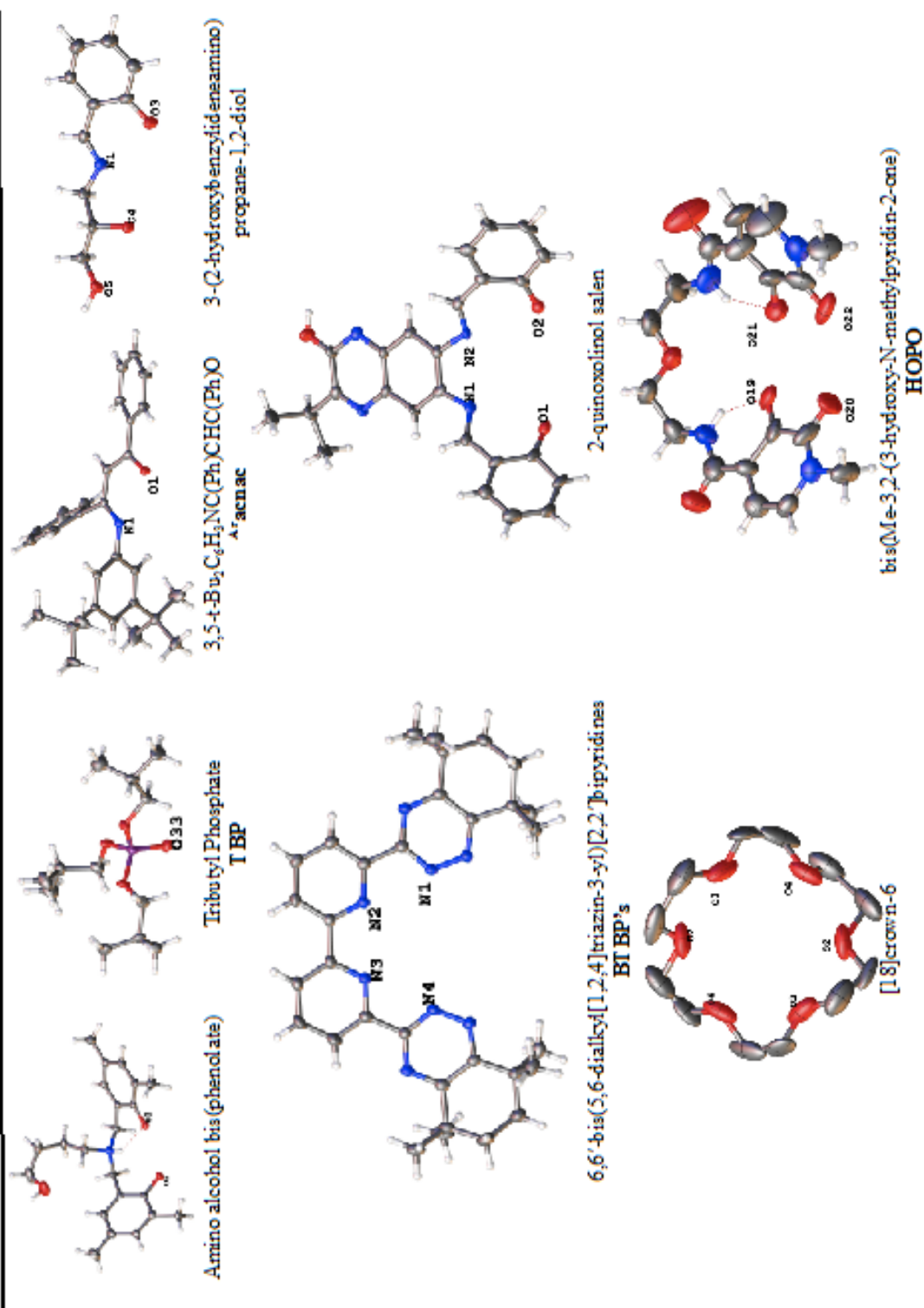
Nowadays, world energy consumption is expected to increase by 47% from 2010 to 2035. This increased energy consumption is proportional to the flourishing economies outside of the Organisation for Economic Co-operation and Development.<sup>6</sup> The United States used coal to provide over 1,700 billion kilowatt hours of electricity in 2009 alone, accounting for almost half of the total electricity produced,<sup>2</sup> but growing environmental concern over the release of greenhouse gases, in particular carbon dioxide from fossil fuels, has caused investigation into incorporating the use of other energy sources.<sup>7</sup> Nuclear energy can help meet these growing demands and offers energy production in a cleaner fashion with lower atmospheric emission.

The first full-scale nuclear power plant began operation in 1957 in Shippingport, Pennsylvania, marking the United States entry into the civilian nuclear power industry.<sup>4</sup> The United States has adopted a once-through fuel cycle, where nuclear fuel rods are made from naturally occurring sources and all used nuclear fuel is disposed of after a single use. For this type of fuel cycle, enriched uranium fuel or thorium-uranium fuel are the only fuels that can be used in order to create a sustainable fission chain reaction without a large input of an external neutron source.<sup>7</sup>

Today, there are over 400 nuclear power plants worldwide, generating about 12% of civilian electricity use.<sup>5</sup> In fact, nuclear power already provides 70 percent of carbon-free electricity in the United States. The energy density of nuclear fuel is another desirable quality; the amount of energy in a single uranium fuel pellet is equal to that of 149 gallons of oil or 1,780 pounds of coal.<sup>6</sup>

The relatively recent discovery of the *5f* elements coupled with these elements' ability to undergo natural fission, manmade fission, and manmade fusion leading to high sums of energy sets the foundation for understanding their chemistry.<sup>4,5</sup> At the first publicly accepted report of fission, researchers were primarily interested with harvesting the energy released from a fission incident. Notoriously, the end of World War II was brought on by the release of two atomic bombs (Little Boy = 141 pounds of fissile mass, Fat Man 56 pounds of fissile mass) on the cities of Hiroshima and Nagasaki in 1945.<sup>8</sup> This release of roughly 200 pounds of fissile material, along with other fissile material releases in the last 70 years has spurred the fundamental and applied chemistry in attempt to be able to understand and ultimately control these atoms in our environment.<sup>8,9</sup> What follows is an overview of the past decade of solid state actinide coordination compounds and how these coordination compounds have been related to waste remediation.

Table 1. Projections of only the ligand of interest in the solid state. The labeled atoms in the ligands are the binding atoms found in the CIF for each dataset.



## **5f Coordination Compounds**

Currently 3936 of the 4165 (94.5%) structures containing a 5f element reported to the Cambridge Crystallographic Data Centre, CCDC, are composed of structures containing Th and U, while 1869 of the 4165 (44.5%) structures contain the  $\text{UO}_2^{2+}$  ion.<sup>10</sup> One reason that the overwhelming majority of the reported actinide structures contain the Th or U atoms is because these atoms provide long lived radioisotopes with lower radioactive emissions.<sup>9</sup> The ligands described below have been looked at for liquid-liquid extraction of trivalent lanthanides and actinides of different oxidation states. Generally, multidentate ligands that contains soft donors, such as nitrogen and sulfur, are used for such separations. Why? Because the behavior of the 5f-elements has been studied much less, it is a challenging task to predict what ligands would have optimum efficiency and selectivity in separations and provide the optimal coordination environment for these 5f metal ions in the solid state.<sup>11</sup>

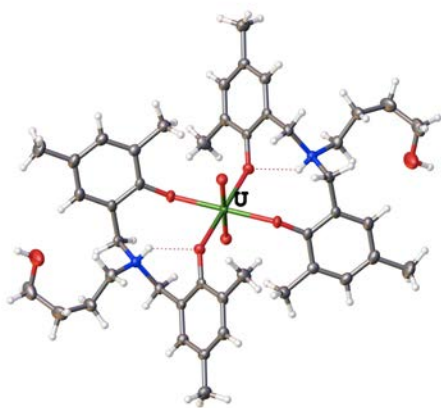


Figure 1 Thermal ellipsoid projection of ammonium type  $[\text{UO}_2(\text{N,N-bis(2-hydroxy-3,5-dimethylbenzyl)-4-amino-1-butanol})_2]$ . The carbon atoms are depicted as gray, the oxygen red, the nitrogen blue, the central uranium atoms green, and the hydrogen atom are omitted for clarity.<sup>12</sup>

In 2006 and 2007, uranyl complexes coordinated to a series aminoalcoholbis(phenolate) ligands were reported. These ligands provide three hard oxygen donors in the form of 2 phenol and one alkyl chain alcohol; the amine group provides a hard nitrogen donor. The ultimate goal of these ligands was to be used as chelation therapy for overexposure to uranium. These ligands contain an [O,N,O,O'] binding pocket and were studied for their chelating effects. Figure 1 shows the  $[UO_2(N,N\text{-bis}(2\text{-hydroxy-3,5-dimethylbenzyl)\text{-}4\text{-amino-1-butanol})_2]$  complex. The two aminoalcoholbis(phenolate) ligands bind the uranyl metal centers in a bidentate fashion with the ligand forming the equatorial plane. The coordination number of these complexes is 6 and is best described as octahedral, with the -yl oxygens binding at the axial positions and the remaining equatorial sites filled by the oxo- donors of the aminoalcoholbis(phenolate) ligands, the amine groups are protonated and do not bind the uranyl center.<sup>12,13</sup>

In the continuation of research, uranyl complexes coordinated with a series of diaminobisphenolates were reported.<sup>14,15</sup> Two types of structures are reported, a 1:1 and a 2:1 ligand to metal ratio. In the 1:1 complexes, the coordination number around the uranium center is 7 and is best described as pentagonal bipyramidal polyhedron. The two -yl oxygens are found at the axial positions and the equatorial plane is defined by two different pentagons depending on whether the central nitrogen in the ligand is an amine or an ammonium. In the amine type ligands, one site is the amine, and four coordination sites are filled by oxygens, two from the ligand and two from a bidentate nitrate. In the ammonium type ligands, the nitrogen uranium bond is replaced by a water molecule. The difference between the amine and ammonium type ligand is the protonation of the central

nitrogen atom. In the 2:1 complexes the coordination number around the uranium center is 6 and is best described as octahedral. Figure 2 shows the 2:1 ligand to metal complex of  $[\text{UO}_2(\text{N}',\text{N}'\text{-bis}(2\text{-hydroxy-3-methoxy-5-(propen-2-yl)benzyl-N-(2-aminoethyl)morpholine})_2]2\text{CH}_3\text{CN}$ . The two -yl oxygens are found at the axial positions and the equatorial plane is defined by four oxygens, two from each ligand.<sup>15</sup>

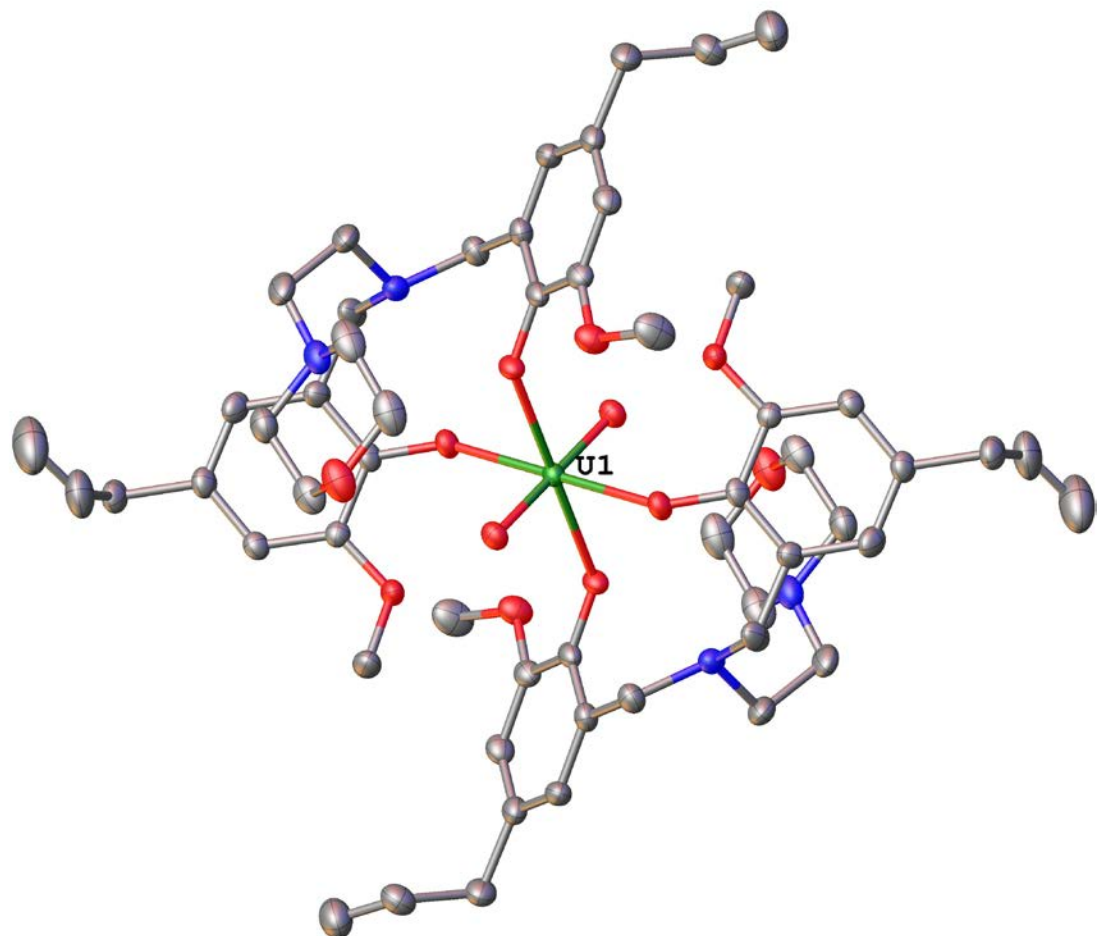


Figure 2 Thermal ellipsoid projection of the ammonium type  $[\text{UO}_2(\text{N}',\text{N}'\text{-bis}(2\text{-hydroxy-3-methoxy-5-(propen-2-yl)benzyl-N-(2-aminoethyl)morpholine})_2]2\text{CH}_3\text{CN}$ . The carbon atoms are depicted as gray, the oxygen red, the nitrogen blue, the central uranium atoms green, and the hydrogen atoms are omitted for clarity.<sup>15</sup>

In 2007, it was reported that derivatives of the ligand (Figure 3), tributyl phosphate (TBP), used in the PUREX process formed coordination structures with uranyl,  $\text{UO}_2^{2+}$ , and perrhenate,  $\text{RhO}_4^-$ .<sup>16</sup> The perrhenate ion is of interest because it has been shown to be a suitable mimic for pertechnetate ( $\text{TcO}_4^-$ ), another potentially hazardous fission product that is also a  $\gamma$ -emitter and readily transportable in aqueous media.<sup>17</sup> The two complexes reported are similar, with the difference being the TBP ligand derivative. In both structures, the coordination number of the uranium is seven and best described as a pentagonal bipyramidal polyhedron. The –yl oxygens are found at the two axial positions. Three sites of the equatorial pentagon are occupied by oxygens from the perrhenate anions. The remaining two sites are occupied by the oxygens of the TBP derivative ligand.<sup>16</sup>

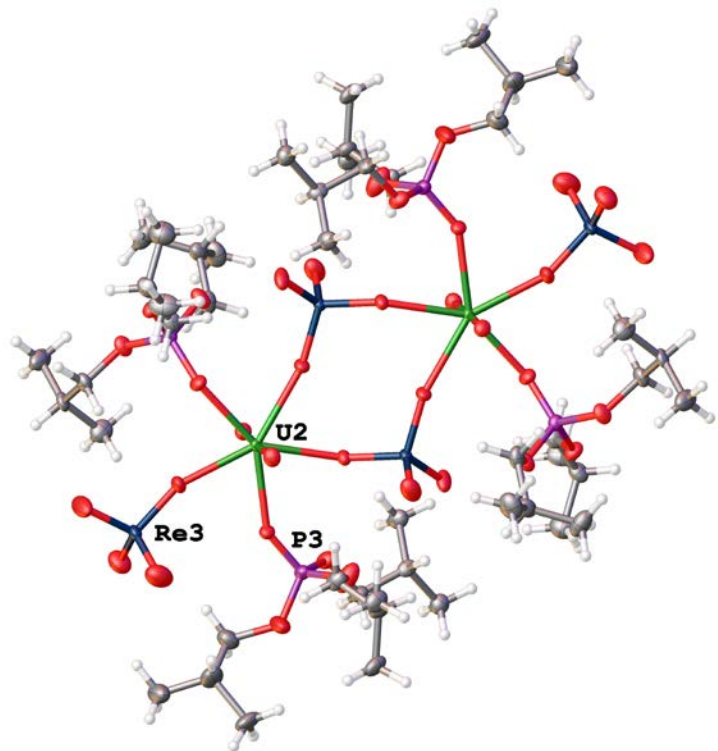


Figure 3 Thermal ellipsoid projection of  $\{\text{UO}_2(\mu_2\text{-ReO}_4)(\text{ReO}_4)(\text{TBPO})_2\}_2$ . The carbon atoms are depicted as gray, the oxygen red, the rhenium metallic blue, the phosphorus metallic purple and the central uranium atoms green.<sup>16</sup>

The first *5f*-BTBP, bis-triazinyl bipyridine, complex was reported in 2008.<sup>18</sup> This report also contains three mononuclear and a dinuclear UO<sub>2</sub>-BTBP complex and also a dinuclear UO<sub>2</sub>-TPTZ, tripyridyl triazine, complex. In all five of these structures, the coordination number around the uranium site is seven and is best described by a pentagonal bipyramidal polyhedron with the -yl oxygens found at the two axial positions. In the four BTBP complexes, the BTBP ligand coordinates the uranium center in a tetradentate fashion that defines the equatorial plane.<sup>18</sup>

Schnaars and coworkers, reported three complexes, AnX<sub>2</sub>(<sup>Ar</sup>acnac)<sub>2</sub> where <sup>Ar</sup>acnac = (ArNC(Ph)CHC(Ph)O<sup>-</sup>) (Ar = 3,5-tBu<sub>2</sub>C<sub>6</sub>H<sub>3</sub>), containing U and Pu in 2011.<sup>11</sup> Among the interesting features of this report is that both the U and Pu metals in the +4 oxidation state were used to prepare complexes and the authors prepared a detailed, comprehensive look at that oxidation state.<sup>11</sup> Two of the isostructural complexes contain U(IV) with the difference being the halides, Cl or I, bonded to the metal center. The Pu(IV) structure will be discussed below. The  $\beta$ -ketoiminate ligand, containing a hard and soft donor, was used because of its ability to stabilize weak Lewis acids, UO<sub>2</sub><sup>2+</sup>, and thus was thought to be able to coordinate to the stronger Lewis acids, An(IV). The coordination number around the uranium center is six and is best described as a distorted octahedral polyhedron. The halides are found at the axial positions and the <sup>Ar</sup>acnac ligands are found in the equatorial plane and are trans to each other, as seen in the isostructural PuI<sub>2</sub>(<sup>Ar</sup>acnac)<sub>2</sub> shown in figure 9. The differing halides do not affect the bonding parameters of the <sup>Ar</sup>acnac ligand.<sup>11</sup>

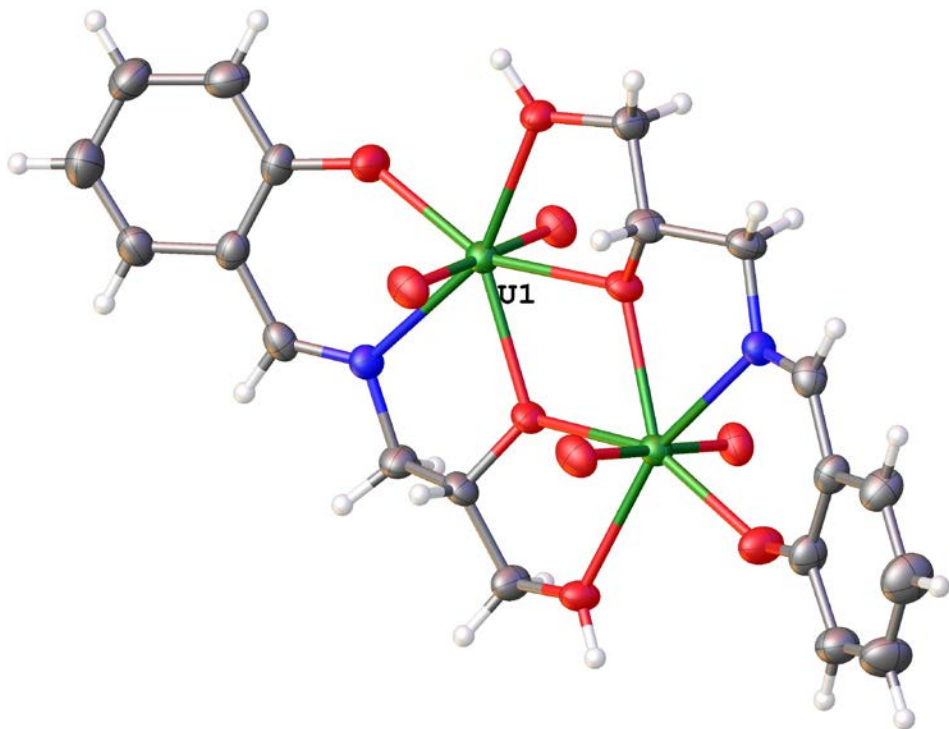


Figure 4 Thermal ellipsoid projection of  $[\text{UO}_2(3\text{-}(2\text{-hydroxybenzylideneamino)\text{propane-}1,2\text{-diol})]_2\cdot\text{DMF}$ . The carbon atoms are depicted as gray, the hydrogen atoms white, the oxygen red, the nitrogen blue, the central uranium atoms green.<sup>19</sup>

Salen-type and Schiff base- $\text{UO}_2^{2+}$  structures were reported by our group previously.<sup>19-21</sup> The coordination number of the uranium center, in both the salen-type and Schiff base systems, is seven and is best described by a pentagonal bipyramid polyhedron, as seen in Figure 4.<sup>19</sup> The salen-type ligands -called the salen quinoxalinols or salqu ligands, were designed with a quinoxaline backbone to enable the readily distinguishable properties either by fluorescence or UV-Vis between different metal complexes. In the  $\text{UO}_2^{2+}$  structures, the -yl oxygens sit at the axial positions while the two oxo- and two aza-coordination sites of the ligand occupy four of the positions in the pentagon. The remaining site of the pentagon is occupied by a solvent molecule. In both

the Schiff base- $\text{UO}_2$  (Figure 4) and salen- $\text{UO}_2$  (Figure 5) compounds the ligand must twist from a planar conformation to accommodate the uranyl ion. This results in a large change in the overlap of the  $\pi$ -bonds in the conjugated back bone, and consequently, a large change in the spectroscopy.<sup>20</sup>

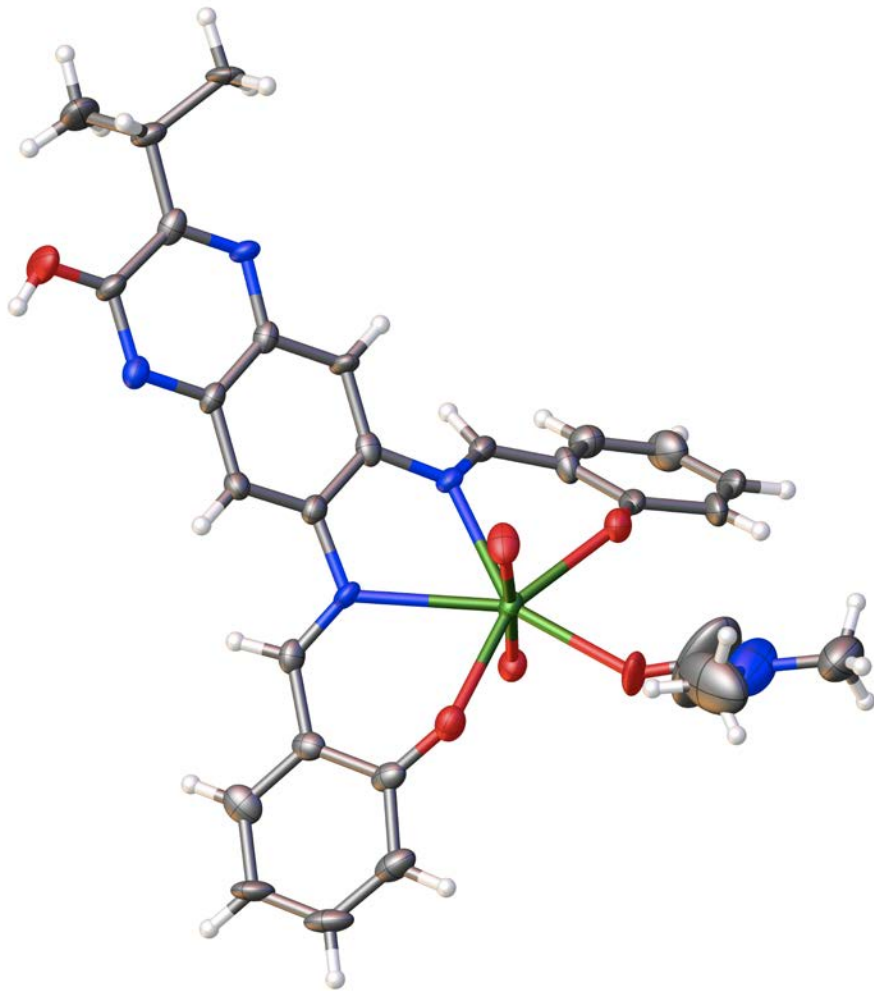


Figure 5 Thermal ellipsoid projection of  $\text{UO}_2(2\text{-quinazolinol})$ . The carbon atoms are depicted as gray, the hydrogen atoms white, the oxygen red, the nitrogen blue, the central uranium atom green.<sup>20</sup>

In the asymmetric Schiff-base structures, the -yl oxygens sit at the axial positions while the equatorial pentagonal coordination is very different. Two ligands bind two metals and exclude the solvent molecule, forming a dinuclear  $\text{U}_2\text{O}_2$  species. This  $\text{U}_2\text{O}_2$

species is composed of two uranium sites, bridged by an alkoxy and hydroxyl oxygen. This U<sub>2</sub>O<sub>2</sub> core is reported as stable to hydrolysis and transamination and could potentially be used to remediate waste stored under alkaline conditions. The shape of this species forms a diamond with each vertex alternating between uranium atom and oxygen atom. (See example with ligand (E)-3-((2-hydroxybenzylidene)amino)propane-1,2-diol - Figure 4) The coordinating pentagon around the metal ion is composed of a phenolic oxygen, imine nitrogen, bridging alkoxy and hydroxyl group with the remaining site of the pentagon occupied by a solvent molecule.<sup>19</sup> These ligand systems offer the U···U interaction found at 3.8794 Å in Figure 4 of [UO<sub>2</sub>(3-(2-hydroxybenzylideneamino)propane-1,2-diol)]<sub>2</sub>·C<sub>3</sub>H<sub>7</sub>NO. In the series of these complexes, prepared with different substituents on the aryl backbone, the resultant complexes were always dinuclear 2:2 metal:ligand complexes. Simple extraction studies proved that they could be effective for removing uranyl from aqueous solutions (up to 99% in 24 hours); however, the presence of iron or copper in mixed solutions would later demonstrate complications to selective extractions. Hydrolysis of this extraction agent does occur, but at extreme pH, conditions (i.e. 1-3 and 13-14); this is important as nuclear waste is found at high and low pH and a one ligand processing system will need a stable ligand over a wide pH range.<sup>19,22,23</sup>

With additional bridged structures, an attempt was made to limit the formation of dinuclear complexes to prepare a 1:1 ligand to metal complex with the preparation of a 2,2'-(1E,1'E)-((2-hydroxypropane-1,3-diyl)bis(azanylylidene))bis(methanylylidene)diphenol ligand.<sup>23</sup> In resulting complexation structures, the coordination number of the uranium site is seven and is best

described as a pentagonal bipyramid polyhedron. The -yl oxygens sit at the axial positions while the equatorial pentagonal coordination is different. The 1:2 ligand to metal pentagon is composed of a phenolic oxygen, imine nitrogen, bridging alkoxy and hydroxyl group with the remaining site of the pentagon occupied by a solvent molecule. The 2:2 ligand to metal pentagonal geometry is the same as the 2:1, in that the coordination bite angles and bond distances are very similar, but one bridging hydroxyl group has been replaced by a coordinating solvent molecule the bridging hydroxyl group in the 2:1 system. Coordinated to uranyl, these Schiff base complexes are very stable - in particular as compared to their transition metal counterparts, and may be useful in the alkaline nuclear waste solutions.<sup>19,22,23</sup> This still may be of use as a final back extraction polishing step in that the ligand could be used to retain uranium in organic solutions after adjusting to a basic pH which would release complexed transition metals.<sup>24,25</sup>

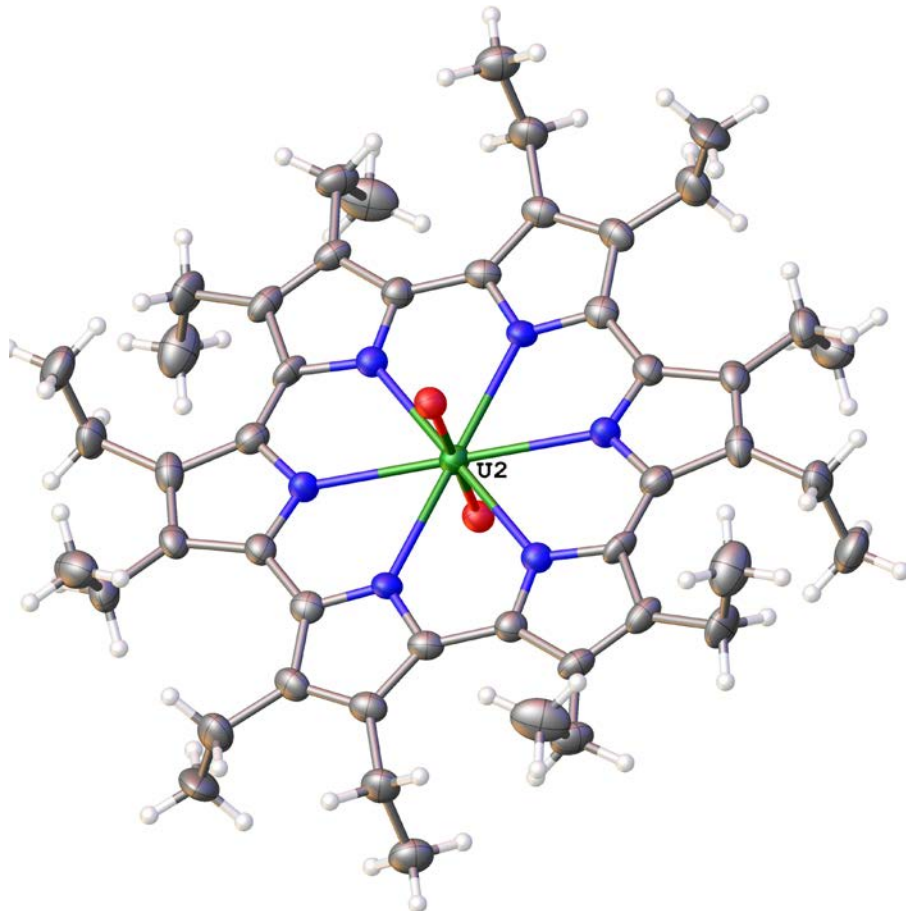


Figure 6 Thermal ellipsoid projection of [cyclo[6]pyrrole ( $\text{UO}_2$ )]. The carbon atoms are depicted as gray, the hydrogen white, the oxygen red, the nitrogen blue, the central uranium atoms green.<sup>26</sup>

The all aza [cyclo[6]pyrrole( $\text{UO}_2$ )] coordination complex was reported in 2007.<sup>26</sup> The ligand was first noted in the synthesis of cyclo[8]pyrrole.<sup>27</sup> The authors held that the cyclo[6]pyrrole would bind uranyl more readily than the earlier reported cyclo[8]pyrrole because of its cavity size and favorable donor number. The coordination number of the uranium site is 8 and is best described as a hexagonal bipyramid, as seen in Figure 6. The -yl oxygens are found at the axial position, and the nitrogen atoms from the ligand define

the hexagonal equatorial plane. This is the first metal complex of the cyclo[N]pyrrole series of expanded porphyrins.<sup>26</sup>

In 2009 and 2010, uranyl structures of the bis(Me-3,2-HOPO), 3-hydroxy-N-methylpyridin-2-one, ligand derivatives were reported.<sup>28,29</sup> The uranium sites in the reported structures have a coordination number of seven and are best described as bicapped pentagonal polyhedra. This ligand architecture coordinates the uranyl unit in a tetradentate fashion, through the four hydroxypyridonate oxygens, leaving one site open for coordination through another ligand or a solvent. In 2011, two uranyl structures of a MeTAM - methyl terephlalamide - ligand were reported.<sup>30</sup> Previous studies have demonstrated that the MeTAM ligand can act as a decorporation agent, and it was found to be more efficient in reducing the  $[UO_2^{2+}]$  in the kidneys and deposited bone than the hydroxypyridonate ligands.<sup>31,32</sup>

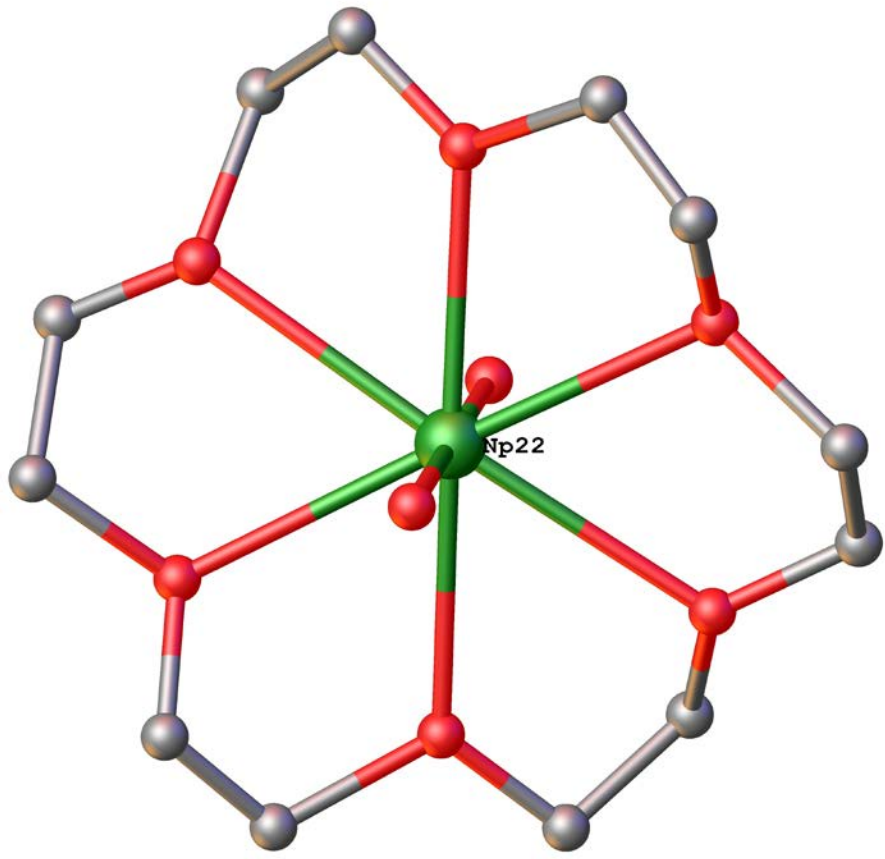


Figure 7 The ball and stick projection of  $[NpO_2([18]\text{crown-6})]^+$ . The perchlorate anion and the hydrogen atoms have been omitted for clarity. The carbon atoms are depicted as gray, the oxygen red, the central neptunium atom green.<sup>33</sup>

Coordination structures that contain neptunium have been few and far between. The first transuranic ether inclusion complex,  $[NpO_2([18]\text{crown-6})][X]$  (where  $X = ClO_4^-$  or  $CF_3SO_3^-$ ), with single crystal diffraction data, was reported by Clark and coworkers in 1998 (See Figure 7). The  $NpO_2^+$  ion is of particular interest because of the problems associated with extracting it from high level nuclear waste, stemming from the low positive charge and relatively high solubility in aqueous media of the neptunyl ion.<sup>33</sup> This also makes neptunyl of great potential environmental and health consequence,

because it could be easily transported in ground water or introduced into the food chain after a waste spill.<sup>34,35</sup> The Np=O bond length of 1.800 (5) Å is unusually short for an  $\text{NpO}_2^+$  ion; it is found at a distance that is 0.05 Å shorter in the  $[\text{NpO}_2(\text{H}_2\text{O})_5]^+$  ion.<sup>33</sup> The [18]crown-6 ligand completely encapsulates the  $\text{NpO}_2^+$  ion. The Np(V) center is best described by an approximate hexagonal bipyramid. The short –yl oxygens are found at the axial positions and the ligands O<sub>ether</sub> coordinate forming the equatorial hexagonal plane.

A neptunium<sup>V</sup>-hexaphyrin expanded porphyrin type complex was reported in 2001.<sup>36</sup> The neptunium(V) center has a coordination number of 8 and is best described as a hexagonal bipyramidal polyhedron. The –yl oxygens are found at the axial positions, with the remaining six coordination sites filled by nitrogen donors from the ligand. The hexaphyrin ligand does have a slight twist when bound to the  $\text{NpO}_2^+$  center, but the distortion is not as pronounced as in the uranyl hexaphyrin structure described in the same paper. The authors reason that the larger ionic radius of the  $\text{NpO}_2^+$  is a better fit for the hexaphyrin ligand as opposed to the uranyl unit.<sup>36</sup> It was later characterized with substituted versions of this ring to determine how this distortion affects coordination.<sup>37</sup> This was the first reported all aza- coordinating system for neptunium, and its selectivity for actinides and intense color were characterized in potential sensing applications.<sup>38-41</sup>

Of the actinide structures reported in the CCDC, the 134 neptunium and 77 plutonium-containing crystal structures represent 3.2 and only 1.8% of the actinide compounds reported respectively (CCDC database search). The remaining 0.5% of the actinides structures reported are the rest of the actinides besides those previously described (i.e. not U, Th, Pu, or Np). This is a problem as the fundamental bonding

parameters and coordination chemistry behavior need to be better understood to be able to intelligently design ligands for separations, perform detailed calculations, and ultimately to formulate new processes using these ligands.

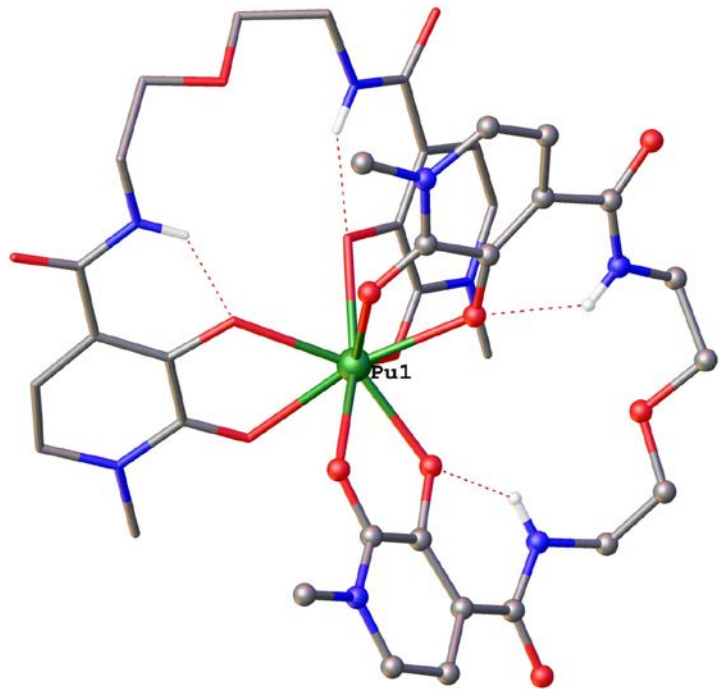


Figure 8 Projection of  $[Pu(5LIO(Me-3,2-HOPO))_2]$ , one ligand shown as a ball and stick and the other as tube, lacking non hydrogen bonding hydrogens for clarity. The carbon atoms are depicted as gray, the oxygen red, the nitrogen blue, and the central plutonium atom green.<sup>42</sup>

In 2000 the first structure reported of an organic extraction agent with a plutonium metal resolved by single crystal analysis was  $[Pu(1)_2(NO_3)_2][(NO_3)_2]$ , where 1 is the trifunctional ligand  $2,6-[{(C_6H_5)_2P(O)CH_2}_2]C_5H_3NO$  and can also be abbreviated to NOPOPO.<sup>42</sup> The coordination number around the plutonium center is 10 and is best

described as a distorted bicapped square antiprism. All ten of the inner sphere coordinating atoms are oxygens. Two of the ligands bind the plutonium center in a tridentate fashion, each ligand binds once through the O<sub>pyridine N-Oxide</sub> and twice through the O<sub>phosphoryl</sub> sites. The M-O<sub>ligand</sub> bond distances of the Pu(IV) structure are shorter than the Th(IV) complex. While the actinide contraction is not as linear as the lanthanide contraction, it still exists and these systems are evidence of this.<sup>43</sup> Typically, a ligand that forms complexes with the lighter actinides forms shorter bonds with the heavier actinides.<sup>42</sup> Later, the compound [Pu(2)<sub>2</sub>(NO<sub>3</sub>)<sub>3</sub><sup>+</sup>][Pu(NO<sub>3</sub>)<sub>6</sub><sup>2-</sup>]<sub>0.5</sub> was reported, where 2 is the bifunctional 2-[(C<sub>6</sub>H<sub>5</sub>)<sub>2</sub>P(O)CH<sub>2</sub>]C<sub>5</sub>H<sub>4</sub>NO.<sup>44</sup> The coordination number of this complex is 10 and is best described as an average of a bicapped antiprism and a sphenocorona. There are two idealized 10 vertex polyhedra; one is a bicapped antiprism, and the other is a sphenocorona. The complex is not described by either of these polyhedra, rather it is better described as a combination of the two. These complexes are examples of and could lead to the further development of phosphinopyridine ligands in separations of nuclear waste.<sup>44</sup>

Linear and cyclic hydroxamates containing the building block 1-amino-5-hydroxamino-pentane as a building block have been found in the naturally occurring compounds known as siderophores, that bacteria have as a way to sequester naturally occurring iron.<sup>45</sup> These complexes were of interest because they are potentially useful in medical treatments as chelators for iron and aluminum overload.<sup>31,45-49</sup> The first plutonium-siderophore complex to be structurally characterized was [Al(H<sub>2</sub>O)<sub>6</sub>][Pu(DFE)(H<sub>2</sub>O)<sub>3</sub>]<sub>2</sub>(CF<sub>3</sub>SO<sub>3</sub>)<sub>5</sub>·14H<sub>2</sub>O, where DFE is an abbreviation for desferrioxamine E. The coordination number around the plutonium metal center is 9, and

can be best described as a distorted tricapped trigonal prism. The ligand coordinates the metal center through six oxygens, three from O<sub>carbonyl</sub> and three from the O<sub>oximate</sub>. Three water molecules complete the coordination sphere. This compound is the first discrete molecule structurally characterized with a plutonium(IV) ion that is 9 coordinate.<sup>50</sup> These siderophore type complexes are interesting, as they biologically function to separate a metal from the environment, transport it across an organic layer, and release the metal under the desired conditions.<sup>50</sup> The DFE ligand undergoes the same conformational changes when binding Pu<sup>IV</sup> as Fe<sup>III</sup> ions. This fact coupled with the known recruitment of iron from the environment into a cell is via DFE leads to the hypothesis that the Pu(DFE) complex could cross the cell membrane with relative ease as compared to the relatively aqueous insoluble Pu<sup>IV</sup>(OH)<sub>4</sub> and Pu<sup>IV</sup>O<sub>2</sub> species.

The first structure of a plutonium<sup>IV</sup> hydroxypyridonate (HOPO) was reported in 2005. The complex is modeled after coordination systems found in siderophores with two N-methyl-3-hydroxy-2-pyridinone groups linked by a 5-membered ether linker. The coordination number of the plutonium atom is 8 and best described as a bicapped trigonal prism. The metal complex is formed by two of the 5LIO(Me-3,2-HOPO) ligands with one plutonium atom. The 5LIO(Me-3,2-HOPO) ligand contains two types of oxygens, the phenolic and amide nitrogen oxygens. Four oxygens from each ligand bind the plutonium metal in a sandwich type complex, as seen in figure 8. In part because of the flexible geometry allowed by the Pu ion, this is the first structure to have two different chiralities of metal complex in one unit cell.<sup>51</sup> This structure was later followed by other related 1,2-HOPO Pu(IV) and Pu(IV)-maltol structures, which were reported with the comparable Ce(IV) structures for comparison. There was a remarkable difference

between these structures which had very dissimilar geometries although they had similar size metal ions, and it points to a significant concern about the viability of Ce(IV) as a model for Pu(IV).<sup>52,53</sup>

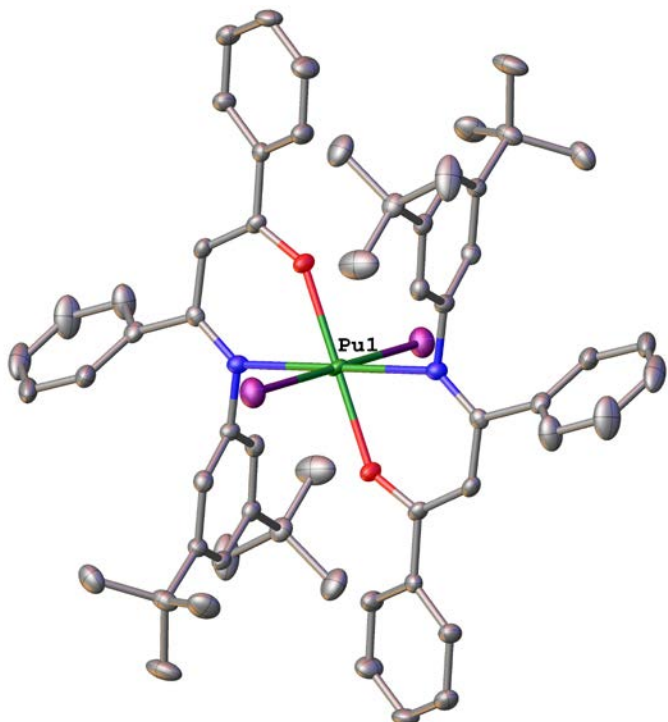


Figure 9 Projection of  $\text{PuI}_2(\text{^Aracnac})_2$ , model shown as a ball and stick projection, lacking hydrogens for clarity. The carbon atoms are depicted in gray, the oxygen atoms red, the nitrogen atoms blue, the iodine atoms as purple and the central plutonium atom is in green.<sup>11</sup>

As described above, three isostructural compounds with the general formula  $\text{AnX}_2(\text{^Aracnac})_2$  were reported. The  $\text{PuI}_2(\text{^Aracnac})_2$  complex is shown in figure 9. The starting material for the Pu isostructure was  $\text{Pu}^0$ , partially because of the lack of suitable Pu(IV) starting materials.<sup>11</sup> This structure reported is the first example of a Pu-I bond. The actinide contraction and ionic bonding models alone are not enough to explain the

difference in the An-O and An-N bond lengths of the  $\text{PuI}_2(^{\text{Ar}}\text{acnac})_2$  and the  $\text{UI}_2(^{\text{Ar}}\text{acnac})_2$  isostructures. The  ${}^{\text{Ar}}\text{acnac}$  ligand may be a useful probe in elucidating an all exclusive comparative bonding study of the actinides because it is not limited by cavity size or sterics. The solid state plutonium structures reported within have one common feature, excluding  $\text{PuI}_2(^{\text{Ar}}\text{acnac})_2$ ; this feature is that the metal center is completely bound by oxygen atoms.<sup>11</sup>

In general soft donors are preferred for separations purposes, yet, with the majority of reported structures, hard donors appear favored for the isolation of single crystals suitable for X-ray diffraction. One reason for the lack of plutonium containing coordination structures reported is the lack of readily available starting materials. This is complicated by the fact that materials must be carefully handled and that plutonium can have up to five oxidation states in aqueous solutions. Thus, preparing solutions containing ions in a single oxidation state for use in metal complexes requires additional preparation.<sup>9</sup> Because of these facts regarding the complications of working with plutonium no reactions containing plutonium were completed in my research career.

The majority of this text is devoted to structural elucidation of thorium and uranium containing coordination compounds and how these structural characterizations are related to the observed optical properties. The hope is that this research has broadened the scope of the solid state actinide containing coordination compounds and that these new insights may lead to long term, solid state, waste remediation solutions.

## References Cited

- (1) Weeks, M. E. *Discovery of the Elements*; Kessinger Publishing Co., 2003.
- (2) Fermi, E. *Nature (London, U. K.)* **1934**, *133*, 898.
- (3) Noddack, I. *Angew. Chem.* **1934**, *47*, 653.
- (4) Meitner, L.; Frisch, O. R. *Nature (London, U. K.)* **1939**, *143*, 239.
- (5) Einstein, A. *Ann. Phys-Berlin* **1905**, *18*, 639.
- (6) Conti, J. J.; Holtberg, P. D.; Beamon, J. A.; Napolitano, J. A.; Schaal, S. A.; Turnure, J. T. *Annual Energy Outlook 2012 with Projections to 2035*, 2012.
- (7) DiMeglio, J. L.; Rosenthal, J. *J. Am. Chem. Soc.* **2013**, *135*, 8798.
- (8) Coster-Mullen, J. *Atom bombs: the top secret inside story of Little Boy and Fat Man*; J. Coster-Mullen: United States, 2008.
- (9) *The Chemistry of the Actinide and Transuranic Elements*; 3rd ed.; Morss, L.; Edelstein; Fuger, J.; Katz, J. J., Eds.; Springer: Dordrecht, The Netherlands, 2006.
- (10) Cambridge Structural Database. Actinide Structure Search. Published Online: 2012. (Accessed 04-13-2012).
- (11) Schnaars, D. D.; Batista, E. R.; Gaunt, A. J.; Hayton, T. W.; May, I.; Reilly, S. D.; Scott, B. L.; Wu, G. *Chem. Commun. (Camb)* **2011**, *47*, 7647.
- (12) Sopo, H.; Sviili, J.; Valkonen, A.; Sillanpaeae, R. *Polyhedron* **2006**, *25*, 1223.
- (13) Sopo, H.; Vaeisaenen, A.; Sillanpaeae, R. *Polyhedron* **2007**, *26*, 184.
- (14) Sopo, H.; Lehtonen, A.; Sillanpaa, R. *Polyhedron* **2008**, *27*, 95.
- (15) Wichmann, O.; Ahonen, K.; Sillanpaa, R. *Polyhedron* **2011**, *30*, 477.
- (16) John, G. H.; May, I.; Sarsfield, M. J.; Collison, D.; Helliwell, M. *Dalton T.* **2007**, *1603*.
- (17) Sutton, A. D.; John, G. H.; Sarsfield, M. J.; Renshaw, J. C.; May, L.; Martin, L. R.; Selvage, A. J.; Collison, D.; Helliwell, M. *Inorg. Chem.* **2004**, *43*, 5480.
- (18) Berthet, J. C.; Thuery, P.; Foreman, M. R. S.; Ephritikhine, M. *Radiochim. Acta* **2008**, *96*, 189.
- (19) Bharara, M. S.; Strawbridge, K.; Vilsek, J. Z.; Bray, T. H.; Gorden, A. E. V. *Inorg. Chem.* **2007**, *46*, 8309.

- (20) Wu, X. H.; Bharara, M. S.; Bray, T. H.; Tate, B. K.; Gorden, A. E. V. *Inorg. Chim. Acta* **2009**, *362*, 1847.
- (21) Wu, X. G.; Hubbard, H. K.; Tate, B. K.; Gorden, A. E. V. *Polyhedron* **2009**, *28*, 360.
- (22) Bharara, M. S.; Hefflin, K.; Tonks, S.; Strawbridge, K. L.; Gorden, A. E. V. *Dalton Trans.* **2008**, 2966.
- (23) Bharara, M. S.; Tonks, S. A.; Gorden, A. E. V. *Chem. Commun.* **2007**, 4006.
- (24) Joshi, J. M.; Pathak, P. N.; Manchanda, V. K. *Solvent Extr. Ion Exch.* **2005**, *23*, 663.
- (25) May, I.; Taylor, R. J.; Wallwork, A. L.; Hastings, J. J.; Fedorov, Y. S.; Zilberman, B. Y.; Mishin, E. N.; Arkhipov, S. A.; Blazheva, I. V.; Poverkova, L. Y.; Livens, F. R.; Charnock, J. M. *Radiochim. Acta* **2000**, *88*, 283.
- (26) Melfi, P. J.; Kim, S. K.; Lee, J. T.; Bolze, F.; Seidel, D.; Lynch, V. M.; Veauthier, J. M.; Gaunt, A. J.; Neu, M. P.; Ou, Z.; Kadish, K. M.; Fukuzumi, S.; Ohkubo, K.; Sessler, J. L. *Inorg. Chem. (Washington, DC, U. S.)* **2007**, *46*, 5143.
- (27) Seidel, D.; Lynch, V.; Sessler, J. L. *Angew. Chem. Int. Ed.* **2002**, *41*, 1422.
- (28) Szigethy, G.; Raymond, K. N. *Inorg. Chem.* **2009**, *48*, 11489.
- (29) Szigethy, G.; Raymond, K. N. *Inorg. Chem.* **2010**, *49*, 6755.
- (30) Ni, C. B.; Shuh, D. K.; Raymond, K. N. *Chem. Commun.* **2011**, *47*, 6392.
- (31) Gorden, A. E. V.; Xu, J. D.; Raymond, K. N.; Durbin, P. *Chem. Rev.* **2003**, *103*, 4207.
- (32) Durbin, P. W.; Kullgren, B.; Ebbe, S. N.; Xu, J. D.; Raymond, K. N. *Health Phys.* **2000**, *78*, 511.
- (33) Clark, D. L.; Keogh, D. W.; Palmer, P. D.; Scott, B. L.; Tait, C. D. *Angew. Chem. Int. Ed.* **1998**, *37*, 164.
- (34) Prosser, S. L.; Popplewell, D. S.; Lloyd, N. C. *J. Environ. Radioactiv.* **1994**, *23*, 123.
- (35) Capdevila, H.; Vitorge, P. *Radiochim. Acta* **1995**, *68*, 51.
- (36) Sessler, J. L.; Seidel, D.; Vivian, A. E.; Lynch, V.; Scott, B. L.; Keogh, D. W. *Angew. Chem. Int. Ed.* **2001**, *40*, 591.

- (37) Sessler, J. L.; Melfi, P. J.; Lynch, V. M. *J. Porphyr. Phthalocya.* **2007**, *11*, 287.
- (38) Sessler, J. L.; Melfi, P. J.; Seidel, D.; Gorden, A. E. V.; Ford, D. K.; Palmer, P. D.; Tait, C. D. *Tetrahedron* **2004**, *60*, 11089.
- (39) Hayes, N. W.; Tremlett, C. J.; Melfi, P. J.; Sessler, J. D.; Shaw, A. M. *Analyst* **2008**, *133*, 616.
- (40) Iordache, A.; Melfi, P.; Bucher, C.; Buda, M.; Moutet, J. C.; Sessler, J. L. *Org. Lett.* **2008**, *10*, 425.
- (41) Melfi, P. J.; Camiolo, S.; Lee, J. T.; Ali, M. F.; McDevitt, J. T.; Lynch, V. M.; Sessler, J. L. *Dalton Trans.* **2008**, 1538.
- (42) Bond, E. M.; Duesler, E. N.; Paine, R. T.; Neu, M. P.; Matonic, J. H.; Scott, B. L. *Inorg. Chem.* **2000**, *39*, 4152.
- (43) Huheey, J. E.; Huheey, C. L. *J. Chem. Educ.* **1972**, *49*, 227.
- (44) Matonic, J. H.; Neu, M. P.; Enriquez, A. E.; Paine, R. T.; Scott, B. L. *J. Chem. Soc., Dalton Trans.* **2002**, 2328.
- (45) Stintzi, A.; Barnes, C.; Xu, L.; Raymond, K. N. P. *Natl. Acad. Sci. USA* **2000**, *97*, 10691.
- (46) John, S. G.; Ruggiero, C. E.; Hersman, L. E.; Tung, C. S.; Neu, M. P. *Environ. Sci. Technol.* **2001**, *35*, 2942.
- (47) Stintzi, A.; Raymond, K. N. *J. Biol. Inorg. Chem.* **2000**, *5*, 57.
- (48) Turcot, I.; Stintzi, A.; Xu, J. D.; Raymond, K. N. *J. Biol. Inorg. Chem.* **2000**, *5*, 634.
- (49) Jurchen, K. M. C.; Raymond, K. N. *J. Coord. Chem.* **2005**, *58*, 55.
- (50) Neu, M. P.; Matonic, J. H.; Ruggiero, C. E.; Scott, B. L. *Angew. Chem. Int. Ed.* **2000**, *39*, 1442.
- (51) Gorden, A. E. V.; Shuh, D. K.; Tiedemann, B. E. F.; Wilson, R. E.; Xu, J. D.; Raymond, K. N. *Chem. Eur. J.* **2005**, *11*, 2842.
- (52) Gorden, A. E. V.; Xu, J.; Szigethy, G.; Oliver, A.; Shuh, D. K.; Raymond, K. N. *J. Am. Chem. Soc.* **2007**, *129*, 6674.
- (53) Szigethy, G.; Xu, J.; Gorden, A. E. V.; Teat, S. J.; Shuh, D. K.; Raymond, K. N. *Eur. J. Inorg. Chem.* **2008**, 2143.

# **Chapter 2: Solid state structural elucidation of the Th<sup>IV</sup>, UO<sub>2</sub><sup>VI</sup>, and U<sup>IV</sup> cyanometallates**

## **5f-Cyanometallate Coordination Complexes**

Increasing the use of nuclear energy is one alternative to generate significant amounts of energy with low atmospheric emissions;<sup>1</sup> however, the extraction and use of uranium for nuclear fuel leads to many environmental concerns including long term storage and remediation.<sup>2-6</sup> In the United States nuclear power plants each 100 million watts of electric capacity (mWe) produced required 0.18 metric tons of uranium metal.<sup>10</sup> Thorium is also being used increasingly in the design of new reactor systems, and thorium is estimated to be four times more abundant than uranium.<sup>11</sup> One strategy in the development of improved methods of uranium processing is to continue to further our understanding of actinide chemistry with detailed characterization of actinide coordination complexes.<sup>11</sup> For these reasons, the fundamental chemistry of actinide complexes has become of broad interest.<sup>9,12-18</sup>

Metal complex salts containing tetracyanoplatinate (TCPt) anions have been investigated for roughly 200 years.<sup>19</sup> Initial interest was in the differing colors of the complexes. The optical properties of these complexes could be altered by simply changing the cation in the solid state; the clear, colorless aqueous solutions were not as optically elegant.<sup>19</sup> These compounds have been reported in some alluring applications: they have been suggested for use in polymer electrolyte membrane fuel cells,<sup>20</sup> as catalyst precursors,<sup>21</sup> and in vapochromic sensing.<sup>22</sup> Prussian blue and Berlin blue analogs contain

identical cyanide linkages between metal centers as the TCPt complexes. These cyano-bridged metal, M-N-C-M', compounds have been shown to demonstrate intriguing magnetic behavior.<sup>23-26</sup>

In the mid-1980s, Gliemann and Yersin reviewed the properties of 36 solid state TCPt compounds known at that time<sup>19</sup> ranging from lithium as the lightest to thulium as the heaviest cation in the  $\text{Li}_2[\text{Pt}(\text{CN})_4] \cdot 4\text{H}_2\text{O}$  and  $\text{Tm}_2[\text{Pt}(\text{CN})_4]_3 \cdot 21\text{H}_2\text{O}$  compounds respectively.<sup>19</sup> This review outlined several structural features and parameters inherent to the TCPt class of compounds all relating to the quasi one-dimensional Pt chains observed in the solid-state structures. Quasi one-dimensional chains are formed in the solid state; platinophilic interactions may guide the square planar TCPt anions tendency to stack. These parallel columns are thus thought to be responsible for the optical properties of this class of compounds.<sup>19</sup> The distance, R, between adjacent Pt atoms in these chains is considered critical in determining the characteristic emission properties. A simple equation has been derived to relate observed emission to the distance, R, between Pt atoms.<sup>27</sup> It has been noted that this distance can be altered by pressure, temperature, choice of cation, or magnetic fields.<sup>19</sup>

These early solid state TCPt compounds were noteworthy because of their striking optical features in the visible range.<sup>19</sup> Since this review was written, more than 30 years ago, the TCPt class of compounds has been expanded.<sup>27-30</sup> The pseudo one-dimensional Pt···Pt structural feature was allowed in the initial work, because the solvent used for these compounds, primarily, was  $\text{H}_2\text{O}$ . Since the early work in aqueous chemistry, several other polar solvents have successfully been used such as dimethyl sulfoxide, N,N-dimethyl acetamide, and N,N-dimethyl formamide;<sup>28</sup> however, solvation

of the cation with larger solvent molecules tends to preclude the formation of the pseudo one-dimensional Pt···Pt interactions and subsequent visible emission. Further extension of this class continued with the addition of aromatic ligands coordinating to the cationic metal center allowing for subsequent tuning of R in the TCPt chains. This also aided in the characterization of internal energy processes with the sensitization of weakly emitting lanthanide cations.<sup>29</sup> Work in this field after the Gliemann and Yersin review has focused on solvent and ancillary ligand effects and not incorporated actinide metal ions.<sup>9</sup>

Recent research on TCPt systems has involved the incorporation of lanthanides into novel TCPt systems.<sup>27,29,31-33</sup> The complexation of the lanthanides with transition metal cyanides have resulted in new compounds with a CN<sup>-</sup> bridging the *d* and *4f* metal centers. As expected, the optical properties of these compounds are of interest as the LnTCPt systems have been shown to undergo intramolecular energy transfer processes that can either enhance<sup>29,34</sup> or weaken<sup>32</sup> the lanthanide emission.<sup>30,35</sup> The discovery of transition metal cyanide complexes with interesting magnetic behavior coupled with a report demonstrating strong ferromagnetic coupling between an actinide ion and transition metals has sparked our interest in exploring the magnetic properties of the *f* orbitals by bridging the *5d* and *5f* metals with a CN<sup>-</sup> ligand.<sup>31,33</sup> These reports support the idea of enhanced magnetic properties with the possibility of forming discrete molecules exhibiting slow magnetic relaxation, known as single-molecule magnets (SMMs).<sup>33</sup> At present, the magnetic properties of cyanoplatinate-based lanthanide systems have not been described. As compared to the *5f* orbitals of the actinides, the radial extension of the *4f* orbitals of the lanthanides are smaller and therefore these latter orbitals are more ionic in nature. The essential lack of covalency by the *4f* orbitals is thought to not allow

strong enough orbital overlap to provide magnetic coupling in the  $4f$ - $5d$  CN bridged compounds.

Cyanide metallocenes<sup>31</sup> and cyanide bridged bimetallic  $3d$ - $5f$  complexes<sup>36</sup> have been reported recently, with evidence to support increased covalent character in the An-C cyanide bond of the metallocenes. Our interest lies in the actinides and their  $5f$  orbitals, rather than the  $4f$  orbitals, because the radial extension of these orbitals may provide enough overlap to significantly raise the relaxation barrier height and thus increase the possibility of cyano bridged  $5d$ - $5f$  SMMs. Compounds containing the tetracyanoplatinate anion have been characterized by their one dimensional Pt-Pt chains,<sup>37</sup> and a simple equation has been derived to determine the Pt-Pt spacing using UV-visible bands.<sup>27</sup> The TCPt anion also offers the ability of the terminal nitrogens to bind metals in low and high oxidation states, with multiple binding modes.<sup>29-31,34,35</sup>

Here, we report on the first  $5f$ -element TCPt compounds,  $\text{Th}(\text{H}_2\text{O})_7[\text{Pt}(\text{CN})_4]_2 \bullet 10\text{H}_2\text{O}$  (**Th1**),  $\text{Th}(\text{H}_2\text{O})_7[\text{Pt}(\text{CN})_4]_2 \bullet 10\text{H}_2\text{O}$  (**Th2**),  $\text{K}_3[(\text{UO}_2)_2(\text{OH})(\text{Pt}(\text{CN})_4)_2]_2 \bullet \text{NO}_3 \bullet 1.5\text{H}_2\text{O}$  (**U3**),  $\{\text{U}_2(\text{H}_2\text{O})_{10}(\text{O})[\text{Pt}(\text{CN})_4]_3\} \bullet 4\text{H}_2\text{O}$  (**U4**),  $\{\text{Th}_2(\text{H}_2\text{O})_{10}(\text{OH})_2[\text{Pd}(\text{CN})_4]_3\} \bullet 8\text{H}_2\text{O}$  (**Th5**),  $\{(\text{UO}_2)_2(\text{C}_2\text{H}_6\text{SO})_4(\text{OH})_2[\text{Ni}(\text{CN})_4]\}$  (**U6**),  $[\text{Th}(\text{C}_2\text{H}_6\text{SO})_9][\text{Pt}(\text{CN})_4]_2 \bullet 4\text{H}_2\text{O}$  (**Th7**), and  $[\text{Th}(\text{C}_2\text{H}_6\text{SO})_8][\text{Fe}(\text{CN})_6] \bullet \text{NO}_3$  (**Th8**) of the actinide tetracyanometallate,  $\text{An}_x[\text{M}(\text{CN})_4]_y$ , class of compounds. They have been characterized by confocal Raman spectroscopy and single crystal X-ray diffraction. It was remarkable that the thorium compounds, **Th1** and **Th2**, emitted while the uranyl compound, **U3**, lacked any observed emission.<sup>9</sup> These compounds contain unique structures illustrating dimeric actinide species. The absence of any significant charge transfer emission in the visible range as

compared to the platinum starting material for  $\{U_2(H_2O)_{10}(O)[Pt(CN)_4]_3\} \cdot 4H_2O$  is unusual because of the presence of pseudo one-dimensional Pt···Pt chains in this compound. Confocal Raman spectroscopy of the cyanide stretching region provides insight into the binding domain (mono- bi- tri- tetradentate) of the tetracyanometallates in these novel structures. The synthesis for compounds **Th1**, **Th2**, **U3**, **U4**, **Th5**, **U6**, **Th7**, and **Th8** can be found below.

## Synthesis of Actinide Cyanometallates

**Caution!** The  $\text{Th}(\text{NO}_3)_4 \cdot 6\text{H}_2\text{O}$ ,  $\text{UO}_2(\text{NO}_3)_2 \cdot 6\text{H}_2\text{O}$  and  $\text{UCl}_4$  used in this study contained depleted uranium, standard precautions for handling radioactive materials or heavy metals, such as uranyl nitrate and thorium nitrate, were followed.

Potassium tetracyanonickelate (II) hydrate (99.9%, Strem), potassium tetracyanopalladate(II) hydrate (98%, Strem), and potassium tetracyanoplatinate(II) hydrate (98%, Strem),  $\text{UO}_2(\text{NO}_3)_2 \cdot 6\text{H}_2\text{O}$  (98%, J. T. Baker),  $\text{Th}(\text{NO}_3)_4 \cdot 6\text{H}_2\text{O}$  (99%, Fluka), and DMSO (99.9%, ACROS), ortho-phenylenediamine (98%, Acros), 2,3-diaminophenazine (90%, Aldrich) were used as received without further purification. Deionized  $\text{H}_2\text{O}$  ( $7.2 \text{ M}\Omega \text{ cm}$ ) was obtained and used on site.  $\text{UCl}_4$  was synthesized by the reaction of  $\text{U}_3\text{O}_8$  with hexachloropropene reported by Hashimoto, *et al.*<sup>1</sup>

**General Synthesis:** Complexes **Th1** and **Th2** were synthesized by weighing out a roughly equimolar amount of  $\text{Th}(\text{NO}_3)_4 \cdot 6\text{H}_2\text{O}$  and  $\text{K}_2[\text{Pt}(\text{CN})_4] \cdot 3\text{H}_2\text{O}$  and dissolving in  $\text{H}_2\text{O}$ . The addition of dilute  $\text{HNO}_3$  was used to synthesize complex **1**. Complex **3** was synthesized in the same fashion, an equimolar amount of  $\text{UO}_2(\text{NO}_3)_2 \cdot 6\text{H}_2\text{O}$  and  $\text{K}_2[\text{Pt}(\text{CN})_4] \cdot 3\text{H}_2\text{O}$  were dissolved in  $\text{H}_2\text{O}$ . Crystals suitable for X-ray diffraction were observed within 2-4 weeks, and yields were found to be 85, 80 and 56% for **Th1**, **Th2**, and **U3** respectively.

**Th(H<sub>2</sub>O)<sub>7</sub>[Pt(CN)<sub>4</sub>]<sub>2</sub>•10H<sub>2</sub>O (Th1)** was prepared by dissolving 0.0250 g (0.04 mmol) of Th(NO<sub>3</sub>)<sub>4</sub>·6H<sub>2</sub>O and 0.0235 g (0.06 mmol) of K<sub>2</sub>[Pt(CN)<sub>4</sub>]·xH<sub>2</sub>O in 3 mL of H<sub>2</sub>O in a test tube. The pH was brought to 2.5 with a small amount of 0.01 M KOH. The test tube was placed in a slow evaporation chamber, after 29 days green-yellow plates suitable for single crystal X-ray diffraction were observed.

**Th<sub>2</sub>(H<sub>2</sub>O)<sub>10</sub>(OH)[Pt(CN)<sub>4</sub>]<sub>2</sub>•5H<sub>2</sub>O (Th2)** was prepared out by dissolving 0.0246 g (0.04 mmol) of Th(NO<sub>3</sub>)<sub>4</sub>·6H<sub>2</sub>O and 0.0237 g (0.06 mmol) of K<sub>2</sub>[Pt(CN)<sub>4</sub>]·3H<sub>2</sub>O in 3 mL of H<sub>2</sub>O in a test tube. The test tube was placed in a slow evaporation chamber, after 14 days green-yellow plates suitable for single crystal X-ray diffraction were observed.

**K<sub>3</sub>[(UO<sub>2</sub>)<sub>2</sub>(OH)(Pt(CN)<sub>4</sub>)<sub>2</sub>]<sub>2</sub>•NO<sub>3</sub>•1.5H<sub>2</sub>O (U3)** was prepared dissolving 0.0248 g (0.05 mmol) of UO<sub>2</sub>(NO<sub>3</sub>)<sub>2</sub>·6H<sub>2</sub>O and 0.0190 g (.05 mmol) of K<sub>2</sub>[Pt(CN)<sub>4</sub>]·xH<sub>2</sub>O in 3 mL of H<sub>2</sub>O. The test tube was placed in a slow evaporation chamber, after 20 days yellow plates suitable for single crystal X-ray diffraction were observed.

**{U<sub>2</sub>(H<sub>2</sub>O)<sub>10</sub>(O)[Pt(CN)<sub>4</sub>]<sub>3</sub>}•4H<sub>2</sub>O Complex U4** was synthesized in an inert atmosphere, employing Schlenk techniques to avoid the inclusion of O<sub>2</sub> into the system. Nitrogen gas was bubbled through H<sub>2</sub>O contained in a Schlenk flask to exchange the dissolved O<sub>2</sub> gas with N<sub>2</sub> gas. The H<sub>2</sub>O was cycled three times using a freeze-pump-thaw method to completely degas the H<sub>2</sub>O. A portion of 0.0216 g (0.0569 mmol) of UCl<sub>4</sub> was weighed out inside an argon atmosphere glove box and placed into a 200 mL Schlenk flask. Slightly less than 1 equivalent, 0.0207 g (0.0549 mmol) of K<sub>2</sub>[Pt(CN)<sub>4</sub>]·3H<sub>2</sub>O, was

weighed out and placed into a 50 mL Schlenk flask. With all three Schlenk flasks connected to the Schlenk line, a cannula was used to transfer the deoxygenated H<sub>2</sub>O to the Schlenk flasks containing the starting materials. The solutions were stirred to allow the solids to dissolve. The K<sub>2</sub>[Pt(CN)<sub>4</sub>]•3H<sub>2</sub>O solution was then transferred by cannula into the Schlenk flask containing the UCl<sub>4</sub> solution. A small amount of precipitate that formed was removed by filtration. The mother liquor was placed in a -19 °C freezer where crystals suitable for single crystal X-ray diffraction (XRD) were observed to have formed after 6 days. Crystalline yield was not determined as the air sensitivity of the sample is significant and therefore, cannot be accurately weighed on the bench. The presence of H<sub>2</sub>O precluded sample manipulation or weighing in the Ar inert atmosphere glove box.

**{Th<sub>2</sub>(H<sub>2</sub>O)<sub>10</sub>(OH)<sub>2</sub>[Pd(CN)<sub>4</sub>]<sub>3</sub>}•8H<sub>2</sub>O** Complex **Th5** was synthesized by weighing out 0.0200 g (0.0387 mmol) of Th(NO<sub>3</sub>)<sub>4</sub>•6H<sub>2</sub>O and 0.0146 (0.0506 mmol) of K<sub>2</sub>[Pd(CN)<sub>4</sub>]•xH<sub>2</sub>O. Each was dissolved in a minimal amount of H<sub>2</sub>O. The K<sub>2</sub>[Pd(CN)<sub>4</sub>]•xH<sub>2</sub>O solution was layered onto the Th(NO<sub>3</sub>)<sub>4</sub> solution in a 5 mL test tube. The test tube was exposed to atmospheric conditions in a slow evaporation chamber where crystals suitable for single crystal XRD were observed to have formed after 27 days. Crystalline yield of 0.0148 g (67%).

**{(UO<sub>2</sub>)<sub>2</sub>(DMSO)<sub>4</sub>(OH)<sub>2</sub>[Ni(CN)<sub>4</sub>]}** Complex **U6** was synthesized by weighing out 0.0251 g (0.0500 mmol) of UO<sub>2</sub>(NO<sub>3</sub>)<sub>2</sub>•6H<sub>2</sub>O and 0.0140 g (0.0581 mmol) of K<sub>2</sub>[Ni(CN)<sub>4</sub>]•xH<sub>2</sub>O. Each was dissolved in a minimal amount of H<sub>2</sub>O. The

$K_2[Ni(CN)_4] \cdot xH_2O$  solution was layered onto the  $UO_2(NO_3)_2 \cdot H_2O$  solution in a 5 mL test tube. The test tube was exposed to atmospheric conditions where crystals suitable for single crystal XRD were observed to have formed after 32 days. Crystalline yield of 0.0118 g (45%).

**[Th(C<sub>2</sub>H<sub>6</sub>SO)<sub>9</sub>][Pt(CN)<sub>4</sub>]<sub>2</sub>•4H<sub>2</sub>O** Complex **Th7** was synthesized by weighing out 0.0200 grams (0.0387 mmol) of  $Th(NO_3)_4 \cdot 6H_2O$  and 0.0146 grams (0.0387 mmol) of  $K_2[Pt(CN)_4] \cdot 3H_2O$ . Each was dissolved in the smallest amount of DMSO neccessary to produce a clear solution. Solutions were heated to aid the dissolution. The  $K_2[Pt(CN)_4] \cdot 3H_2O$  solution was transferred to the  $Th(NO_3)_4 \cdot 6H_2O$  solution *via* pipette. The solution was allowed to mix and it remained clear and colorless immediately after transfer. The solution was allowed to cool at room temperature and left open to air. Suitable crystals for single crystal XRD were observed after 10 days.

**[Th(C<sub>2</sub>H<sub>6</sub>SO)<sub>8</sub>][Fe(CN)<sub>6</sub>]•NO<sub>3</sub>** Complex **Th8** was synthesized by weighing out 0.0200 grams (0.0387 mmol) of  $Th(NO_3)_4 \cdot 6H_2O$  and 0.0143 grams (0.0387 mmol) of  $K_3[Fe(CN)_6] \cdot 3H_2O$ . Each was dissolved in a minimal amount of DMSO. In addition to heating, the  $K_4[Fe(CN)_6] \cdot 3H_2O$  solution was filtered twice through glass wool before added to the  $Th(NO_3)_4 \cdot 6H_2O$  solution via pipette. The solution was allowed to mix and remained clear and colorless immediately after transfer. The solution was allowed to cool at room temperature and left open to air. Suitable crystals for single crystal XRD were collected after 12 days.

## 5f-Cyanometallate Coordination Complexes

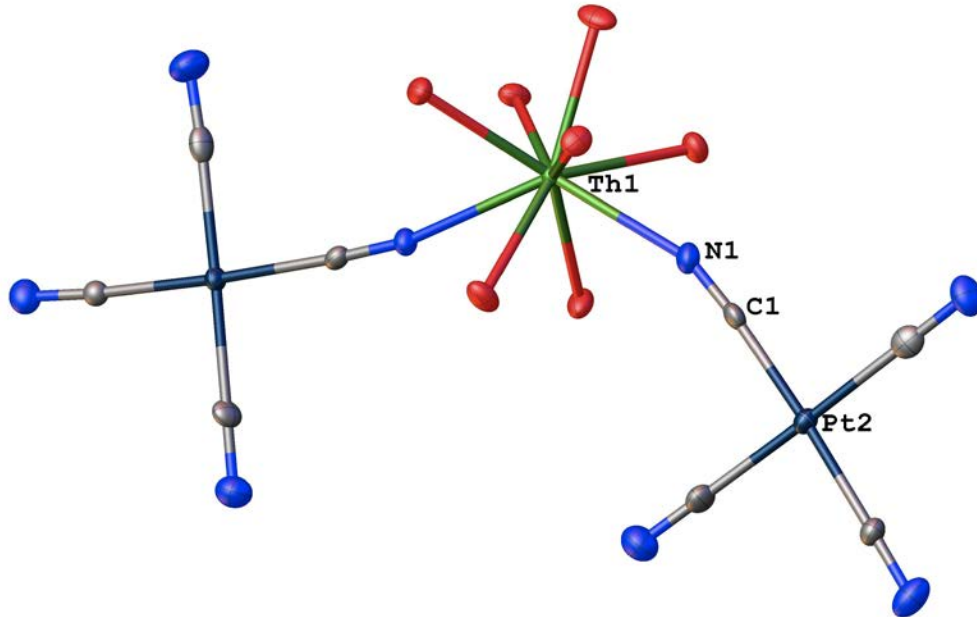


**Figure 10** Asymmetric unit of  $\text{Th}(\text{H}_2\text{O})_7[\text{Pt}(\text{CN})_4]_2 \cdot 10\text{H}_2\text{O}$  (Th1). Atoms as shown are labeled: Th in green, O in red, N in blue, C in grey, and Pt in metallic blue.<sup>9</sup>

The structure of **Th1** (Figure 10) is molecular and consists of  $[\text{Th}(\text{H}_2\text{O})_7(\text{Pt}(\text{CN})_4)_2]$  monomers. The Th metal center is coordinated by two nitrogens from the tetracyanoplatinate anions and seven oxygens from water molecules. The overall coordination environment of the Th site is nine, which is best described as a tricapped trigonal prism. The Th-O bonds range from 2.420(4) to 2.494(4) and the two Th-N bonds are significantly longer at 2.552(5) and 2.571(4) Å. The Th-O bonds correlate well with reported Th-OH<sub>2</sub> data.<sup>38</sup> The Th-N bonds are longer than reported Th-N bonds;<sup>39,40</sup> however these complexes are the first reported N bonded cyanide complexes coordinated

to thorium. The packing diagram of **Th1** (Figure 11) shows the extension of quasi one dimensional linear chains with non-equidistant Pt-Pt distances at 3.371 and 3.351 Å. These distances are ~0.1 Å longer and consistent with the shorter wavelength emission (~50 nm shorter) relative to that compound. These interactions are formed by the interaction of monomers between two tetracyanoplatinate anions.

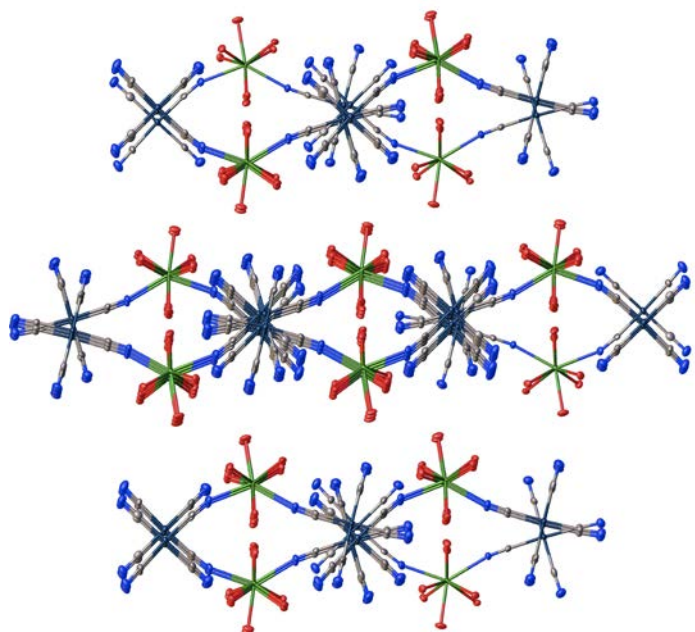


**Figure 11** Packing diagram of  $\text{Th}(\text{H}_2\text{O})_7[\text{Pt}(\text{CN})_4]_2 \cdot 10\text{H}_2\text{O}$  (**Th1**). Atoms as shown are labeled: Th in green, O in red, N in blue, C in grey, and Pt in metallic blue.<sup>9</sup>

**Th<sub>2</sub>(H<sub>2</sub>O)<sub>10</sub>(OH)[Pt(CN)<sub>4</sub>]•5H<sub>2</sub>O (Th2)**

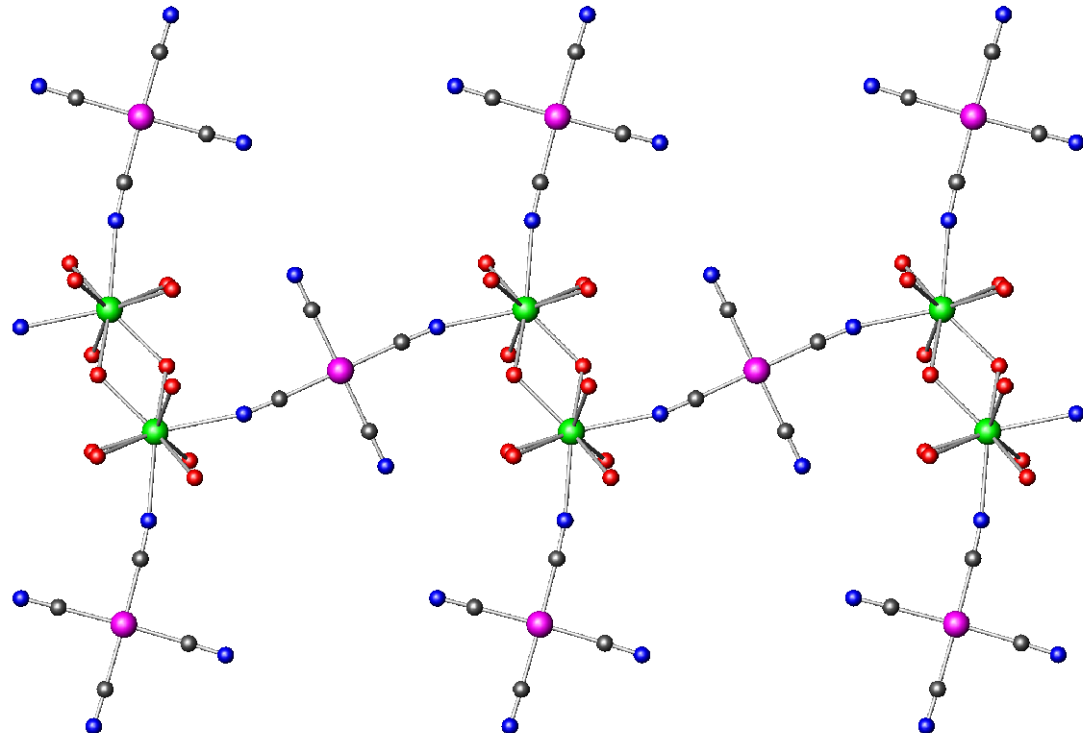


**Figure 12** Projection of Th<sub>2</sub>(H<sub>2</sub>O)<sub>10</sub>(OH)<sub>2</sub>[Pt(CN)<sub>4</sub>]<sub>3</sub>•5H<sub>2</sub>O (Th2) showing the extension of the 1 dimensional chain and the Th-O-Th units. Atoms as shown are labeled: Th in green, O in red, N in blue, C in black, and Pt in magenta.<sup>9</sup>

The structure of **Th2** (Figure 12) consists of one-dimensional [Th<sub>2</sub>(H<sub>2</sub>O)<sub>10</sub>(OH)<sub>2</sub>(Pt(CN)<sub>4</sub>)<sub>3</sub>] chains. Th dimers are formed by linking each Th site with hydroxyls at the bridging oxygen position as seen in figure 12. The Th metal centers are each coordinated by five water molecules. The overall coordination environment of the Th site is nine, and the coordination geometry about the metal center is best described as a tricapped trigonal prism. The Th-O and Th-N bonds range from 2.348(4)–2.500(4) and 2.615(4)–2.653(5) Å respectively. The Th-O bonds correlate with the Th-OH<sub>2</sub> data, with

the Th-OH being slightly truncated at 2.348(4) Å.<sup>38</sup> The Th-N bonds are longer than

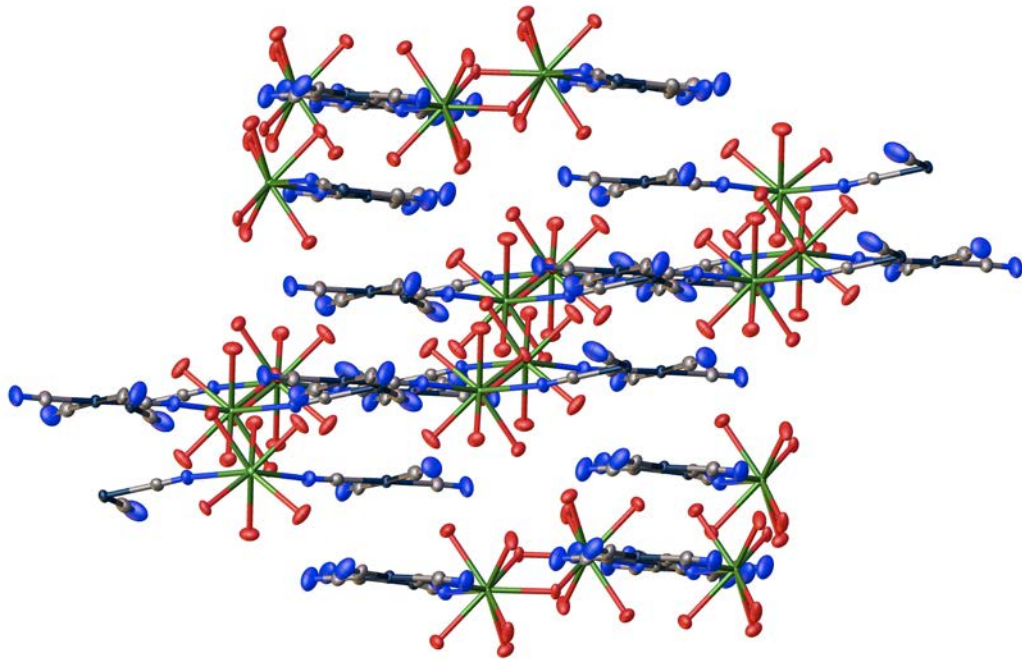


**Figure 13** Packing diagram of  $\text{Th}_2(\text{H}_2\text{O})_{10}(\text{OH})_2[\text{Pt}(\text{CN})_4]_3 \cdot 5\text{H}_2\text{O}$  (Th2). Atoms as shown are labeled: Th in green, O in red, N in blue, C in grey, and Pt in magenta.<sup>9</sup>

reported bonds and probably better described as a dative interaction.<sup>39,41</sup> The elongation of the one dimensional structure is visualized in Figure 12 through the Th-O-Th-TCPt-Th-O-Th-TCPt-Th-O-Th chain. The packing diagram of **2** (Figure 13) shows the extension of quasi one dimensional chains with equal Pt-Pt distances at 3.272 Å representing an equidistant linear chain. These interactions are formed by the interaction of dimers between two tetracyanoplatinate anions.

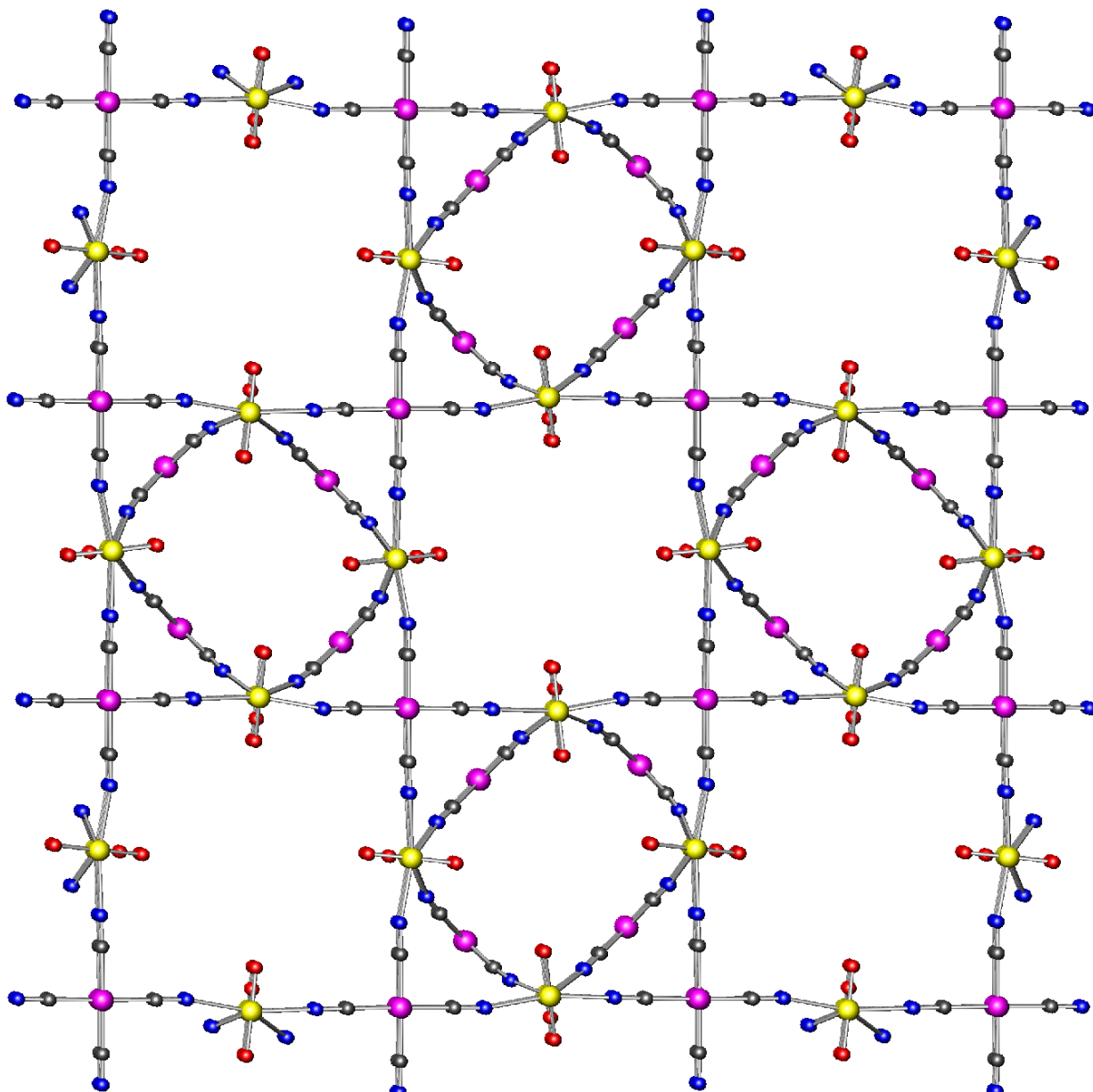


**Figure 14** Packing diagram of  $\text{K}_3[(\text{UO}_2)_2(\text{OH})(\text{Pt}(\text{CN})_4)_2]_2 \cdot \text{NO}_3 \cdot 1.5\text{H}_2\text{O}$  (**U3**) viewed along the  $c$  axis.  $\text{K}^+$ ,  $(\text{NO}_3)^-$ , waters of hydration and hydrogen atoms omitted for clarity. Atoms as shown are labeled: U in yellow, O in red, N in blue, C in black, and Pt in purple.<sup>9</sup>

### $\text{K}_3[(\text{UO}_2)_2(\text{OH})(\text{Pt}(\text{CN})_4)_2]_2 \cdot \text{NO}_3 \cdot 1.5\text{H}_2\text{O}$ (**U3**)

The structure of **U3** (Figure 14) consists of a complex three dimensional lattice made from units of  $[\text{UO}_2(\text{OH})(\text{Pt}(\text{CN})_4)_4]$ . The lattice in 3 consists of layers of cubes with

TCPt anions at the eight vertices. In turn, these layers are bridged by hydroxyl units between uranyl units. The uranium sites are cis bridged within each respective cube and are found at the midpoint of each edge of the cube. The overall coordination environment of the U site is seven, which is best described as a pentagonal bipyramid. Three oxygens coordinate the U center. The “-yl” oxygen distances U–O1 and U–O2 are significantly shorter at 1.774(12) and 1.720(12) Å, forming a O–U–O angle of 179.1(5) $^{\circ}$ ; this confirms the retention of the uranyl subunit. The third oxygen, a hydroxyl group, coordinates the uranium at a distance of 2.310(6) Å. The four U–N bonds range from 2.482(12) to 2.531(14) Å. The packing of **U3** in the structure does not result in quasi one dimensional chains as seen in **Th1** and **Th2**. Instead, in the structure of **U3**, dimeric Pt–Pt interactions are observed at 3.2214(15) Å. These interactions are found between the layers of cube vertices giving the spacing between layers. The Pt–Pt distances are shorter in complex **U3** as compared to complexes **Th1** and **Th2**, and the expected emission should be blue shifted relative to these; however, the lack of emission from **U3**, as observed in the emission spectra (Chapter 3), may be caused by the missing quasi one dimensional Pt-Pt chains.

While the nature of the energy sink is not definitely known at this time, we believe that the source is most likely due to its open-framework nature. Within the channels of the structure there is a large amount of thermal motion of the potassium and nitrate ions as well as the hydrate water molecules. This is seen in the large thermal parameters found in the anisotropic refinement of these nitrate ions and water molecules. These large thermal parameters could be explained in at least two different ways. First, it would be probable that within this metal framework of U3 that the charge balance nitrate

ions and waters of hydration are weakly structurally ordered. This weak ordering allows the atom positions of the nitrate and water molecules to “drift” from one unit cell compared to another. This positional disorder would lead to elongated thermal parameters. Second, it is plausible that an energy transfer mechanism exists in the compound that results in the lack of visible emission of both the uranyl and TCPt portions, but rather results in non-radiative vibrational relaxation of the channel components. Further studies, such as low-temperature emission, are needed to support this hypothesis.

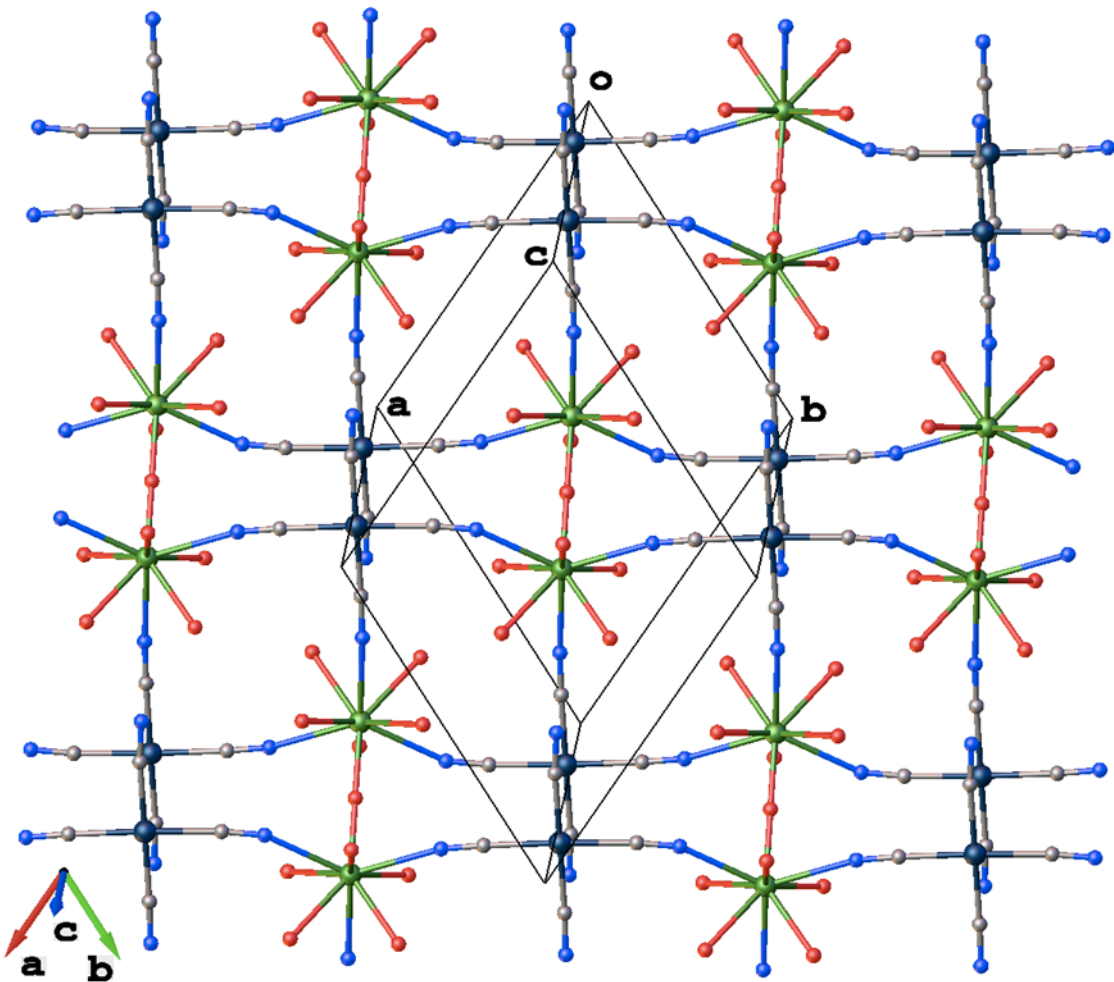


**Figure 15** Projection of  $\{U_2(H_2O)_{10}(O)[Pt(CN)_4]_3\} \cdot 4H_2O$  with lattice vectors shown. Hydration water molecules and hydrogens have been removed for clarity.<sup>7</sup>

**$\{U_2(H_2O)_{10}(O)[Pt(CN)_4]_3\} \cdot 4H_2O$  (U4)** The structure of **U4** has two dimensional, bonding interactions, contains U(IV) as the actinide metal cation, and consists of  $[U(H_2O)_5(O)(Pt(CN)_4)]$  units. Three tetracyanoplatinate anions and five water molecules coordinate the U(IV) metal center. One additional oxygen bridges two uranium sites to complete the coordination sphere as shown in Figure 15. The U(1)-O(1) bond distance at

2.0706(7) Å and the U-O-U bond angle of 180° corresponds well with another U-O<sub>oxo</sub>-U bridged species.<sup>17</sup> The overall coordination environment of the U(IV) site is nine, and this is best described geometrically as a tricapped trigonal prism. There are two distinct crystallographic tetracyanoplatinate anions in this structure. The structure is extended in two dimensions by the tetracyanoplatinate anions containing Pt1, which are tridentate and bridge three U sites, and the oxo bridge which links together two U sites as shown in Figure 16. The second tetracyanoplatinate anion containing Pt2 does not coordinate uranium, but is present for charge balance and is involved in the formation of the pseudo one-dimensional stacks.

Each uranium center is coordinated by three tetracyanoplatinate anions and in turn, each tridentate tetracyanoplatinate anion coordinates three U(IV) centers. An oxo bridge spans the U(IV) centers on the ladder structural features, thus forming the second dimension of the sheet. This forms a series of parallel ridges and furrows in conjunction with a macrostructure like a corrugated sheet. This structure does contain pseudo one-dimensional tetracyanoplatinate chains, as shown in Figure 16, which is common with square planar cyanometallate complexes. In the pseudo one-dimensional chains, there are two crystallographically independent Pt···Pt distances, 3.266(1) and 3.493(1) Å. These chains are described in the earlier literature as linear and non-equidistant with Pt

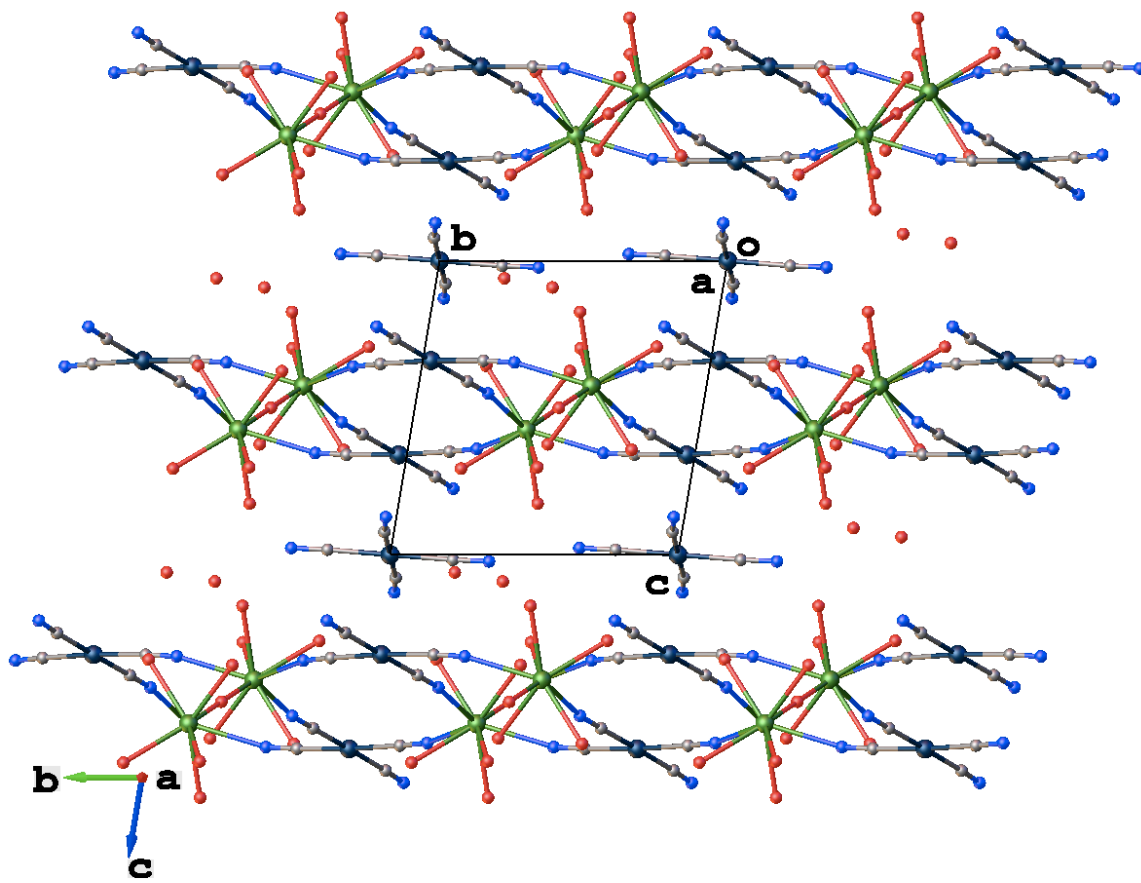


**Figure 16** Packing diagram of (U4) showing the 2-D structural motif and the one-dimensional linear nonequidistant Pt-Pt chains along the *c* axis.<sup>7</sup>

atoms forming a x-y-y-x type structure. In this structure, x = a free  $\text{Pt}(\text{CN})_4^{2-}$  anion and y = a complexed  $\text{Pt}(\text{CN})_4^{2-}$  anion.<sup>19</sup> This type of chain structure is also described previously as linear non-equidistant, and it is often associated with partially oxidized systems.<sup>19</sup> The coordinating tetracyanoplatinate anions coordinate the uranium centers through three different U-N≡C bond angles 172.3(15), 165.2(12), and 155.3(12)°. The U-OH<sub>2</sub> bonds range from 2.456(1) to 2.514(1) Å. The U-O<sub>oxo</sub> bond is 2.0706(7) Å and the three U-N bonds range from 2.543(1) to 2.565(1) Å.

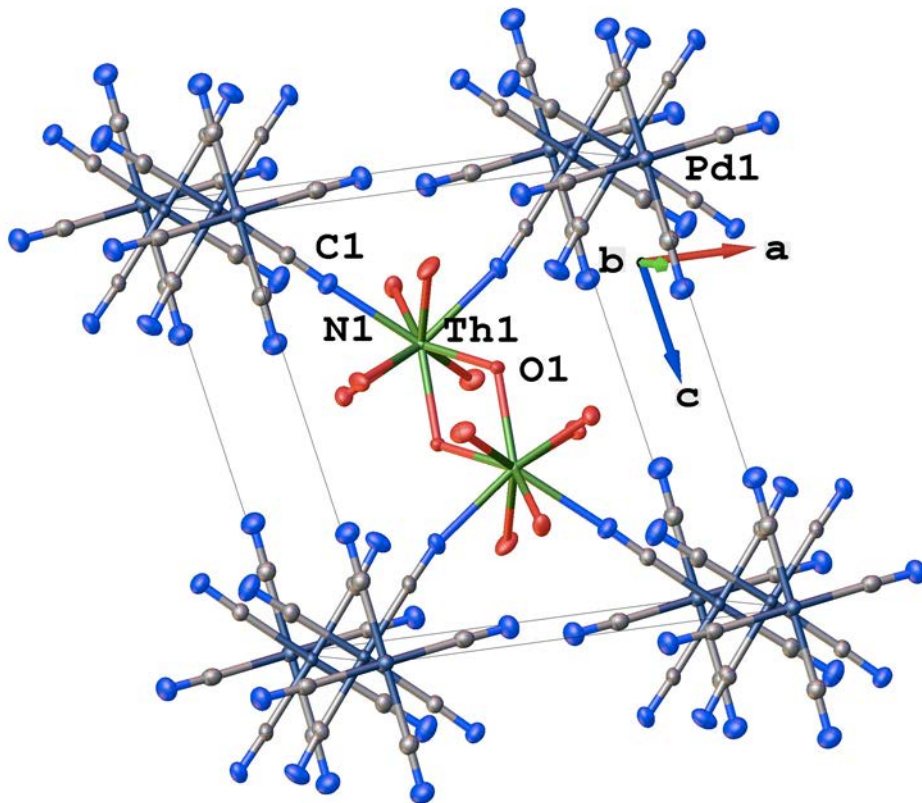


**Figure 17** Projection of  $\{\text{Th}_2(\text{H}_2\text{O})_{10}(\text{OH})_2[\text{Pd}(\text{CN})_4]_3\} \cdot 8\text{H}_2\text{O}$  (**Th5**) showing the pseudo-one dimensional  $\text{Pd}\cdots\text{Pd}$  interactions, along the  $b$  axis, with the unit cell superimposed. Thorium atoms are labeled in green, oxygen atoms in red, nitrogen atoms in blue and palladium atoms in metallic blue.<sup>7</sup>

### $\{\text{Th}_2(\text{H}_2\text{O})_{10}(\text{OH})_2[\text{Pd}(\text{CN})_4]_3\} \cdot 8\text{H}_2\text{O}$ (**Th5**)

The key feature of the structure of **Th5** is a series of one-dimensional chains of  $\{\text{Th}_2(\text{OH})_2(\text{H}_2\text{O})(\text{Pd}(\text{CN})_4)_3\}$ . There is one crystallographically independent  $\text{Th}^{4+}$  center with a coordination number of nine, and it is best described geometrically as a tricapped trigonal prism. Three monodentate tetracyanopalladate anions and six oxygens coordinate the  $\text{Th}^{4+}$  metal center. Five of the coordinating oxygens are from water molecules, and the other two are from bridging hydroxides. Two hydroxide ions link the two  $\text{Th}^{4+}$  sites together, and do not form bonds of equal length. The inversion symmetry is shown in two unique Th-OH bond distances of 2.337(3) and 2.371(3) Å. Two  $\text{Th}^{4+}$  ions sit

3.9858(4) Å apart from each other, which is a shorter distance than the sum of the Van der Waals radii. The tetracyanopalladate anion bound to the Th<sup>4+</sup> site extends the chain by binding to another asymmetric unit in a cis fashion. The pseudo one-dimensional Pd···Pd chains are present and can be visualized in Figure 17. Again, chains like these are described in the earlier literature as linear and non-equidistant. The two crystallographically independent Pd···Pd distances are found at 3.2512(5) and 3.4960(9) Å. At first glance, the structure of **Th2** and **Th5** appear very similar as both are described as one-dimensional.<sup>9</sup> Upon closer observation the structure of **Th2** can be described as a polymeric structure consisting of  $[-\text{TCPt-Th-(OH)}_2\text{-Th-}]^{+4}$  monomers. Inspection of **Th5** reveals that the polymeric structure is composed of  $[-(\text{OH})\text{-Th-(TCPd)}_2\text{-Th-(OH)-}]^{+2}$  monomers and is not isostructural with **Th2**.

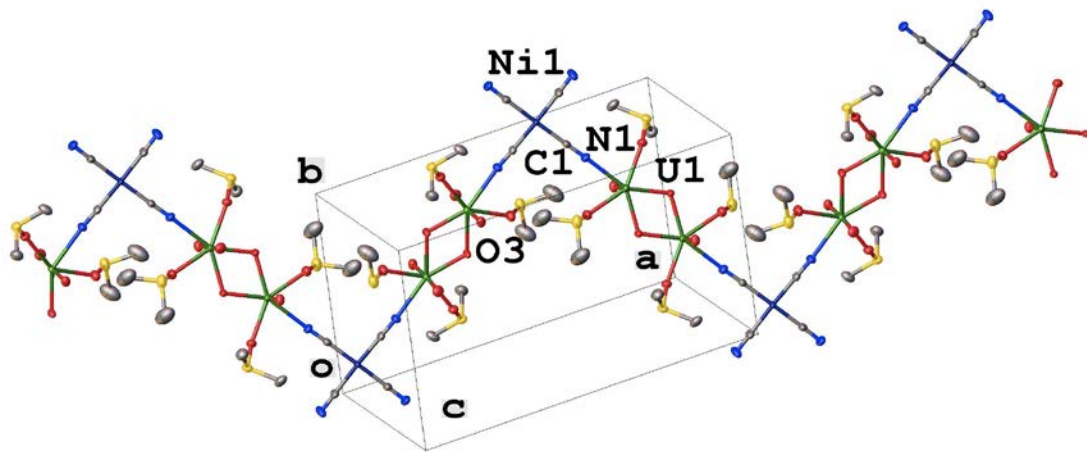


**Figure 18** Extension of the one-dimensional structure of  $\{(UO_2)_2(DMSO)_4(OH)_2[Ni(CN)_4]\}$  (**U6**) with the unit cell superimposed. Uranium atoms are labeled in green, oxygen atoms in red, nitrogen atoms in blue and platinum atoms in blue metal. Hydrogen atoms are not shown for clarity.<sup>7</sup>

### $\{(UO_2)_2(DMSO)_4(OH)_2[Ni(CN)_4]\}$ (**U6**)

The structure of  $\{(UO_2)_2(DMSO)_4(OH)_2[Ni(CN)_4]\}$  (**U6**) has one-dimensional bonding interactions and consists of extended chains made up of  $\{UO_2(DMSO)_4(OH)_2[Ni(CN)_4]\}$  units. There is one crystallographically independent  $UO_2^{2+}$  site. It has a coordination number of seven and is best described as a pentagonal bipyramid. Each  $UO_2^{2+}$  site is coordinated by six oxygen atoms and one tetracyanonicinate anion. Two oxygens are from the uranyl oxygen atoms and are found at distances of 1.776(4) and 1.779(4) Å from the metal ion. The second pair of coordinating oxygens are from the DMSO solvent molecule, and these are found at 2.380(4) and 2.391(4) Å. The third pair of coordinating oxygens are from the bridging hydroxides and have bond distances of 2.321(4) and 2.334(4) Å. One nitrogen from a cis bridging tetracyanonicinate anion also coordinates the  $UO_2^{2+}$  site. The structure is extended by two structural features along the one-

dimensional chain; two bridging hydroxides connect uranyl sites and the cis bridging tetracyanonickelate anion connects these uranyl sites extending the chain indefinitely. As compared to **Th2** and **Th5** only a single TCNi unit bonds each  $\text{UO}_2^{2+}$  center. The polymeric structure of **U6** is clearly seen in Figure 18 consisting of  $[-(\text{OH})-\text{UO}_2-\text{TCNi}-\text{UO}_2-(\text{OH})-]$  monomers. The monomer of **U6** resembles the monomer of **Th5**. In contrast, 3d metallophilicity is not observed, because the one-dimensional chains do not pack in such a way that  $\text{Ni} \cdots \text{Ni}$  interactions are observed. The central reason for this is the small, hard 3d  $\text{Ni}^{2+}$  ions do not readily allow for metallophilic interactions. In addition, the inclusion of DMSO prohibits the stacking of TCNi, while by comparison, in **Th5**, the inclusion of  $\text{H}_2\text{O}$  allows for the TCPd anions to form the pseudo one-dimensional chains.

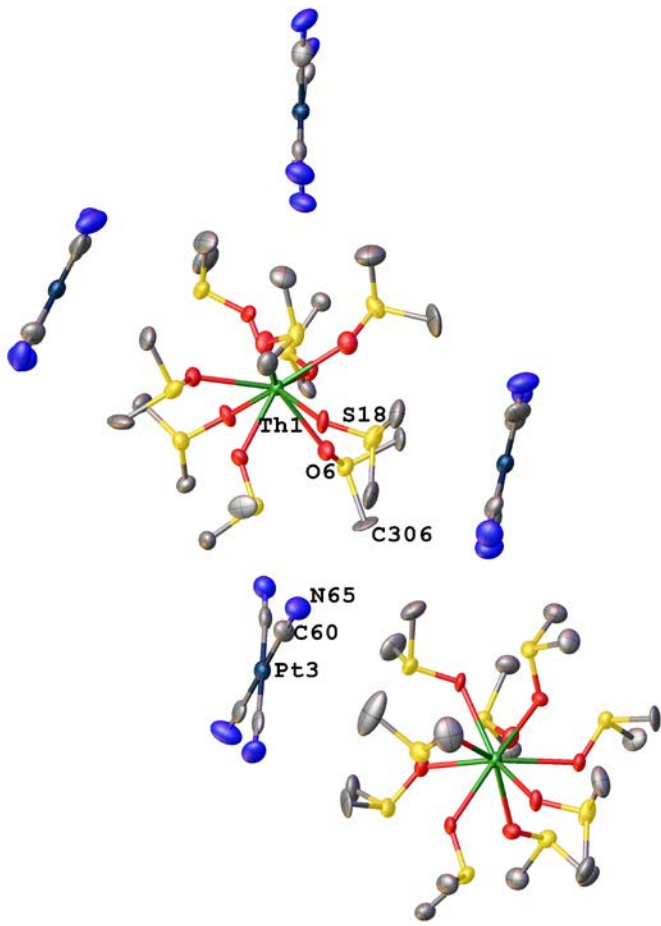


**Figure 19** Projection of the ionic structure of  $[\text{Th}(\text{C}_2\text{H}_6\text{SO})_9][\text{Pt}(\text{CN})_4]_2 \cdot 4\text{H}_2\text{O}$  (**Th7**). Thorium atoms are labeled in green, oxygen atoms in red, nitrogen atoms in blue and platinum atoms in blue metal. Hydrogen atoms are not shown for clarity.<sup>8</sup>

### [ $\text{Th}(\text{C}_2\text{H}_6\text{SO})_9][\text{Pt}(\text{CN})_4]_2 \cdot 4\text{H}_2\text{O}$ (**Th7**)

The structure of  $[\text{Th}(\text{C}_2\text{H}_6\text{SO})_9][\text{Pt}(\text{CN})_4]_2 \cdot 4\text{H}_2\text{O}$  (**Th7**) is ionic in nature. The structure is formed by anions of  $[\text{Pt}(\text{CN})_4]^{2-}$  and cations of  $[\text{Th}(\text{C}_2\text{H}_6\text{SO})_8]^{4+}$ . The  $\text{Th}^{4+}$  site is coordinated in a bicapped trigonal prismatic fashion by eight monodentate DMSO molecules. The structure is completed by two uncoordinated tetracyanoplatinate anions and four  $\text{H}_2\text{O}$  molecules. As shown in Figure 19, columns of tetracyanoplatinate ions do form but the Pt spacing between tetracyanoplatinate anions are found to be 8.696 Å, too long to be considered pseudo one dimensional Pt chains.

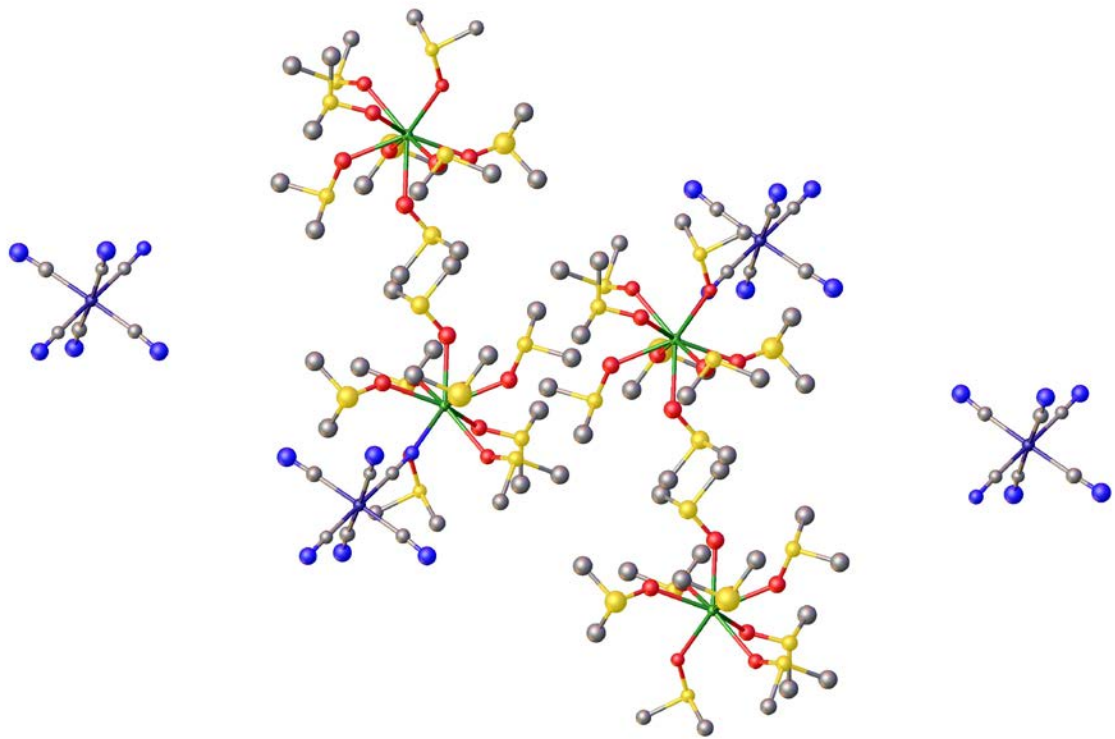


**Figure 20** Projection of the structure of  $[\text{Th}(\text{C}_2\text{H}_6\text{SO})_8][\text{Fe}(\text{CN})_6]\cdot\text{NO}_3$  (Th8). Thorium atoms are labeled in green, oxygen atoms in red, nitrogen atoms in blue and iron atoms in blue metal. Hydrogen atoms and nitrate anions are not shown for clarity.<sup>8</sup>

### $[\text{Th}(\text{C}_2\text{H}_6\text{SO})][\text{Fe}(\text{CN})_6]\cdot\text{NO}_3$ (Th8)

The structure of  $[\text{Th}(\text{C}_2\text{H}_6\text{SO})_8][\text{Fe}(\text{CN})_6]\cdot\text{NO}_3$  (**Th8**) is molecular in nature. It is composed of a unit of  $[\text{Fe}(\text{CN})_6]^{3-}$  and a unit of  $[\text{Th}(\text{C}_2\text{H}_6\text{SO})_8]^{4+}$  to form the  $[(\text{Th}(\text{C}_2\text{H}_6\text{SO})_8)(\text{Fe}(\text{CN})_6)]^+$  cation. The structure is charge balanced by the presence of a nitrate anion which is not shown in figure 20. The  $\text{Th}^{4+}$  site is coordinated in a tricapped trigonal prismatic fashion by one nitrogen from the hexacyanoferrate anion and eight monodentate DMSO molecules. Because the hexacyanoferrate molecular geometry is octahedral and not square planar it does not allow the formation of  $\text{Fe}\cdots\text{Fe}$  pseudo one dimensional chains as in other compounds in this class. As shown in Figure 20, a

nitrogen from the hexacyanoferrate ion covalently binds the thorium center with a bond length of 2.674 Å which is probably better described as a dative interaction.<sup>39,41</sup>

**Table 2**

Formula	$\text{Th}(\text{H}_2\text{O})_7[\text{Pt}(\text{CN})_4]_2 \bullet 10\text{H}_2\text{O}$ <b>Th1</b>	$\text{Th}_2(\text{H}_2\text{O})_{10}(\text{OH})_2[\text{Pt}(\text{CN})_4]_3 \bullet 5\text{H}_2\text{O}$ <b>Th2</b>	$\text{K}_3[(\text{UO}_2)_2(\text{OH})(\text{Pt}(\text{CN})_4)_2]_2 \bullet \text{NO}_3 \bullet 1.5\text{H}_2\text{O}$ <b>U3</b>
Formula mass	1136.65	1665.85	2517.15
Color	Yellow Green	Yellow Green	Yellow
Crystal system	Orthorhombic	Monoclinic	Tetragonal
Space group	<i>Pbca</i>	<i>C2/c</i>	<i>P4/mbm</i>
a (Å)	13.2464(6)	16.4915(4)	22.1073(2)
b (Å)	20.5599(10)	12.1941(4)	22.1073(2)
c (Å)	22.4536(11)	19.5380(5)	12.6202(2)
$\alpha$ (°)	90	90	90
$\beta$ (°)	90	114.016(4)	90
$\gamma$ (°)	90	90	90
V (Å <sup>3</sup> )	6115.1(5)	3588.9(2)	6167.9(1)
Z	8	4	4
T (K)	193 (2)	295 (2)	290 (2)
$\lambda$ (Å)	0.71073	0.71073	0.71073
$\mu$ (mm <sup>-1</sup> )	14.053	19.989	19.75
Reflections collected	59819	32269	26733
Unique reflections	7574	5166	3423
Rint	0.0737	0.0281	0.0564
$R_1$ [ $I > 2\sigma(I)$ ]	0.0301	0.0141	0.0522
wR <sub>2</sub> (all data)	0.0781	0.0244	0.01562

**Table 3**

Formula	$\{\text{U}_2(\text{H}_2\text{O})_{10}(\text{O})[\text{Pt}(\text{CN})_4]_3\} \bullet 4\text{H}_2\text{O}$ <b>U4</b>	$\{\text{Th}_2(\text{H}_2\text{O})_{10}(\text{OH})_2[\text{Pd}(\text{CN})_4]_3\} \bullet 8\text{H}_2\text{O}$ <b>Th5</b>	$\{(\text{UO}_2)_2(\text{DMSO})_4(\text{OH})_2[\text{Ni}(\text{CN})_4]\}$ <b>U6</b>
Formula mass	1613.57	1415.52	2094.72
Color	Emerald green	Colorless	Yellow
Crystal system	Triclinic	Triclinic	Monoclinic
Space group	$P\bar{1}$	$P\bar{1}$	$C2/c$
a (Å)	9.716 (4)	9.6141 (6)	21.5224(11)
b (Å)	9.823 (4)	9.9479 (6)	10.2531(5)
c (Å)	9.926 (4)	11.1360 (7)	13.3170(6)
$\alpha$ ( $^{\circ}$ )	74.191 (7)	73.7480 (10)	90
$\beta$ ( $^{\circ}$ )	70.734 (7)	78.0950 (10)	111.9430(10)
$\gamma$ ( $^{\circ}$ )	67.242 (7)	68.6530 (10)	90
V (Å $^3$ )	813.2 (6)	945.82 (10)	2725.8(2)
Z	1	1	2
T (K)	183 (2)	183 (2)	183 (2)
$\lambda$ (Å)	0.71073	0.71073	0.71073
$\mu$ (mm $^{-1}$ )	22.857	9.315	2.552
Reflections collected	7998	9619	10040
Unique reflections	3940	4604	3358
Rint	0.0582	0.0270	0.0292
R <sub>1</sub> [I > 2σ(I)]	0.0669	0.0282	0.0298
wR <sub>2</sub> (all data)	0.1681	0.0715	0.0746

**Table 4**

Formula	[Th(C <sub>2</sub> H <sub>6</sub> SO) <sub>9</sub> ][Pt(CN) <sub>4</sub> ] <sub>2</sub> •4H <sub>2</sub> O <b>Th7</b>	[Th(C <sub>2</sub> H <sub>6</sub> SO) <sub>8</sub> ][Fe(CN) <sub>6</sub> ] <sub>2</sub> •NO <sub>3</sub> <b>Th8</b>
Formula mass	3066.60	1131.13
Color	colorless	colorless
Crystal system	Triclinic	Monoclinic
Space group	<i>P</i> ī	<i>P</i> 2 <sub>1</sub> n
a (Å)	12.4199(6)	11.9796(9)
b (Å)	20.3265(10)	17.7389(13)
c (Å)	21.1132(10)	20.0389(15)
α (°)	102.080(1)	90
β (°)	98.2710(1)	90.117(2)
γ (°)	96.694(01)	90
V (Å <sup>3</sup> )	5098.25(4)	4258.4(6)
Z	4	4
T (K)	183 (2)	183 (2)
λ (Å)	0.71073	0.71073
μ (mm <sup>-1</sup> )	8.803	4.276
Reflections collected	25422	10600
Unique reflections	15375	8144
R <sub>int</sub>	0.0579	0.0690
R <sub>1</sub> [I > 2σ(I)]	0.0585	0.0840
wR <sub>2</sub> (all data)	0.1402	0.2164

## Crystallographic Overview

A brief review of the structural characteristics of these complexes is presented here in an attempt to aid in the discussion of all eight compounds (**Th1**, **Th2**, **U3**, **U4**, **Th5**, **U6**, **Th7**, and **Th8**) in the following chapters.  $\text{Th}(\text{H}_2\text{O})_7[\text{Pt}(\text{CN})_4]_2 \cdot 10\text{H}_2\text{O}$  (**Th1**) is composed of monomers,  $[\text{Th}(\text{H}_2\text{O})_7(\text{Pt}(\text{CN})_4)_2]$ . The  $\text{Th}^{4+}$  metal center is bound by two monodentate tetracyanoplatinate anions. These monomers are not covalently bonded to another monomer, subsequently, the structural motif is best described as zero-dimensional. The formation of pseudo one-dimensional Pt···Pt chains is observed from the stacking of the monomers. There are two Pt···Pt R values found at 3.3712(2) and 3.3515(2) Å.  $\text{Th}_2(\text{H}_2\text{O})_{10}(\text{OH})_2[\text{Pt}(\text{CN})_4]_3 \cdot 5\text{H}_2\text{O}$  (**Th2**) is composed of  $[\text{Th}_2(\text{H}_2\text{O})_{10}(\text{OH})_2(\text{Pt}(\text{CN})_4)_3]$  chains, and is best described as one-dimensional. Each  $\text{Th}^{4+}$  metal center is bound by two tetracyanoplatinate anions via two different modes of coordination, mono- and bidentate. The bidentate tetracyanoplatinate anion covalently extends the global structure in chains along one dimension. These chains pack in a way that formation of pseudo one-dimensional Pt···Pt chains is observed. The Pt atoms in the pseudo one-dimensional chains are spaced equidistant at 3.272(2) Å. The three-dimensional structure of (**U3**) is composed of  $[\text{UO}_2(\text{OH})(\text{Pt}(\text{CN})_4)_4]$  units. Each  $\text{UO}_2^{2+}$  is bound by four tetradentate tetracyanoplatinate anions. The tetradentate tetracyanoplatinate anions extend the global structure in all three dimensions. The packing of this structure only allows the formation of Pt···Pt dimers, found at 3.221(1) Å.<sup>9</sup> The two dimensional structure of  $\{\text{U}_2(\text{H}_2\text{O})_{10}(\text{O})[\text{Pt}(\text{CN})_4]_3\} \cdot 4\text{H}_2\text{O}$  (**U4**) is composed of  $[\text{U}(\text{H}_2\text{O})_5(\text{O})(\text{Pt}(\text{CN})_4)]$  units. The structure contains two crystallographically independent types of tetracyanometallate anions: one form binds three  $\text{U}^{\text{IV}}$  centers and

the other form is incorporated into the structure for charge balance. Pt $\cdots$ Pt interactions are found in this structure at 3.266(1) and 3.493(1) Å. The one dimensional structure of {Th<sub>2</sub>(H<sub>2</sub>O)<sub>10</sub>(OH)<sub>2</sub>[Pd(CN)<sub>4</sub>]<sub>3</sub>}•8H<sub>2</sub>O (**Th5**) is composed of one-dimensional chains of {Th<sub>2</sub>(OH)<sub>2</sub>(H<sub>2</sub>O)(Pd(CN)<sub>4</sub>)<sub>3</sub>}. These one dimensional chains line up so that the tetracyanopalladate ions form Pd $\cdots$ Pd interactions found at 3.2512(5) and 3.4960(9) Å. The one dimensional structure of {(UO<sub>2</sub>)<sub>2</sub>(DMSO)<sub>4</sub>(OH)<sub>2</sub>[Ni(CN)<sub>4</sub>] } (**U6**) is composed {UO<sub>2</sub>(DMSO)<sub>4</sub>(OH)<sub>2</sub>[Ni(CN)<sub>4</sub>] } units. The structure is extended by two structural features along the one-dimensional chain; two bridging hydroxides connect uranyl sites and the cis bridging tetracyanonickelate anion connects these uranyl sites extending the chain indefinitely. The ionic structure of [Th(C<sub>2</sub>H<sub>6</sub>SO)<sub>9</sub>][Pt(CN)<sub>4</sub>]<sub>2</sub>•4H<sub>2</sub>O (**Th7**) is zero dimensional and the simplest and possibly least interesting in regards to the structural properties of all eight of these compounds. A thorium center is coordinated by eight monodentate DMSO molecules bound through the oxygen atom and the tetrapositive charge on the thorium atom is charge balanced by two tetracyanoplatinate anions. Chemically it is interesting to note that the DMSO molecules must have a higher affinity to the thorium center than the cyanide group from the tetracyanoplatinate. The ionic structure of [Th(C<sub>2</sub>H<sub>6</sub>SO)<sub>8</sub>][Fe(CN)<sub>6</sub>]•NO<sub>3</sub> (**Th8**) is zero dimensional in nature and composed of the simple hexacyanoferrate bound via one cyanide group to the hepta DMSO coordinated thorium metal with a nitrate ion included for charge balance.

In summary, eight cyano bridged 5*d*-5*f* complexes **Th1**, **Th2**, **U3**, **U4**, **Th5**, **U6**, **Th7**, and **Th8** have been synthesized. These complexes represent the first d<sup>8</sup> metal cyanides coordinated to actinide metals. The thorough structure elucidation and analysis starts to establish An-N-C bonding parameters. Complexes **Th1** and **Th2** contain long

range Pt-Pt interactions manifested in the quasi one dimensional chains, while complex **U3** lacks this long range order. Incorporation of the solvent DMSO into the structures negatively impacts the formation of the square planar d<sup>8</sup> metal interactions. The synthesis of **Th1**, **Th2**, and **Th5** provides a readily available way to access the Th-N bond without having to prepare the thorium starting material as the halide salt, or as an organometallic starting material Cp, or Cp\*.<sup>39-43</sup> The combined preparation simplicity, Th–N bond accessibility at bench top conditions, ambient atmospheric conditions, and in the presence of H<sub>2</sub>O is unique in the field of actinide chemistry.

## References Cited

- (1) *Nuclear Technology Review 2010*, International Atomic Energy Agency, 2010.
- (2) Albright, D.; Berkout, F.; Walker, W. *Plutonium and Highly Enriched Uranium 1996: World Inventories, Capabilities, and Policies*; Stockholm International Peace Research Institute: Oxford University Press: New York, 1997.
- (3) Gorden, A. E.; Xu, J.; Raymond, K. N.; Durbin, P. *Chem. Rev.* **2003**, *103*, 4207.
- (4) Nuclear Energy Advisory Committee *Nuclear Energy: Policies and Technology for the 21st Century*, 2008.
- (5) United States Energy Administration *Annual Energy Review 2010*, U. S. Department of Energy, 2011
- (6) MIT Nuclear Fuel Cycle Study Advisory Committee *The Future of the Nuclear Fuel Cycle: An Interdisciplinary Study*, Massachusetts Institute of Technology (MIT), 2011.
- (7) Maynard, B. A.; Lynn, K. S.; Sykora, R. E.; Gorden, A. E. V. *Inorg. Chem.* **2013**, *52*, 4880.
- (8) Maynard, B. A.; Lynn, K. S.; Sykora, R. E.; Gorden, A. E. V. *J. Radioanal. Nucl. Chem.* **2013**, *296*, 453.
- (9) Maynard, B. A.; Sykora, R. E.; Mague, J. T.; Gorden, A. E. *Chem. Commun. (Camb.)* **2010**, *46*, 4944.
- (10) *Forty Years of Uranium Resources, Production and Demand in Perspective "The Red Book Retrospective."*, Organisation for Economic Co-operation and Development Nuclear Energy Agency, 2006.
- (11) Britt, P.; Forsberg, C.; Herring, S. *Technology and Applied R&D Needs for Nuclear Fuel Resources*, 2010.
- (12) Cantat, T.; Graves, C. R.; Scott, B. L.; Kiplinger, J. L. *Angew. Chem., Int. Ed.* **2009**, *48*, 3681.
- (13) DeVore, M. A.; Gorden, A. E. V. *Polyhedron* **2012**, *42*, 271.
- (14) Melfi, P. J.; Kim, S. K.; Lee, J. T.; Bolze, F.; Seidel, D.; Lynch, V. M.; Veauthier, J. M.; Gaunt, A. J.; Neu, M. P.; Ou, Z.; Kadish, K. M.; Fukuzumi, S.; Ohkubo, K.; Sessler, J. L. *Inorg. Chem. (Washington, DC, U. S.)* **2007**, *46*, 5143.

- (15) Pasquale, S.; Sattin, S.; Escudero-Adan, E. C.; Martinez-Belmonte, M.; de, M. J. *Nat. Commun.* **2012**, *3*, 1793/1.
- (16) Schnaars, D. D.; Batista, E. R.; Gaunt, A. J.; Hayton, T. W.; May, I.; Reilly, S. D.; Scott, B. L.; Wu, G. *Chem Commun (Camb)* **2011**, *47*, 7647.
- (17) Daly, S. R.; Ephritikhine, M.; Girolami, G. S. *Polyhedron* **2012**, *33*, 41.
- (18) Montreal, M. J.; Thomson, R. K.; Cantat, T.; Travia, N. E.; Scott, B. L.; Kiplinger, J. L. *Organometallics* **2011**, *30*, 2031.
- (19) Gliemann, G.; Yersin, H. *Struct. Bond.* **1985**, *62*, 87.
- (20) Di, N. V.; Negro, E.; Vezzu, K.; Toniolo, L.; Pace, G. *Electrochim. Acta* **2011**, *57*, 257.
- (21) Ding, E.; Sturgeon, M. R.; Rath, A.; Chen, X.; Keane, M. A.; Shore, S. G. *Inorg. Chem. (Washington, DC, U. S.)* **2009**, *48*, 325.
- (22) Cich, M. J.; Hill, I. M.; Lackner, A. D.; Martinez, R. J.; Ruthenburg, T. C.; Takeshita, Y.; Young, A. J.; Drew, S. M.; Buss, C. E.; Mann, K. R. *Sens. Actuators, B* **2010**, *B149*, 199.
- (23) Perrier, M.; Long, J.; Paz, F. A. A.; Guari, Y.; Larionova, J. *Inorg. Chem. (Washington, DC, U. S.)* **2012**, *51*, 6425.
- (24) Dumont, M. F.; Knowles, E. S.; Guiet, A.; Pajerowski, D. M.; Gomez, A.; Kycia, S. W.; Meisel, M. W.; Talham, D. R. *Inorg. Chem. (Washington, DC, U. S.)* **2011**, *50*, 4295.
- (25) Le, B. R.; Tsunobuchi, Y.; Mathoniere, C.; Tokoro, H.; Ohkoshi, S.-i.; Ould-Moussa, N.; Molnar, G.; Bousseksou, A.; Letard, J.-F. *Inorg. Chem. (Washington, DC, U. S.)* **2012**, *51*, 2852.
- (26) Mizuno, Y.; Okubo, M.; Kagesawa, K.; Asakura, D.; Kudo, T.; Zhou, H.; Ohishi, K.; Okazawa, A.; Kojima, N. *Inorg. Chem. (Washington, DC, U. S.)*, Ahead of Print.
- (27) Loosli, A.; Wermuth, M.; Gudel, H. U.; Capelli, S.; Hauser, J.; Burgi, H. B. *Inorg. Chem.* **2000**, *39*, 2289.
- (28) Du, B.; Meyers, E. A.; Shore, S. G. *Inorg. Chem.* **2001**, *40*, 4353.
- (29) Maynard, B. A.; Kalachnikova, K.; Whitehead, K.; Assefa, Z.; Sykora, R. E. *Inorg. Chem. (Washington, DC, U. S.)* **2008**, *47*, 1895.
- (30) Maynard, B. A.; Sykora, R. E. *Acta Crystallogr., Sect. E: Struct. Rep. Online* **2008**, *E64*, m138.

- (31) Maynadie, J.; Berhet, J.-C.; Thuery, P.; Ephritikhine, M. *Organometallics* **2007**, *26*, 2623.
- (32) Zhu, X.; Wong, W.-K.; Guo, J.; Wong, W.-Y.; Zhang, J.-P. *Eur. J. Inorg. Chem.* **2008**, 3515.
- (33) Rinehart, J. D.; Harris, T. D.; Kozimor, S. A.; Bartlett, B. M.; Long, J. R. *Inorg. Chem.* **2009**, *48*, 3382.
- (34) Maynard, B. A.; Smith, P. A.; Ladner, L.; Jaleel, A.; Beedoe, N.; Crawford, C.; Assefa, Z.; Sykora, R. E. *Inorg. Chem. (Washington, DC, U. S.)* **2009**, *48*, 6425.
- (35) Maynard, B. A.; Smith, P. A.; Sykora, R. E. *Acta Crystallogr., Sect. E: Struct. Rep. Online* **2009**, *65*, m1132.
- (36) Zhang, L.-P.; Tanner, P. A.; Mak, T. C. W. *Eur. J. Inorg. Chem.* **2006**, 1543.
- (37) Holzapfel, W.; Yersin, H.; Gliemann, G. *Z. Kristallogr.* **1981**, *157*, 47.
- (38) Wilson, R. E.; Skanthakumar, S.; Burns, P. C.; Soderholm, L. *Angew. Chem., Int. Ed.* **2007**, *46*, 8043.
- (39) Schelter, E. J.; Morris, D. E.; Scott, B. L.; Kiplinger, J. L. *Chem. Commun. (Cambridge, U. K.)* **2007**, 1029.
- (40) Pool, J. A.; Scott, B. L.; Kiplinger, J. L. *Chem. Commun. (Cambridge, U. K.)* **2005**, 2591.
- (41) Drew, M. G. B.; Willey, G. R. *J. Chem. Soc., Dalton Trans.* **1984**, 727.
- (42) Cantat, T.; Scott, B. L.; Kiplinger, J. L. *Chem. Commun. (Cambridge, U. K.)* **2010**, *46*, 919.
- (43) Jantunen, K. C.; Burns, C. J.; Castro-Rodriguez, I.; Da, R. R. E.; Golden, J. T.; Morris, D. E.; Scott, B. L.; Taw, F. L.; Kiplinger, J. L. *Organometallics* **2004**, *23*, 4682.

## **Chapter 3: Emission and Raman Spectroscopy of the Actinide Tetracyanometallates**

In chapter 2, the solid state structural elucidation of the actinide tetracyanoplatinate compounds was discussed in detail. Figures from chapter 2 have been included along with the spectra to help coordinate the features observed in the spectra with the structural features. As with any coordination compound, the structural features found from the single crystal x-ray diffraction experiment dictate what can be observed *via* other solid state experimental methods (i.e. photoluminescence and Raman spectroscopy). Chapter 3 will focus on these two experimentation methods with an emphasis of pointing out why the observations can be made when considering the structural features.

## Excitation and Emission

### CRAIC Microspectrophotometer

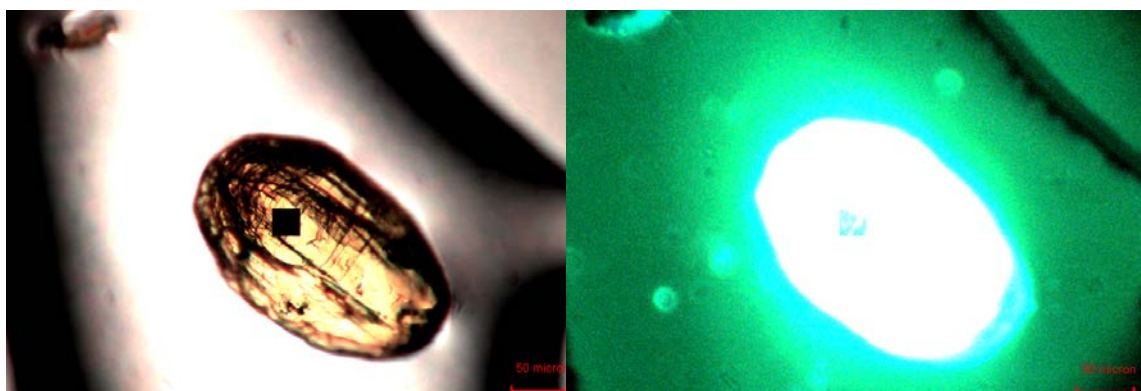


**Figure 21** Single crystal sample of  $\text{Th}(\text{H}_2\text{O})_7[\text{Pt}(\text{CN})_4]_2 \cdot 10\text{H}_2\text{O}$  (TH1), on the left the sample is viewed under a magnification of x10. The same single crystal sample is viewed on the right under a magnification of x10 and 365 nm excitation with the CRAIC microspectrophotometer.

As shown in Figure 21 the single crystal samples of TH1 are luminescent when excited with ultraviolet radiation. This was first observed on the bench top using a standard ultraviolet (UV) lamp (425 nm). The CRAIC microspectrophotometer now allows for a single crystal sample to be used for fluorescence and UV experiments. A single crystal sample can be mounted on a goniometer head to undergo a structural analysis via X-ray diffraction, with the same mounted crystal later placed on a sample slide for observation under the microspectrophotometer and then the Raman spectrophotometer. This experimental configuration allows for exact determination of

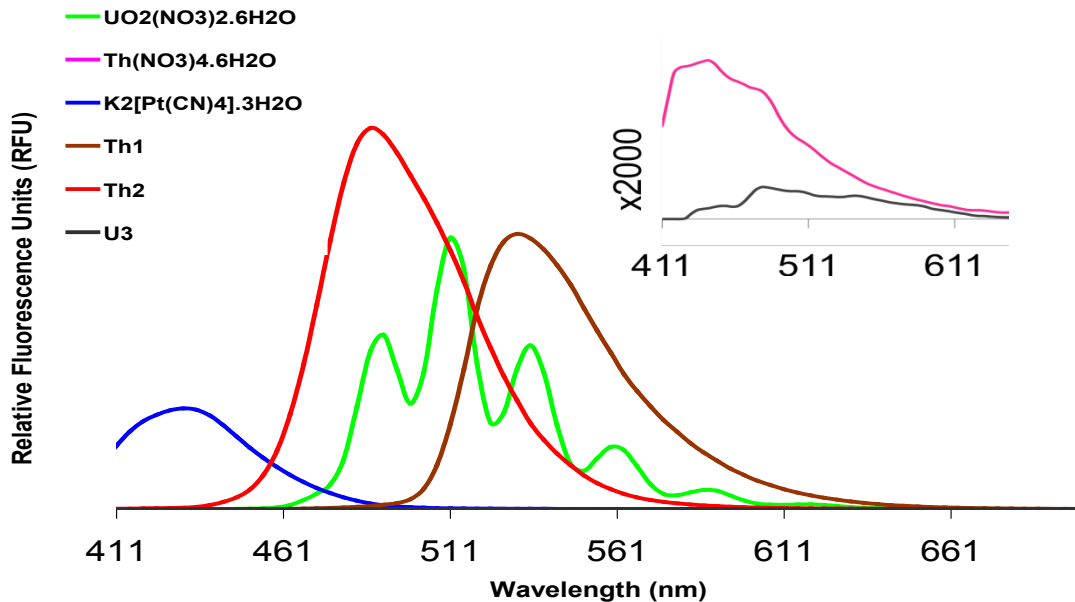


**Figure 22** Emission spectra of starting materials, **Th1**, **Th2** and **U3** excited at 400 nm. The emission of **U3** and thorium nitrate are so weak as to be at background levels, as seen by the inset in the upper right hand corner which is presented with a y-axis magnification of x2000.

the structural features and one to one correspondence with the observed spectral features.

### Thermo NanoDrop Fluorimeter

At first, the emission characterization was done on a Thermo NanoDrop Fluorimeter. The emission spectra of **Th1** ( $\text{Th}(\text{H}_2\text{O})_7[\text{Pt}(\text{CN})_4]_2 \cdot 10\text{H}_2\text{O}$ ), **Th2** ( $\text{Th}_2(\text{H}_2\text{O})_{10}(\text{OH})_2[\text{Pt}(\text{CN})_4]_3 \cdot 5\text{H}_2\text{O}$ ), **U3** ( $\text{K}_3[(\text{UO}_2)_2(\text{OH})(\text{Pt}(\text{CN})_4)_2]_2 \cdot \text{NO}_3 \cdot 1.5\text{H}_2\text{O}$ ) and starting materials ( $\text{K}_2[\text{Pt}(\text{CN})_4] \cdot 3\text{H}_2\text{O}$ ,  $\text{UO}_2(\text{NO}_3)_2 \cdot 6\text{H}_2\text{O}$  and  $\text{Th}(\text{NO}_3)_4 \cdot 6\text{H}_2\text{O}$ ) are shown in Figure 22. The emission of **U3** and the  $\text{Th}(\text{NO}_3)_4 \cdot 6\text{H}_2\text{O}$  are on the same order of magnitude as the background. The  $\text{UO}_2(\text{NO}_3)_2 \cdot 6\text{H}_2\text{O}$  emission spectrum is characteristic of that salt.<sup>1</sup> The emission of the  $\text{K}_2[\text{Pt}(\text{CN})_4] \cdot 3\text{H}_2\text{O}$  starting material shows a broad peak centered at 440 nm;<sup>2</sup> however, both **Th1** and **Th2** fluoresce further into the visible region. Both thorium compounds have broad-band emission, red shifted by about 40 nm for **Th1**

and 90 nm for **Th2**, relative to  $K_2[Pt(CN)_4] \cdot 3H_2O$ . Since  $Th^{4+}$  is a known non-emitting ion, we can assign the broad band emission from **Th1** and **Th2** as originating from the TCPt portions of the structures.<sup>3</sup> The dominant electronic form of thorium is the tetrapositive  $Th^{4+}$  species which contains a  $5f^0$  configuration.<sup>4</sup> All of the electrons are spin paired in this electronic state and emission is not expected. The broad emission features in both **Th1** and **Th2** are very unusual for a  $Th^{4+}$  complex and can be assigned to a charge transfer state within the tetracyanoplatinate ion since the  $Th^{4+}$  ion is non-fluorescent. On the other hand, the complete lack of observed emission in **U3** is rather intriguing since both of the starting materials,  $K_2[Pt(CN)_4] \cdot 3H_2O$  and  $UO_2(NO_3)_2 \cdot 6H_2O$ , have strong emission when excited at 400 nm.

### **Photon Technology International spectrometer**

The photoluminescence spectra were collected using a Photon Technology International spectrometer (model QM-7/SE). The system uses a high intensity xenon source for excitation. Selection of excitation and emission wavelengths are conducted by means of computer controlled, autocalibrated “QuadraScopic” monochromators and are equipped with aberration corrected emission and excitation optics. Signal detection is accomplished with a photomultiplier tube detector (Hamamatsu model 928) that can work either in analog or digital (photon counting) modes. The instrument operation, data collection, and handling were all controlled using the FeliX32 fluorescence spectroscopic package. UV-vis absorption data was acquired using a Craic Technologies 20/20 PV UV-visible microspectrophotometer. All of the spectroscopic experiments were conducted on neat crystalline samples held in sealed quartz capillary tubes at room temperature.

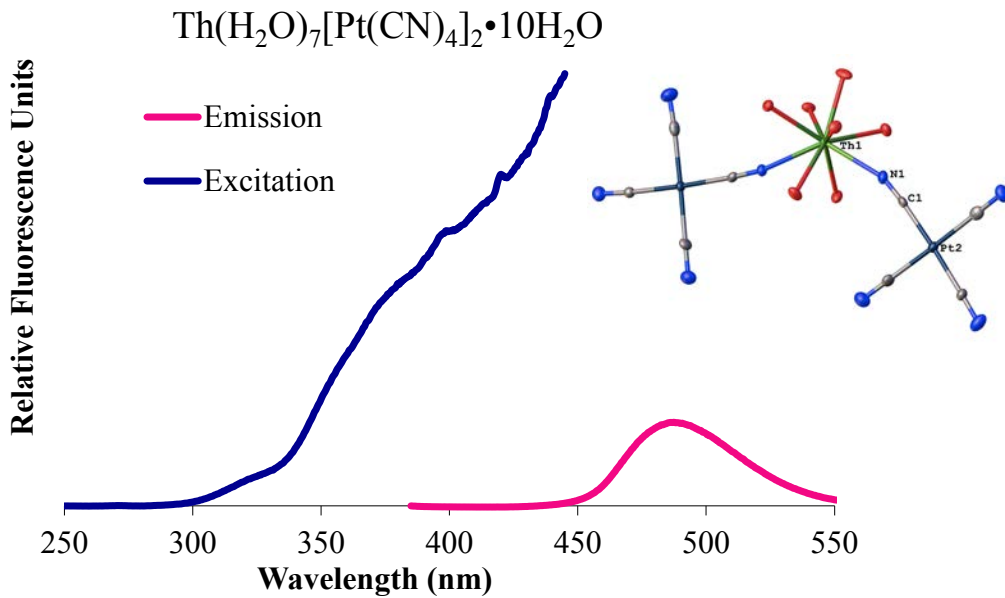


**Figure 23** Excitation spectrum of  $\text{Th}(\text{H}_2\text{O})_7[\text{Pt}(\text{CN})_4]_2 \cdot 10\text{H}_2\text{O}$  in blue was monitored at a wavelength of 487 nm and the emission spectrum in pink was excited at 370 nm.

To try to further extend our characterization of these actinide tetracyanoplatinate compounds, photoluminescence measurements were performed to give insight into the excitation species. **Th1** and **Th2** have the most compelling absorption/emission properties. An example of the contrast upon excitation of the neat, solid samples with ambient or 365 nm radiation is shown in Figure 21. The excitation spectra of  $\text{K}_2[\text{Pt}(\text{CN})_4] \cdot 3\text{H}_2\text{O}$  can be characterized by the large band at 385 nm which corresponds to a charge transfer state, on the TC $\text{Pt}$  anion, and the broadband emission feature at 425 nm is the relaxation of this excited charge transfer state.<sup>5</sup> Broad band excitation features are found in all three spectra; however, since it is known that the dominant form of thorium will be the  $\text{Th}^{4+}$  species, and thus, all electrons will be spin paired in the electronic ground state, the excitation spectrum does not originate from the  $\text{Th}^{4+}$  site.<sup>6</sup> This broad band excitation can be attributed to the charge transfer state on the  $[\text{Pt}(\text{CN})_4]^{2-}$

anion, which is what would be expected from the tetracyanoplatinate class of compounds featuring the Pt $\cdots$ Pt one-dimensional columns. Of note in a compound that contains a filled valence shell are the low energy features found at 400, 425 and 440 nm in the excitation spectrum of **Th1** (Figure 23). It is likely that these features can be attributed to vibronic coupling as only one electronic transition is reported for Th $^{4+}$  in this energy range, the 6d to 7s transition around 432 nm,<sup>6</sup> which does not match with these observed bands.

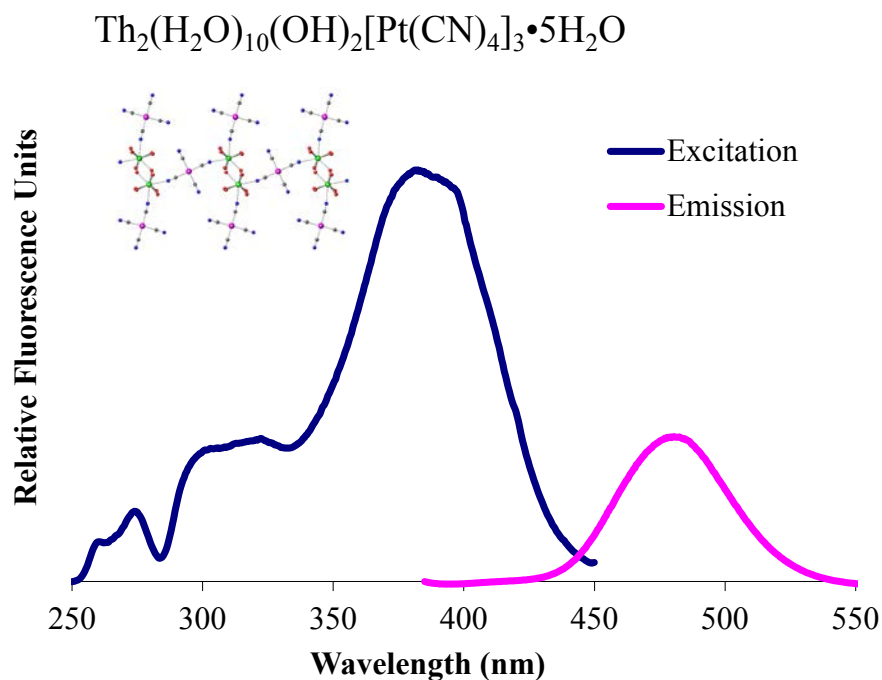


**Figure 24** Excitation spectrum of  $\text{Th}_2(\text{H}_2\text{O})_{10}(\text{OH})_2[\text{Pt}(\text{CN})_4]_3 \cdot 5\text{H}_2\text{O}$  in blue was monitored at a wavelength of 480 nm and the emission spectrum in red was excited at 370 nm.

A correlation has been described in previous works that the separation of the Pt sites in the pseudo one-dimensional chains directly corresponds to the emission wavelength.<sup>7</sup> It states that the shorter the distance, R, between the Pt $\cdots$ Pt sites within the

chain, the lower the energy emission. The **Th1** and **Th2** compounds appear to follow this trend. The shortest Pt···Pt spacings in **Th1** and **Th2** are 3.3515(2) and 3.272(2) Å respectively, with the  $\lambda_{\text{max}}$  of **Th2** red shifted by ~50 nm as compared to the  $\lambda_{\text{max}}$  of **Th1**,<sup>8</sup> however, since Th<sup>4+</sup> should not have excitation, and thus should not be emissive, the thorium sites of **Th1** and **Th2** seem to only function to adjust the Pt···Pt distance in these compounds. While there is a difference between the excitation profiles of the starting material, K<sub>2</sub>[Pt(CN)<sub>4</sub>]•3H<sub>2</sub>O, as compared to **Th1** and **Th2**, the emission profiles can be characterized as the same and resultant of the relaxation of the charge transfer state.

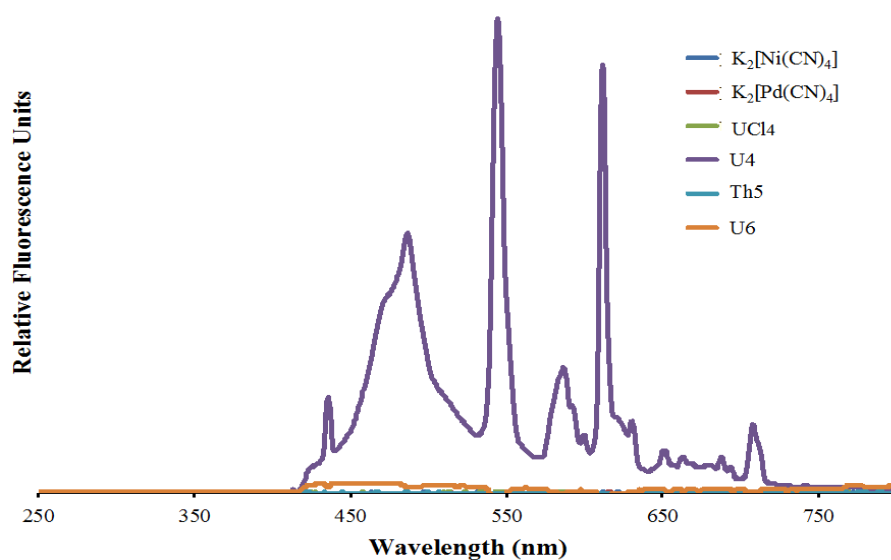


**Figure 25** Emission spectra of the K<sup>+</sup> salts of the d<sup>8</sup> tetracyanometallates and the complexes U4, Th5, and U6.

Spectral features are also observed in the emission spectra (Figure 25) of U4 at 435, 485, 544, 583, 611, and 707 nm. These features are weaker in intensity and sharper, as can be surmised with emission originating from the U(IV) site,<sup>9,10</sup> as opposed

to the charge transfer state on the TCPt anion that has broad intense emission features as seen in Figure 23, 24, and 25.

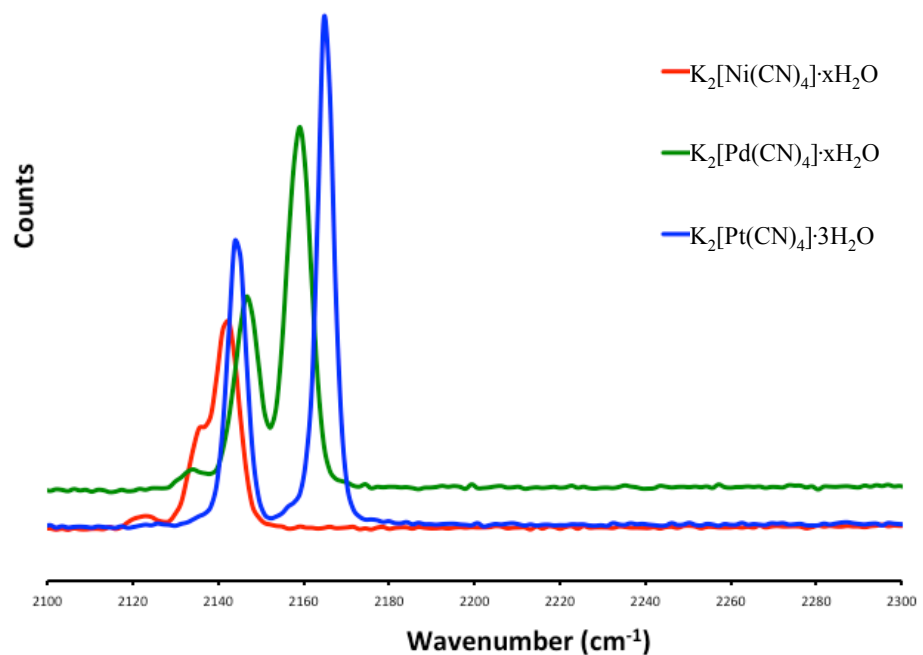


**Figure 26** Raman spectra of the  $\text{K}^+$  salts of the  $d^8$  tetracyanometallates in the  $\text{CN}^-$  stretching region.

## Raman Spectroscopy

The square planar tetracyanometallate anions are able to adopt several coordination modes (i.e. monodentate, trans- or cis-bridging, tri and even tetradentate

bridging) and uncoordinated tetracyanometallate anions can also be incorporated into the structure. For the simple potassium salts,  $A_{1g}$  and  $B_{1g}$  are the two CN vibrational modes expected in the cyanide stretching region between 2100 and 2300  $\text{cm}^{-1}$ . The  $A_{1g}$  is more intense and has a larger Raman shift as compared to the  $B_{1g}$ . Our values correlate well with data reported as seen in Table 5.<sup>11-13</sup> The assignment of the observed Raman shifts in our compounds is made easier if the square planar cyanometallates are considered as maintaining  $D_{4h}$  symmetry in the solid state. In this report, we have chosen to focus on the cyanide region.

Raman spectroscopy was performed using the 514 nm line (20 mW) from an air-cooled Argon ion laser (model 163-C42, Spectra-Physics Lasers, Inc.) as the excitation source. Raman spectra were collected and analyzed using a Renishaw inVia Raman microscope system. All of the spectroscopic experiments were conducted on neat crystalline samples held in sealed quartz capillary tubes at room temperature.

**Table 5** Vibrational modes of the  $d^8$  cyanometallate  $K^+$  salts given in  $\text{cm}^{-1}$ .

Assignment	$K_2[Ni(CN)_4] \cdot H_2O$	$K_2[Pd(CN)_4] \cdot H_2O$	$K_2[Pt(CN)_4] \cdot 3H_2O$
$v(CN)A_{1g}$	2132 (2132) <sup>13</sup>	2159 (2150) <sup>12</sup>	2164 (2168) <sup>11</sup>
$v(CN)B_{1g}$	2125 (2128) <sup>13</sup>	2146 (2139) <sup>12</sup>	2143 (2149) <sup>11</sup>

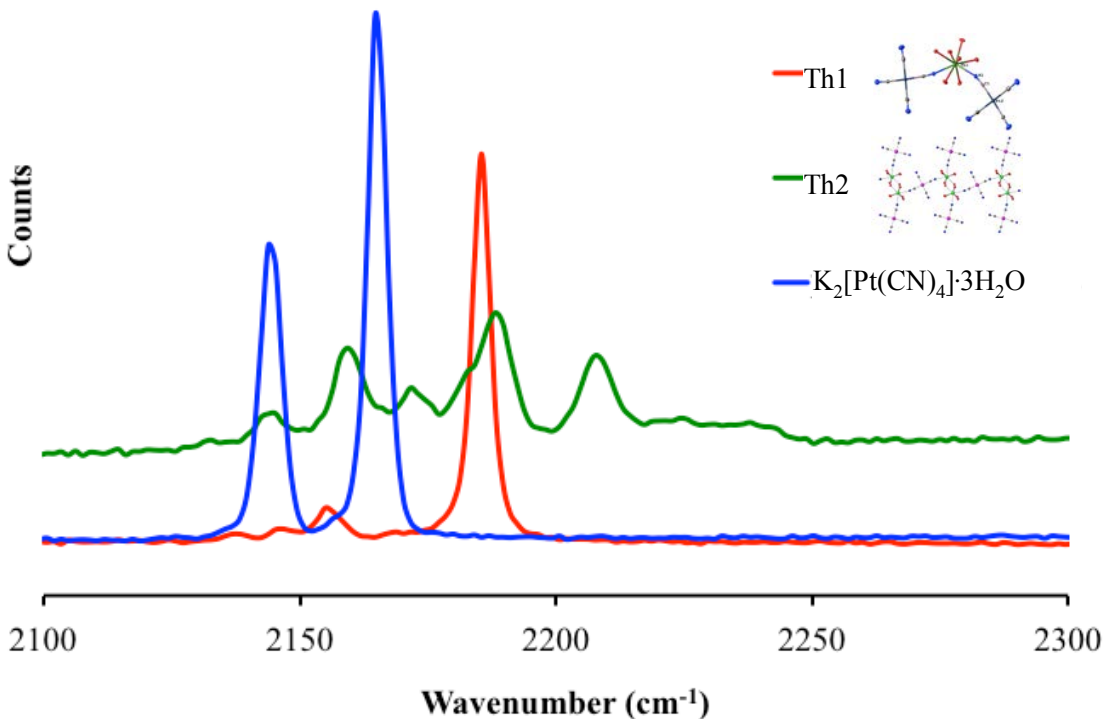


**Figure 27** Raman data of  $\text{Th}_x[\text{Pt}(\text{CN})_4]_y$  compounds and the  $\text{K}_2[\text{Pt}(\text{CN})_4]\cdot 3\text{H}_2\text{O}$  starting material.

Little has been reported previously about thorium compounds and identifiable features of Raman spectroscopy, and we wanted to further characterize these using the Raman features of these compounds. The compound  $\text{Th}(\text{H}_2\text{O})_7[\text{Pt}(\text{CN})_4]_2\cdot 10\text{H}_2\text{O}$  (**Th1**) has two unique cyanide environments. One cyanide environment is only coordinated to the Pt center and the other cyanide environment is coordinated to both the platinum and thorium metal center. As compared to the starting material, the peak height ratio of the  $A_{1g}$  and  $B_{1g}$  is altered, and the Raman shifts are larger. The  $B_{1g}$  band blue shifts  $\sim 13 \text{ cm}^{-1}$  while the  $A_{1g}$  band blue shifts  $\sim 20 \text{ cm}^{-1}$ . Although the Th-N bonds in the  $\text{Th}(\text{H}_2\text{O})_7[\text{Pt}(\text{CN})_4]_2\cdot 10\text{H}_2\text{O}$  compound, (2.552(5) and 2.571(4) Å) are longer than other reported Th-N bonds,<sup>14,15</sup> the blue shift in the  $A_{1g}$  and  $B_{1g}$  bands of Figure 27 indicate electron density withdrawal from the N lone pair.<sup>16,17</sup>

In the next thorium cyanoplatinate compound,  $\text{Th}_2(\text{H}_2\text{O})_{10}(\text{OH})_2[\text{Pt}(\text{CN})_4]_3 \bullet 5\text{H}_2\text{O}$  (**Th2**), there are two cyanide environments. One cyanide environment is coordinated to only the platinum center, while the other center is linked to both the platinum center and thorium center. This second environment is located trans to another such environment. As compared to  $\text{Th}(\text{H}_2\text{O})_7[\text{Pt}(\text{CN})_4]_2 \bullet 10\text{H}_2\text{O}$  (**Th1**), the  $\text{Th}_2(\text{H}_2\text{O})_{10}(\text{OH})_2[\text{Pt}(\text{CN})_4]_3 \bullet 5\text{H}_2\text{O}$  (**Th2**) Raman spectra have more features, and the features are blue shifted to a greater degree. The  $\text{B}_{1g}$  band appears at  $2160\text{ cm}^{-1}$ , this peak blue shifts roughly  $\sim 17\text{ cm}^{-1}$  as compared to the starting material,  $\text{K}_2[\text{Pt}(\text{CN})_4] \bullet 3\text{H}_2\text{O}$ . We believe the  $\text{A}_{1g}$  vibration has been blue shifted  $\sim 26\text{ cm}^{-1}$  in agreement with the notion that the  $\text{Th}^{4+}$  withdraws electron density from the N lone pair. Three other spectral bands are seen at roughly  $2145$ ,  $2173$ , and  $2209\text{ cm}^{-1}$  respectively.

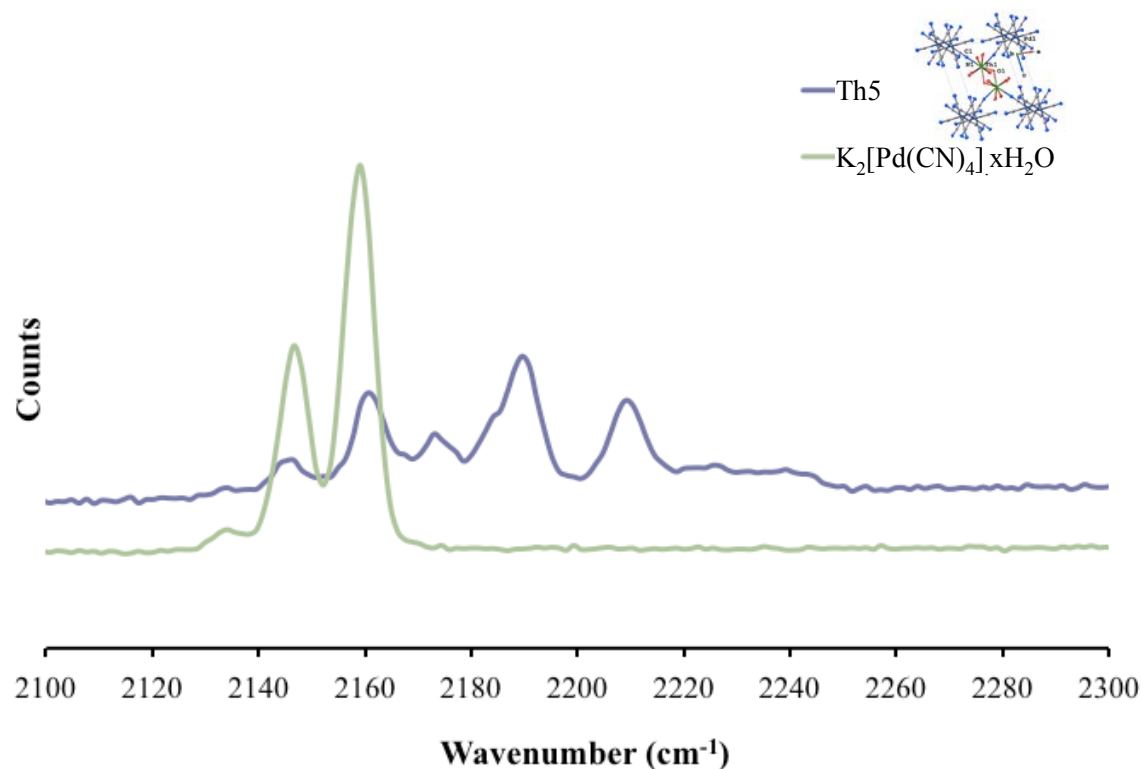


**Figure 28** Raman spectra of  $\text{Th}_2(\text{OH})_2(\text{H}_2\text{O})_{10}[\text{Pd}(\text{CN})_4]_3 \bullet 8\text{H}_2\text{O}$  and  $\text{K}_2[\text{Pd}(\text{CN})_4] \bullet x\text{H}_2\text{O}$ .

In the first Th[Pd(CN)<sub>4</sub>] structure reported, Th<sub>2</sub>(OH)<sub>2</sub>(H<sub>2</sub>O)<sub>10</sub>[Pd(CN)<sub>4</sub>]<sub>3</sub>•8H<sub>2</sub>O, like Th<sub>2</sub>(H<sub>2</sub>O)<sub>10</sub>(OH)<sub>2</sub>[Pt(CN)<sub>4</sub>]<sub>3</sub>•5H<sub>2</sub>O, there are two cyanide environments. One cyanide environment is coordinated to only the palladium center, while the other

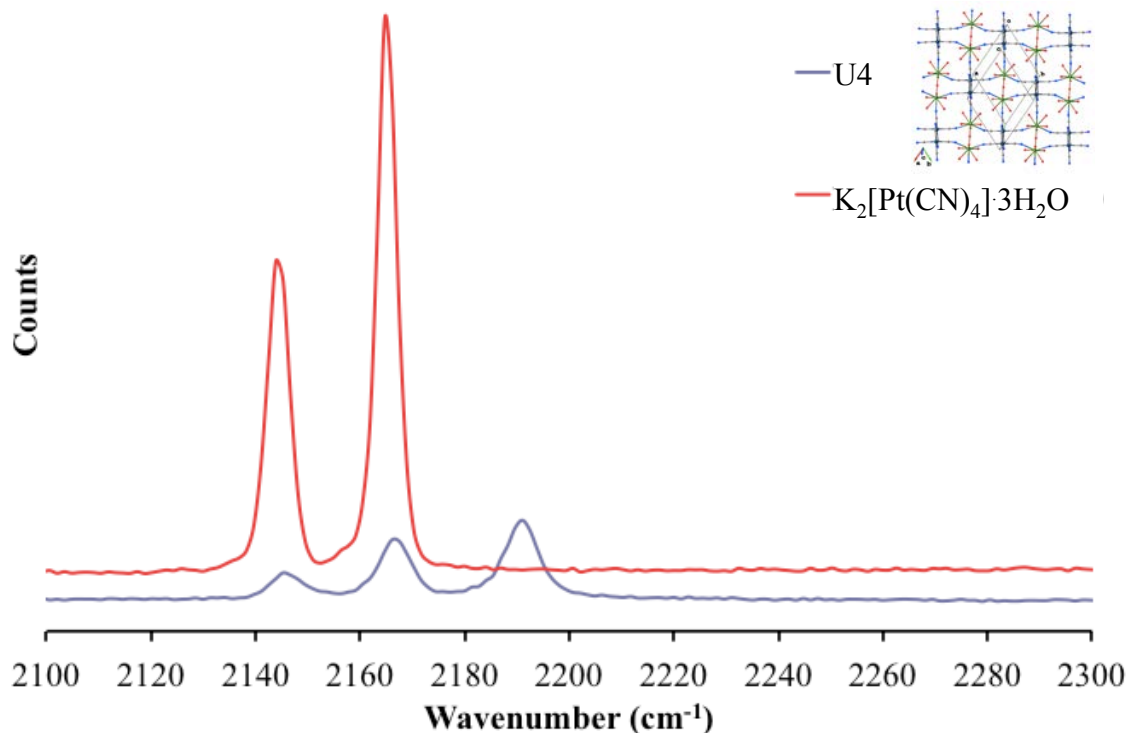


**Figure 29** Raman spectrum of  $\{U_2(H_2O)_{10}(O)\}[Pt(CN)_4]_3 \cdot 4H_2O$ .

environment is linked to both the palladium center and the thorium center. This second environment is located cis to another such environment. In good agreement with the Th<sub>2</sub>(H<sub>2</sub>O)<sub>10</sub>(OH)<sub>2</sub>[Pt(CN)<sub>4</sub>]<sub>3</sub>•5H<sub>2</sub>O compound a total of five spectral features are seen (Figure 28) with the same peak trends. The B<sub>1g</sub> band appears at 2162 cm<sup>-1</sup>, this peak blue shifts roughly ~16 cm<sup>-1</sup> as compared to the K<sub>2</sub>[Pt(CN)<sub>4</sub>] starting material. We believe the A<sub>1g</sub> vibration has been blue shifted ~32 cm<sup>-1</sup>, found at 2191 cm<sup>-1</sup>, and this would be in agreement with the notion that the Th<sup>4+</sup> withdraws electron density from the N lone pair. Three other spectral bands are seen at roughly 2147, 2174, and 2210 cm<sup>-1</sup>, respectively.

In the first U(IV)[Pt(CN)<sub>4</sub>] structure reported, ( $\{U_2(H_2O)_{10}(O)[Pt(CN)_4]_3\} \cdot 4H_2O$ ) (**U6**) there are three cyanide environments. The first cyanide environment is coordinated to only the platinum atom, the second cyanide environment is coordinated to both the platinum atom and the uranium (IV) center and is trans to another identical environment, and the third cyanide environment is coordinated to both the platinum and the uranium (IV) center and is trans to the cyanide environment coordinated to only the platinum metal.

### DFT Analysis

Electronic structure calculations were performed, to give insight into the vibrational frequencies resulting from the An-NC-M bonding interactions in these actinide cyanometallate compounds, using the unrestricted B3LYP hybrid density functional theory (DFT)<sup>18,19</sup> in the *Gaussian 09* code.<sup>20</sup> The Th and U were modeled with the Stuttgart relativistic effective core potential and basis set<sup>21-23</sup> with the C and H atoms modeled using a Pople style double- $\zeta$  6-31++G\* basis set with polarization function optimized for heavy atoms.<sup>24,25</sup> The proper  $f$  electron configurations, based on experimental results, were used for the appropriate ion. For calculations involving the Th<sup>4+</sup> and the UO<sub>2</sub><sup>2+</sup> ion this corresponds to a  $f^0$  electron configuration. For calculations involving the U<sup>4+</sup> ion a  $f^2$  electron configuration was employed. Calculations were carried out using the spin-unrestricted formalism with  $\alpha$  spins in excess of  $\beta$  spins. The simplest, full unit was assembled using the crystallographic information files from the reported Th1, Th2, U3, and U4 compounds.<sup>26,27</sup> It is important to note that the CIF files for structure Th1, Th2, U3, and U4 were manipulated and the calculated structure is a pruned version of the CIF file. These pruned versions of the molecules were used to

simplify the gas phase calculations. For example the U4 structure contains a U(IV) center coordinated by 8 water molecules and a single nitrogen from a tetracyanoplatinate anion as compared to the solid state structure that is coordinated by 6 water molecules and 3 nitrogens from 3 tetracyanoplatinate anions. Using the lowest calculated energy from different multiplicities a geometry optimization was performed to alleviate any solid state crystallographic strain in the molecule.

**Table 6** Single point energy calculations performed using the unrestricted B3LYP functional in Gaussian09 revB.01. Energy given in Hartree-Fock units.

Job	Multiplicity	E (HF)	ΔE (HF)
Th1	1	-2688.102335	0.000000
Th1	3	-2688.044021	-0.000778712
Th1	5	-2687.945887	-4.979E-09
Th1	7	-2687.629621	0.000307
Th1	9	-2757.039314	-2.24973E-06
U(Th1)	1	-2757.262479	-4.00424E-05
U(Th1)	3	-2757.327569	-0.000074
U(Th1)	5	-2757.318271	-0.000030
U(Th1)	7	-2757.219955	-1.65928E-06
U1(Th1)	9	-2757.039314	-0.000002
Th2	1	-3586.11963	-2.32893E-06
Th2	3	-3585.775907	-2.8973E-06
Th2	5	-3585.726351	-3.22697E-06

Th2	7	-3585.581883	1.12344E-07
Th2	9	-3585.412239	-0.000004
U(Th2)	1	-3724.119042	-0.000216
U(Th2)	3	-3585.775907	-6.94523E-07
U(Th2)	5	-3585.726452	-0.000014
U(Th2)	7	-3585.581837	0.000002
U(Th2)	9	-3585.412239	-0.000003
U3	1	-1500.363653	-2.60991E-06
U3	3	-1500.332201	-0.000002
U3	5	-1500.211464	-4.00184E-06
U3	7	-1500.030710	-9.11421E-07
U3	9	-1499.797249	-0.000012
U4	1	-1578.415620	-0.000062
U4	3	-1578.495487	-0.000002
U4	5	-1578.490605	-0.000006
U4	7	-1578.334771	-0.000050
U4	9	-1578.132857	-0.000002
Th(U4)	1	-1509.244857	-3.9408E-08
Th(U4)	3	-1509.217155	-6.00242E-07
Th(U4)	5	-1509.073826	-9.28127E-06
Th(U4)	7	-1508.856842	-4.39347E-07

Th(U4)	9	-1508.639400	-0.000215098
--------	---	--------------	--------------

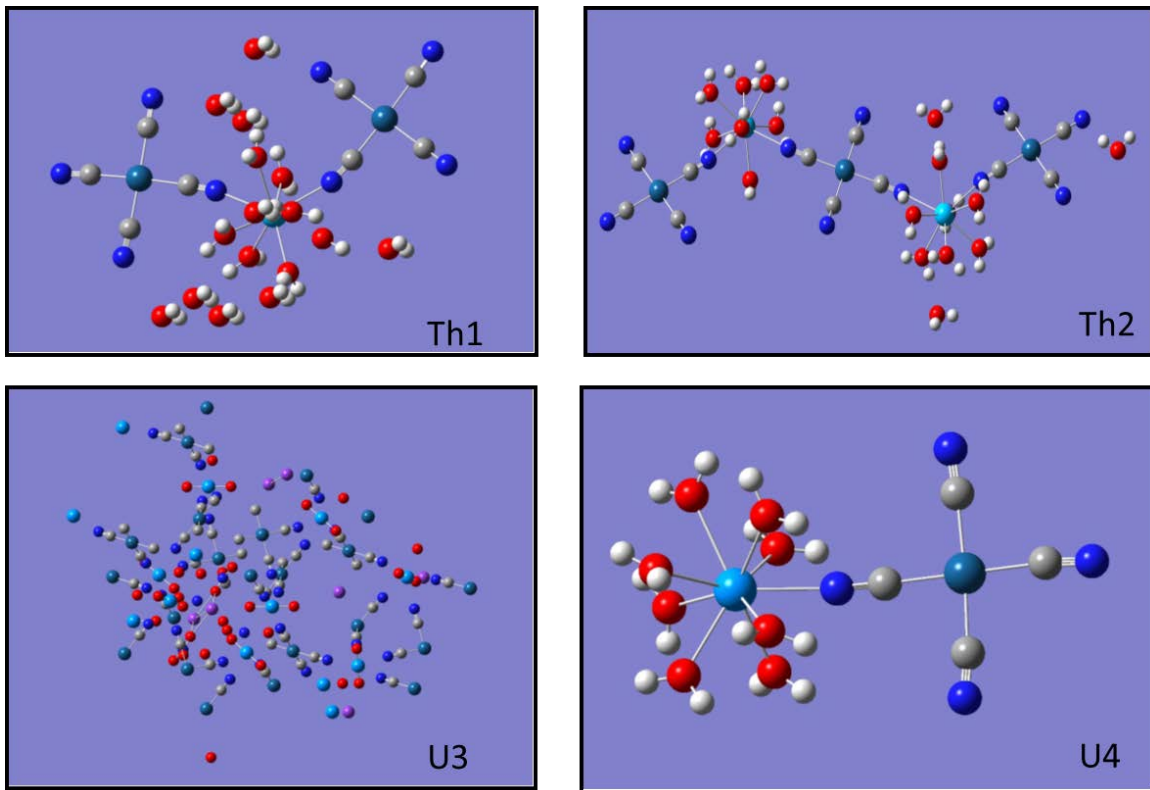


**Figure 30** Projections of the atom positions from jobs run in Gaussian. The crystallographic information files were used as a starting point for atom positions.

## Discussion

### Emission

An earlier paper reports (Capelin 1970) the luminescent detection of metal ions including the limit of detection, 20 ppm, for the  $\text{Th}^{4+}$  metal ion.<sup>28</sup> The mode of characterization is described as ultraviolet examination with the emission characterization results for the white  $\text{Th}^{4+}$  precipitate given as green. The precipitate is formed under

basic conditions by the addition of NH<sub>3</sub>. The ThTCPt compounds that we reported formed greenish-yellow crystals, and when irradiated with UV light gave a green emission (Figure 21). We attempted to grow ThTCPt crystals at higher pH, but the formation of Th(OH)<sub>4</sub> prevented this. For these reasons, we do not believe that the compounds we reported and the compounds from this much earlier report are the same.<sup>28</sup>

The lack of intense charge transfer emission in both the uranyl compound previously characterized, K<sub>3</sub>[(UO<sub>2</sub>)<sub>2</sub>(OH)(Pt(CN)<sub>4</sub>)<sub>2</sub>]<sub>2</sub>•NO<sub>3</sub>•1.5H<sub>2</sub>O (**U3**),<sup>8</sup> and the U(IV) compound reported here, {U<sub>2</sub>(H<sub>2</sub>O)<sub>10</sub>(O)[Pt(CN)<sub>4</sub>]<sub>3</sub>}•4H<sub>2</sub>O (**U4**), is curious. The pseudo one-dimensional Pt···Pt chains are not present in **U3**, only dimeric interactions are found at 3.2214(15) Å. Both the K<sub>2</sub>[Pt(CN)<sub>4</sub>]•3H<sub>2</sub>O and UO<sub>2</sub>(NO<sub>3</sub>)<sub>2</sub>•6H<sub>2</sub>O starting materials emit in the visible range, and it is odd that the product of these two materials is not emissive. Because **U3** lacks the long range Pt···Pt interactions, the lack of intense charge transfer emission seen from **U4** may be of more interest as it contains the pseudo one-dimension chains with R spacings of 3.266(1) and 3.493(1) Å. Further, any electronic energy transfer quenching should be forbidden as the TCPt does not change its multiplicity upon going from the ground state to the lowest excited state.<sup>29</sup>

The lack of emission in **Th5** and **U6** is expected. The Pd···Pd pseudo one-dimensional structural feature is not linked to the same metal-to-ligand charge transfer visible emission as its 5d Pt···Pt counterpart. The formation of pseudo one dimensional Ni···Ni interactions in the covalently bound TCNi class of compounds does not appear previously in the literature. However these structural interactions do exist in the ionic compounds with longer Ni...Ni interactions found at 3.567(2), 3.804(1), and 3.733(1) for the strontium, rubidium, and sodium [Ni(CN)<sub>4</sub>]<sup>2-</sup> salts.<sup>30</sup> The inclusion of DMSO may

play a role in the lack of Ni $\cdots$ Ni interactions, but it is not solely responsible. The lack of these interactions is probably due to the smaller, harder nature of the 3d Ni atom as compared to the larger, softer nature of the corresponding 4d and 5d Pd and Pt atoms.

### Raman Spectroscopy

Table 7

Compound		B <sub>1g</sub>		A <sub>1g</sub>		Mode
Th(H <sub>2</sub> O) <sub>7</sub> [Pt(CN) <sub>4</sub> ] <sub>2</sub> •10H <sub>2</sub> O	2146vw	2156w		2185s		monodentate
Th <sub>2</sub> (H <sub>2</sub> O) <sub>10</sub> (OH) <sub>2</sub> [Pt(CN) <sub>4</sub> ] <sub>3</sub> •5H <sub>2</sub> O	2141w	2160m	2173w	2189m	2209m	bidentate
K <sub>3</sub> [(UO <sub>2</sub> ) <sub>2</sub> (OH)(Pt(CN) <sub>4</sub> ) <sub>2</sub> ] <sub>2</sub> •NO <sub>3</sub> •1.5H <sub>2</sub> O		2143s		2164s		tetridentate
{U <sub>2</sub> (H <sub>2</sub> O) <sub>10</sub> (O)[Pt(CN) <sub>4</sub> ]} <sub>3</sub> •4H <sub>2</sub> O	2146w	2167m		2191s		uncoordinated tridentate
{Th <sub>2</sub> (OH) <sub>2</sub> (H <sub>2</sub> O) <sub>10</sub> [Pd(CN) <sub>4</sub> ] <sub>3</sub> }•8H <sub>2</sub> O	2142w	2161m	2174w	2189s	2210m	uncoordinated bidentate
{(UO <sub>2</sub> ) <sub>2</sub> (DMSO) <sub>4</sub> (OH) <sub>2</sub> [Ni(CN) <sub>4</sub> ]}		2138w		2161m		bidentate

Few reports exist with Raman spectroscopy and structural data to accompany it involving TCNi interested in the mode of bridging of the TCNi anion.<sup>31-35</sup> Within these reports, only one structure is characterized as a cis or trans bridging structure<sup>31</sup>, and the rest involve the square planar TCNi that is either unbound or all nitrogens bind a metal and the D<sub>4h</sub> symmetry is roughly preserved. In all of these reports, only a single A<sub>1g</sub> and B<sub>1g</sub> vibration are reported in the cyanide region. We report all the peaks present in the vCN region of the Raman spectra and believe they correlate to the mode of binding of the d<sup>8</sup> tetracyanometallate, thus originating from the binding of the actinide metal. To our knowledge, there are no single crystal structural reports containing covalently bound metals to TCPd or TCPt with Raman data to accompany it, making comparing assignments with other work a moot point. This is not to say that structural elucidation of the tetracyanometallate ions, and their ionic complexes, have not been reported previously, or that Raman spectroscopy has not been performed in separate reports.<sup>11-13</sup>

However, the blue shift of the Raman bands does correlate well with other cyanide bridged 4f and 5f and transition metal complexes.<sup>16,17</sup>

At first glance, the different actinide metal ions ( $\text{Th}^{4+}$ , U(IV), and  $\text{UO}_2^{\text{VI}}$ ) appear to affect the cyanide region of the Raman data in different ways. The  $\text{UO}_2^{2+}$  has little to no effect on shifting the vibrational modes in the cyanide region. When a  $[\text{Pt}(\text{CN})_4]^{2-}$  coordinates to a tetra positive uranium site, the cyanide region of the Raman spectrum displays a peak at  $2192 \text{ cm}^{-1}$ , roughly  $28 \text{ cm}^{-1}$  higher in energy than the  $A_{1g}$  vibration in the starting material. The largest difference occurs when a tetracyanometallate anion coordinates to a thorium. This is most likely a structural restriction, but this is hard to confirm, as an isostructural series has not as yet been characterized. In the three compounds containing U, as either  $\text{UO}_2^{2+}$  or  $\text{U}^{4+}$ , there are not any structural trends that correspond with the features seen in the Raman spectra. This makes the spectral features hard to elucidate.

Upon closer inspection, it seems that it is the binding modes, (uncoordinated, mono- bi- tri- and tetradentate) in which the tetracyanometallate anions are incorporated, that are responsible for the spectrum in the cyanide region. A monodentate tetracyanometallate, found in  $\text{Th}(\text{H}_2\text{O})_7[\text{Pt}(\text{CN})_4]_2 \bullet 10\text{H}_2\text{O}$ , gives rise to three peaks, the two typical  $A_{1g}$  and  $B_{1g}$  peaks are still observed, but a significant third vibration also appears at lower frequency. When the tetracyanometallate coordinates the tetra positive thorium metal in a bridging, cis or trans, fashion as in,  $\text{Th}_2(\text{H}_2\text{O})_{10}(\text{OH})_2[\text{Pt}(\text{CN})_4]_3 \bullet 5\text{H}_2\text{O}$  and  $\{\text{Th}_2(\text{H}_2\text{O})_{10}(\text{OH})_2[\text{Pd}(\text{CN})_4]_3\} \bullet 8\text{H}_2\text{O}$ , five peaks are seen in the cyanide region of the spectrum. Again, the typical  $A_{1g}$  and  $B_{1g}$  vibrations are found, but three other vibrations are observed at lower frequency. The tridentate bridging species

$\{U_2(H_2O)_{10}(O)[Pt(CN)_4]_3\} \cdot 4H_2O$  gives three vibrations in the cyanide stretching region, again the  $A_{1g}$  and  $B_{1g}$  vibrations similar to the potassium salt are found, but a third vibration is found at lower frequency.

In the compounds containing  $Th^{4+}$ , the similarity of the Raman features in the  $Th_2(H_2O)_{10}(OH)_2[Pt(CN)_4]_3 \cdot 5H_2O$  and  $Th_2(OH)_2(H_2O)_{10}[Pd(CN)_4]_3 \cdot 8H_2O$  structures is remarkable. In the spectrum of each, there are five spectral features. Assigning the first two spectral features to the  $B_{1g}$  and  $A_{1g}$  vibrations, respectively, would indicate backbonding from the Th metal. Instead, the  $B_{1g}$  and  $A_{1g}$  vibrations are assigned to more blue shifted spectral features in accordance with a bound metal withdrawing electron density form the N lone pair. The same spectral features are not observed in the  $Th(H_2O)_7[Pt(CN)_4]_2 \cdot 10H_2O$  compound (**Th1**). One possible explanation for this is the bridging features of the cyanometallate anion observed in the compounds. In both the  $Th_2(H_2O)_{10}(OH)_2[Pt(CN)_4]_3 \cdot 5H_2O$  (**Th2**) and  $Th_2(OH)_2(H_2O)_{10}[Pd(CN)_4]_3 \cdot 8H_2O$  (**Th5**) structures, the cyanometallates coordinate the  $Th^{4+}$  centers in a bidentate bridging fashion and five spectral features are observed in the vCN region. This is in contrast to the  $Th(H_2O)_7[Pt(CN)_4]_2 \cdot 10H_2O$  (**Th1**) structure in which the coordinating cyanometallate only binds in a monodentate fashion and three spectral features are observed in the vCN region.

The tetradentate species found in  $K_3[(UO_2)_2(OH)(Pt(CN)_4)_2]_2 \cdot NO_3 \cdot 1.5H_2O$  shows only the  $A_{1g}$  and  $B_{1g}$  vibrations. Interesting is that the bridging cyanometallate species in  $\{(UO_2)_2(DMSO)_4(OH)_2[Ni(CN)_4]\}$  show a similar spectrum as  $K_2[Ni(CN)_4] \cdot xH_2O$ , but the  $A_{1g}$  and  $B_{1g}$  vibrations are at lower frequency. The  $v1$   $(UO_2)^{2+}$  symmetric stretching vibration is observed at  $826\text{ cm}^{-1}$  and correlates well with

previous reports.<sup>36,37</sup> A weakness in characterizing these compounds by Raman spectroscopy alone is if the solid state structure contains more than one type of tetracyanometallate binding. With Raman data alone in the cyanide region of the spectrum you could only classify the tetracyanometallate mode of binding as tetradentate, monodentate-tridentate, and bidentate.

## Computational Analysis

In the tetracyanoplatinate free anion the  $A_{1g}$  vibration corresponds to all four cyanide groups stretching and compressing in phase. The  $B_{1g}$  corresponds to two trans cyanide groups stretching while the other two trans cyanide groups are compressing. Experimental data has shown that there are two stretches in the CN region that correspond to the  $A_{1g}$  ( $2164\text{ cm}^{-1}_{\text{exp}}, 2225\text{ cm}^{-1}_{\text{cal}}$ ) and  $B_{1g}$  ( $2143\text{ cm}^{-1}_{\text{exp}}, 2202.05\text{ cm}^{-1}_{\text{cal}}$ ) vibrational modes in the square planar tetracyanoplatinate molecule. The difference between the experimental and calculated  $A_{1g}$  and  $B_{1g}$  vibrational frequencies seem to correlate ( $A_{1g}-B_{1g\text{exp}}=21\text{ cm}^{-1}$ , and  $A_{1g}-B_{1g\text{cal}}=23\text{ cm}^{-1}$ ). When the symmetry of the free tetracyanoplatinate anion is disturbed by binding a  $5f$  center, more spectral features are observed in the experimental data. This can be visualized if each individual cyanide bond has its own environment. As seen in Table 8 additional vibrational modes are calculated when the smallest whole unit is used. The smallest whole unit is different than the crystallographic asymmetric unit as symmetry operations are not considered. Because the  $D_{4h}$  symmetry is broken with the binding of an actinide metal, confirmed by the structural elucidation in chapter 2, this computational data aligns with the observed

experimental data. Additional support is given by the calculation of the lone, uncoordinated tetracyanoplatinate anion giving only two vibrations.

**Table 8** Vibrational modes calculated by the unrestricted B3LYP functional.

	Frequency	Raman Activity		Frequency	Raman Activity		Frequency	Raman Activity
U4	2103.74	101759.0311	Th1	2177.27	1534.8014	U(Th1)	2151.37	53458.0379
	2222.04	2599.8266		2191.58	426.6418		2164.68	420128.9835
	2527.76	9165.9218		2206.36	37.671		2311.63	10164.5883
	2585.19	13900.2591		2207.63	447.2925		2356.1	40649.9583
Th(U4)	2036.35	23747.7646		2216.27	1431.607	U(Th1)	2387.14	7106.9728
	2352.23	17668.2092		2224.88	939.9632		2455.58	6568.2785
	2572.09	16816.6473		2244.67	1115.5023		2462.23	372429.9
	2634.19	25849.0315		2245.95	2597.1117			

## Conclusions

A thorough characterization of the actinide cyanometallates has been presented here. In general, the An[CM] class of compounds synthesized and structurally characterized during the course of research represents the first time these type of complexes with the 5f elements have been reported in the literature.<sup>26,27</sup> Solid state characterization illustrates the structural novelty of this class of compounds. The most outstanding example of this is the Th-NC bond found in **Th1**, **Th2**, **Th5**, and **Th8** represent the total known Th-NC linkages in the Cambridge Crystallographic Database.<sup>38</sup> Also interesting are the oxygen (hydroxyl and oxo) bridging species observed in **Th2**, **U4**, **Th5**, and **U6** are not observed in the analogous 4f, Ln[CM] literature.<sup>39-42</sup>

Further experimental techniques were employed to investigate the electronics of these An[CN] compounds. Of note, only the thorium containing compounds (**Th1** and **Th2**) gave observable emission in the visible region of the spectra.<sup>27</sup> Again, this is an interesting aspect of these compounds as the Th<sup>4+</sup> has a completely empty O electron shell, thus no electrons are able to be excited and subsequent emission should not be observed (CATE Vol. 1, pg 59).<sup>6</sup> It is important to note that this research does not make the claim that the emission from **Th1** and **Th2** originates from the thorium sites. Instead, the broad band in the excitation spectra of these compounds is attributed to the ligand to metal charge transfer band from the cyanide groups bound to the platinum atoms.<sup>5</sup> The packing structure of these compounds in the solid state leads to the observed differences in emission between **Th1** and **Th2**. The observed Pt···Pt distances in **Th1** are 3.371 and 3.351 Å, and a single Pt···Pt distance is observed in **Th2** at 3.272 Å. The Pt···Pt distances in **Th1** and **Th2** differ by roughly 0.010 Å and, correspondingly, the  $\lambda_{\max}$  of **Th2** is red shifted by ~50 nm as compared to the  $\lambda_{\max}$  of **Th1**. Effectively, the thorium atoms are placeholders, they directly affect the Pt···Pt spacings in these two compounds, which results in the difference of observed emission in the solid state.<sup>8</sup> While there is a difference between the excitation profiles of the starting material, K<sub>2</sub>[Pt(CN)<sub>4</sub>]•3H<sub>2</sub>O, as compared to **Th1** and **Th2**, the emission profiles can be characterized as the same feature and resultant of the relaxation of the charge transfer state.

The lack of observable intense charge transfer bands in the uranyl, **U3**, containing compound and the U(IV), **U4**, containing compound is confounding at first. Upon looking at the solid state structural features of **U3** it is apparent that only dimeric Pt···Pt interactions found at 3.2214(15) Å are observed. Effectively, the lack of overlap from

“infinite”  $d_z^2$  orbitals in the Pt...Pt chains quenches the emission from metal to ligand charge transfer bands seen in Th1, Th2, and other previously reported tetracyanoplatinate compounds. The lack of intense charge transfer emission seen from **U4** may be of more interest as it contains the pseudo one-dimension chains with R spacings of 3.266(1) and 3.493(1) Å. Any electronic energy transfer quenching should be forbidden, because the TCPt does not change its multiplicity upon going from the ground state to the lowest excited state.<sup>29</sup> The lack of emission in **Th5**, **U6**, **Th7**, and **Th8** is expected as the actinide metal centers have an empty O electronic shell.<sup>6</sup> The Pd···Pd pseudo one-dimensional structural feature is not linked in the literature to the same metal-to-ligand charge transfer visible emission as its 5d Pt···Pt counterpart.<sup>43</sup> When a covalent bond is formed between a cyanide group of a tetracyanonickelate and another metal the formation of pseudo one dimensional Ni···Ni interactions in the TCNi class of compounds has not been observed previously in the literature. The inclusion of DMSO may play a role in the lack of Ni···Ni interactions in U6 and the lack of Pt...Pt interactions in **Th7**, but it is not solely responsible. The lack of these interactions is probably due to the smaller, harder nature of the 3d Ni atom as compared to the larger, softer nature of the corresponding 4d and 5d Pd and Pt atoms. The octahedral molecular structure of the hexacyanoferrate anion forbids packing interaction of Fe···Fe atoms.

Vibrational spectra of the actinide cyanometallates were observed with a confocal Raman Microscope. For the simple potassium tetracyanoplatinate salt, the A<sub>1g</sub> and B<sub>1g</sub> are the two CN vibrational modes expected in the cyanide stretching region between 2100 and 2300 cm<sup>-1</sup>. The cyanide region of the spectrum provides the most information regarding the solid state structure of these compounds. Previous reports of other

cyanometallates<sup>31-35</sup> only reported two stretches in this region. In our spectra, we were able to observe multiple stretches in this cyanide region.

It seems that it is the binding modes, (uncoordinated, mono- bi- tri- and tetradentate) in which the tetracyanometallate anion is incorporated, that are responsible for distinct changes in the spectrum in the cyanide region. A monodentate tetracyanometallate, found in  $\text{Th}(\text{H}_2\text{O})_7[\text{Pt}(\text{CN})_4]_2 \cdot 10\text{H}_2\text{O}$ , gives rise to three peaks, the two typical  $A_{1g}$  and  $B_{1g}$  peaks are still observed, but a significant third vibration also appears at lower frequency.<sup>26</sup> When the tetracyanometallate coordinates the tetra positive thorium metal in a bridging, cis or trans, fashion as in,  $\text{Th}_2(\text{H}_2\text{O})_{10}(\text{OH})_2[\text{Pt}(\text{CN})_4]_3 \cdot 5\text{H}_2\text{O}$  and  $\{\text{Th}_2(\text{H}_2\text{O})_{10}(\text{OH})_2[\text{Pd}(\text{CN})_4]_3\} \cdot 8\text{H}_2\text{O}$ , five peaks are seen in the cyanide region of the spectrum. Again, the typical  $A_{1g}$  and  $B_{1g}$  vibrations are found, but three other vibrations are observed at lower frequency. The tridentate bridging species  $\{\text{U}_2(\text{H}_2\text{O})_{10}(\text{O})[\text{Pt}(\text{CN})_4]_3\} \cdot 4\text{H}_2\text{O}$  gives three vibrations in the cyanide stretching region, again the  $A_{1g}$  and  $B_{1g}$  vibrations similar to the potassium salt are found, but a third vibration is found at lower frequency.

Of note in the compounds containing  $\text{Th}^{4+}$  are the similarity of the Raman features in the  $\text{Th}_2(\text{H}_2\text{O})_{10}(\text{OH})_2[\text{Pt}(\text{CN})_4]_3 \cdot 5\text{H}_2\text{O}$  and  $\text{Th}_2(\text{OH})_2(\text{H}_2\text{O})_{10}[\text{Pd}(\text{CN})_4]_3 \cdot 8\text{H}_2\text{O}$  structures. In the spectrum of each, there are five spectral features. Assigning the first two spectral features to the  $B_{1g}$  and  $A_{1g}$  vibrations, respectively, would indicate backbonding from the Th metal. Instead, the  $B_{1g}$  and  $A_{1g}$  vibrations are assigned to more blue shifted spectral features in accordance with a bound metal withdrawing electron density form the N lone pair. The same spectral features are not observed in the  $\text{Th}(\text{H}_2\text{O})_7[\text{Pt}(\text{CN})_4]_2 \cdot 10\text{H}_2\text{O}$  compound (**Th1**). One possible explanation for this is the

bridging features of the cyanometallate anion observed in the compounds. In both the  $\text{Th}_2(\text{H}_2\text{O})_{10}(\text{OH})_2[\text{Pt}(\text{CN})_4]_3 \cdot 5\text{H}_2\text{O}$  (**Th2**) and  $\text{Th}_2(\text{H}_2\text{O})_{10}[\text{Pd}(\text{CN})_4]_3 \cdot 8\text{H}_2\text{O}$  (**Th5**) structures, the cyanometallates coordinate the  $\text{Th}^{4+}$  centers in a bidentate bridging fashion and five spectral features are observed in the vCN region. This is in contrast to the  $\text{Th}(\text{H}_2\text{O})_7[\text{Pt}(\text{CN})_4]_2 \cdot 10\text{H}_2\text{O}$  (**Th1**) structure in which the coordinating cyanometallate only binds in a monodentate fashion and three spectral features are observed in the vCN region.

The tetradentate species found in  $\text{K}_3[(\text{UO}_2)_2(\text{OH})(\text{Pt}(\text{CN})_4)_2]_2 \cdot \text{NO}_3 \cdot 1.5\text{H}_2\text{O}$  shows only the  $A_{1g}$  and  $B_{1g}$  vibrations. Interesting is that the bridging cyanometallate species in  $\{(\text{UO}_2)_2(\text{DMSO})_4(\text{OH})_2[\text{Ni}(\text{CN})_4]\}$  show a similar spectrum as  $\text{K}_2[\text{Ni}(\text{CN})_4] \cdot x\text{H}_2\text{O}$ , but the  $A_{1g}$  and  $B_{1g}$  vibrations are at lower frequency. The  $v1$   $(\text{UO}_2)^{2+}$  symmetric stretching vibration is observed at  $826\text{ cm}^{-1}$  and correlates well with previous reports.<sup>36,37</sup> A weakness in characterizing these compounds by Raman spectroscopy alone is if the solid state structure contains more than one type of tetracyanometallate binding. With Raman data alone in the cyanide region of the spectrum, you could only classify the tetracyanometallate mode of binding as tetradentate-anionic, monodentate-tridentate, and bidentate.

The computational analysis of the compounds was done using DFT methods with the unrestricted B3LYP hybrid functional. In the actinide cyanometallates, the interesting structural features that give rise to the observed electronic properties, arise from the long-range packing interactions of the  $\text{Pt}\cdots\text{Pt}$  interactions. This is unfortunate because defining enough heavy atoms in a calculation was computationally time consuming and not practically possible to be carried out during my time at Los Alamos National

Laboratory. What was able to be calculated were the Raman vibrations of the simplest actinide cyanometallates. These calculations involved the appropriate actinide unit, including the oxo bridged species, and the full metal cyanides coordinating these units along with the coordinated and uncoordinated solvent molecules. The coordinates of the atoms for these calculations were directly taken from the crystallographic information files of the appropriate compounds (Th1, Th2, U3, U4, Th5 U6). These computational analysis provided insight into the growth of vibrational bands in the Raman spectrum. Additional bands were seen in the calculated structures as compared to the experimental work. Each of these bands seen in the calculated vibrational spectra corresponds to a breaking of the idealized  $D_{4h}$  symmetry square planar geometry of the anions. It can be clearly seen in the crystallographic description that the symmetry is broken, however, neither earlier reports nor our experimental work were able to observe all of the bands predicted by the calculations.

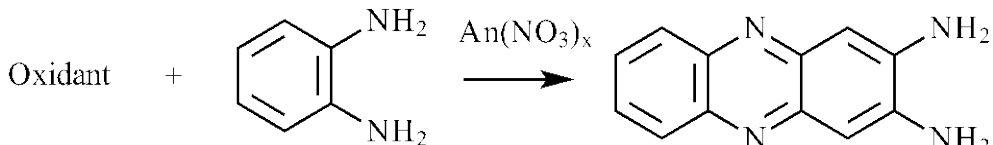
## References Cited

- (1) Pant, D. D.; Khandelwal, D. P.; Bist, H. D. *Curr. Sci.* **1959**, *28*, 483.
- (2) Baril-Robert, F.; Guo, Z.; Patterson, H. H. *Chem. Phys. Lett.* **2009**, *471*, 258.
- (3) Gliemann, G.; Yersin, H. *Struct. Bond.* **1985**, *62*, 87.
- (4) *The Chemistry of the Actinide and Transuranic Elements*; 3rd ed.; Morss, L.; Edelstein; Fuger, J.; Katz, J. J., Eds.; Springer: Dordrecht, The Netherlands, 2006.
- (5) Cowman, C. D.; Gray, H. B. *Inorg. Chem.* **1976**, *15*, 2823.
- (6) Morss, L.; Edelstein, N. M.; Fuger, J. *The Chemistry of the Actinide and Transactinide Elements* Springer, 2006; Vol. 1.
- (7) Loosli, A.; Wermuth, M.; Guedel, H.-U.; Capelli, S.; Hauser, J.; Buergi, H.-B. *Inorg. Chem.* **2000**, *39*, 2289.
- (8) Maynard, B. A.; Sykora, R. E.; Mague, J. T.; Gorden, A. E. *Chem Commun (Camb)* **2010**, *46*, 4944.
- (9) Simoni, E.; Hubert, S.; Genet, M. *J. Phys. (Paris)* **1988**, *49*, 1425.
- (10) Godbole, S. V.; Page, A. G.; Sangeeta; Sabharwal, S. C.; Gesland, J. Y.; Sastry, M. D. *J. Lumin.* **2001**, *93*, 213.
- (11) Benner, R. E.; Von, R. K. U.; Lee, K. C.; Owen, J. F.; Chang, R. K.; Laube, B. L. *Chem. Phys. Lett.* **1983**, *96*, 65.
- (12) Gans, P.; Gill, J. B.; Johnson, L. H. *J. Chem. Soc. Dalton.* **1993**, 345.
- (13) McCullough, R. L.; Jones, L. H.; Crosby, G. A. *Spectrochim. Acta* **1960**, *16*, 929.
- (14) Pool, J. A.; Scott, B. L.; Kiplinger, J. L. *Chem. Commun. (Cambridge, U. K.)* **2005**, 2591.
- (15) Schelter, E. J.; Morris, D. E.; Scott, B. L.; Kiplinger, J. L. *Chem. Commun. (Cambridge, U. K.)* **2007**, 1029.
- (16) Assefa, Z.; Haire, R. G.; Sykora, R. E. *J. Solid State Chem.* **2008**, *181*, 382.
- (17) Assefa, Z.; Kalachnikova, K.; Haire, R. G.; Sykora, R. E. *J. Solid State Chem.* **2007**, *180*, 3121.
- (18) Becke, A. D. *J. Chem. Phys.* **1993**, *98*, 5648.

- (19) Lee, C.; Yang, W.; Parr, R. G. *Phys. Rev. B: Condens. Matter* **1988**, *37*, 785.
- (20) Frisch, M. J.; Trucks, G. W.; Schlegel, H. B.; Scuseria, G. E.; Robb, M. A.; Cheeseman, J. R.; Scalmani, G.; Barone, V.; Mennucci, B.; Petersson, G. A.; Nakatsuji, H.; Caricato, M.; Li, X.; Hratchian, H. P.; Izmaylov, A. F.; Bloino, J.; Zheng, G.; Sonnenberg, J. L.; Hada, M.; Ehara, M.; Toyota, K.; Fukuda, R.; Hasegawa, J.; Ishida, M.; Nakajima, T.; Honda, Y.; Kitao, O.; Nakai, H.; Vreven, T.; Montgomery, J. A., Jr.; Peralta, J. E.; Ogliaro, F.; Bearpark, M.; Heyd, J. J.; Brothers, E.; Kudin, K. N.; Staroverov, V. N.; Kobayashi, R.; Normand, J.; Raghavachari, K.; Rendell, A.; Burant, J. C.; Iyengar, S. S.; Tomasi, J.; Cossi, M.; Rega, N.; Millam, N. J.; Klene, M.; Knox, J. E.; Cross, J. B.; Bakken, V.; Adamo, C.; Jaramillo, J.; Gomperts, R.; Stratmann, R. E.; Yazyev, O. A.; A. J.; Cammi, R.; Pomelli, C.; Ochterski, J. W.; Martin, R. L.; Morokuma, K.; Zakrzewski, V. G.; Voth, G. A.; Salvador, P.; Dannenberg, J. J.; Dapprich, S.; Daniels, A. D.; Farkas, Ö.; Foresman, J. B.; Ortiz, J. V.; Cioslowski, J.; Fox, D. J. 2009.
- (21) Feller, D. *J. Comput. Chem.* **1996**, *17*, 1571.
- (22) Kuechle, W.; Dolg, M.; Stoll, H.; Preuss, H. *Mol. Phys.* **1991**, *74*, 1245.
- (23) Schuchardt, K. L.; Didier, B. T.; Elsethagen, T.; Sun, L.; Gurumoorthi, V.; Chase, J.; Li, J.; Windus, T. L. *J. Chem. Inf. Model.* **2007**, *47*, 1045.
- (24) Petersson, G. A.; Bennett, A.; Tensfeldt, T. G.; Al-Laham, M. A.; Shirley, W. A.; Mantzaris, J. *J. Chem. Phys.* **1988**, *89*, 2193.
- (25) Petersson, G. A.; Al-Laham, M. A. *J. Chem. Phys.* **1991**, *94*, 6081.
- (26) Maynard, B. A.; Lynn, K. S.; Sykora, R. E.; Gorden, A. E. V. *Inorg. Chem.* **2013**, *52*, 4880.
- (27) Maynard, B. A.; Sykora, R. E.; Mague, J. T.; Gorden, A. E. V. *Chem. Commun. (Cambridge, U. K.)* **2010**, *46*, 4944.
- (28) Capelin, B. C.; Ingram, G. *Talanta* **1970**, *17*, 187.
- (29) Matsushi.R; Fujimori, H.; Sakuraba, S. *J. Chem. Soc. Farad. T 1* **1974**, *70*, 1702.
- (30) Fronczek, F. R.; Delord, T. J.; Watkins, S. F.; Gueorguieva, P.; Stanley, G. G.; Zizza, A. S.; Cornelius, J. B.; Mantz, Y. A.; Musselman, R. L. *Inorg. Chem.* **2003**, *42*, 7026.
- (31) Kuerkcueoglu, G. S.; Hoekelek, T.; Aksel, M.; Yesilel, O. Z.; Dal, H. J. *Inorg. Organomet. Polym. Mater.* **2011**, *21*, 602.

- (32) Kurkcuoglu, G. S.; Yesilel, O. Z.; Kavlak, I.; Buyukgungor, O. *Struct. Chem.* **2008**, *19*, 879.
- (33) Agusti, G.; Cobo, S.; Gaspar, A. B.; Molnar, G.; Moussa, N. O.; Szilagyi, P. A.; Palfi, V.; Vieu, C.; Munoz, M. C.; Real, J. A.; Bousseksou, A. *Chem. Mater.* **2008**, *20*, 6721.
- (34) Lemus-Santana, A. A.; Rodriguez-Hernandez, J.; del, C. L. F.; Basterrechea, M.; Reguera, E. *J. Solid State Chem.* **2009**, *182*, 757.
- (35) Kurkcuoglu, G. S.; Yesilel, O. Z.; Cayli, I.; Buyukgungor, O. *J. Mol. Struct.* **2011**, *994*, 39.
- (36) Frost, R. L.; Cejka, J.; Weier, M. L.; Martens, W. *J. Raman Spectrosc.* **2006**, *37*, 538.
- (37) Frost, R. L.; Cejka, J.; Dickfos, M. J. *J. Raman Spectrosc.* **2009**, *40*, 38.
- (38) Cambridge Structural Database, Actinide Structure Search Published Online: 2012, (Accessed 04-13-2012).
- (39) Maynard, B. A.; Smith, P. A.; Ladner, L.; Jaleel, A.; Beedoe, N.; Crawford, C.; Assefa, Z.; Sykora, R. E. *Inorg. Chem.* **2009**, *48*, 6425.
- (40) Maynard, B. A.; Smith, P. A.; Sykora, R. E. *Acta Crystallogr., Sect. E: Struct. Rep. Online* **2009**, *65*, m1132.
- (41) Maynard, B. A.; Kalachnikova, K.; Whitehead, K.; Assefa, Z.; Sykora, R. E. *Inorg. Chem.* **2008**, *47*, 1895.
- (42) Maynard, B. A.; Sykora, R. E. *Acta Crystallogr., Sect. E: Struct. Rep. Online* **2008**, *64*, m138.
- (43) Stojanovic, M.; Robinson, N. J.; Assefa, Z.; Sykora, R. E. *Inorg. Chim. Acta* **2011**, *376*, 414.

## Chapter 4: Synergistic Thorium Mediated Synthesis of 2,3-diaminophenazine



**Scheme 1** Oxidation of ortho-phenylenediamine to 2,3-diaminophenazine.

In the last decade, reports detailing metal mediated synthetic methods<sup>1-4</sup> or catalysis<sup>5-8</sup> incorporating the use of actinide metals have become more common. The focal point of this research is typically an actinide metal center saddled with sterically hindered ligands (such as cyclopentadiene, pentamethylcyclopentadienyl,<sup>7,9</sup> and N-ethylmethylamine).<sup>7,9</sup> Ultimately, the ligand and the metal are bound covalently, to some degree, and the electronics of these ligand-actinide complexes and their subsequent reactivity have not been clearly explained.<sup>7,9</sup>

The heterocycle 2,3-diaminophenazine is thought to play a role in iron-sequestration in some bacteria, and is of interest for the self-assembly of nanobelts and “green” fluorescence sensitive assays.<sup>10</sup> 2,3-diaminophenazine is produced *via*  $H_2O_2$  catalysis by horseradish peroxidase and fungal laccase enzymes;<sup>11</sup> non-biological synthetic pathways are known including catalysis by Cu(II) and Fe(III).<sup>10,12,13</sup> We wanted to observe the metal mediation of the unencumbered actinide cations. Here, we report the thorium nitrate, uranyl nitrate, and oxygen mediated synthesis of 2,3-diaminophenazine.

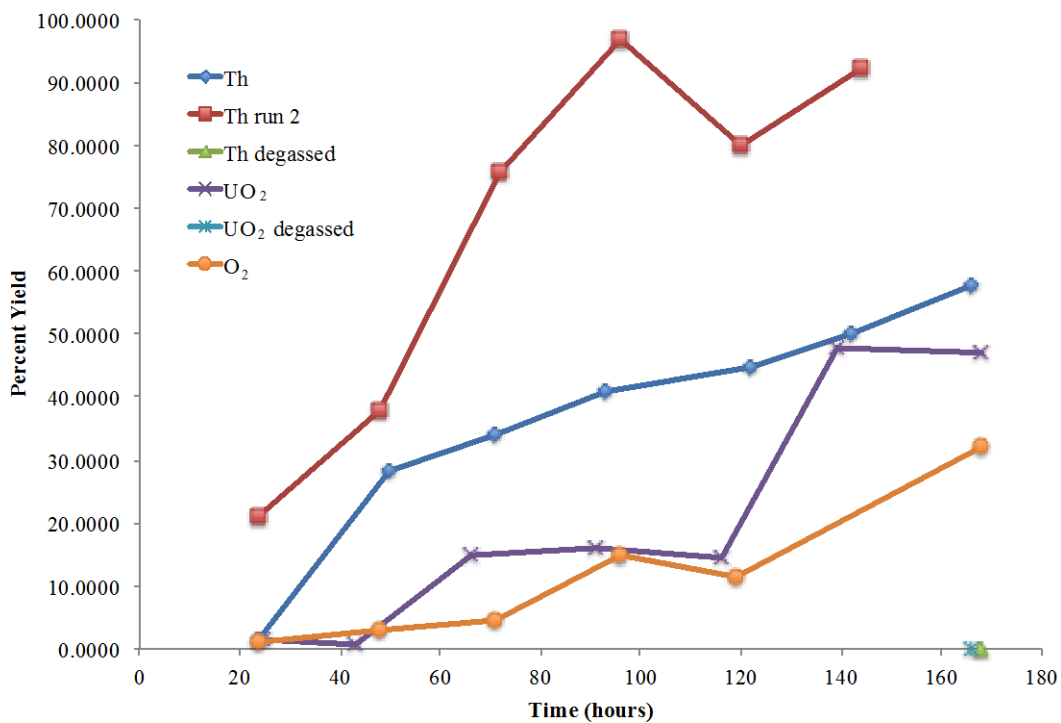


**Figure 31** Chart depicting the data from table 1.

As seen in Figure 31, dioxygen alone oxidizes ortho-phenylenediamine to 2,3-diaminophenazine. Figure 31 also shows that incorporating the simple actinide nitrate salts [Th(NO<sub>3</sub>)<sub>4</sub> and UO<sub>2</sub>(NO<sub>3</sub>)<sub>4</sub>] enhances the oxidation of *ortho*-diaminobenzene to 2,3-diaminophenazine in the presence of dioxygen. While this oxidation occurs at order of magnitudes slower than the simple FeCl<sub>3</sub> salt,<sup>10</sup> we wanted to investigate this oxidation reaction because simple, sterically unencumbered actinide centers are not unusual. The results of the actinide containing reactions are of interest. It is evident that the addition of actinide ions (Th<sup>+4</sup> and UO<sub>2</sub><sup>2+</sup>) to the aqueous solution provide metal mediation for the oxidative generation of 2,3-diaminophenazine. Increasing the Th<sup>+4</sup> concentration by a factor of 2 increases the formation of the 2,3-diaminophenazine product as seen in Figure

31 (Th and Th run 2). This data appears to indicate that including the actinide ( $\text{Th}^{+4}$  or  $\text{UO}_2^{+2}$ ) ions in the presence of dioxygen examples a synergistic behavior, as the sum of the “ $\text{O}_2$ ” and degassed “actinide salt” reactions are less than the isolated product in the “ $\text{Th}^{+4} + \text{O}_2$ ” reaction alone.

To better understand the influence of dioxygen in the mechanism of the oxidation reaction, two reactions were set up to run seven days; the first reaction Schlenk flask was degassed to remove as much dioxygen as possible and contained  $\text{Th}(\text{NO}_3)_4$  as the actinide source, the second reaction Schlenk flask was also degassed to remove as much dioxygen as possible and contained  $\text{UO}_2(\text{NO}_3)_2$  as the actinide source. After 7 days, no observable precipitate was present in the reaction flask containing  $\text{Th}^{+4}$ , and the solution appeared to be the same color as at time 0. No phenazine was detected. The reaction flask with  $\text{UO}_2^{+2}$  as the actinide source was found to contain 0.0230 grams of isolable 2,3-diaminophenazine. This result appears to indicate that in the presence of oxygen, in the form of terminal oxo's of the uranyl subunit, are needed for the oxidation to occur and that the oxo's from the actinyl units may also be a useful oxygen source in this reaction pathway.<sup>9</sup>

A third reaction was started to determine whether oxygen was important in the role of the reaction scheme. A Schlenk flask was set up with only a stir bar in an aqueous solution of *ortho*-phenylenediamine. Argon was bubbled through the solution for two hours, and then put through three cycles of freeze-pump-thaw in an effort to remove all possible traces of  $\text{O}_2$ . Two reaction attempts have been made to rid the Schlenk flask of  $\text{O}_2$ , in both instances a 25% yield of 2,3-diaminophenazine has been observed. If these results are found to remain accurate it would give evidence that any

oxygen donor will mediate the reaction as this reaction would require the oxygen from H<sub>2</sub>O to serve as the oxidant. Interestingly, as this reaction contained only H<sub>2</sub>O and *ortho*-phenylenediamine, a literature search was unable to find any information on the temperature induced oxidation of *ortho*-phenylenediamine in an inert atmosphere.

Previous reports in the literature of phenazines prepared in this fashion feature metals that are able to go through one electron oxidations (Cu(II)<sup>13</sup> and Co(II)<sup>14</sup>) and proposed mechanisms have involved  $\mu$ -dioxygen with hydrogen peroxide evolution. This mechanism would be highly unlikely, for either the Th<sup>+4</sup> or the UO<sub>2</sub><sup>+2</sup> ions, as both metal centers contain complete electronic shells K, L, M and N; also neither ion possess paired or unpaired electrons in the O shell.<sup>15</sup> Further observation of the data in the chart of Figure 31 may give some insight into how the reaction proceeds. If the data were examined then the trace of the Th<sup>+4</sup> (exponential) as compared to the trace of the UO<sub>2</sub><sup>+2</sup> (stepwise) data appear to follow different paths. This may be rationalized if the reaction proceeds in two different pathways.

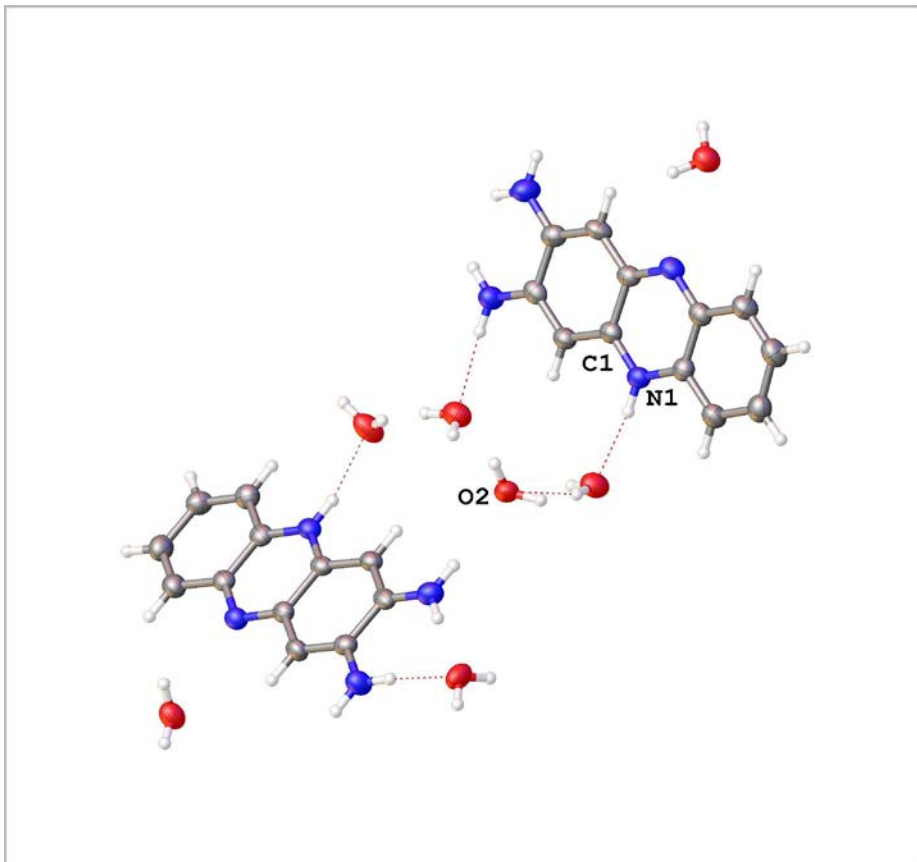


**Figure 32** Projection of the asymmetric unit of  $(C_{12}H_{10}N_4)_2 \bullet 7H_2O$ .

Single crystals of X-ray diffraction quality 2,3-diaminophenazine were grown directly from the reaction flasks. After a reaction had been heated, it was set aside undisturbed to cool for two days. While the structure of 2,3-diaminophenazine is known, this structure crystal structure  $(C_{12}H_{10}N_4)_2 \bullet 7H_2O$  differs from other known reports by the number of waters of hydration in the lattice as can be seen in figure 32. As would be expected,  $\pi \cdots \pi$  stacking interactions are found at 3.838 Å. Also interesting in the crystal structure is the seven member ring formed by the hydrogen bonding of the terminal amine groups and a water of hydration. This may give some insight into how the mechanism of the reaction proceeds.

## Conclusions

Fundamentally, these observations engage the idea of using the depleted actinide reserve, especially depleted  $^{238}\text{U}$ , as a source for new routes of metal mediation. In future research we plan to monitor these reactions using a UV-vis spectrometer to more precisely document the concentrations of both the *ortho*-phenylenediamine starting material and the 2,3-diaminophenazine product. We plan on investigating the electronic role of these actinide centers,  $\text{UO}_2^{2+}$  and  $\text{Th}^{4+}$ , and also if the  $\text{Np}^{5+}$  and  $\text{PuO}_2^{2+}$  can mediate this reaction. It would be very unlikely that these actinide ions go through one electron oxidations that have been proposed for other metal centers as this would lead to removal of a single electron from a filled shell. If these metal units go though one electron oxidations or reductions then a signal would be evident from the corresponding unpaired electron in an electron paramagnetic resonance experiment. It is tough to argue that incorporating actinide ions into reaction pathways can result in green chemistry following the principles established by Anastas and Warner. Yet, these reaction conditions do abide by several principles of green chemistry including: mild reaction conditions, safer solvents, and catalysis.

## Synthesis

Typical Reaction: 0.0040 moles of *ortho*-phenylenediamine was heated at 80° C in a 100 ml round bottom flask charged with a stir bar and 100 ml of deionized  $\text{H}_2\text{O}$ . When the o-phenylenediamine dissolved the appropriate volume of a stock actinide starting material solution was added to the mixture to allow a 1:100 stoichiometric ratio. The reaction was

allowed to stir and heat at 80° C for the duration of the experiment. When the experiment time had lapsed; the solution was filtered, the solid was washed with hexanes, and dried in a vacuum oven. The dried material was then scraped from the filter paper and weighed. Mass spectrometry analysis was performed on the dried material and a mass of 211.0961 ( $M+1$ ) was obtained.

**Table 9** Experiments were run with Th(NO<sub>3</sub>)<sub>4</sub> and UO<sub>2</sub>(NO<sub>3</sub>)<sub>2</sub> as the metal mediator. Ortho-phenylenediamine has been abbreviated OPD. 2,3-diaminophenazine has been abbreviated DAP.

	Temp	Time	OPD mmol	Th(NO <sub>3</sub> ) <sub>4</sub> mmol	UO <sub>2</sub> (NO <sub>3</sub> ) <sub>2</sub> mmol	DAP mmol	% yield	DAP/Metal mmol ratio
Th	80	24	3.997	0.03953		0.03223	1.613	101.1
	80	50	4.005	0.03973		0.56730	28.33	100.8
	80	71	4.002	0.03953		0.68057	34.01	101.2
	80	93	4.003	0.03973		0.81754	40.85	100.8
	80	122	4.005	0.03953		0.89242	44.57	101.3
	80	142	3.991	0.04128		0.99763	49.99	96.68
	80	166	4.003	0.04109		1.15261	57.59	97.43
	80	24	8.597	0.08973		0.91137	21.20	95.82
	80	48	8.580	0.09070		1.62085	37.78	94.60
	80	72	8.591	0.09070		3.25687	75.81	94.72
	80	96	8.495	0.08857		4.11991	96.99	95.91
	80	120	8.550	0.09244		3.41517	79.88	92.49
	80	144	8.537	0.08857		3.92986	92.06	96.39
	Th Degassed	80	168	3.990	0.04070	Trace Amount		98.04
UO <sub>2</sub>	80	25	3.949		0.03953	0.02844	1.440	99.90
	80	43	3.949		0.03953	0.01137	0.5761	99.90
	80	66	3.949		0.03953	0.29147	14.76	99.90
	80	91	3.949		0.03953	0.31659	16.034	99.90

	80	116	3.949		0.03953	0.28531	14.45	99.90	
	80	139	3.949		0.03953	0.94550	47.89	99.90	
	80	168	3.949		0.03953	0.92891	47.05	99.90	
UO <sub>2</sub> Degassed	80	166	3.990		0.03952	0.10284	5.155	100.0	
No Metal	80	24	3.987			0.02275	1.141		
	80	48	3.987			0.06019	3.019		
	80	71	3.987			0.08768	4.400		
	80	96	3.987			0.29573	14.83		
	80	119	3.987			0.22749	11.41		
	80	168	3.987			0.64218	32.21		
Degassed	80	165	3.989			0.49905	25.02		

## References Cited

- (1) Schelter, E. J.; Morris, D. E.; Scott, B. L.; Kiplinger, J. L. *Chem. Commun. (Cambridge, U. K.)* **2007**, 1029.
- (2) Weiss, C. J.; Marks, T. J. *Dalton Trans.* **2010**, 39, 6576.
- (3) Weiss, C. J.; Wobser, S. D.; Marks, T. J. *Organometallics* **2010**, 29, 6308.
- (4) Kiplinger, J. L.; Pool, J. A.; Schelter, E. J.; Thompson, J. D.; Scott, B. L.; Morris, D. E. *Angew. Chem., Int. Ed.* **2006**, 45, 2036.
- (5) Hayes, C. E.; Platel, R. H.; Schafer, L. L.; Leznoff, D. B. *Organometallics* **2012**, 31, 6732.
- (6) Wobser, S. D.; Marks, T. J. *Organometallics* **2013**, 32, 2517.
- (7) Barnea, E.; Moradove, D.; Berthet, J.-C.; Ephritikhine, M.; Eisen, M. S. *Organometallics* **2006**, 25, 320.
- (8) Stubbert, B. D.; Marks, T. J. *J. Am. Chem. Soc.* **2007**, 129, 4253.
- (9) Andrea, T.; Barnea, E.; Eisen, M. S. *J. Am. Chem. Soc.* **2008**, 130, 2454.
- (10) He, D.; Wu, Y.; Xu, B.-Q. *Eur. Polym. J.* **2007**, 43, 3703.
- (11) Zhou, P.; Liu, H.; Chen, S.; Lucia, L.; Zhan, H.; Fu, S. *Molbank* **2011**, M730.
- (12) Nemeth, S.; Simandi, L. I.; Argay, G.; Kalman, A. *Inorg. Chim. Acta* **1989**, 166, 31.
- (13) Peng, S. M.; Liaw, D. S. *Inorg. Chim. Acta* **1986**, 113, L11.
- (14) Rosso, N. D.; Szpoganicz, B.; Martell, A. E. *Inorg. Chim. Acta* **1999**, 287, 193.
- (15) Morss, L.; Edelstein, N. M.; Fuger, J. *The Chemistry of the Actinide and Transactinide Elements* Springer, **2006**; Vol. 1.

## Chapter 5: Synthesis, Isolation, Structural Characterization and Emission Spectroscopy of Salzine Compounds

One new 2-(1H-imidazo[4,5-b] phenazin-2-yl)phenol (salzine) derivative has been synthesized and the structural elucidation of three novel solid state structures are reported in this chapter. The salzine class of molecules were reported first in 2011 with the several different substituents on the benzene ring (X= H, CH<sub>3</sub>O, CH<sub>2</sub>OH, Br, and Cl).<sup>1</sup> In this report only the synthesis *via* a Mn<sup>III</sup> mediated reaction and the solution phase UV and fluorescence spectra were reported. These salzine derivatives offer the common five atom ligand geometry (N-C-C-C-O) found in chapter 1 to bind actinide atoms and have solid state structural characterization.<sup>2</sup>

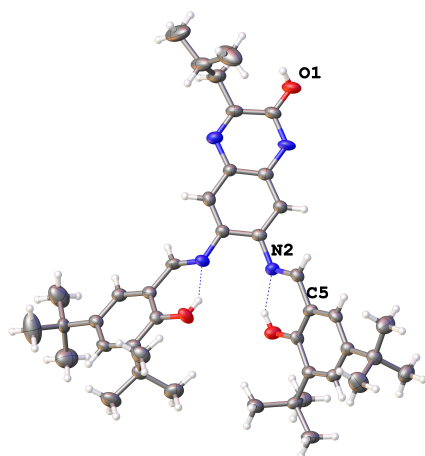


**Figure 33** Projection of the 2-quinoxalinol salen molecule. Atoms as shown are labeled: H in white, O in red, N in blue, and C in grey.

The 2-quinoxolinol salen ligand (salqu) was first synthesized in the Gorden group in 2007, and this report included the synthesis of the ligand and other related ligands.<sup>3</sup> This ligand system contains two (N-C-C-C-O) structural motifs per molecule. Yet, only structures with a bound uranyl ion have been reported with this 2-quinoxalinol salen ligand system. Until now, the free 2-quinoxalinol salen ligand has only been characterized in the solution phase. The quinoxolinol salen ligand features an (O-N-N-O) tetradentate binding pocket, as shown in Figure 33, which can be used in metal coordination. The O32-N3 distance is 2.596(4), the N3-N2 distance is 2.737(6), the N2-O31 distance is 2.568(4), and the O31-O32 distance is 4.037(5) Å. Several metals have been shown to coordinate to the ligand including; Cu(II), Mn(II), Co(II), Ni<sup>2+</sup>, and UO<sub>2</sub><sup>2+</sup>.<sup>4</sup> The 2-quinoxalinol salen-Cu(II) complexes have been shown to be active towards C-H activation and oxidation. The tetradentate O-N-N-O binding pocket of the 2-quinoxalinol salen ligand coordinates UO<sub>2</sub><sup>+2</sup> and several solid state structural reports were made of this solid state structure with different solvents incorporated into the crystal lattice.<sup>5</sup> It was thought that increasing the conjugation of the 2-quinoxalinol with two additional aromatic rings, formed from condensation with salicylaldehyde, would increase the emission properties of the ligand metal complexes. Exploring along these same lines, it was thought that increasing the conjugation of the backbone by starting with 2,3-diaminophenazine, then subsequent condensation with salicylaldehyde derivatives, would provide a larger aromatic scaffold system with a O-N-N-O pocket for metal binding.

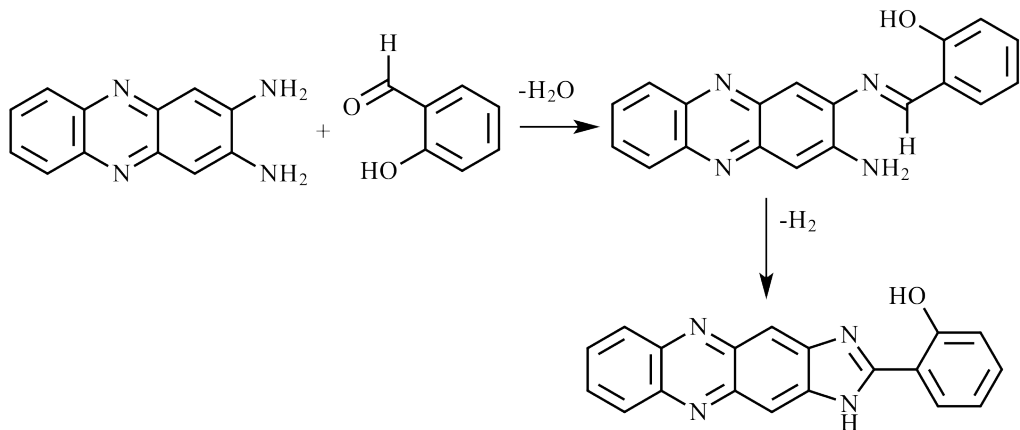
## Synthesis of the benzimidazole ligands

**C<sub>19</sub>H<sub>12</sub>N<sub>4</sub>O** Compound **Salzine** was synthesized by dissolving 0.05052 grams of 2,3-diaminophenazine in 20 ml of salicylaldehyde in a round bottom flask, charged with a stir bar. The reaction was heated at 80 °C for 24 hours. The solution changes color during the heating phase from red to very dark red/black. The reaction solution was then filtered and washed with ethanol leaving the crude yellow product.

**C<sub>27</sub>H<sub>28</sub>N<sub>4</sub>O** Compound **t-butsalzine** was synthesized by dissolving 0.2371 grams of 2,3-diaminophenazine in 25 ml of pyridine in a round bottom flask, charged with a stir bar. The reaction was heated at 110 °C for until all the 2,3-diaminophenazine had dissolved, then 0.2630 grams of 3,4-ditertbutyl-2-hydroxy benzaldehyde was added. The reaction was heated at 110 °C for 24 hours. The reaction solution was then filtered and washed with hexane, leaving the crude brown product. This brown product was passed through a silica gel column during column chromatography using ethyl acetate as the mobile phase. The yellow fractions were collected and rotovapped to dryness to recover the pure product.

**[UO<sub>2</sub>(C<sub>19</sub>H<sub>11</sub>N<sub>4</sub>O)(DMSO)]•DMSO** complex **Usalzine** was synthesized by dissolving 0.0201 grams of salzine in 1 ml of DMSO in a test tube. This solution was then layered with a ethanol solution containing 0.0117 grams of UO<sub>2</sub>(NO<sub>3</sub>)<sub>2</sub>. This test tube was set up for crystal growth in a slow diffusion 20 dram vial with hexanes as the diffusion solvent. After 4 days quality single crystals were observed and used for X-ray diffraction.

## X-ray Diffraction



Scheme 2 Shows the starting materials, 2,3-diaminophenazine and salicyaldehyde the product [2-(1H-imidazo[4,5-b]phenazin-2-yl)phenol], and a possible Schiff base intermediate.

Figure 34 of the salzine [2-(1H-imidazo[4,5-b]phenazin-2-yl)phenol] molecule shows that a different condensation result is observed for the 2,3-diaminophenazine starting material as opposed to the 2-quinoxolinol. As seen in the hypothesized scheme 2, during a condensation event between the aldehyde and the amine functional group of 2-quinoxalinol, a single condensation occurs forming a Schiff base. This leaves the second amine site on the 2-quinoxolinol available for another condensation with an aldehyde. Figure 33 shows that the reaction does not lead down the same pathway when 2,3-diaminophenazine provides the amine source. Instead, it is postulated, that the aldehyde and an amine go through a second condensation resulting in the evolution of  $H_2O$ , then the lone pair on the remaining amine attacks the imine, forming an imidazole in this process. Two representative structures were synthesized and isolated as shown in Figure 34 and Figure 35. As seen in Figure 35, the O1-N2 distance is found at 2.5866 (19) Å. In comparison to the two O-N distances of the 2-quinoxolinol salen compound found at 2.596(4) and 2.568(4) Å the distance is shorter between these two atoms.

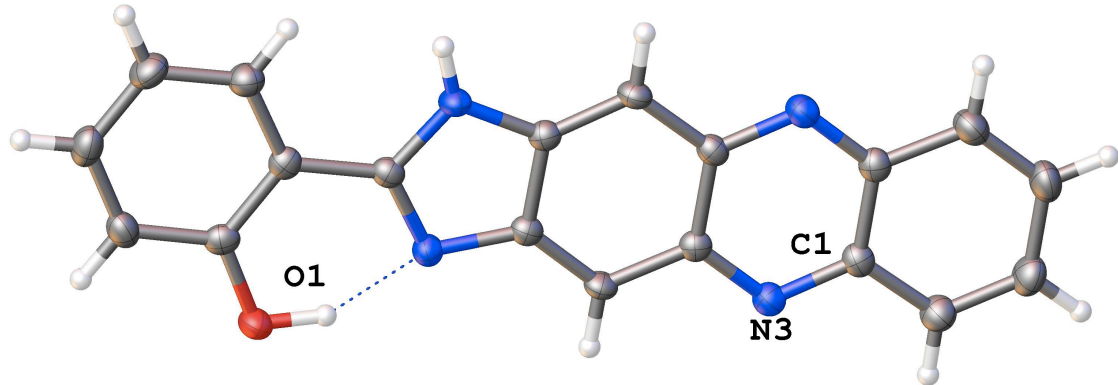


**Figure 34** Projection of the asymmetric unit of the salzine molecule. Atoms as shown are labeled: H in white, O in red, N in blue, and C in grey.

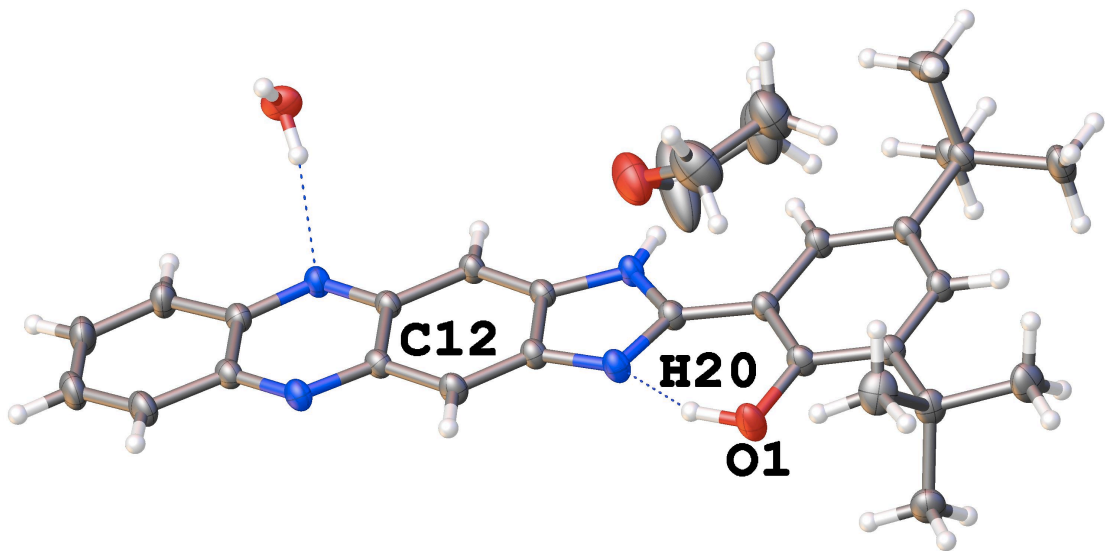


**Figure 15** Projection of the asymmetric unit of tbu-salzine. Atoms as shown are labeled: H in white, O in red, N in blue, and C in grey.

As seen in Figure 35, the O1-N2 distance is found at 2.5569(18) Å in comparison to the two O-N distances of the 2-quinoxolinol salen compound found at 2.596(4) and 2.568(4) Å the distance is shorter between these two atoms.

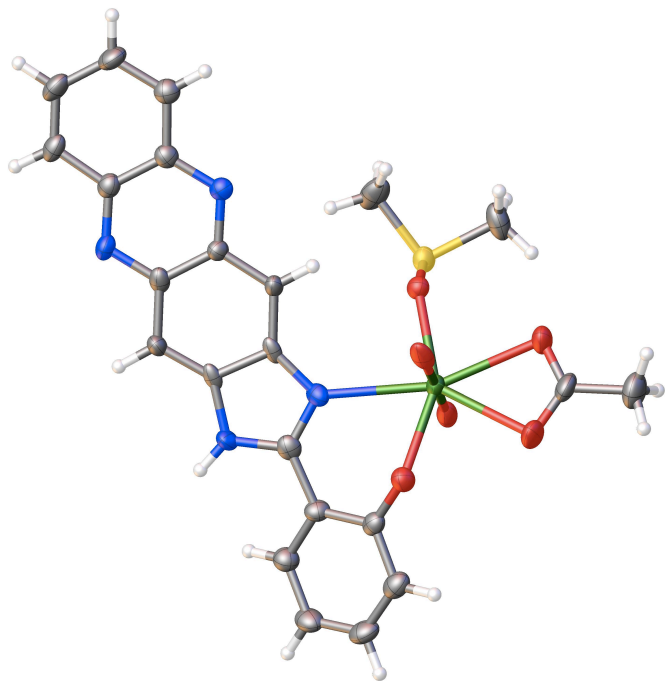


**Figure 36** Projection of the asymmetric unit of salzine- $\text{UO}_2$ . The non-coordinating solvent DMSO molecule has been removed for clarity. Atoms as shown are labeled: H in white, O in red, N in blue, C in grey, and sulfur in yellow.

As seen in Figure 36, the O3-N1 distance is found at 2.767(9) Å in comparison to the O-N distance of the salzine ligand found at 2.5866(19) Å. Clearly, upon binding of this bidentate O-N binding site, the O-N distance expands to accommodate the metal. The uranium center is seven coordinate and shown to have a beautiful symmetrical pentagonal bipyramidal geometry. These seven sites are coordinated by six oxygen atoms and one nitrogen atom. Two terminal oxo atoms of the  $\text{UO}_2^{+2}$  unit account for two of the six oxygen atoms. Three addition oxygen atoms can be accounted for by the coordination of a DMSO solvent molecule and an acetate anion. The remaining oxygen and nitrogen atoms that fill the coordination sphere of the uranium are from the **salzine** ligand. The U-N distance is observed at 2.558(6) Å. The U-O distance is found at 2.220(6) Å.

## CRAIC Microspectrophotometer

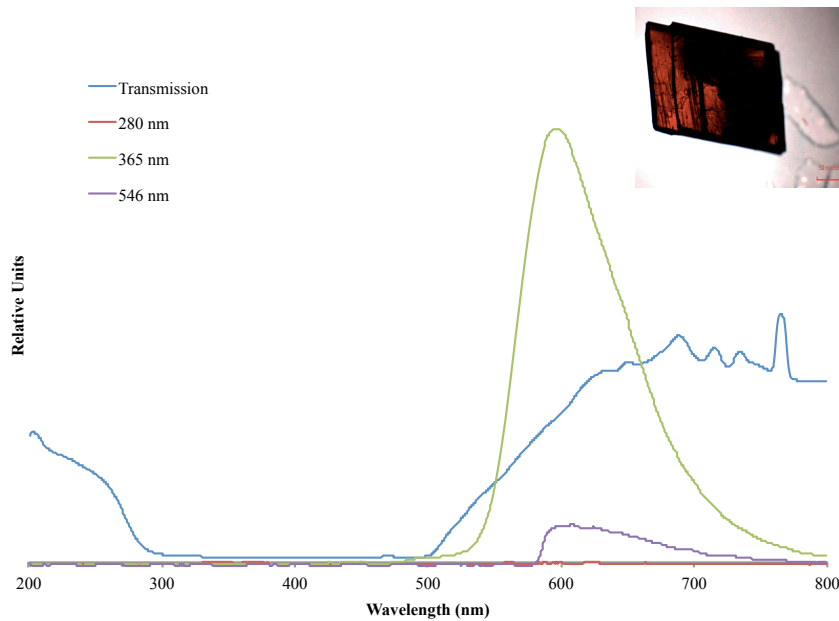


**Figure 37** Transmission and emission spectra of the salzine ligand. The image in the upper right corner is at a magnification of x10 and shows the sample this data was taken from.

The transmission and emission spectra of the salzine ligand were obtained by taking the single crystal used in the structural elucidation and directly putting it onto a quartz slide for further characterization with the CRAIC microspectrophotometer. As seen in Figure 37 there are two dominate spectral features seen in the emission spectra of the salzine compound. The emission resulting from an excitation at 280 nm results in a featureless spectrum. The emission resulting from an excitation wavelength of 365 nm results in a broad band feature centering around 605 nm. The emission resulting from an excitation wavelength of 546 nm results in a shoulder centered around the same 605 nm region.

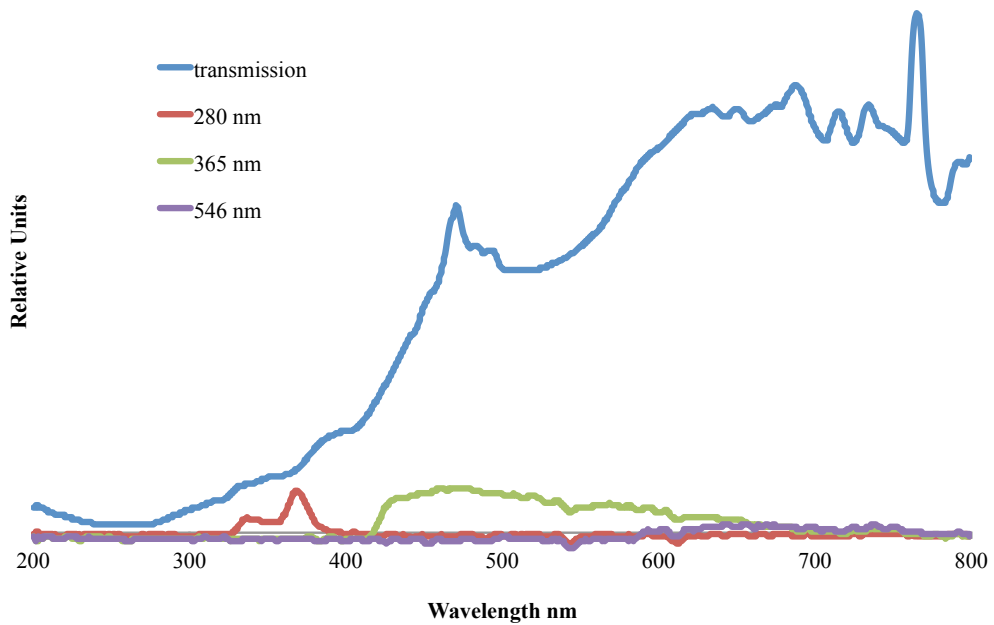


**Figure 38** Transmission and emission spectra of the salzine- $\text{UO}_2$  complex.

The transmission and emission spectra of the salzine- $\text{UO}_2$  complex were obtained by taking the single crystal used in the structural elucidation and directly putting it onto a quartz slide for further characterization with the CRAIC microspectrophotometer. As seen in Figure 38, and in comparison to Figure 38, there are two dominate spectral features seen in the emission spectra of the salpen- $\text{UO}_2$  complex. In contrast to just the salzine ligand, a spectral feature is observed from the 280 nm excitation at 362 nm with a shoulder observed at 328 nm. The emission resulting from an excitation wavelength of 365 nm results in a broad shoulder feature around 365 nm. The emission resulting from an excitation wavelength of 546 nm results is featureless. The growth of spectral features in the salzine- $\text{UO}_2$  complex in both the transmission and 280 nm excitation spectra are ways to tell if the ligand has bound the  $\text{UO}_2$  center in the solid state. Curious

is the loss of the large, broad band excitation feature found in the 365 nm emission spectrum of the salzine ligand.

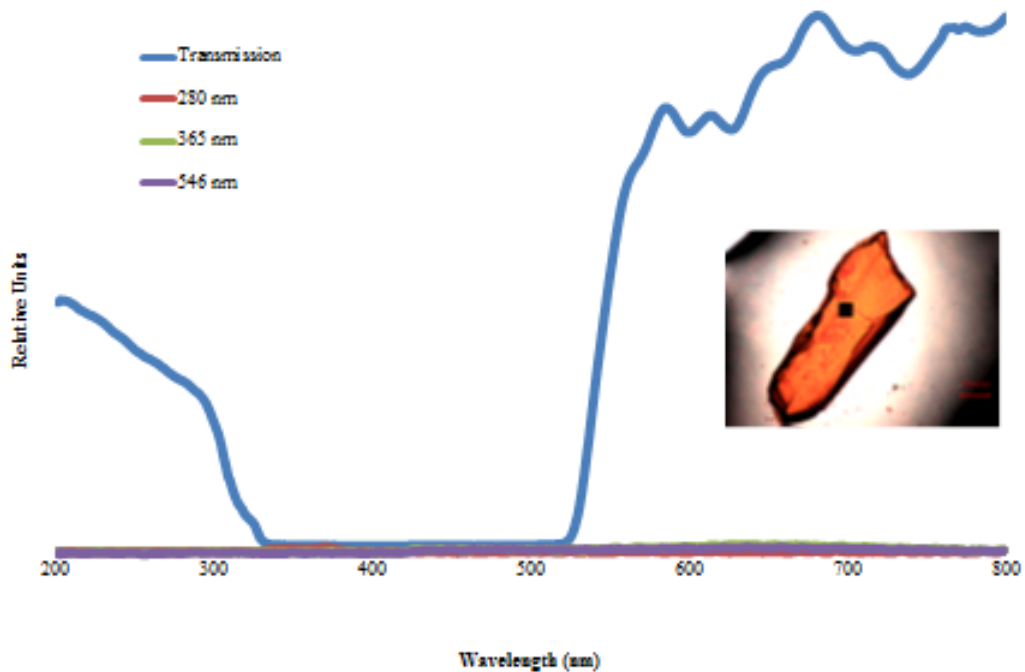


**Figure 39** Transmission and emission spectra of the tbut-salzine. The image in the upper right corner is at a magnification of x10 and shows the sample this data was taken from.

The transmission and emission spectra of the tbut-salzine ligand were obtained by taking the single crystal used in the structural elucidation and directly putting it onto a quartz slide for further characterization with the CRAIC microspectrophotometer. There are no spectral features seen in the emission spectra of the salpen compound. This is a result worth investigating further as comparison with salzine in Figure 37 some emission features would be expected. Unfortunately, a metal complex with the tbutyl-salzine ligand has not been isolated yet so no comparison can be made in the solid state of the electronic properties.

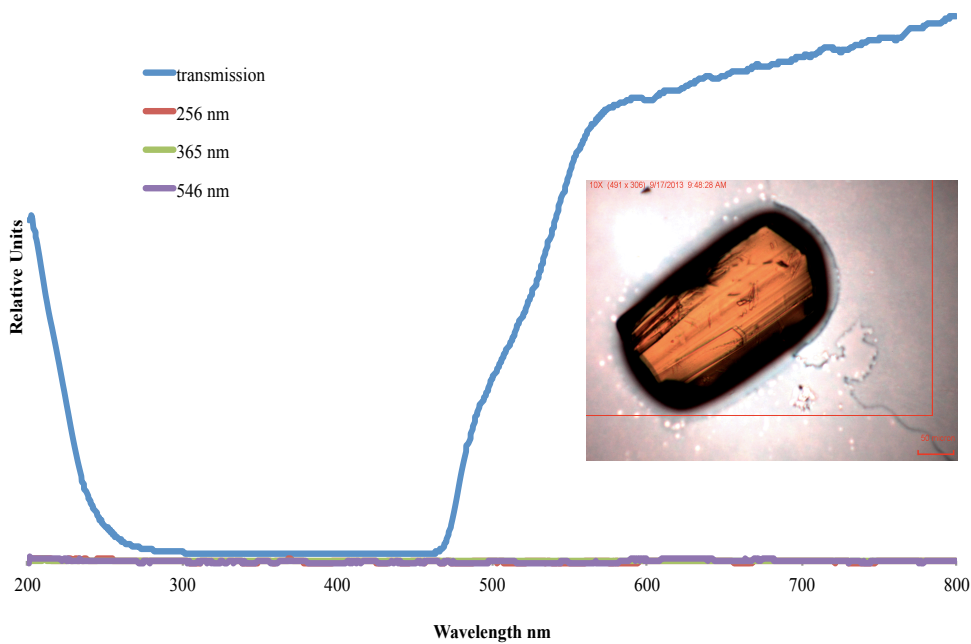


**Figure 40** Transmission and emission spectra of 2-quinoxalinol salen. The image in the upper right corner is at a magnification of x10 and shows the sample this data was taken from.

The transmission and emission spectra of the 2-quinoxalinol ligand were obtained by taking the single crystal used in the structural elucidation and directly putting it onto a quartz slide for further characterization with the CRAIC microspectrophotometer. As seen in Figure 40 there are no spectral features seen in the emission spectra of the 2-quinoxalinol salen compound. This is a result worth further investigation in comparison with the solution phase UV-vis data of just the 2-quinoxalinol salen ligand and the 2-quinoxalinol salen- $\text{UO}_2$  complex.

Synthesizing additional ligands with this common five atom (N-C-C-C-O) ligand geometry is worthy of note as several other solid state structures over the last decade have included the structural motif when coordinating to an actinide center.<sup>2</sup> Also, in future work, the 2-quinoxalinol salen-UO<sub>2</sub> single crystal should be regrown. Comparing the solid state spectra of the 2-quinoxolinol salen ligand with that of the UO<sub>2</sub> complexed 2-quinoxalinol structure with the CRAIC microspectrophotometer may give valuable insight into the electronics of the metal-ligand interactions.

## **References Cited**

- (1) Lei, Y.; Li, D.; Ouyang, J.; Shi, J. *Adv. Mater. Res. (Durnten-Zurich, Switz.)* **2011**, *311-313*, 1286.
- (2) Gorden, A. E. V.; DeVore, M. A.; Maynard, B. A. *Inorg. Chem. (Washington, DC, U. S.)*, Ahead of Print.
- (3) Wu, X.; Gorden, A. E. V. *J. Comb. Chem.* **2007**, *9*, 601.
- (4) Wu, X. G.; Hubbard, H. K.; Tate, B. K.; Gorden, A. E. V. *Polyhedron* **2009**, *28*, 360.
- (5) Wu, X. H.; Bharara, M. S.; Bray, T. H.; Tate, B. K.; Gorden, A. E. V. *Inorg. Chim. Acta* **2009**, *362*, 1847.

# Chapter 6: Conclusions and Future Work

## Actinide Cyanometallates

The ThTCPt compounds, **Th1** and **Th2**, are unique among the reported thorium literature, because we believe they are the first reported Th(IV) containing compounds to have both emission and structural work reported. The metal cation acts as a placeholder that tunes the R-value between Pt centers in the pseudo one-dimensional chains. **Th5** extends the set of reported, solid state thorium isocyanide complexes to a total of three. Mono- bi- and tridentate bridging TCM's, where M = Pt or Pd, has been shown in the solid state to give a fingerprint in the CN region of the Raman spectrum. The computational analysis performed using the unrestricted b3lyp functional gave valuable insight into the vibrational frequencies observed in the Raman spectrum of these compounds. This work lends support to the hypothesis that the spectral features seen in the experimental work are related to the incorporation mode of the tetracyanoplatinate anion (un-, mono-, bi-, tri-, and/or ter-dentate); however, when more than one tetracyanoplatinate anion binds a *5f* center, assigning the spectral features become less clear.

A reasonable conclusion from this computational analysis is that coordination of an actinide metal center breaks the symmetry of the  $D_{4h}$  cyanometallate anion and this leads to an increased number of vibrational stretches in the cyanide region. These vibrational modes may not have been observed in the experimental work because the sensitivity of the instrument. Unfortunately, we were unable to synthesize an  $An_x[Ni(CN)_4]_y$  analog in aqueous solution, and the DMSO incorporated into **U6** prohibits

the formation of more peaks in the cyanide region of the Raman spectrum. Previous literature has only reported two vibrations,  $A_{1g}$  and  $B_{1g}$ , in the  $2000\text{ cm}^{-1}$  region. We report on one molecular unit and three bridging compounds that have more than two vibrations in this region of the Raman spectrum. This will provide valuable structural information when single crystal XRD analysis is not possible.

## Future Work

### Actinide cyanometallates

Furthering the work in the actinide cyanometallate class of compounds will require synthesizing new compounds, containing transuranic elements. Multiple reactions have been attempted using an aqueous solution of  $\text{Np(V)O}_2\text{Cl}$  and these attempts resulted in the formation of a black non-crystalline solid precipitate probably a result of the reduction potential of Pt(II) [ $\text{Pt}^{\text{II}} + 2\text{e}^- > \text{Pt}_{(\text{s})}, E^\circ = +1.18\text{ V}$ .]<sup>1</sup> Two possible avenues to further pursue with the transuranic elements are available; first would be to use a cyanometallate with a lower reduction potential,  $\text{K}_2[\text{Ni(CN)}_4]$  or  $\text{K}_2[\text{Pd(CN)}_4]$ , and second would be to use a different solvent (DMSO, DMF, DMA, ...) to reduce the possibility of reducing the metal from the cyanometallate. Also, transition metal cyanides were purchased to be studied in these complexes ( $\text{Zn(CN)}_2$ ,  $\text{Pt(II)(CN)}_2$ ,  $\text{Cu(I)CN}$ ,  $\text{K}_3[\text{Co(CN)}_6]$ ,  $\text{K}_3[\text{Fe(CN)}_6]$ , and  $\text{K}_4[\text{Fe(CN)}_6]$ ). In aqueous solution they precipitated out as microcrystalline products and were never characterized. Using a polar organic solvent (such as DMSO, DMA, or DMF) may provide the environment needed

to properly crystallize the material in X-ray diffraction quality samples. The most interesting compounds may come from the solvent DMA. DMA is a planar, polar, organic solvent which may allow for platinophilic stacking interactions to be observed.

### **Oxidation of *ortho*-phenylenediamine**

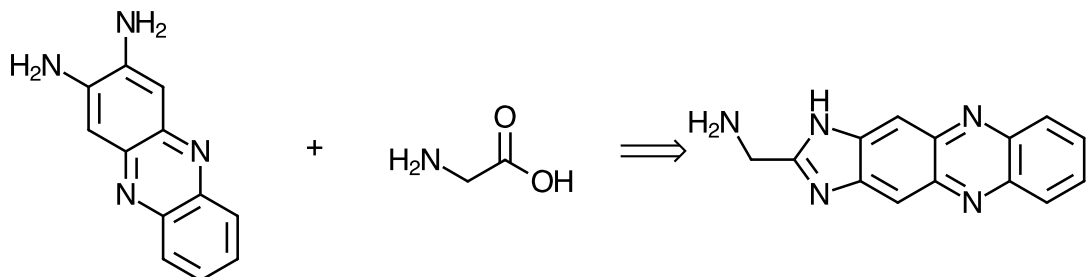
A flaw in the reporting of the isolated yield of the oxidation of *ortho*-phenylenediamine is the method in which it is obtained. Differing amounts of product are lost in the filtering steps for each reaction, making the results qualitative, but hardly quantitative. To improve these results UV-vis should be employed to get accurate measurements of the concentration of *ortho*-phenylenediamine when the reaction starts and when the reaction has completed. Further, it should be seen if the reaction can go to completion and what the most efficient mediation loading could be. Dioxygen is thought to play an important role in the reaction pathway, to explore this the dioxygen pressure can be increased using a Parr bomb. Future efforts should also focus on attempting to use other benzene derivatives, with *ortho* amine and alcohol functional groups, to prepare larger ring systems from different starting materials. Two examples of these starting materials would be 2-aminophenol and 1,2-dihydroxybenzene. Simple combinatorial enumeration [possible molecules =  $2^N$ ] would need to be done to figure amount the number of possible product molecules available when N number of different starting materials are available.

## Salzine

The salzine project has a huge potential for expansion by a future researcher. The most important facet of synthesizing these reactions is that the salicylaldehyde needs to be soluble in the reaction solvent. Pyridine seems to be an optimum solvent for the reaction, less optimal for the researcher considering the health implications by accidental exposure. When 2,3-diaminophenazine is used as the starting backbone, so far, only the monosubstituted imidazole has been observed, as seen in chapter 5. One aspect of a more careful synthetic researcher would be to try to isolate the disubstituted compound. This may not be possible under the current reaction conditions. Also, using different benzaldehyde starting materials can increase the number of different salzine molecules. A search of commercially available materials shows several options: 2-hydroxy-5-nitrobenzaldehyde, 3-tert-butyl-2-hydroxybenzaldehyde, 5-chloro-2-hydroxybenzaldehyde, 3-bromo-5-chloro-2-hydroxybenzaldehyde, 2,4,6-trihydroxybenzaldehyde, 2,3-dihydroxybenzaldehyde, and 2-hydroxy-5-methylbenzaldehyde. One metal complex has been isolated, salpen-UO<sub>2</sub>. Further salzine complexes need to be synthesized, isolated, and characterized. Several other metals can be used for example: VO<sup>2+</sup>, Cu (I), Cu (II), Cu (III), Ce(IV), Gd<sup>3+</sup>, Th+4, U(IV), U(VI), NpO<sub>2</sub><sup>+</sup>, and PuO<sub>2</sub><sup>2+</sup>.

Using these newly synthesized salzine molecules, synthesized from the hydroxybenzaldehydes listed above, and the metals available it should be a possibility to isolate these metal complexes. When the complexes have been isolated it should be attempted to grow single crystals. The most successful method to this point in crystallizing out the salen/salzine complexes has been slow diffusion. Slow evaporation has been useful in obtaining single crystals from a pure source of ligand. When single

crystals have been isolated structure elucidation using the X-ray diffractometer should be used. The single crystals can then be put through a series of spectrometer methods using the Craic microspectrophotometer to understand the electronic properties. Further, the electrochemical properties should be characterized using cyclic voltammetry. This will give insight into the bonding interaction between the ligand and the metal.

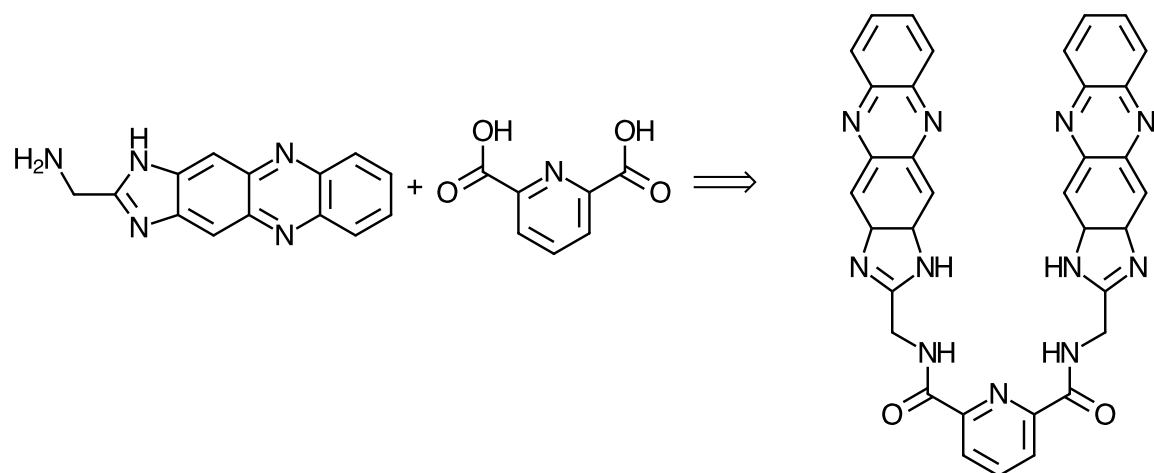


**Scheme 3** Reaction of 2,3-diaminophenazine with glycine under 4 N HCl conditions and reflux should produce the phenazineimidazole product which can be used in further synthetic steps.

### Phenazineimidazole

Another possible avenue for exploration is reaction of 2,3-diaminophenazine with glycine under 4 N HCl at reflux. This has been reported to give a glycine benzimidazole in previous work with *ortho*-phenylenediamine.<sup>2</sup> This reaction should produce the glycine phenazineimidazole, as seen in scheme 3, with the amine group available for condensation with a dicarboxylic acid to produce a new series of molecules with large sections of aromaticity and several hard and soft donor binding sites. This proposed molecule can be seen in the following reaction scheme 4. It may be just as interesting to start with the 2-quinoxalinol diamine, make the imidazole via addition of 4 N HCl and follow with the condensation with 2,6-pyridinedicarboxylic acid. The reason why this

may be more interesting is that the 2-quinoxalinol has orders of magnitude higher emission when excited *via* a simple UV lamp.



**Scheme 4** Starting with the phenazineimidazole starting material.

The same synthetic methods can be employed as with the salzine project. All the amino acids can be used as starting material in place of glycine. This creates a large array of ligands possible for coordination with the typical metals:  $\text{VO}^{2+}$ , Cu (I), Cu (II), Cu (III), Ce(IV),  $\text{Gd}^{3+}$ ,  $\text{Th}^{4+}$ , U(IV),  $\text{UO}_2^{2+}$ ,  $\text{U}^{\text{VI}}$ ,  $\text{NpO}_2^+$ , and  $\text{PuO}_2^{2+}$ . Using these newly synthesized salzine molecules, synthesized from the hydroxybenzaldehydes listed above, and the phenazineimidazoles and the metals available it should be a possibility to isolate these metal complexes. Also the stoichiometry between the metal and the salzine ligands should be explored as a 2:1 salzine metal complex would be expected and can be visualized in Figure 41 and Figure 42. When the complexes have been isolated it should be attempted to grow single crystals. The most successful method to this point in crystallizing out the salen/salzine complexes has been slow diffusion. Slow evaporation has been useful in obtaining single crystals from a pure source of ligand. When single crystals have been isolated structure elucidation using the X-ray diffractometer should be

used. The single crystals can then be put through a series of spectrometer methods using the Craic microspectrophotometer to understand the electrochemical properties. Further, the electrochemical properties should be characterized using cyclic voltammetry. This will give insight into the bonding interaction between the ligand and the metal.

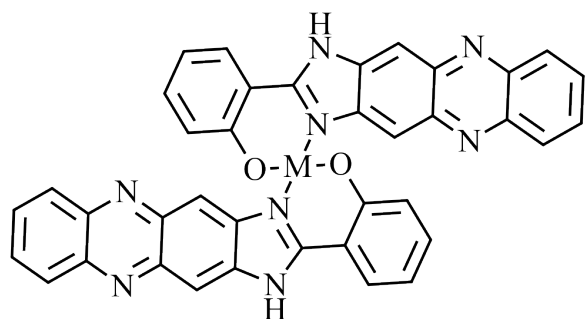


Figure 41 Possible 2:1 salzine metal complex.

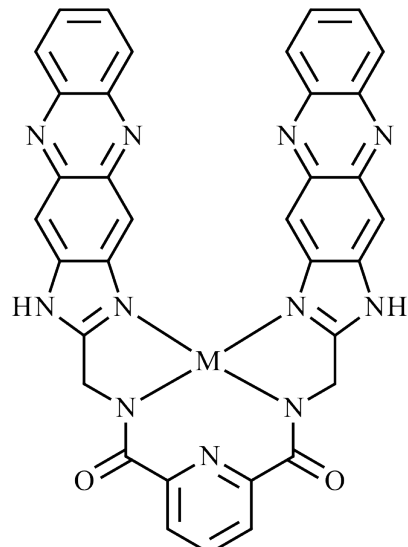


Figure 42 Possible 1:1 phenezeneimidazole metal complex.

### **References Cited**

- (1) Housecroft, C.; Sharpe, A. *Inorganic Chemistry*; Pearson Education Limited, 2007; Vol. 3. Pg. 1022.
- (2) Tyagi, N.; Mathur, P. *Spectrochim. Acta, Part A* **2012**, *96*, 759.

## Appendix 1: Crystallographic Tables

### Crystallographic Data Collection for Th1, Th2, and U3

Crystals of compounds **2** and **3** were obtained in good yield from slow evaporation in water at room temperature. Crystals of **1** were obtained by slow evaporation of a water solution with a pH of 2.5. X-ray diffraction data for **1** were collected at -80 °C on a Bruker SMART APEX CCD X-ray diffractometer unit using Mo K $\alpha$  radiation from crystals mounted in Paratone-N oil on glass fibers. SMART (v 5.624) was used for preliminary determination of cell constants and data collection control. Determination of integrated intensities and global cell refinement were performed with the Bruker SAINT Software package using a narrow-frame integration algorithm. X-ray data for **2** and **3** were collected using a Varian Oxford Xcalibur E single-crystal X-ray diffractometer. Intensity measurements were performed using Mo K $\alpha$  radiation, from a sealed-tube Enhance X-ray source, and an Eos area detector. CrysAlis<sup>R1</sup> was used for preliminary determination of the cell constants, data collection strategy, and for data collection control. Following data collection, CrysAlis was also used to integrate the reflection intensities, apply an absorption correction to the data, and perform a global cell refinement. The program suite SHELXTL (v 5.1) was used for space group determination, structure solution, and refinement.<sup>1</sup> Refinement was performed against  $F^2$  by weighted full-matrix least square, and empirical absorption correction (SADABS<sup>2</sup>) was applied. H atoms were found from the difference fourier maps.

#### **U4, Th5, U6, Th7, Th8, salzine, Usalzine, and t-butosalzine**

The X-ray diffraction datasets were collected at 183 K, on a Bruker SMART APEX CCD X-ray diffractometer unit using Mo K $\alpha$  radiation, from crystals mounted in Paratone-N oil on glass fibers. SMART (v 5.624) was used for preliminary determination of cell constants and data collection control. Determination of integrated intensities and global cell refinement were performed with the Bruker SAINT software package using a narrow-frame integration algorithm. The program suite SHELXTL (v 5.1) was used for space group determination, structure solution, and refinement.<sup>3</sup> Refinement was performed against  $F^2$  by weighted full-matrix least squares, and empirical absorption correction (SADABS) was applied. Hydrogen atoms for **U6** were found from the difference fourier maps. Projections were generated in the Olex2.1-1 graphics program.<sup>4</sup> Table 1 contains key results of the X-ray experiments and additional crystallographic information is included as Supporting Information.

**Crystallographic Table 1.**

Crystal data and structure refinement for Th1, **Th(H<sub>2</sub>O)<sub>7</sub>[Pt(CN)<sub>4</sub>]<sub>2</sub>•10H<sub>2</sub>O**.

Identification code	Th1
Empirical Formula	C <sub>8</sub> H <sub>34</sub> N <sub>8</sub> O <sub>17</sub> Pt <sub>2</sub> Th
Formula weight	1136.65
Temperature	193(2) K
Wavelength	0.71071
Crystal System	Orthorhombic
Spacegroup	<i>Pbca</i>
Unit cell dimensions	a = 13.2464(6) Å      α = 90.0 ° b = 20.5599(10) Å      β = 90.0 ° c = 22.4536(11) Å      γ = 90.0 °
Volume	6115.1(5) Å <sup>3</sup>
Z	8
Calculated density	2.469 Mg/m <sup>3</sup>
Absorption coefficient	14.053 mm <sup>-1</sup>
F(000)	4160
Crystal size	0.80 x 0.80 x 0.09 mm
Theta range for data collection	1.81 to 28.27 °
Limiting indices	-17<=h<=17, -27<=k<=27, 29<=l<=29
Reflections collected / unique	59819 / 7574 [R(int) = 0.0737]
Completeness to theta = 28.27	99.9 %
Absorption correction	Analytical
Max. and min. transmission	0.3710 and 0.0314
Refinement method	Full-matrix least squares on F <sup>2</sup>
Data / restraints / parameters	7574 / 0 / 313
Goodness-of-fit on F <sup>2</sup>	0.999
Final R indices [I>2sigma(I)]	R1 = 0.0301, wR2 = 0.0766
R indices (all data)	R1 = 0.0373, wR2 = 0.0781
Largest diff. peak and hole	2.154 and -3.034 e. Å <sup>-3</sup>

**Crystallographic Table 2.** Atomic coordinates ( $\times 10^4$ ) and equivalent isotropic displacement parameters ( $\text{\AA}^2 \times 10^3$ )  $\text{Th}(\text{H}_2\text{O})_7[\text{Pt}(\text{CN})_4]_2 \bullet 10\text{H}_2\text{O}$ . U(eq) is defined as one third of the trace of the orthogonalized  $U^{ij}$  tensor.

	x	y	z	U(eq)
Th(1)	3617(1)	3956(1)	8669(1)	14(1)
Pt(1)	3747(1)	6259(1)	7345(1)	16(1)
O(1)	2519(3)	3947(2)	7783(2)	28(1)
N(1)	3683(3)	5121(2)	8278(2)	22(1)
C(1)	3711(4)	5557(2)	7954(2)	18(1)
O(2)	4947(3)	3941(2)	7922(2)	25(1)
Pt(2)	3733(1)	1421(1)	7668(1)	15(1)
N(2)	1312(3)	2367(3)	8310(3)	33(1)
C(2)	3733(4)	6956(3)	7957(3)	21(1)
O(3)	2275(3)	3225(2)	9036(2)	23(1)
N(3)	6121(4)	2301(2)	8688(2)	31(1)
C(3)	3809(4)	6923(3)	6703(3)	24(1)
O(4)	2058(3)	4602(2)	8865(2)	25(1)
N(4)	3619(4)	5162(3)	6382(2)	35(1)
C(4)	3683(4)	5561(3)	6732(3)	26(1)
O(5)	5104(3)	4559(2)	9052(2)	25(1)
N(5)	3705(3)	2874(2)	8098(2)	18(1)
C(5)	3725(4)	2356(3)	7925(2)	18(1)
O(6)	4743(3)	3181(2)	9197(2)	24(1)
N(6)	3954(4)	1798(3)	6321(2)	33(1)
C(6)	3872(4)	1663(3)	6813(3)	22(1)
O(7)	3459(3)	4136(2)	9730(2)	27(1)
C(7)	3567(4)	1168(3)	8520(3)	20(1)
N(7)	3449(4)	1006(2)	9002(2)	31(1)
O(8)	127(3)	4252(2)	8998(2)	32(1)
N(8)	6239(3)	4929(3)	7635(2)	28(1)
C(8)	3755(4)	487(3)	7462(2)	21(1)
O(9)	4100(4)	2602(2)	10200(2)	36(1)
O(10)	4764(3)	3339(2)	6865(2)	30(1)
O(11)	4819(3)	1362(2)	9962(2)	38(1)

O(12)	6790(3)	3788(2)	177(2)	35(1)
O(13)	2101(3)	4223(2)	5978(2)	32(1)
O(14)	5082(3)	5813(2)	9419(2)	28(1)
O(15)	2691(3)	3258(2)	6760(2)	30(1)
O(16)	2020(4)	2537(2)	10071(2)	38(1)
O(17)	1751(4)	4061(3)	10301(3)	74(2)

**Crystallographic Table 3.** Bond lengths [ $\text{\AA}$ ] and angles [ $^\circ$ ] for  $\text{Th}(\text{H}_2\text{O})_7[\text{Pt}(\text{CN})_4]_2 \bullet 10\text{H}_2\text{O}$ .

Th(1)-O(7)	2.420(4)
Th(1)-O(2)	2.434(4)
Th(1)-O(1)	2.464(4)
Th(1)-O(3)	2.469(4)
Th(1)-O(5)	2.481(4)
Th(1)-O(6)	2.485(4)
Th(1)-O(4)	2.494(4)
Th(1)-N(1)	2.552(5)
Th(1)-N(5)	2.570(4)
Pt(1)-C(2)	1.985(6)
Pt(1)-C(3)	1.986(6)
Pt(1)-C(1)	1.990(6)
Pt(1)-C(4)	1.991(6)
N(1)-C(1)	1.155(7)
Pt(2)-C(8)	1.975(6)
Pt(2)-C(6)	1.991(6)
Pt(2)-C(7)	1.995(6)
Pt(2)-C(5)	2.007(6)
N(2)-C(2)#1	1.160(8)
C(2)-N(2)#2	1.160(8)
N(3)-C(3)#3	1.176(8)
C(3)-N(3)#4	1.176(8)
N(4)-C(4)	1.139(8)
N(5)-C(5)	1.135(7)
N(6)-C(6)	1.146(7)
C(7)-N(7)	1.142(8)
N(8)-C(8)#4	1.168(8)
C(8)-N(8)#3	1.168(8)
O(7)-Th(1)-O(2)	138.02(13)
O(7)-Th(1)-O(1)	138.15(13)
O(2)-Th(1)-O(1)	82.58(15)
O(7)-Th(1)-O(3)	72.68(13)

O(2)-Th(1)-O(3)	138.01(13)
O(1)-Th(1)-O(3)	80.77(13)
O(7)-Th(1)-O(5)	69.61(14)
O(2)-Th(1)-O(5)	70.74(14)
O(1)-Th(1)-O(5)	138.78(14)
O(3)-Th(1)-O(5)	139.48(14)
O(7)-Th(1)-O(6)	71.35(13)
O(2)-Th(1)-O(6)	83.43(13)
O(1)-Th(1)-O(6)	137.26(12)
O(3)-Th(1)-O(6)	83.24(13)
O(5)-Th(1)-O(6)	71.25(13)
O(7)-Th(1)-O(4)	70.93(13)
O(2)-Th(1)-O(4)	136.75(13)
O(1)-Th(1)-O(4)	70.01(13)
O(3)-Th(1)-O(4)	70.69(12)
O(5)-Th(1)-O(4)	109.29(13)
O(6)-Th(1)-O(4)	138.98(13)
O(7)-Th(1)-N(1)	101.46(15)
O(2)-Th(1)-N(1)	75.52(14)
O(1)-Th(1)-N(1)	75.52(14)
O(3)-Th(1)-N(1)	135.31(13)
O(5)-Th(1)-N(1)	67.86(14)
O(6)-Th(1)-N(1)	138.21(13)
O(4)-Th(1)-N(1)	65.79(13)
O(7)-Th(1)-N(5)	128.82(15)
O(2)-Th(1)-N(5)	67.17(13)
O(1)-Th(1)-N(5)	67.51(13)
O(3)-Th(1)-N(5)	70.85(13)
O(5)-Th(1)-N(5)	124.67(13)
O(6)-Th(1)-N(5)	69.82(13)
O(4)-Th(1)-N(5)	125.91(13)
N(1)-Th(1)-N(5)	129.71(15)
C(2)-Pt(1)-C(3)	90.4(2)
C(2)-Pt(1)-C(1)	92.6(2)
C(3)-Pt(1)-C(1)	176.8(2)
C(2)-Pt(1)-C(4)	177.0(2)

C(3)-Pt(1)-C(4)	89.8(2)
C(1)-Pt(1)-C(4)	87.2(2)
C(1)-N(1)-Th(1)	161.2(4)
N(1)-C(1)-Pt(1)	175.5(5)
C(8)-Pt(2)-C(6)	90.9(2)
C(8)-Pt(2)-C(7)	88.5(2)
C(6)-Pt(2)-C(7)	178.8(2)
C(8)-Pt(2)-C(5)	176.8(2)
C(6)-Pt(2)-C(5)	92.2(2)
C(7)-Pt(2)-C(5)	88.5(2)
N(2)#2-C(2)-Pt(1)	177.5(5)
N(3)#4-C(3)-Pt(1)	177.1(5)
N(4)-C(4)-Pt(1)	178.1(5)
C(5)-N(5)-Th(1)	170.1(4)
N(5)-C(5)-Pt(2)	176.4(5)
N(6)-C(6)-Pt(2)	179.5(6)
N(7)-C(7)-Pt(2)	177.6(5)
N(8)#3-C(8)-Pt(2)	177.1(5)

Symmetry transformations used to generate equivalent atoms:

#1 -x+1/2,y-1/2,z #2 -x+1/2,y+1/2,z #3 -x+1,y-1/2,-z+3/2

#4 -x+1,y+1/2,-z+3/2

**Crystallographic Table 4.** Anisotropic displacement parameters ( $\text{\AA}^2 \times 10^3$ ) for  $\text{Th}(\text{H}_2\text{O})_7[\text{Pt}(\text{CN})_4]_2 \cdot 10\text{H}_2\text{O}$ . The anisotropic displacement factor exponent takes the form:  $-2\pi^2 [ h^2 a^* U^{11} + \dots + 2 h k a^* b^* U^{12} ]$

	U <sup>11</sup>	U <sup>22</sup>	U <sup>33</sup>	U <sup>23</sup>	U <sup>13</sup>	U <sup>12</sup>
Th(1)	18(1)	14(1)	10(1)	0(1)	0(1)	0(1)
Pt(1)	19(1)	16(1)	14(1)	2(1)	1(1)	0(1)
O(1)	38(2)	26(2)	19(2)	-3(2)	-8(2)	6(2)
N(1)	27(3)	18(2)	20(3)	2(2)	-2(2)	-1(2)
C(1)	24(3)	16(3)	14(3)	-4(2)	0(2)	0(2)
O(2)	36(2)	24(2)	16(2)	-2(2)	10(2)	-3(2)
Pt(2)	19(1)	15(1)	13(1)	-2(1)	1(1)	0(1)
N(2)	31(3)	30(3)	38(3)	-8(3)	3(2)	-1(2)
C(2)	21(3)	19(3)	23(3)	-1(2)	0(2)	-1(2)
O(3)	24(2)	24(2)	19(2)	-1(2)	3(2)	-6(2)
N(3)	35(3)	30(3)	29(3)	-9(2)	3(2)	0(2)
C(3)	25(3)	21(3)	25(3)	-1(2)	0(2)	0(2)
O(4)	23(2)	24(2)	27(2)	2(2)	5(2)	5(2)
N(4)	47(3)	36(3)	21(3)	-7(2)	-4(2)	0(2)
C(4)	35(3)	26(3)	16(3)	9(2)	0(2)	-1(2)
O(5)	26(2)	27(2)	23(2)	-3(2)	-6(2)	-3(2)
N(5)	26(2)	15(2)	13(2)	-2(2)	2(2)	-1(2)
C(5)	16(3)	25(3)	13(3)	4(2)	1(2)	0(2)
O(6)	31(2)	24(2)	16(2)	1(2)	-1(2)	6(2)
N(6)	40(3)	39(3)	21(3)	0(2)	3(3)	-4(2)
C(6)	24(3)	23(3)	18(3)	-6(2)	0(2)	0(2)
O(7)	26(2)	42(2)	12(2)	-3(2)	2(2)	-1(2)
C(7)	22(3)	18(3)	19(3)	-4(2)	1(2)	-3(2)
N(7)	43(3)	27(3)	24(3)	2(2)	3(2)	-6(2)
O(8)	31(2)	31(2)	35(3)	-2(2)	-1(2)	-1(2)
N(8)	32(3)	20(3)	32(3)	4(2)	5(2)	-1(2)
C(8)	28(3)	23(3)	11(3)	-3(2)	4(2)	0(2)
O(9)	56(3)	35(2)	16(2)	1(2)	4(2)	-1(2)
O(10)	37(2)	32(2)	21(2)	-2(2)	0(2)	1(2)
O(11)	45(3)	41(3)	28(3)	-1(2)	-6(2)	4(2)

O(12)	36(2)	40(3)	28(3)	1(2)	0(2)	4(2)
O(13)	30(2)	36(2)	29(3)	-3(2)	-4(2)	-2(2)
O(14)	37(2)	29(2)	18(2)	-6(2)	-4(2)	-3(2)
O(15)	39(2)	30(2)	21(2)	-2(2)	-3(2)	-1(2)
O(16)	58(3)	36(2)	20(2)	7(2)	6(2)	-1(2)
O(17)	44(3)	139(6)	40(3)	-45(4)	17(3)	-24(3)

---

**Crystallographic Table 5.** Crystal data and structure refinement for (Th2), Th<sub>2</sub>(H<sub>2</sub>O)<sub>10</sub>(OH)<sub>2</sub>[Pt(CN)<sub>4</sub>]<sub>3</sub>•5H<sub>2</sub>O.

Identification code	Th2
Empirical formula	C <sub>12</sub> H <sub>32</sub> N <sub>12</sub> O <sub>17</sub> Pt <sub>3</sub> Th <sub>2</sub>
Formula weight	1665.85
Temperature	295(2) K
Wavelength	0.71073 Å
Crystal system	Monoclinic
Space group	C2/c
Unit cell dimensions	a = 16.4915(4) Å      α = 90°. b = 12.1941(4) Å      β = 114.016(4)°. c = 19.5380(5) Å      γ = 90°.
Volume	3588.9(2) Å <sup>3</sup>
Z	4
Density (calculated)	3.083 Mg/m <sup>3</sup>
Absorption coefficient	19.989 mm <sup>-1</sup>
F(000)	2952
Crystal size	0.29 x 0.03 x 0.03 mm <sup>3</sup>
Theta range for data collection	3.34 to 30.61°.
Index ranges	-22<=h<=23, -16<=k<=17, -27<=l<=27
Reflections collected	32269
Independent reflections	5166 [R(int) = 0.0281]
Completeness to theta = 29.00°	99.6 %
Absorption correction	Semi-empirical from equivalents
Max. and min. transmission	1.0 and 0.30
Refinement method	Full-matrix least-squares on F <sup>2</sup>
Data / restraints / parameters	5166 / 0 / 211
Goodness-of-fit on F <sup>2</sup>	0.918
Final R indices [I>2sigma(I)]	R1 = 0.0141, wR2 = 0.0239
R indices (all data)	R1 = 0.0211, wR2 = 0.0244
Extinction coefficient	0.000167(4)
Largest diff. peak and hole	0.652 and -0.703 e.Å <sup>-3</sup>

**Crystallographic Table 6.** Atomic coordinates ( $\times 10^4$ ) and equivalent isotropic displacement parameters ( $\text{\AA}^2 \times 10^3$ ) for  $\text{Th}_2(\text{H}_2\text{O})_{10}(\text{OH})_2[\text{Pt}(\text{CN})_4]_3 \bullet 5\text{H}_2\text{O}$ . U(eq) is defined as one third of the trace of the orthogonalized  $U^{ij}$  tensor.

	x	y	z	U(eq)
Th(1)	1439(1)	1950(1)	149(1)	15(1)
Pt(1)	-838(1)	2711(1)	1667(1)	19(1)
Pt(2)	2500	-2500	0	19(1)
O(1)	2912(1)	1674(1)	321(1)	21(1)
O(2)	327(1)	3347(2)	-470(1)	39(1)
O(3)	2138(1)	1128(2)	1407(1)	36(1)
O(4)	978(1)	1541(2)	-1193(1)	32(1)
O(5)	1993(2)	3462(2)	1087(1)	41(1)
O(6)	-40(1)	1005(2)	-412(1)	31(1)
O(7)	0	2667(3)	-2500	48(1)
O(8)	1252(2)	-571(2)	1772(1)	52(1)
O(9)	-1371(2)	6087(2)	2690(1)	51(1)
C(1)	-39(2)	2306(2)	1173(2)	25(1)
C(2)	-1040(2)	1152(2)	1838(2)	30(1)
C(3)	-1609(2)	3159(2)	2176(2)	28(1)
C(4)	-705(2)	4284(2)	1463(2)	30(1)
C(5)	1985(2)	-1034(2)	46(1)	22(1)
C(6)	1855(2)	-3191(2)	550(2)	32(1)
N(1)	429(2)	2110(2)	888(1)	30(1)
N(2)	-1182(2)	261(2)	1927(2)	53(1)
N(3)	-2028(2)	3433(2)	2486(2)	47(1)
N(4)	-661(2)	5176(2)	1329(2)	49(1)
N(5)	1694(2)	-181(2)	51(1)	27(1)
N(6)	1490(2)	-3589(3)	873(2)	63(1)

**Crystallographic Table 7.** Bond lengths [Å] and angles [°] for  $\text{Th}_2(\text{H}_2\text{O})_{10}(\text{OH})_2[\text{Pt}(\text{CN})_4]_3 \bullet 5\text{H}_2\text{O}$ .

---

Th(1)-O(1)	2.3369(17)
Th(1)-O(1)#1	2.3675(17)
Th(1)-O(2)	2.4342(18)
Th(1)-O(3)	2.4631(18)
Th(1)-O(4)	2.4650(18)
Th(1)-O(5)	2.4962(19)
Th(1)-O(6)	2.5113(18)
Th(1)-N(1)	2.619(2)
Th(1)-N(5)	2.651(2)
Th(1)-Th(1)#1	4.0045(2)
Pt(1)-C(2)	1.982(3)
Pt(1)-C(3)	1.982(3)
Pt(1)-C(1)	1.987(3)
Pt(1)-C(4)	1.988(3)
Pt(2)-C(6)#2	1.982(3)
Pt(2)-C(6)	1.982(3)
Pt(2)-C(5)#2	1.997(3)
Pt(2)-C(5)	1.997(3)
O(1)-Th(1)#1	2.3675(17)
O(1)-H(1A)	0.8501
O(2)-H(2A)	0.8500
O(2)-H(2B)	0.8499
O(3)-H(3A)	0.8500
O(3)-H(3B)	0.8501
O(4)-H(4A)	0.8500
O(4)-H(4B)	0.8500
O(5)-H(5A)	0.8500
O(5)-H(5B)	0.8500
O(6)-H(6A)	0.8500
O(6)-H(6B)	0.8501
O(7)-H(7)	0.8501
O(8)-H(8A)	0.8499

---

O(8)-H(8B)	0.8500
O(9)-H(9A)	0.8500
O(9)-H(9B)	0.8500
C(1)-N(1)	1.145(3)
C(2)-N(2)	1.140(4)
C(3)-N(3)	1.139(4)
C(4)-N(4)	1.129(4)
C(5)-N(5)	1.147(3)
C(6)-N(6)	1.141(4)
O(1)-Th(1)-O(1)#1	63.31(7)
O(1)-Th(1)-O(2)	134.55(6)
O(1)#1-Th(1)-O(2)	71.29(6)
O(1)-Th(1)-O(3)	76.19(6)
O(1)#1-Th(1)-O(3)	125.04(6)
O(2)-Th(1)-O(3)	137.08(7)
O(1)-Th(1)-O(4)	88.66(7)
O(1)#1-Th(1)-O(4)	73.94(6)
O(2)-Th(1)-O(4)	76.67(7)
O(3)-Th(1)-O(4)	142.68(7)
O(1)-Th(1)-O(5)	87.31(7)
O(1)#1-Th(1)-O(5)	70.95(6)
O(2)-Th(1)-O(5)	79.88(8)
O(3)-Th(1)-O(5)	71.65(7)
O(4)-Th(1)-O(5)	142.45(6)
O(1)-Th(1)-O(6)	139.91(6)
O(1)#1-Th(1)-O(6)	131.91(6)
O(2)-Th(1)-O(6)	72.66(7)
O(3)-Th(1)-O(6)	103.04(6)
O(4)-Th(1)-O(6)	67.57(6)
O(5)-Th(1)-O(6)	131.24(7)
O(1)-Th(1)-N(1)	142.06(7)
O(1)#1-Th(1)-N(1)	130.56(7)
O(2)-Th(1)-N(1)	72.63(7)
O(3)-Th(1)-N(1)	67.93(7)
O(4)-Th(1)-N(1)	127.69(7)
O(5)-Th(1)-N(1)	70.37(7)

O(6)-Th(1)-N(1)	63.37(7)
O(1)-Th(1)-N(5)	71.54(6)
O(1)#1-Th(1)-N(5)	123.85(7)
O(2)-Th(1)-N(5)	139.42(7)
O(3)-Th(1)-N(5)	69.49(7)
O(4)-Th(1)-N(5)	73.40(6)
O(5)-Th(1)-N(5)	139.08(7)
O(6)-Th(1)-N(5)	70.93(7)
N(1)-Th(1)-N(5)	105.55(7)
O(1)-Th(1)-Th(1)#1	31.89(4)
O(1)#1-Th(1)-Th(1)#1	31.43(4)
O(2)-Th(1)-Th(1)#1	102.69(5)
O(3)-Th(1)-Th(1)#1	101.54(5)
O(4)-Th(1)-Th(1)#1	79.79(5)
O(5)-Th(1)-Th(1)#1	77.27(5)
O(6)-Th(1)-Th(1)#1	147.28(4)
N(1)-Th(1)-Th(1)#1	147.64(5)
N(5)-Th(1)-Th(1)#1	98.31(5)
C(2)-Pt(1)-C(3)	89.65(11)
C(2)-Pt(1)-C(1)	91.90(11)
C(3)-Pt(1)-C(1)	178.04(11)
C(2)-Pt(1)-C(4)	176.96(12)
C(3)-Pt(1)-C(4)	88.88(12)
C(1)-Pt(1)-C(4)	89.63(11)
C(6)#2-Pt(2)-C(6)	180.00(19)
C(6)#2-Pt(2)-C(5)#2	91.37(11)
C(6)-Pt(2)-C(5)#2	88.63(11)
C(6)#2-Pt(2)-C(5)	88.63(11)
C(6)-Pt(2)-C(5)	91.37(11)
C(5)#2-Pt(2)-C(5)	180.00(15)
Th(1)-O(1)-Th(1)#1	116.69(7)
Th(1)-O(1)-H(1A)	121.4
Th(1)#1-O(1)-H(1A)	121.1
Th(1)-O(2)-H(2A)	118.3
Th(1)-O(2)-H(2B)	119.7
H(2A)-O(2)-H(2B)	120.5

Th(1)-O(3)-H(3A)	123.6
Th(1)-O(3)-H(3B)	120.5
H(3A)-O(3)-H(3B)	115.6
Th(1)-O(4)-H(4A)	124.4
Th(1)-O(4)-H(4B)	124.7
H(4A)-O(4)-H(4B)	110.7
Th(1)-O(5)-H(5A)	109.8
Th(1)-O(5)-H(5B)	128.6
H(5A)-O(5)-H(5B)	121.4
Th(1)-O(6)-H(6A)	129.4
Th(1)-O(6)-H(6B)	112.5
H(6A)-O(6)-H(6B)	112.0
H(8A)-O(8)-H(8B)	104.9
H(9A)-O(9)-H(9B)	108.9
N(1)-C(1)-Pt(1)	177.6(3)
N(2)-C(2)-Pt(1)	177.9(3)
N(3)-C(3)-Pt(1)	177.7(3)
N(4)-C(4)-Pt(1)	177.5(3)
N(5)-C(5)-Pt(2)	177.6(3)
N(6)-C(6)-Pt(2)	179.4(3)
C(1)-N(1)-Th(1)	171.5(2)
C(5)-N(5)-Th(1)	165.5(2)

Symmetry transformations used to generate equivalent atoms:

#1 -x+1/2,-y+1/2,-z #2 -x+1/2,-y-1/2,-z

**Crystallographic Table 8.** Anisotropic displacement parameters ( $\text{\AA}^2 \times 10^3$ ) for  $\text{Th}_2(\text{H}_2\text{O})_{10}(\text{OH})_2[\text{Pt}(\text{CN})_4]_3 \bullet 5\text{H}_2\text{O}$ . The anisotropic displacement factor exponent takes the form:  $-2\pi^2 [ h^2 a^*{}^2 U^{11} + \dots + 2 h k a^* b^* U^{12} ]$

	U <sup>11</sup>	U <sup>22</sup>	U <sup>33</sup>	U <sup>23</sup>	U <sup>13</sup>	U <sup>12</sup>
Th(1)	15(1)	15(1)	18(1)	1(1)	10(1)	1(1)
Pt(1)	21(1)	21(1)	19(1)	1(1)	12(1)	2(1)
Pt(2)	16(1)	16(1)	24(1)	0(1)	9(1)	2(1)
O(1)	19(1)	17(1)	33(1)	9(1)	15(1)	5(1)
O(2)	24(1)	38(1)	61(1)	26(1)	24(1)	11(1)
O(3)	32(1)	48(1)	25(1)	10(1)	8(1)	-2(1)
O(4)	44(1)	29(1)	23(1)	0(1)	13(1)	5(1)
O(5)	61(2)	39(1)	34(1)	-15(1)	32(1)	-23(1)
O(6)	23(1)	43(1)	29(1)	-3(1)	13(1)	-9(1)
O(7)	61(2)	42(2)	39(2)	0	18(2)	0
O(8)	41(1)	80(2)	32(1)	-5(1)	12(1)	9(1)
O(9)	45(2)	66(2)	36(1)	-4(1)	11(1)	6(1)
C(1)	23(1)	28(2)	23(1)	-1(1)	10(1)	-2(1)
C(2)	39(2)	30(2)	27(2)	-3(1)	20(1)	4(1)
C(3)	33(2)	27(2)	27(1)	6(1)	17(1)	6(1)
C(4)	29(2)	34(2)	28(2)	3(1)	15(1)	1(1)
C(5)	17(1)	23(1)	25(1)	-1(1)	7(1)	-2(1)
C(6)	22(1)	36(2)	37(2)	7(1)	13(1)	4(1)
N(1)	27(1)	41(2)	29(1)	-3(1)	18(1)	-1(1)
N(2)	90(2)	28(2)	55(2)	-1(1)	42(2)	-2(2)
N(3)	57(2)	55(2)	45(2)	11(1)	36(2)	23(2)
N(4)	57(2)	31(2)	60(2)	14(1)	25(2)	0(1)
N(5)	26(1)	20(1)	33(1)	-2(1)	11(1)	2(1)
N(6)	35(2)	97(3)	64(2)	31(2)	28(2)	6(2)

**Crystallographic Table 9.** Hydrogen coordinates ( $\times 10^4$ ) and isotropic displacement parameters ( $\text{\AA}^2 \times 10^3$ ) for  $\text{Th}_2(\text{H}_2\text{O})_{10}(\text{OH})_2[\text{Pt}(\text{CN})_4]_3 \bullet 5\text{H}_2\text{O}$ .

	x	y	z	U(eq)
H(1A)	3224	1161	599	32
H(2A)	-179	3287	-455	58
H(2B)	404	3789	-774	58
H(3A)	2634	1337	1739	54
H(3B)	1864	649	1548	54
H(4A)	1123	964	-1361	48
H(4B)	686	1975	-1548	48
H(5A)	2123	4017	890	61
H(5B)	2032	3478	1535	61
H(6A)	-392	931	-870	47
H(6B)	-316	1026	-127	47
H(7)	-404	3069	-2467	72
H(8A)	1693	-1006	1930	78
H(8B)	1195	-358	2164	78
H(9A)	-1049	5514	2794	76
H(9B)	-1483	6254	3064	76

**Crystallographic Table 10** Crystal data and structure refinement for U3,  
 $K_3[(UO_2)_2(OH)(Pt(CN)_4)_2]_2 \cdot NO_3 \cdot 1.5H_2O$ .

Identification code	U3
Empirical formula	$C_{16} H_5 K_3 N_{17} O_{14.50} Pt_4 U_4$
Formula weight	2517.15
Temperature	290(2) K
Wavelength	0.71073 Å
Crystal system, space group	Tetragonal, P 4/m b m
Unit cell dimensions	$a = 22.1073(2)$ Å $\alpha = 90^\circ$ . $b = 22.1073(2)$ Å $\beta = 90^\circ$ . $c = 12.6202(2)$ Å $\gamma = 90^\circ$ .
Volume	6167.90(13) Å <sup>3</sup>
Z, Calculated density	4, 2.711 Mg/m <sup>3</sup>
Absorption coefficient	19.750 mm <sup>-1</sup>
F(000)	4292
Crystal size	0.344 x 0.174 x 0.096 mm
Theta range for data collection	2.91 to 26.37 °.
Limiting indices	-27<=h<=27, -25<=k<=26, -15<=l<=15
Reflections collected / unique	6733 / 3423 [R(int) = 0.0564]
Completeness to theta = 26.37	99.7 %
Absorption correction	Semi-empirical from equivalents
Max. and min. transmission	1.00 and 0.31193
Refinement method	Full-matrix least-squares on F <sup>2</sup>
Data / restraints / parameters	3423 / 55 / 146
Goodness-of-fit on F <sup>2</sup>	1.058
Final R indices [I>2sigma(I)]	R1 = 0.0522, wR2 = 0.1500
R indices (all data)	R1 = 0.0687, wR2 = 0.1562
Largest diff. peak and hole	4.241 and -9.542 e. Å <sup>-3</sup>

**Crystallographic Table 11.** Atomic coordinates ( $\times 10^4$ ) and equivalent isotropic displacement parameters ( $\text{\AA}^2 \times 10^3$ ) for  $\text{K}_3[\text{(UO}_2)_2\text{(OH)(Pt(CN)}_4\text{)}_2\text{]}\cdot\text{NO}_3\cdot1.5\text{H}_2\text{O}$ . U(eq) is defined as one third of the trace of the orthogonalized  $U^{ij}$  tensor.

	x	y	z	U(eq)
K(1)	607(3)	5607(3)	0	51(2)
K(2)	3617(7)	3695(7)	-5000	152
U(1)	2379(1)	5072(1)	-1713(1)	19(1)
Pt(1)	1464(1)	6464(1)	-5000	22(1)
Pt(2)	1234(1)	3766(1)	-5000	22(1)
Pt(3)	2432(1)	2568(1)	-1276(1)	15(1)
C(1)	1902(7)	6004(6)	-3904(11)	22(3)
C(2)	1676(8)	4216(7)	-3896(12)	26(3)
C(3)	2423(7)	3463(7)	-1306(12)	24(3)
C(4)	3325(6)	2575(7)	-1294(11)	20(3)
N(1)	2118(7)	5718(6)	-3255(11)	39(3)
N(2)	1937(7)	4471(7)	-3235(11)	39(3)
N(3)	2409(7)	3985(6)	-1344(11)	39(3)
N(4)	2579(7)	6157(6)	-1344(11)	38(3)
N(5)	0	5000	-2660(20)	74(11)
O(1)	1634(5)	5159(5)	-1214(9)	36(2)
O(2)	3103(5)	5001(5)	-2198(9)	33(2)
O(3)	2746(8)	5044(7)	0	29(3)
O(4)	0	5000	-1682(19)	55(5)
O(5)	326(12)	5326(12)	-3270(30)	210(20)
O(6)	728(10)	4272(10)	0	63(6)
O(7)	0	0	5000	56(12)

**Crystallographic Table 12.** Bond lengths [ $\text{\AA}$ ] and angles [ $^\circ$ ] for  $\text{K}_3[(\text{UO}_2)_2(\text{OH})(\text{Pt}(\text{CN})_4)_2]_2 \cdot \text{NO}_3 \cdot 1.5\text{H}_2\text{O}$ .

K(1)-O(4)	2.848(19)
K(1)-O(4)#1	2.848(19)
K(1)-O(1)#2	2.912(12)
K(1)-O(1)#3	2.912(12)
K(1)-O(1)	2.912(12)
K(1)-O(1)#4	2.912(12)
K(1)-O(6)#1	2.96(3)
K(1)-O(6)	2.96(3)
K(1)-K(1)#1	3.80(2)
U(1)-O(2)	1.720(12)
U(1)-O(1)	1.774(12)
U(1)-O(3)	2.310(6)
U(1)-N(3)	2.449(14)
U(1)-N(1)	2.482(13)
U(1)-N(4)	2.483(14)
U(1)-N(2)	2.531(14)
Pt(1)-C(1)#5	1.971(15)
Pt(1)-C(1)#4	1.971(15)
Pt(1)-C(1)	1.971(15)
Pt(1)-C(1)#6	1.971(15)
Pt(2)-C(2)#7	1.971(15)
Pt(2)-C(2)	1.971(15)
Pt(2)-C(2)#8	1.971(15)
Pt(2)-C(2)#6	1.971(15)
Pt(3)-C(4)	1.975(14)
Pt(3)-C(4)#8	1.975(14)
Pt(3)-C(3)	1.978(15)
Pt(3)-C(3)#8	1.978(15)
Pt(3)-Pt(3)#2	3.2214(15)
C(1)-N(1)	1.139(19)
C(2)-N(2)	1.16(2)
C(3)-N(3)	1.16(2)

C(4)-N(4)#9	1.15(2)
N(4)-C(4)#10	1.15(2)
N(5)-O(4)	1.238(18)
N(5)-O(5)#11	1.279(18)
N(5)-O(5)	1.279(18)
O(3)-U(1)#2	2.310(6)
O(4)-K(1)#1	2.848(19)
O(6)-K(1)#1	2.96(3)
O(4)-K(1)-O(4)#1	96.4(7)
O(4)-K(1)-O(1)#2	126.8(3)
O(4)#1-K(1)-O(1)#2	79.3(3)
O(4)-K(1)-O(1)#3	126.8(3)
O(4)#1-K(1)-O(1)#3	79.3(3)
O(1)#2-K(1)-O(1)#3	104.7(5)
O(4)-K(1)-O(1)	79.3(3)
O(4)#1-K(1)-O(1)	126.8(3)
O(1)#2-K(1)-O(1)	63.5(5)
O(1)#3-K(1)-O(1)	143.8(6)
O(4)-K(1)-O(1)#4	79.3(3)
O(4)#1-K(1)-O(1)#4	126.8(3)
O(1)#2-K(1)-O(1)#4	143.8(6)
O(1)#3-K(1)-O(1)#4	63.5(5)
O(1)-K(1)-O(1)#4	104.7(5)
O(4)-K(1)-O(6)#1	64.7(3)
O(4)#1-K(1)-O(6)#1	64.7(3)
O(1)#2-K(1)-O(6)#1	143.8(3)
O(1)#3-K(1)-O(6)#1	65.9(4)
O(1)-K(1)-O(6)#1	143.8(3)
O(1)#4-K(1)-O(6)#1	65.9(4)
O(4)-K(1)-O(6)	64.7(3)
O(4)#1-K(1)-O(6)	64.7(3)
O(1)#2-K(1)-O(6)	65.9(4)
O(1)#3-K(1)-O(6)	143.8(3)
O(1)-K(1)-O(6)	65.9(4)
O(1)#4-K(1)-O(6)	143.8(3)

O(6)#1-K(1)-O(6)	100.3(9)
O(4)-K(1)-K(1)#1	48.2(4)
O(4)#1-K(1)-K(1)#1	48.2(4)
O(1)#2-K(1)-K(1)#1	108.1(3)
O(1)#3-K(1)-K(1)#1	108.1(3)
O(1)-K(1)-K(1)#1	108.1(3)
O(1)#4-K(1)-K(1)#1	108.1(3)
O(6)#1-K(1)-K(1)#1	50.1(4)
O(6)-K(1)-K(1)#1	50.1(4)
O(2)-U(1)-O(1)	179.1(5)
O(2)-U(1)-O(3)	90.2(5)
O(1)-U(1)-O(3)	89.8(5)
O(2)-U(1)-N(3)	87.3(5)
O(1)-U(1)-N(3)	93.7(5)
O(3)-U(1)-N(3)	77.6(5)
O(2)-U(1)-N(1)	89.4(5)
O(1)-U(1)-N(1)	90.0(5)
O(3)-U(1)-N(1)	146.2(5)
N(3)-U(1)-N(1)	136.1(5)
O(2)-U(1)-N(4)	89.4(5)
O(1)-U(1)-N(4)	89.7(5)
O(3)-U(1)-N(4)	77.8(5)
N(3)-U(1)-N(4)	155.1(5)
N(1)-U(1)-N(4)	68.5(5)
O(2)-U(1)-N(2)	92.3(5)
O(1)-U(1)-N(2)	88.2(5)
O(3)-U(1)-N(2)	146.2(5)
N(3)-U(1)-N(2)	68.9(5)
N(1)-U(1)-N(2)	67.5(5)
N(4)-U(1)-N(2)	135.9(5)
C(1)#5-Pt(1)-C(1)#4	89.1(8)
C(1)#5-Pt(1)-C(1)	178.0(9)
C(1)#4-Pt(1)-C(1)	90.8(8)
C(1)#5-Pt(1)-C(1)#6	90.8(8)
C(1)#4-Pt(1)-C(1)#6	178.0(9)
C(1)-Pt(1)-C(1)#6	89.1(8)

C(2)#7-Pt(2)-C(2)	179.3(10)
C(2)#7-Pt(2)-C(2)#8	90.0(8)
C(2)-Pt(2)-C(2)#8	90.0(8)
C(2)#7-Pt(2)-C(2)#6	90.0(8)
C(2)-Pt(2)-C(2)#6	90.0(8)
C(2)#8-Pt(2)-C(2)#6	179.3(10)
C(4)-Pt(3)-C(4)#8	90.8(9)
C(4)-Pt(3)-C(3)	90.1(6)
C(4)#8-Pt(3)-C(3)	178.0(6)
C(4)-Pt(3)-C(3)#8	178.0(6)
C(4)#8-Pt(3)-C(3)#8	90.1(6)
C(3)-Pt(3)-C(3)#8	88.9(9)
C(4)-Pt(3)-Pt(3)#2	90.6(4)
C(4)#8-Pt(3)-Pt(3)#2	90.6(4)
C(3)-Pt(3)-Pt(3)#2	91.1(4)
C(3)#8-Pt(3)-Pt(3)#2	91.1(4)
N(1)-C(1)-Pt(1)	175.3(15)
N(2)-C(2)-Pt(2)	178.8(15)
N(3)-C(3)-Pt(3)	178.3(15)
N(4)#9-C(4)-Pt(3)	177.5(13)
C(1)-N(1)-U(1)	168.5(15)
C(2)-N(2)-U(1)	172.8(15)
C(3)-N(3)-U(1)	171.4(13)
C(4)#10-N(4)-U(1)	166.7(13)
O(4)-N(5)-O(5)#11	127(2)
O(4)-N(5)-O(5)	127(2)
O(5)#11-N(5)-O(5)	106(5)
U(1)-O(1)-K(1)	161.3(6)
U(1)-O(3)-U(1)#2	138.7(8)
N(5)-O(4)-K(1)	138.2(4)
N(5)-O(4)-K(1)#1	138.2(4)
K(1)-O(4)-K(1)#1	83.6(7)
K(1)-O(6)-K(1)#1	79.7(9)

---

Symmetry transformations used to generate equivalent atoms:

#1 -x,-y+1,-z #2 x,y,-z #3 y-1/2,x+1/2,-z

#4 y-1/2,x+1/2,z #5 y-1/2,x+1/2,-z-1  
#6 x,y,-z-1 #7 -y+1/2,-x+1/2,-z-1  
#8 -y+1/2,-x+1/2,z #9 -y+1,x,z #10 y,-x+1,z  
#11 -x,-y+1,z

**Crystallographic Table 13.** Anisotropic displacement parameters ( $\text{\AA}^2 \times 10^3$ ) for  $\text{K}_3[(\text{UO}_2)_2(\text{OH})(\text{Pt}(\text{CN})_4)_2]_2 \bullet \text{NO}_3 \bullet 1.5\text{H}_2\text{O}$ . The anisotropic displacement factor exponent takes the form:  $-2\pi^2 [ h^2 a^{*2} U^{11} + \dots + 2 h k a^{*} b^{*} U^{12} ]$

	U <sup>11</sup>	U <sup>22</sup>	U <sup>33</sup>	U <sup>23</sup>	U <sup>13</sup>	U <sup>12</sup>
K(1)	50(3)	50(3)	53(5)	0	0	5(4)
U(1)	27(1)	11(1)	18(1)	0(1)	-2(1)	-1(1)
Pt(1)	25(1)	25(1)	14(1)	0	0	5(1)
Pt(2)	25(1)	25(1)	15(1)	0	0	-8(1)
Pt(3)	11(1)	11(1)	23(1)	0(1)	0(1)	0(1)
C(1)	36(9)	13(7)	17(6)	-5(5)	0(6)	-1(6)
C(2)	36(9)	22(8)	21(7)	4(6)	2(6)	-12(7)
C(3)	24(8)	16(5)	33(8)	-8(6)	1(7)	2(6)
C(4)	9(6)	27(8)	24(7)	4(6)	-5(5)	-1(5)
N(1)	55(10)	29(7)	33(6)	9(5)	-12(6)	0(7)
N(2)	53(9)	32(7)	30(6)	-2(5)	-11(6)	-13(7)
N(3)	58(10)	20(4)	39(7)	2(5)	-10(7)	2(5)
N(4)	55(10)	22(5)	36(7)	2(5)	-8(7)	-8(6)
N(5)	86(17)	86(17)	48(10)	0	0	20(20)
O(1)	31(5)	37(6)	41(6)	-4(5)	1(4)	0(4)
O(2)	34(5)	31(6)	35(5)	1(5)	1(4)	0(4)
O(3)	36(8)	29(8)	22(5)	0	0	-3(7)
O(4)	61(8)	61(8)	45(10)	0	0	-8(12)
O(5)	240(30)	240(30)	140(30)	100(20)	100(20)	20(40)
O(6)	54(8)	54(8)	83(18)	0	0	-16(10)
O(7)	72(19)	72(19)	22(17)	0	0	0

**Crystallographic Table 14.** Crystal data and structure refinement for  $\{U_2(H_2O)_{10}(O)[Pt(CN)_4]_3\} \cdot 4H_2O$  (U4) .

Identification code	U4
Empirical formula	C <sub>12</sub> N <sub>12</sub> O <sub>15</sub> Pt <sub>3</sub> U <sub>2</sub>
Formula weight	1613.57
Temperature	183(2) K
Wavelength	0.71073 Å
Crystal system, space group	Triclinic, P-1
Unit cell dimensions	a = 9.716(4) Å   α = 74.191(7) ° b = 9.823(4) Å   β = 70.734(7) ° c = 9.926(4) Å   γ = 67.242(7) °
Volume	813.2(6) Å <sup>3</sup>
Z, Calculated density	1, 3.295 Mg/m <sup>3</sup>
Absorption coefficient	22.857 mm <sup>-1</sup>
F(000)	694
Crystal size	0.10 x 0.10 x 0.10 mm
Theta range for data collection	2.28 to 28.31 deg.
Limiting indices	-12<=h<=12, -13<=k<=13, -13<=l<=13
Reflections collected / unique	7998 / 3940
[R(int) = 0.0582]	
Completeness to theta = 28.31	97.7 %
Absorption correction	Numerical
Max. and min. transmission	0.2083 and 0.2083
Refinement method	Full-matrix least-squares on F <sup>2</sup>
Data / restraints / parameters	3940 / 0 / 184
Goodness-of-fit on F <sup>2</sup>	1.103
Final R indices [I>2sigma(I)]	R1 = 0.0669, wR2 = 0.1618
R indices (all data)	R1 = 0.0781, wR2 = 0.1681
Largest diff. peak and hole	3.760 and -4.888 e. Å <sup>-3</sup>

**Crystallographic Table 15.** Atomic coordinates ( $\times 10^4$ ) and equivalent isotropic displacement parameters ( $\text{\AA}^2 \times 10^3$ ) for  $\{\text{U}_2(\text{H}_2\text{O})_{10}(\text{O})[\text{Pt}(\text{CN})_4]_3\} \cdot 4\text{H}_2\text{O}$ . U(eq) is defined as one third of the trace of the orthogonalized  $U_{ij}$  tensor.

	x	y	z	U(eq)
U(1)	3933(1)	-6003(1)	4254(1)	18(1)
N(1)	-3216(15)	2390(15)	3598(15)	27(3)
N(2)	2717(15)	-3189(14)	3459(16)	26(3)
N(3)	1899(12)	1804(13)	2245(13)	17(1)
N(4)	-2136(13)	-2455(13)	4513(13)	17(1)
N(5)	-1730(20)	3471(18)	9774(19)	45(4)
N(6)	-3250(20)	-370(20)	11280(20)	58(5)
Pt(1)	-140(1)	-286(1)	3396(1)	17(1)
Pt(2)	0	0	10000	24(1)
C(1)	-2092(16)	1456(14)	3509(16)	18(3)
C(2)	1741(18)	-2101(16)	3400(18)	24(3)
C(3)	1085(15)	1104(15)	2659(16)	17(1)
C(4)	-1371(17)	-1665(16)	4100(18)	26(3)
C(5)	-1080(20)	2204(19)	9828(19)	38(5)
C(6)	-2063(19)	-330(20)	10779(19)	32(4)
O(1)	5000	-5000	5000	28(4)
O(2)	5195(14)	-5176(13)	1741(13)	36(3)
O(3)	4603(16)	-7770(15)	6431(14)	40(3)
O(4)	4464(16)	-8043(18)	2930(19)	55(4)
O(5)	1764(15)	-4828(15)	6247(16)	45(3)
O(6)	1874(16)	-5401(15)	2975(17)	45(3)
O(7)	5120(20)	-2350(20)	600(20)	85(6)
O(8)	1570(30)	-5930(20)	9090(20)	89(7)

**Crystallographic Table 16.** Bond lengths [ $\text{\AA}$ ] and angles [ $^\circ$ ] for  $\{\text{U}_2(\text{H}_2\text{O})_{10}(\text{O})[\text{Pt}(\text{CN})_4]_3\} \cdot 4\text{H}_2\text{O}$ .

---

U(1)-O(1)	2.0706(7)
U(1)-O(2)	2.456(12)
U(1)-O(3)	2.473(12)
U(1)-O(4)	2.489(13)
U(1)-O(5)	2.509(12)
U(1)-O(6)	2.514(13)
U(1)-N(4)#1	2.543(12)
U(1)-N(2)	2.561(13)
U(1)-N(1)#2	2.565(13)
N(1)-C(1)	1.117(18)
N(1)-U(1)#3	2.565(13)
N(2)-C(2)	1.125(19)
N(3)-C(3)	1.148(19)
N(4)-C(4)	1.18(2)
N(4)-U(1)#1	2.543(12)
N(5)-C(5)	1.15(2)
N(6)-C(6)	1.11(2)
Pt(1)-C(4)	1.985(18)
Pt(1)-C(3)	1.989(14)
Pt(1)-C(1)	1.997(13)
Pt(1)-C(2)	2.000(15)
Pt(1)-Pt(2)	6.685(3)
Pt(2)-C(5)#4	1.995(17)
Pt(2)-C(5)	1.995(17)
Pt(2)-C(6)	2.014(18)
Pt(2)-C(6)#4	2.014(18)
O(1)-U(1)#5	2.0706(7)
O(1)-U(1)-O(2)	90.5(3)
O(1)-U(1)-O(3)	75.9(3)
O(2)-U(1)-O(3)	139.6(4)
O(1)-U(1)-O(4)	142.7(3)
O(2)-U(1)-O(4)	74.7(5)
O(3)-U(1)-O(4)	93.3(6)
O(1)-U(1)-O(5)	78.9(3)
O(2)-U(1)-O(5)	137.0(4)
O(3)-U(1)-O(5)	78.2(5)
O(4)-U(1)-O(5)	134.5(5)
O(1)-U(1)-O(6)	142.0(3)
O(2)-U(1)-O(6)	77.9(5)
O(3)-U(1)-O(6)	134.2(5)

O(4)-U(1)-O(6)	68.9(5)
O(5)-U(1)-O(6)	85.4(5)
O(1)-U(1)-N(4)#1	134.0(3)
O(2)-U(1)-N(4)#1	135.5(4)
O(3)-U(1)-N(4)#1	66.8(4)
O(4)-U(1)-N(4)#1	67.6(4)
O(5)-U(1)-N(4)#1	68.1(4)
O(6)-U(1)-N(4)#1	67.4(4)
O(1)-U(1)-N(2)	75.1(3)
O(2)-U(1)-N(2)	68.5(4)
O(3)-U(1)-N(2)	139.2(5)
O(4)-U(1)-N(2)	126.8(5)
O(5)-U(1)-N(2)	68.5(5)
O(6)-U(1)-N(2)	66.9(4)
N(4)#1-U(1)-N(2)	117.8(4)
O(1)-U(1)-N(1)#2	76.7(3)
O(2)-U(1)-N(1)#2	69.1(4)
O(3)-U(1)-N(1)#2	70.7(5)
O(4)-U(1)-N(1)#2	66.0(5)
O(5)-U(1)-N(1)#2	144.2(5)
O(6)-U(1)-N(1)#2	129.3(5)
N(4)#1-U(1)-N(1)#2	113.2(4)
N(2)-U(1)-N(1)#2	128.1(5)
C(1)-N(1)-U(1)#3	164.9(13)
C(2)-N(2)-U(1)	155.2(13)
C(4)-N(4)-U(1)#1	171.5(12)
C(4)-Pt(1)-C(3)	179.1(6)
C(4)-Pt(1)-C(1)	89.5(6)
C(3)-Pt(1)-C(1)	90.2(6)
C(4)-Pt(1)-C(2)	87.4(6)
C(3)-Pt(1)-C(2)	92.9(6)
C(1)-Pt(1)-C(2)	176.2(6)
C(4)-Pt(1)-Pt(2)	94.7(5)
C(3)-Pt(1)-Pt(2)	86.2(4)
C(1)-Pt(1)-Pt(2)	90.8(4)
C(2)-Pt(1)-Pt(2)	87.2(5)
C(5)#4-Pt(2)-C(5)	180.000(3)
C(5)#4-Pt(2)-C(6)	90.7(8)
C(5)-Pt(2)-C(6)	89.3(8)
C(5)#4-Pt(2)-C(6)#4	89.3(8)
C(5)-Pt(2)-C(6)#4	90.7(8)
C(6)-Pt(2)-C(6)#4	180.0(4)
C(5)#4-Pt(2)-Pt(1)	86.0(5)
C(5)-Pt(2)-Pt(1)	94.0(5)
C(6)-Pt(2)-Pt(1)	88.5(5)
C(6)#4-Pt(2)-Pt(1)	91.5(5)

N(1)-C(1)-Pt(1)	177.2(14)
N(2)-C(2)-Pt(1)	174.2(14)
N(3)-C(3)-Pt(1)	174.3(11)
N(4)-C(4)-Pt(1)	178.3(12)
N(5)-C(5)-Pt(2)	177.9(17)
N(6)-C(6)-Pt(2)	172.0(19)
U(1)-O(1)-U(1)#5	180.000(18)

---

Symmetry transformations used to generate equivalent atoms:

#1 -x,-y,-z+2 #2 x-1,y+1,z #3 -x,-y-1,-z+1  
#4 x+1,y-1,z #5 -x+1,-y-1,-z+1

**Crystallographic Table 17.** Anisotropic displacement parameters ( $\text{\AA}^2 \times 10^3$ ) for  $\{\text{U}_2(\text{H}_2\text{O})_{10}(\text{O})[\text{Pt}(\text{CN})_4]_3\} \cdot 4\text{H}_2\text{O}$ . The anisotropic displacement factor exponent takes the form:  $-2 \pi^2 [ h^2 a^{*2} U_{11} + \dots + 2 h k a^* b^* U_{12} ]$ .

	U11	U22	U33	U23	U13	U12
U(1)	12(1)	14(1)	28(1)	-7(1)	-3(1)	-2(1)
N(1)	27(7)	20(6)	32(7)	-14(5)	-7(6)	2(5)
N(2)	22(6)	19(6)	37(8)	-4(6)	-10(6)	-6(5)
N(3)	11(1)	14(1)	25(1)	-6(1)	-3(1)	-1(1)
N(4)	11(1)	14(1)	25(1)	-6(1)	-3(1)	-1(1)
N(5)	53(10)	29(8)	42(10)	-7(7)	-10(8)	-2(8)
N(6)	38(10)	66(13)	55(12)	3(10)	0(9)	-21(9)
Pt(1)	11(1)	14(1)	25(1)	-6(1)	-3(1)	-1(1)
Pt(2)	22(1)	23(1)	22(1)	-6(1)	-2(1)	-4(1)
C(1)	20(7)	11(6)	22(7)	-2(5)	-6(6)	-4(5)
C(2)	24(7)	20(7)	30(9)	-9(6)	-3(7)	-9(6)
C(3)	11(1)	14(1)	25(1)	-6(1)	-3(1)	-1(1)
C(4)	18(7)	18(7)	32(9)	-6(6)	-13(7)	9(6)
C(5)	44(10)	25(8)	30(9)	-8(7)	-9(8)	6(8)
C(6)	24(8)	36(9)	28(9)	-4(7)	-1(7)	-7(7)
O(1)	17(7)	11(6)	49(11)	-4(7)	-8(7)	2(6)
O(2)	36(7)	29(6)	32(7)	-3(5)	-2(6)	-4(5)
O(3)	46(8)	48(8)	37(8)	14(6)	-21(6)	-32(7)
O(4)	33(7)	63(9)	80(11)	-53(9)	5(7)	-16(7)
O(5)	36(7)	39(7)	50(9)	-17(6)	9(6)	-12(6)
O(6)	43(8)	36(7)	66(10)	1(7)	-34(7)	-14(6)
O(7)	72(13)	86(14)	102(16)	29(12)	-40(12)	-44(11)
O(8)	125(18)	83(14)	61(12)	-33(11)	-3(12)	-41(13)

**Crystallographic Table 18.** Crystal data and structure refinement for  $\{\text{Th}_2(\text{H}_2\text{O})_{10}(\text{OH})_2[\text{Pd}(\text{CN})_4]_3\cdot 8\text{H}_2\text{O}$ , Th5.

Identification code	Th5
Empirical formula	$\text{C}_{12}\text{N}_{12}\text{O}_{20}\text{Pd}_3\text{Th}_2$
Formula weight	1415.52
Temperature	183(2) K
Wavelength	0.71073 Å
Crystal system, space group	Triclinic, P-1
Unit cell dimensions	$a = 9.6141(6)$ Å $\alpha = 73.7480(10)$ ° $b = 9.9479(6)$ Å $\beta = 78.0950(10)$ ° $c = 11.1360(7)$ Å $\gamma = 68.6530(10)$ °
Volume	945.82(10) Å <sup>3</sup>
Z, Calculated density	1, 2.485 Mg/m <sup>3</sup>
Absorption coefficient	9.315 mm <sup>-1</sup>
F(000)	634
Crystal size	0.10 x 0.10 x 0.10 mm
Theta range for data collection	1.92 to 28.30 deg.
Limiting indices	-12<=h<=11, -13<=k<=13, -14<=l<=14
Reflections collected / unique	9619 / 4604 [R(int) = 0.0270]
Completeness to theta = 28.30	98.0 %
Absorption correction	None
Max. and min. transmission	0.4560 and 0.4560
Refinement method	Full-matrix least-squares on F <sup>2</sup>
Data / restraints / parameters	4604 / 0 / 223
Goodness-of-fit on F <sup>2</sup>	1.055
Final R indices [I>2sigma(I)]	R1 = 0.0282, wR2 = 0.0705
R indices (all data)	R1 = 0.0307, wR2 = 0.0715
Largest diff. peak and hole	1.971 and -1.153 e. Å <sup>-3</sup>

**Crystallographic Table 19.** Atomic coordinates ( $\times 10^4$ ) and equivalent isotropic displacement parameters ( $\text{\AA}^2 \times 10^3$ ) for  $\{\text{Th}_2(\text{H}_2\text{O})_{10}(\text{OH})_2[\text{Pd}(\text{CN})_4]_3\} \cdot 8\text{H}_2\text{O}$ . U(eq) is defined as one third of the trace of the orthogonalized  $U_{ij}$  tensor.

	x	y	z	U(eq)
Th(1)	14489(1)	4502(1)	3568(1)	14(1)
Pd(1)	10269(1)	6655(1)	-29(1)	15(1)
Pd(2)	10000	10000	0	19(1)
C(1)	11742(6)	5874(5)	1220(5)	19(1)
C(2)	11950(6)	6406(6)	-1433(5)	19(1)
C(3)	8729(6)	7455(6)	-1214(5)	22(1)
C(4)	8649(6)	6816(5)	1402(5)	20(1)
C(5)	12223(6)	9136(6)	-235(5)	23(1)
C(6)	10053(6)	9469(6)	1838(5)	25(1)
N(1)	12559(5)	5457(5)	1968(5)	26(1)
N(2)	12946(5)	6228(5)	-2209(5)	23(1)
N(3)	7840(6)	7917(6)	-1900(5)	35(1)
N(4)	7757(6)	6832(6)	2270(5)	32(1)
N(5)	13498(6)	8561(6)	-337(5)	32(1)
N(6)	10063(6)	9136(6)	2920(5)	35(1)
O(1)	15863(4)	5615(4)	4239(3)	15(1)
O(2)	14684(4)	2638(4)	2358(4)	24(1)
O(3)	12531(4)	3314(4)	4517(4)	25(1)
O(4)	15960(5)	1979(4)	4598(4)	30(1)
O(6)	12295(4)	6616(4)	4095(4)	29(1)
O(7)	14774(5)	6731(4)	1867(4)	33(1)
O(8)	6790(5)	9365(4)	3782(4)	30(1)
O(9)	10241(5)	6175(5)	6143(4)	35(1)
O(10)	4255(7)	9248(5)	2909(5)	51(1)
O(11)	9840(50)	9160(20)	5551(16)	460(20)

**Crystallographic Table 20.** Bond lengths [ $\text{\AA}$ ] and angles [ $^\circ$ ] for  $\{\text{Th}_2(\text{H}_2\text{O})_{10}(\text{OH})_2[\text{Pd}(\text{CN})_4]_3\} \cdot 8\text{H}_2\text{O}$ .

---

Th(1)-O(1)	2.337(3)
Th(1)-O(1)#1	2.371(3)
Th(1)-O(4)	2.468(4)
Th(1)-O(3)	2.482(4)
Th(1)-O(6)	2.484(4)
Th(1)-O(2)	2.516(3)
Th(1)-O(7)	2.541(4)
Th(1)-N(1)	2.579(5)
Th(1)-N(2)#2	2.582(5)
Th(1)-Th(1)#1	3.9858(4)
Pd(1)-C(3)	1.981(5)
Pd(1)-C(4)	1.982(5)
Pd(1)-C(1)	1.988(5)
Pd(1)-C(2)	2.000(5)
Pd(1)-Pd(2)	3.2511(4)
Pd(2)-C(6)	1.973(6)
Pd(2)-C(6)#3	1.973(6)
Pd(2)-C(5)	1.983(6)
Pd(2)-C(5)#3	1.983(6)
Pd(2)-Pd(1)#3	3.2511(4)
C(1)-N(1)	1.150(7)
C(2)-N(2)	1.147(7)
C(3)-N(3)	1.146(7)
C(4)-N(4)	1.152(7)
C(5)-N(5)	1.145(7)
C(6)-N(6)	1.157(8)
N(2)-Th(1)#2	2.582(4)
O(1)-Th(1)#1	2.371(3)

O(1)-Th(1)-O(1)#1	64.30(13)
O(1)-Th(1)-O(4)	93.27(13)
O(1)#1-Th(1)-O(4)	72.64(13)
O(1)-Th(1)-O(3)	137.15(12)
O(1)#1-Th(1)-O(3)	73.01(12)
O(4)-Th(1)-O(3)	77.08(14)
O(1)-Th(1)-O(6)	84.07(13)
O(1)#1-Th(1)-O(6)	69.66(12)
O(4)-Th(1)-O(6)	139.25(14)

O(3)-Th(1)-O(6)	77.70(13)
O(1)-Th(1)-O(2)	144.27(12)
O(1)#1-Th(1)-O(2)	131.48(12)
O(4)-Th(1)-O(2)	68.76(13)
O(3)-Th(1)-O(2)	70.67(13)
O(6)-Th(1)-O(2)	129.88(13)
O(1)-Th(1)-O(7)	70.53(12)
O(1)#1-Th(1)-O(7)	124.53(12)
O(4)-Th(1)-O(7)	141.48(15)
O(3)-Th(1)-O(7)	138.16(13)
O(6)-Th(1)-O(7)	75.43(14)
O(2)-Th(1)-O(7)	103.99(14)
O(1)-Th(1)-N(1)	133.45(13)
O(1)#1-Th(1)-N(1)	130.54(14)
O(4)-Th(1)-N(1)	132.15(14)
O(3)-Th(1)-N(1)	73.74(14)
O(6)-Th(1)-N(1)	68.24(14)
O(2)-Th(1)-N(1)	66.17(13)
O(7)-Th(1)-N(1)	66.76(14)
O(1)-Th(1)-N(2)#2	77.45(13)
O(1)#1-Th(1)-N(2)#2	125.54(13)
O(4)-Th(1)-N(2)#2	72.47(15)
O(3)-Th(1)-N(2)#2	135.05(14)
O(6)-Th(1)-N(2)#2	144.56(14)
O(2)-Th(1)-N(2)#2	67.87(13)
O(7)-Th(1)-N(2)#2	70.00(15)
N(1)-Th(1)-N(2)#2	103.85(15)
O(1)-Th(1)-Th(1)#1	32.41(8)
O(1)#1-Th(1)-Th(1)#1	31.90(8)
O(4)-Th(1)-Th(1)#1	81.72(10)
O(3)-Th(1)-Th(1)#1	104.84(9)
O(6)-Th(1)-Th(1)#1	74.50(10)
O(2)-Th(1)-Th(1)#1	150.45(9)
O(7)-Th(1)-Th(1)#1	98.15(9)
N(1)-Th(1)-Th(1)#1	142.17(10)
N(2)#2-Th(1)-Th(1)#1	102.61(10)
C(3)-Pd(1)-C(4)	89.6(2)
C(3)-Pd(1)-C(1)	177.5(2)
C(4)-Pd(1)-C(1)	87.9(2)
C(3)-Pd(1)-C(2)	92.1(2)
C(4)-Pd(1)-C(2)	177.6(2)
C(1)-Pd(1)-C(2)	90.4(2)
C(3)-Pd(1)-Pd(2)	90.37(15)
C(4)-Pd(1)-Pd(2)	85.76(14)
C(1)-Pd(1)-Pd(2)	89.07(14)

C(2)-Pd(1)-Pd(2)	95.97(14)
C(6)-Pd(2)-C(6)#3	180.00(9)
C(6)-Pd(2)-C(5)	89.3(2)
C(6)#3-Pd(2)-C(5)	90.7(2)
C(6)-Pd(2)-C(5)#3	90.7(2)
C(6)#3-Pd(2)-C(5)#3	89.3(2)
C(5)-Pd(2)-C(5)#3	180.00(16)
C(6)-Pd(2)-Pd(1)	91.79(16)
C(6)#3-Pd(2)-Pd(1)	88.21(16)
C(5)-Pd(2)-Pd(1)	81.32(15)
C(5)#3-Pd(2)-Pd(1)	98.68(15)
C(6)-Pd(2)-Pd(1)#3	88.21(16)
C(6)#3-Pd(2)-Pd(1)#3	91.79(16)
C(5)-Pd(2)-Pd(1)#3	98.68(15)
C(5)#3-Pd(2)-Pd(1)#3	81.32(15)
Pd(1)-Pd(2)-Pd(1)#3	180.0
N(1)-C(1)-Pd(1)	177.5(5)
N(2)-C(2)-Pd(1)	177.6(5)
N(3)-C(3)-Pd(1)	179.9(7)
N(4)-C(4)-Pd(1)	176.1(5)
N(5)-C(5)-Pd(2)	176.1(5)
N(6)-C(6)-Pd(2)	178.3(5)
C(1)-N(1)-Th(1)	177.5(5)
C(2)-N(2)-Th(1)#2	168.0(4)
Th(1)-O(1)-Th(1)#1	115.70(13)

---

Symmetry transformations used to generate equivalent atoms:

#1 -x+3,-y+1,-z+1 #2 -x+3,-y+1,-z  
#3 -x+2,-y+2,-z

**Crystallographic Table 21.** Anisotropic displacement parameters ( $\text{Å}^2 \times 10^3$ ) for  $\{\text{Th}_2(\text{H}_2\text{O})_{10}(\text{OH})_2[\text{Pd}(\text{CN})_4]_3\} \cdot 8\text{H}_2\text{O}$ . The anisotropic displacement factor exponent takes the form:  $-2 \pi^2 [ h^2 a^{*2} U_{11} + \dots + 2 h k a^* b^* U_{12} ]$

	U11	U22	U33	U23	U13	U12
Th(1)	11(1)	18(1)	11(1)	-3(1)	-1(1)	-4(1)
Pd(1)	11(1)	19(1)	13(1)	-4(1)	-1(1)	-4(1)
Pd(2)	18(1)	17(1)	19(1)	-3(1)	-3(1)	-3(1)
C(1)	18(2)	19(2)	19(2)	-3(2)	-3(2)	-7(2)
C(2)	14(2)	25(2)	19(3)	-4(2)	-3(2)	-8(2)
C(3)	20(3)	25(2)	24(3)	-9(2)	-2(2)	-8(2)
C(4)	17(2)	21(2)	23(3)	-4(2)	0(2)	-7(2)
C(5)	26(3)	24(2)	18(3)	-6(2)	-2(2)	-7(2)
C(6)	23(3)	26(2)	24(3)	-6(2)	-4(2)	-6(2)
N(1)	25(2)	27(2)	23(2)	-2(2)	-9(2)	-6(2)
N(2)	17(2)	28(2)	27(2)	-12(2)	1(2)	-8(2)
N(3)	34(3)	31(3)	40(3)	-7(2)	-17(3)	-5(2)
N(4)	32(3)	35(3)	29(3)	-11(2)	10(2)	-17(2)
N(5)	22(3)	36(3)	34(3)	-10(2)	-1(2)	-3(2)
N(6)	33(3)	39(3)	27(3)	-3(2)	-7(2)	-5(2)
O(1)	15(2)	22(2)	12(2)	-3(1)	-1(1)	-10(1)
O(2)	19(2)	28(2)	30(2)	-17(2)	-3(2)	-5(2)
O(3)	22(2)	29(2)	23(2)	1(2)	-4(2)	-13(2)
O(4)	36(2)	18(2)	26(2)	-2(2)	-9(2)	1(2)
O(6)	18(2)	32(2)	23(2)	-3(2)	1(2)	4(2)
O(7)	42(3)	32(2)	26(2)	10(2)	-19(2)	-18(2)
O(8)	32(2)	25(2)	28(2)	-4(2)	0(2)	-8(2)
O(9)	22(2)	55(3)	27(2)	-8(2)	-2(2)	-12(2)
O(10)	65(4)	34(2)	57(3)	-7(2)	-32(3)	-7(2)
O(11)	1090(80)	260(20)	119(14)	-52(15)	50(30)	-360(40)

**Crystallographic Table 22** Crystal data and structure refinement for U<sub>6</sub>{(UO<sub>2</sub>)<sub>2</sub>(DMSO)<sub>4</sub>(OH)<sub>2</sub>[Ni(CN)<sub>4</sub>]}.

Identification code	U6
Empirical formula	C <sub>24</sub> H <sub>48</sub> N <sub>8</sub> Ni <sub>2</sub> O <sub>20</sub> S <sub>8</sub> U <sub>4</sub>
Formula weight	2094.72
Temperature	183(2) K
Wavelength	0.71073 Å
Crystal system, space group	Monoclinic, C 2/c
Unit cell dimensions	a = 21.5224(11) Å α = 90 ° b = 10.2531(5) Å β = 111.9430(10)° c = 13.3170(6) Å γ = 90 °
Volume	2725.8(2) Å <sup>3</sup>
Z, Calculated density	2, 2.552 Mg/m <sup>3</sup>
Absorption coefficient	2.892 mm <sup>-1</sup>
F(000)	1920
Crystal size	0.10 x 0.10 x 0.10 mm
Theta range for data collection	2.04 to 28.32 °
Limiting indices	-28<=h<=25, -13<=k<=13, -12<=l<=17
Reflections collected / unique	10040 / 3358 [R(int) = 0.0292]
Completeness to theta = 28.32	98.9 %
Absorption correction	Empirical
Max. and min. transmission	0.3588 and 0.3588
Refinement method	Full-matrix least-squares on F <sup>2</sup>
Data / restraints / parameters	3358 / 0 / 146
Goodness-of-fit on F <sup>2</sup>	1.057
Final R indices [I>2sigma(I)]	R1 = 0.0298, wR2 = 0.0724
R indices (all data)	R1 = 0.0346, wR2 = 0.0746
Largest diff. peak and hole	1.937 and -1.110 e. Å <sup>-3</sup>

**Crystallographic Table 23.** Atomic coordinates ( $\times 10^4$ ) and equivalent isotropic displacement parameters ( $\text{\AA}^2 \times 10^3$ ) for  $\{(\text{UO}_2)_2(\text{DMSO})_4(\text{OH})_2[\text{Ni}(\text{CN})_4]\}$ . U(eq) is defined as one third of the trace of the orthogonalized  $U_{ij}$  tensor.

	x	y	z	U(eq)
Ni(1)	5000	7183(1)	2500	21(1)
U(1)	3110(1)	11034(1)	503(1)	20(1)
O(1)	3164(2)	11299(4)	1851(3)	27(1)
O(2)	3113(2)	10683(4)	-803(3)	32(1)
O(3)	2997(2)	13276(3)	186(4)	29(1)
O(5)	2493(2)	9073(3)	374(3)	27(1)
O(6)	4224(2)	11862(4)	1002(4)	34(1)
C(1)	4375(3)	8440(5)	1758(5)	26(1)
C(2)	4373(3)	5883(5)	1834(6)	32(1)
C(3)	1886(3)	9276(6)	1750(6)	39(2)
C(4)	2834(3)	7466(6)	2013(5)	37(1)
C(5)	5472(6)	11375(11)	1315(10)	86(3)
C(6)	4797(6)	13323(11)	17(10)	86(3)
S(1)	2159(1)	8211(1)	953(1)	29(1)
S(2)	4682(1)	11754(2)	354(1)	40(1)
N(1)	3979(2)	9209(4)	1294(4)	30(1)
N(2)	3995(3)	5090(5)	1436(6)	49(2)

**Crystallographic Table 24.** Bond lengths [ $\text{\AA}$ ] and angles [ $^\circ$ ] for  $\{(\text{UO}_2)_2(\text{DMSO})_4(\text{OH})_2[\text{Ni}(\text{CN})_4]\}$ .

---

Ni(1)-C(1)#1	1.858(5)
Ni(1)-C(1)	1.858(5)
Ni(1)-C(2)	1.868(6)
Ni(1)-C(2)#1	1.868(6)
U(1)-O(1)	1.776(4)
U(1)-O(2)	1.779(4)
U(1)-O(3)#2	2.321(4)
U(1)-O(3)	2.334(4)
U(1)-O(5)	2.380(4)
U(1)-O(6)	2.391(4)
U(1)-N(1)	2.577(5)
U(1)-U(1)#2	3.8853(4)
O(3)-U(1)#2	2.321(4)
O(5)-S(1)	1.520(4)
O(6)-S(2)	1.538(5)
C(1)-N(1)	1.156(7)
C(2)-N(2)	1.132(7)
C(3)-S(1)	1.769(7)
C(4)-S(1)	1.776(6)
C(5)-S(2)	1.748(12)
C(6)-S(2)	1.712(11)
C(1)#1-Ni(1)-C(1)	92.2(3)
C(1)#1-Ni(1)-C(2)	176.6(3)
C(1)-Ni(1)-C(2)	89.5(2)
C(1)#1-Ni(1)-C(2)#1	89.5(2)
C(1)-Ni(1)-C(2)#1	176.6(3)
C(2)-Ni(1)-C(2)#1	89.0(3)
O(1)-U(1)-O(2)	175.37(18)
O(1)-U(1)-O(3)#2	91.29(17)
O(2)-U(1)-O(3)#2	93.06(18)
O(1)-U(1)-O(3)	89.74(17)
O(2)-U(1)-O(3)	93.45(18)
O(3)#2-U(1)-O(3)	66.83(15)
O(1)-U(1)-O(5)	91.51(17)
O(2)-U(1)-O(5)	87.94(17)
O(3)#2-U(1)-O(5)	76.46(13)
O(3)-U(1)-O(5)	143.29(13)
O(1)-U(1)-O(6)	89.15(17)
O(2)-U(1)-O(6)	88.49(18)
O(3)#2-U(1)-O(6)	140.94(14)
O(3)-U(1)-O(6)	74.12(13)

O(5)-U(1)-O(6)	142.58(14)
O(1)-U(1)-N(1)	86.29(18)
O(2)-U(1)-N(1)	89.14(19)
O(3) <sup>#2</sup> -U(1)-N(1)	149.80(14)
O(3)-U(1)-N(1)	143.13(14)
O(5)-U(1)-N(1)	73.52(14)
O(6)-U(1)-N(1)	69.19(14)
O(1)-U(1)-U(1) <sup>#2</sup>	90.61(13)
O(2)-U(1)-U(1) <sup>#2</sup>	93.90(14)
O(3) <sup>#2</sup> -U(1)-U(1) <sup>#2</sup>	33.52(9)
O(3)-U(1)-U(1) <sup>#2</sup>	33.32(9)
O(5)-U(1)-U(1) <sup>#2</sup>	109.98(9)
O(6)-U(1)-U(1) <sup>#2</sup>	107.43(10)
N(1)-U(1)-U(1) <sup>#2</sup>	175.42(11)
U(1) <sup>#2</sup> -O(3)-U(1)	113.17(15)
S(1)-O(5)-U(1)	144.3(3)
S(2)-O(6)-U(1)	127.2(3)
N(1)-C(1)-Ni(1)	179.0(5)
N(2)-C(2)-Ni(1)	179.5(7)
O(5)-S(1)-C(3)	105.8(3)
O(5)-S(1)-C(4)	104.6(3)
C(3)-S(1)-C(4)	98.3(3)
O(6)-S(2)-C(6)	105.4(4)
O(6)-S(2)-C(5)	104.9(4)
C(6)-S(2)-C(5)	101.7(6)
C(1)-N(1)-U(1)	172.5(5)

---

Symmetry transformations used to generate equivalent atoms:  
#1 -x+1,y,-z+1/2 #2 -x+1/2,-y+5/2,-z

**Crystallographic Table 25.** Anisotropic displacement parameters ( $\text{\AA}^2 \times 10^3$ ) for  $\{(\text{UO}_2)_2(\text{DMSO})_4(\text{OH})_2[\text{Ni}(\text{CN})_4]\}$ . The anisotropic displacement factor exponent takes the form:  $-2\pi^2 [ h^2 a^{*2} U_{11} + \dots + 2 h k a^* b^* U_{12} ]$

	U11	U22	U33	U23	U13	U12
Ni(1)	14(1)	12(1)	29(1)	0	-1(1)	0
U(1)	17(1)	16(1)	24(1)	3(1)	2(1)	2(1)
O(1)	23(2)	33(2)	23(2)	-4(2)	7(2)	1(2)
O(2)	38(2)	32(2)	23(2)	3(2)	7(2)	0(2)
O(3)	17(2)	15(2)	47(2)	6(2)	2(2)	-1(1)
O(5)	27(2)	19(2)	33(2)	2(2)	9(2)	-2(1)
O(6)	23(2)	28(2)	46(3)	5(2)	9(2)	-1(2)
C(1)	19(2)	19(2)	34(3)	0(2)	4(2)	-5(2)
C(2)	22(3)	17(2)	47(4)	-2(2)	2(2)	4(2)
C(3)	40(4)	33(3)	48(4)	-1(3)	21(3)	7(3)
C(4)	42(4)	33(3)	41(4)	14(3)	22(3)	14(3)
C(5)	89(6)	80(5)	113(7)	34(5)	65(5)	28(4)
C(6)	89(6)	80(5)	113(7)	34(5)	65(5)	28(4)
S(1)	28(1)	20(1)	40(1)	-3(1)	13(1)	-4(1)
S(2)	29(1)	50(1)	38(1)	1(1)	10(1)	2(1)
N(1)	25(2)	19(2)	42(3)	3(2)	5(2)	4(2)
N(2)	25(3)	25(3)	82(5)	-15(3)	2(3)	-5(2)

**Crystallographic Table 26.** Hydrogen coordinates ( $\times 10^4$ ) and isotropic displacement parameters ( $\text{\AA}^2 \times 10^3$ ) for  $\{(\text{UO}_2)_2(\text{DMSO})_4(\text{OH})_2[\text{Ni}(\text{CN})_4]\}$ .

	x	y	z	U(eq)
H(3A)	1501	9781	1279	59
H(3B)	2250	9870	2152	59
H(3C)	1754	8765	2261	59
H(4A)	3051	6824	1707	55
H(4B)	2663	7028	2512	55
H(4C)	3160	8134	2406	55
H(5A)	5448	10551	1671	129
H(5B)	5618	12072	1856	129
H(5C)	5793	11289	956	129
H(6A)	4364	13702	-430	129
H(6B)	5095	13323	-389	129
H(6C)	5000	13841	679	129

**Crystallographic Table 27.** Crystal data and structure refinement for  $[\text{Th}(\text{C}_2\text{H}_6\text{SO})_8][\text{Fe}(\text{CN})_6] \cdot \text{NO}_3$ , Th8.

Identification code	Th8
Empirical formula	$\text{C}_{22}\text{H}_{48}\text{FeN}_7\text{O}_{11}\text{S}_8\text{Th}$
Formula weight	1131.08
Temperature	183(2) K
Wavelength	0.71073 Å
Crystal system, space group	Monoclinic, $P2_1/n$
Unit cell dimensions	$a = 11.9796(9)$ Å $\alpha = 90^\circ$ $b = 17.7389(13)$ Å $\beta = 90.117(2)^\circ$ $c = 20.0389(15)$ Å $\gamma = 90^\circ$
Volume	4258.4(5) Å <sup>3</sup>
Z, Calculated density	4, 3.446 Mg/m <sup>3</sup>
Absorption coefficient	4.276 mm <sup>-1</sup>
F(000)	3920
Crystal size	0.10 x 0.10 x 0.10 mm
Theta range for data collection	1.53 to 28.31 deg.
Limiting indices	-15≤h≤15, -23≤k≤23, -26≤l≤26
Reflections collected / unique	43457 / 10579 [R(int) = 0.0690]
Completeness to theta = 28.31	99.8 %
Absorption correction	None
Max. and min. transmission	0.2261 and 0.2261
Refinement method	Full-matrix least-squares on $F^2$
Data / restraints / parameters	10579 / 0 / 452
Goodness-of-fit on $F^2$	1.111
Final R indices [I>2sigma(I)]	R1 = 0.0840, wR2 = 0.2100
R indices (all data)	R1 = 0.1029, wR2 = 0.2164
Largest diff. peak and hole	9.836 and -2.858 e.Å <sup>-3</sup>

**Crystallographic Table 28.** Atomic coordinates ( $\times 10^4$ ) and equivalent isotropic displacement parameters ( $\text{\AA}^2 \times 10^3$ ) for  $[\text{Th}(\text{C}_2\text{H}_6\text{SO})_8][\text{Fe}(\text{CN})_6]\text{NO}_3$ . U(eq) is defined as one third of the trace of the orthogonalized  $U_{ij}$  tensor.

	x	y	z	U(eq)
Th(1)	7548(1)	2367(1)	935(1)	19(1)
Fe(1)	7372(2)	878(1)	-1612(1)	23(1)
S(1)	6844(3)	384(2)	1220(2)	29(1)
O(1)	7600(8)	1011(5)	965(5)	29(2)
C(1)	5757(11)	955(8)	-1711(7)	30(3)
N(1)	4803(11)	1001(8)	-1775(7)	46(3)
N(2)	7303(10)	1761(6)	-278(5)	31(2)
N(3)	9921(10)	747(9)	-1586(8)	53(4)
N(4)	7463(11)	-2(7)	-2944(6)	41(3)
N(5)	7662(12)	2377(8)	-2404(8)	54(4)
N(6)	7200(13)	-623(8)	-805(6)	47(3)
N(7)	7335(18)	6041(9)	709(9)	62(4)
S(2)	4765(3)	2705(2)	348(2)	37(1)
O(2)	5582(7)	2180(6)	722(5)	35(2)
C(2)	7315(10)	1441(7)	-777(6)	25(2)
O(3)	7174(10)	3327(6)	135(5)	40(2)
C(3)	8999(12)	815(8)	-1587(7)	37(3)
S(3)	7015(6)	3602(4)	-567(3)	83(2)
O(4)	6541(9)	3381(6)	1494(5)	40(2)
C(4)	7424(11)	322(7)	-2447(6)	28(3)
S(4)	6707(3)	4228(2)	1459(2)	37(1)
O(5)	6595(9)	1903(6)	1936(5)	42(3)
C(5)	7512(11)	1826(8)	-2095(6)	28(3)
S(5)	5443(3)	2130(2)	2197(2)	37(1)
O(6)	8968(9)	2030(6)	1739(6)	46(3)
C(6)	7254(12)	-69(8)	-1110(7)	34(3)
S(6)	9180(4)	1467(2)	2287(2)	44(1)
O(7)	9306(9)	2256(6)	357(6)	44(3)
C(7)	7511(11)	-457(7)	964(7)	27(2)
S(7)	9791(5)	1865(3)	-244(3)	67(1)
O(8)	8746(8)	3454(6)	1220(6)	47(3)
C(8)	5714(12)	362(9)	631(8)	39(3)
S(8)	9816(4)	3787(2)	955(2)	49(1)
C(9)	4242(14)	2116(11)	-294(7)	47(4)

O(9)	7583(17)	5917(8)	1287(8)	87(5)
C(10)	3544(14)	2720(12)	858(9)	56(5)
O(10)	8020(20)	6089(12)	281(12)	118(7)
C(11)	9290(20)	2069(14)	3016(9)	75(6)
O(11)	6360(16)	6028(10)	504(9)	88(5)
C(12)	10630(14)	1223(11)	2209(10)	57(5)
C(13)	5717(17)	2375(12)	3038(8)	58(5)
C(14)	4737(15)	1248(9)	2303(9)	48(4)
C(15)	6890(30)	4591(13)	-487(11)	130(15)
C(16)	7950(30)	3679(17)	-620(20)	280(40)
C(17)	5311(17)	4589(12)	1499(12)	68(6)
C(18)	7198(18)	4501(10)	2275(8)	54(5)
C(19)	10883(15)	3416(10)	1451(10)	54(4)
C(20)	9860(18)	4696(11)	1283(16)	98(10)
C(21)	9920(20)	884(11)	84(17)	108(12)
C(22)	11165(13)	2077(10)	-260(9)	50(4)

---

**Crystallographic Table 29.** Bond lengths [Å] and angles [°] for,  $[\text{Th}(\text{C}_2\text{H}_6\text{SO})_8][\text{Fe}(\text{CN})_6]\text{NO}_3$ .

---

Th(1)-O(3)	2.379(10)
Th(1)-O(1)	2.407(9)
Th(1)-O(7)	2.413(10)
Th(1)-O(2)	2.415(9)
Th(1)-O(6)	2.416(10)
Th(1)-O(4)	2.439(9)
Th(1)-O(5)	2.453(10)
Th(1)-O(8)	2.470(10)
Th(1)-N(2)	2.674(11)
Fe(1)-C(4)	1.944(13)
Fe(1)-C(5)	1.947(13)
Fe(1)-C(1)	1.950(14)
Fe(1)-C(2)	1.950(12)
Fe(1)-C(3)	1.952(15)
Fe(1)-C(6)	1.964(15)
S(1)-O(1)	1.523(9)
S(1)-C(7)	1.770(12)
S(1)-C(8)	1.795(14)
C(1)-N(1)	1.152(18)
N(2)-C(2)	1.149(16)
N(3)-C(3)	1.111(18)
N(4)-C(4)	1.150(17)
N(5)-C(5)	1.172(19)
N(6)-C(6)	1.158(19)
N(7)-O(10)	1.19(2)
N(7)-O(9)	1.22(2)
N(7)-O(11)	1.24(2)
S(2)-O(2)	1.544(10)
S(2)-C(9)	1.771(15)
S(2)-C(10)	1.787(17)
O(3)-S(3)	1.502(11)
O(3)-C(16)	1.88(4)
S(3)-C(16)	1.14(3)
S(3)-C(15)	1.77(2)
O(4)-S(4)	1.517(11)
S(4)-C(17)	1.792(19)
S(4)-C(18)	1.802(16)
O(5)-S(5)	1.530(11)
S(5)-C(13)	1.770(16)
S(5)-C(14)	1.793(16)
O(6)-S(6)	1.506(11)

S(6)-C(12)	1.797(17)
S(6)-C(11)	1.81(2)
O(7)-S(7)	1.508(12)
S(7)-C(22)	1.689(17)
S(7)-C(21)	1.87(2)
O(8)-S(8)	1.509(12)
S(8)-C(20)	1.742(19)
S(8)-C(19)	1.747(17)
O(3)-Th(1)-O(1)	137.4(3)
O(3)-Th(1)-O(7)	84.2(4)
O(1)-Th(1)-O(7)	84.7(3)
O(3)-Th(1)-O(2)	78.3(4)
O(1)-Th(1)-O(2)	83.8(3)
O(7)-Th(1)-O(2)	139.1(4)
O(3)-Th(1)-O(6)	139.3(4)
O(1)-Th(1)-O(6)	73.6(3)
O(7)-Th(1)-O(6)	71.7(4)
O(2)-Th(1)-O(6)	140.2(4)
O(3)-Th(1)-O(4)	71.9(3)
O(1)-Th(1)-O(4)	137.5(3)
O(7)-Th(1)-O(4)	135.5(4)
O(2)-Th(1)-O(4)	72.5(3)
O(6)-Th(1)-O(4)	103.0(4)
O(3)-Th(1)-O(5)	134.7(4)
O(1)-Th(1)-O(5)	69.9(3)
O(7)-Th(1)-O(5)	140.6(4)
O(2)-Th(1)-O(5)	69.1(4)
O(6)-Th(1)-O(5)	72.5(4)
O(4)-Th(1)-O(5)	68.9(3)
O(3)-Th(1)-O(8)	72.9(4)
O(1)-Th(1)-O(8)	139.4(3)
O(7)-Th(1)-O(8)	70.6(4)
O(2)-Th(1)-O(8)	135.6(3)
O(6)-Th(1)-O(8)	68.3(4)
O(4)-Th(1)-O(8)	66.8(3)
O(5)-Th(1)-O(8)	110.1(4)
O(3)-Th(1)-N(2)	69.9(3)
O(1)-Th(1)-N(2)	67.9(3)
O(7)-Th(1)-N(2)	68.0(4)
O(2)-Th(1)-N(2)	71.3(3)
O(6)-Th(1)-N(2)	125.7(4)
O(4)-Th(1)-N(2)	131.3(4)
O(5)-Th(1)-N(2)	123.9(4)
O(8)-Th(1)-N(2)	126.0(4)
C(4)-Fe(1)-C(5)	90.4(5)

C(4)-Fe(1)-C(1)	88.9(5)
C(5)-Fe(1)-C(1)	88.6(6)
C(4)-Fe(1)-C(2)	179.6(6)
C(5)-Fe(1)-C(2)	89.3(5)
C(1)-Fe(1)-C(2)	90.9(5)
C(4)-Fe(1)-C(3)	87.7(5)
C(5)-Fe(1)-C(3)	88.6(6)
C(1)-Fe(1)-C(3)	175.6(6)
C(2)-Fe(1)-C(3)	92.5(5)
C(4)-Fe(1)-C(6)	90.5(6)
C(5)-Fe(1)-C(6)	178.8(6)
C(1)-Fe(1)-C(6)	92.2(6)
C(2)-Fe(1)-C(6)	89.8(5)
C(3)-Fe(1)-C(6)	90.6(6)
O(1)-S(1)-C(7)	104.4(6)
O(1)-S(1)-C(8)	104.1(6)
C(7)-S(1)-C(8)	97.5(7)
S(1)-O(1)-Th(1)	136.2(5)
N(1)-C(1)-Fe(1)	179.4(14)
C(2)-N(2)-Th(1)	170.9(11)
O(10)-N(7)-O(9)	122(2)
O(10)-N(7)-O(11)	114(2)
O(9)-N(7)-O(11)	123(2)
O(2)-S(2)-C(9)	102.7(7)
O(2)-S(2)-C(10)	104.5(7)
C(9)-S(2)-C(10)	97.8(9)
S(2)-O(2)-Th(1)	128.3(6)
N(2)-C(2)-Fe(1)	178.2(12)
S(3)-O(3)-C(16)	37.2(6)
S(3)-O(3)-Th(1)	152.5(6)
C(16)-O(3)-Th(1)	133.1(12)
N(3)-C(3)-Fe(1)	176.8(14)
C(16)-S(3)-O(3)	89.7(17)
C(16)-S(3)-C(15)	88(2)
O(3)-S(3)-C(15)	104.4(9)
S(4)-O(4)-Th(1)	130.1(6)
N(4)-C(4)-Fe(1)	179.2(14)
O(4)-S(4)-C(17)	103.3(8)
O(4)-S(4)-C(18)	105.5(7)
C(17)-S(4)-C(18)	99.6(10)
S(5)-O(5)-Th(1)	127.8(6)
N(5)-C(5)-Fe(1)	175.4(13)
O(5)-S(5)-C(13)	103.0(8)
O(5)-S(5)-C(14)	103.7(7)
C(13)-S(5)-C(14)	100.9(9)
S(6)-O(6)-Th(1)	140.2(7)

N(6)-C(6)-Fe(1)	178.7(14)
O(6)-S(6)-C(12)	105.0(8)
O(6)-S(6)-C(11)	102.0(9)
C(12)-S(6)-C(11)	98.4(11)
S(7)-O(7)-Th(1)	139.4(7)
O(7)-S(7)-C(22)	106.9(8)
O(7)-S(7)-C(21)	100.3(10)
C(22)-S(7)-C(21)	97.8(10)
S(8)-O(8)-Th(1)	135.9(7)
O(8)-S(8)-C(20)	104.7(11)
O(8)-S(8)-C(19)	105.8(8)
C(20)-S(8)-C(19)	96.4(9)
S(3)-C(16)-O(3)	53.0(18)

---

**Crystallographic Table 30.** Anisotropic displacement parameters ( $\text{Å}^2 \times 10^3$ ) for  $[\text{Th}(\text{C}_2\text{H}_6\text{SO})_8][\text{Fe}(\text{CN})_6]\text{NO}_3$ . The anisotropic displacement factor exponent takes the form:  $-2 \pi^2 [ h^2 a^*{}^2 U_{11} + \dots + 2 h k a^* b^* U_{12} ]$

	U11	U22	U33	U23	U13	U12
Th(1)	20(1)	19(1)	18(1)	-2(1)	1(1)	0(1)
Fe(1)	27(1)	24(1)	18(1)	-3(1)	1(1)	0(1)
S(1)	30(2)	28(2)	27(2)	0(1)	3(1)	2(1)
O(1)	34(5)	21(4)	32(5)	-3(4)	5(4)	0(4)
C(1)	30(7)	33(7)	28(6)	-2(5)	0(5)	-3(5)
N(1)	34(7)	52(8)	52(8)	7(6)	-6(6)	-7(6)
N(2)	42(7)	28(6)	23(5)	-3(4)	2(5)	-3(5)
N(3)	24(6)	71(10)	65(10)	-13(8)	-2(6)	3(6)
N(4)	51(8)	40(7)	32(6)	-11(5)	0(6)	9(6)
N(5)	48(8)	37(7)	76(10)	10(7)	-23(7)	-1(6)
N(6)	70(10)	35(7)	36(7)	-1(6)	-1(6)	2(7)
N(7)	99(14)	34(8)	52(10)	-6(7)	12(10)	11(8)
S(2)	29(2)	39(2)	42(2)	-2(2)	-1(1)	1(1)
O(2)	21(4)	43(6)	42(5)	-5(4)	-3(4)	-2(4)
C(2)	31(6)	26(6)	19(6)	4(5)	3(5)	1(5)
O(3)	66(7)	31(5)	22(4)	2(4)	6(5)	3(5)
C(3)	41(8)	39(8)	30(7)	-14(6)	-8(6)	15(6)
S(3)	111(5)	93(5)	45(3)	16(3)	20(3)	17(4)
O(4)	44(6)	32(5)	44(6)	-9(4)	23(5)	-1(4)
C(4)	27(6)	30(7)	27(6)	-2(5)	-5(5)	3(5)
S(4)	48(2)	31(2)	33(2)	-2(1)	9(2)	4(2)
O(5)	55(7)	40(6)	31(5)	0(4)	20(5)	-1(5)
C(5)	30(6)	31(7)	22(6)	4(5)	3(5)	0(5)
S(5)	39(2)	38(2)	35(2)	5(2)	12(2)	4(2)
O(6)	46(6)	44(6)	49(6)	3(5)	-24(5)	-1(5)
C(6)	39(8)	36(8)	26(6)	-3(6)	5(5)	2(6)
S(6)	50(2)	41(2)	40(2)	7(2)	-7(2)	-12(2)
O(7)	33(5)	46(7)	51(6)	-5(5)	15(5)	2(5)
C(7)	28(6)	18(6)	34(6)	-3(5)	4(5)	1(5)
S(7)	63(3)	66(3)	71(3)	-3(3)	5(3)	3(3)
O(8)	30(5)	29(5)	80(8)	-12(5)	-5(5)	-1(4)
C(8)	28(7)	38(8)	50(9)	10(7)	-11(6)	-1(6)
S(8)	41(2)	46(2)	60(3)	6(2)	-5(2)	-13(2)
C(9)	48(9)	67(11)	27(7)	-8(7)	-13(6)	4(8)
O(9)	143(16)	51(9)	68(10)	2(7)	32(10)	13(9)
C(10)	38(8)	88(14)	42(9)	-10(9)	5(7)	15(9)
O(10)	140(19)	92(14)	121(17)	31(12)	34(15)	-6(13)

C(11)	108(18)	87(16)	31(9)	-2(9)	2(10)	-2(14)
O(11)	89(12)	90(12)	84(11)	-6(9)	-13(10)	29(10)
C(12)	37(9)	58(11)	76(13)	11(10)	1(8)	4(8)
C(13)	62(11)	83(14)	29(7)	-11(8)	-6(7)	10(10)
C(14)	52(10)	35(8)	57(10)	3(7)	19(8)	-4(7)
C(15)	270(40)	66(15)	57(13)	35(12)	70(20)	80(20)
C(16)	200(30)	180(30)	460(60)	280(40)	-320(40)	-190(30)
C(17)	65(13)	54(12)	86(15)	-4(11)	8(11)	19(10)
C(18)	93(14)	41(9)	29(8)	0(7)	-6(8)	6(9)
C(19)	51(10)	46(10)	64(11)	-2(8)	-14(9)	2(8)
C(20)	63(13)	36(10)	200(30)	-30(14)	-73(16)	6(9)
C(21)	81(15)	33(10)	210(30)	2(14)	97(19)	-7(10)
C(22)	38(8)	51(10)	62(11)	-4(8)	18(8)	1(7)

---

**Crystallographic Table 31.** Hydrogen coordinates ( $\times 10^4$ ) and isotropic displacement parameters ( $\text{\AA}^2 \times 10^3$ ) for  $[\text{Th}(\text{C}_2\text{H}_6\text{SO})_8][\text{Fe}(\text{CN})_6]\text{NO}_3$ .

	x	y	z	U(eq)
H(7A)	8180	-540	1237	40
H(7B)	7726	-414	494	40
H(7C)	6998	-883	1019	40
H(8A)	5228	798	703	58
H(8B)	5283	-103	692	58
H(8C)	6014	377	177	58
H(9A)	4820	2041	-633	71
H(9B)	3587	2353	-500	71
H(9C)	4028	1627	-105	71
H(10A)	3687	3026	1257	84
H(10B)	3353	2205	992	84
H(10C)	2922	2939	605	84
H(11A)	8544	2260	3133	113
H(11B)	9782	2495	2918	113
H(11C)	9590	1780	3391	113
H(12A)	10730	891	1823	85
H(12B)	10878	961	2614	85
H(12C)	11073	1682	2148	85
H(13A)	6106	2861	3053	87
H(13B)	6185	1987	3244	87
H(13C)	5011	2414	3281	87
H(14A)	4530	1045	1865	72
H(14B)	4062	1324	2570	72
H(14C)	5232	891	2531	72
H(15A)	6199	4712	-249	195
H(15B)	6871	4821	-932	195
H(15C)	7530	4787	-237	195
H(16A)	8305	3191	-703	424
H(16B)	8253	3890	-200	424
H(16C)	8113	4025	-985	424
H(17A)	4927	4490	1076	103
H(17B)	5335	5134	1580	103
H(17C)	4909	4341	1864	103
H(18A)	7976	4341	2329	81
H(18B)	6737	4260	2617	81
H(18C)	7149	5050	2321	81
H(19A)	11002	2886	1334	81

H(19B)	10673	3454	1922	81
H(19C)	11573	3701	1374	81
H(20A)	9299	5010	1060	148
H(20B)	10603	4912	1212	148
H(20C)	9702	4677	1763	148
H(21A)	9172	666	137	163
H(21B)	10298	894	517	163
H(21C)	10350	578	-230	163
H(22A)	11267	2582	-449	76
H(22B)	11560	1707	-536	76
H(22C)	11466	2065	195	76

---

**Crystallographic Table 32.** Crystal data and structure refinement for  $[\text{Th}(\text{C}_2\text{H}_6\text{SO})_9][\text{Pt}(\text{CN})_4]_2 \cdot 4\text{H}_2\text{O}$ , **Th7**.

Identification code	Th7
Empirical formula	$\text{C}_{40} \text{H}_{96} \text{N}_8 \text{O}_{16} \text{Pt}_4 \text{S}_{16} \text{Th}_2$
Formula weight	2702.65
Temperature	293(2) K
Wavelength	0.71073 Å
Crystal system, space group	Triclinic, P-1
Unit cell dimensions	$a = 12.4199(6)$ Å $\alpha = 102.0800(10)$ $b = 20.3265(10)$ Å $\beta = 98.2710(10)$ $c = 21.1132(10)$ Å $\gamma = 96.6940(10)$
Volume	5098.3(4) Å <sup>3</sup>
Z, Calculated density	2, 1.761 Mg/m <sup>3</sup>
Absorption coefficient	8.745 mm <sup>-1</sup>
F(000)	2536
Crystal size	0.01 x 0.01 x 0.01 mm
Theta range for data collection	1.00 to 28.32 deg.
Limiting indices	-16<=h<=16, -27<=k<=21, -28<=l<=28
Reflections collected / unique	43789 / 23889 [R(int) = 0.0646]
Completeness to theta = 28.32	94.0 %
Absorption correction	None
Refinement method	Full-matrix least-squares on F <sup>2</sup>
Data / restraints / parameters	23889 / 0 / 1031
Goodness-of-fit on F <sup>2</sup>	0.975
Final R indices [I>2sigma(I)]	R1 = 0.0582, wR2 = 0.1214
R indices (all data)	R1 = 0.1013, wR2 = 0.1447
Largest diff. peak and hole	2.651 and -1.963 e.Å <sup>-3</sup>

**Crystallographic Table 33.** Atomic coordinates ( $\times 10^4$ ) and equivalent isotropic displacement parameters ( $\text{\AA}^2 \times 10^3$ ) for  $[\text{Th}(\text{C}_2\text{H}_6\text{SO})_9][\text{Pt}(\text{CN})_4]_2 \cdot 4\text{H}_2\text{O}$ .  
 U(eq) is defined as one third of the trace of the orthogonalized  
 $U_{ij}$  tensor.

---

	x	y	z	U(eq)
Th(1)	4891(1)	7335(1)	2610(1)	24(1)
Pt(1)	3634(1)	396(1)	917(1)	32(1)
O(1)	4232(5)	7950(4)	3604(4)	32(2)
N(1)	9648(10)	7162(7)	757(7)	67(4)
O(1W)	56(12)	5711(10)	3913(8)	105(7)
Th(2)	9886(1)	2346(1)	2368(1)	22(1)
Pt(2)	1326(1)	9159(1)	4251(1)	37(1)
O(2)	5334(6)	6876(4)	3568(4)	33(2)
N(2)	7300(10)	4264(7)	771(7)	67(4)
O(2W)	4386(16)	3360(9)	1226(11)	132(9)
Pt(3)	6097(1)	4069(1)	4141(1)	32(1)
O(3)	5944(5)	8476(4)	3101(4)	35(2)
N(3)	5681(10)	379(6)	1956(6)	64(4)
O(3W)	4970(30)	730(20)	3738(18)	131(19)
Pt(4)	8438(1)	5726(1)	756(1)	34(1)
O(4)	5738(6)	7669(4)	1734(4)	40(2)
O(4W)	9070(30)	8505(16)	1388(17)	75(14)
O(5)	6910(6)	7282(4)	2838(3)	33(2)
O(6)	5299(6)	6201(4)	2189(4)	34(2)
S(7)	6035(2)	6360(1)	3766(1)	31(1)
O(7)	3717(5)	6791(4)	1538(3)	27(2)
S(8)	7618(2)	6902(2)	2393(2)	44(1)
O(8)	3204(6)	6695(4)	2746(3)	34(2)
S(9)	2812(2)	6599(2)	3377(1)	31(1)
O(9)	3614(6)	8075(4)	2304(3)	31(2)
S(10)	10915(2)	1435(1)	3576(1)	28(1)
C(10)	7110(10)	6877(6)	4389(6)	47(3)
S(11)	5391(2)	7770(2)	1045(2)	38(1)
O(11)	11782(5)	2199(4)	2639(3)	30(2)
C(11)	5262(9)	5992(6)	4262(5)	39(3)
S(12)	9335(2)	582(1)	1549(1)	31(1)
O(12)	10892(5)	3193(4)	1914(3)	28(2)
C(12)	2362(9)	7085(6)	609(5)	34(3)
S(13)	8167(2)	3672(2)	2697(2)	36(1)
O(13)	10523(5)	1828(4)	1328(3)	27(2)

---

C(13)	2251(9)	5725(5)	3178(6)	34(3)
S(14)	4985(2)	8248(2)	4255(2)	38(1)
O(14)	10463(6)	3355(4)	3269(3)	33(2)
S(15)	10318(2)	2093(2)	711(1)	30(1)
O(15)	10249(5)	1984(4)	3404(3)	25(2)
S(16)	2476(2)	6754(1)	1331(1)	30(1)
O(16)	8225(5)	2216(4)	2828(3)	30(2)
S(17)	7112(2)	8791(2)	3083(2)	37(1)
O(17)	8410(5)	1916(4)	1449(4)	34(2)
S(18)	4701(2)	5569(1)	1683(1)	33(1)
O(18)	8750(5)	3252(4)	2207(3)	28(2)
S(19)	2834(3)	8495(2)	2635(2)	43(1)
O(19)	9641(6)	1121(4)	2203(4)	32(2)
S(20)	10837(2)	3941(1)	1912(2)	34(1)
S(21)	7855(2)	1806(2)	3320(2)	35(1)
S(25)	7164(2)	1890(2)	1292(1)	30(1)
S(31)	12662(2)	1940(2)	2246(2)	41(1)
N(41)	-274(9)	7880(7)	4318(6)	63(4)
C(51)	7195(9)	3844(6)	4814(6)	35(3)
C(52)	5004(10)	3272(7)	4160(5)	37(3)
N(52)	4356(10)	2825(6)	4144(6)	62(3)
C(55)	7708(9)	4798(7)	756(6)	38(3)
C(56)	7318(10)	5781(6)	-3(7)	42(3)
C(59)	2364(9)	347(6)	196(6)	35(3)
N(59)	1631(9)	356(6)	-187(6)	58(3)
C(60)	7171(9)	4858(7)	4145(6)	38(3)
C(61)	5021(9)	4324(6)	3484(6)	35(3)
N(61)	4378(9)	1917(6)	905(6)	58(3)
N(62)	2934(10)	-1152(6)	850(5)	57(3)
C(62)	2216(10)	9138(7)	5108(7)	47(3)
N(63)	6687(9)	5831(6)	-430(5)	46(3)
C(63)	302(10)	8326(7)	4270(6)	41(3)
C(64)	9225(10)	6635(8)	739(7)	54(4)
N(65)	7830(9)	5318(6)	4140(6)	57(3)
C(65)	3176(10)	-562(7)	896(5)	39(3)
N(66)	4341(8)	4484(5)	3135(5)	45(3)
C(66)	4095(10)	1368(7)	919(7)	46(3)
N(67)	7821(9)	3730(6)	5224(5)	57(3)
C(67)	4921(9)	395(6)	1584(6)	33(3)
C(68)	2339(11)	9951(8)	4213(6)	50(4)
N(68)	2729(9)	9140(6)	5592(5)	57(3)
N(69)	2985(10)	10454(7)	4216(8)	75(4)
C(70)	10028(9)	932(6)	3944(6)	43(3)
C(71)	11645(8)	2219(7)	492(6)	43(3)
C(80)	2012(10)	5902(6)	935(5)	40(3)
C(81)	1558(9)	6947(6)	3351(7)	45(3)

C(82)	5149(10)	5656(6)	949(5)	41(3)
C(84)	6724(9)	1063(6)	789(6)	41(3)
C(85)	9734(10)	1344(6)	83(6)	46(3)
C(86)	11868(9)	1870(6)	4295(6)	42(3)
C(87)	6752(9)	3504(7)	2314(7)	58(4)
C(88)	6984(9)	2363(6)	678(6)	45(3)
C(89)	8238(10)	2388(7)	4112(5)	48(3)
C(90)	6417(9)	1796(7)	3214(6)	50(4)
S(99)	11012(3)	3568(2)	3986(1)	38(1)
N(100)	-68(10)	9246(6)	2919(6)	61(3)
N(101)	10196(10)	5616(6)	1932(6)	64(3)
C(201)	9543(10)	5683(6)	1512(6)	40(3)
C(202)	448(11)	9202(7)	3400(8)	53(4)
C(301)	8780(10)	7496(7)	2431(6)	52(4)
C(302)	7810(9)	8920(7)	3891(6)	46(3)
C(303)	4823(10)	9115(6)	4448(6)	46(3)
C(304)	12178(9)	4254(6)	1838(7)	47(3)
C(305)	10540(9)	191(6)	1511(7)	48(3)
C(306)	5464(10)	4925(6)	1864(7)	52(4)
C(307)	10149(10)	3925(7)	1112(6)	50(3)
C(308)	3392(13)	9337(6)	2668(6)	63(4)
C(309)	6996(10)	9641(6)	3069(7)	55(4)
C(310)	8437(11)	4514(6)	2599(7)	57(4)
C(311)	13671(10)	2652(7)	2354(6)	59(4)
C(312)	1673(10)	8400(8)	1998(7)	65(4)
C(313)	13381(10)	1466(7)	2738(6)	52(4)
C(314)	4240(13)	7961(7)	4843(7)	65(4)
C(315)	5704(13)	8648(7)	1109(9)	81(5)
C(316)	6462(15)	7515(10)	641(7)	99(7)
C(317)	12242(11)	4057(9)	4000(8)	80(5)
C(318)	10330(12)	4235(10)	4323(9)	110(8)
C(319)	8457(10)	-62(6)	1756(6)	43(3)
C(501)	8292(12)	6420(8)	2876(6)	68(5)

---

**Crystallographic Table 34.** Bond lengths [Å] and angles [°] for  $[\text{Th}(\text{C}_2\text{H}_6\text{SO})_9][\text{Pt}(\text{CN})_4]_2 \cdot 4\text{H}_2\text{O}$ .

---

Th(1)-O(2)	2.420(7)
Th(1)-O(8)	2.421(7)
Th(1)-O(9)	2.422(6)
Th(1)-O(6)	2.429(7)
Th(1)-O(4)	2.429(8)
Th(1)-O(3)	2.462(7)
Th(1)-O(7)	2.469(7)
Th(1)-O(1)	2.504(7)
Th(1)-O(5)	2.504(7)
Pt(1)-C(65)	1.954(13)
Pt(1)-C(67)	1.973(12)
Pt(1)-C(66)	1.992(14)
Pt(1)-C(59)	2.006(11)
O(1)-S(14)	1.511(8)
N(1)-C(64)	1.128(17)
Th(2)-O(17)	2.404(7)
Th(2)-O(11)	2.412(6)
Th(2)-O(16)	2.414(7)
Th(2)-O(19)	2.417(7)
Th(2)-O(12)	2.446(7)
Th(2)-O(14)	2.445(7)
Th(2)-O(15)	2.450(6)
Th(2)-O(18)	2.495(6)
Th(2)-O(13)	2.505(7)
Pt(2)-C(68)	1.947(17)
Pt(2)-C(202)	1.986(14)
Pt(2)-C(62)	1.992(12)
Pt(2)-C(63)	2.008(14)
O(2)-S(7)	1.524(7)
N(2)-C(55)	1.152(15)
Pt(3)-C(60)	1.960(13)
Pt(3)-C(61)	1.977(12)
Pt(3)-C(51)	1.987(13)
Pt(3)-C(52)	2.000(14)
O(3)-S(17)	1.526(7)
N(3)-C(67)	1.146(14)
Pt(4)-C(201)	1.974(12)
Pt(4)-C(56)	1.996(13)
Pt(4)-C(55)	1.996(14)
Pt(4)-C(64)	1.997(16)
O(4)-S(11)	1.521(8)

O(5)-S(8)	1.532(7)
O(6)-S(18)	1.522(8)
S(7)-C(11)	1.741(11)
S(7)-C(10)	1.791(10)
O(7)-S(16)	1.529(7)
S(8)-C(301)	1.751(13)
S(8)-C(501)	1.750(13)
O(8)-S(9)	1.524(7)
S(9)-C(13)	1.771(11)
S(9)-C(81)	1.782(10)
O(9)-S(19)	1.515(7)
S(10)-O(15)	1.536(7)
S(10)-C(86)	1.780(11)
S(10)-C(70)	1.783(12)
S(11)-C(315)	1.754(14)
S(11)-C(316)	1.752(14)
O(11)-S(31)	1.540(7)
S(12)-O(19)	1.539(8)
S(12)-C(319)	1.772(12)
S(12)-C(305)	1.779(11)
O(12)-S(20)	1.531(7)
C(12)-S(16)	1.784(10)
S(13)-O(18)	1.522(7)
S(13)-C(310)	1.766(12)
S(13)-C(87)	1.787(11)
O(13)-S(15)	1.512(7)
S(14)-C(303)	1.767(12)
S(14)-C(314)	1.800(14)
O(14)-S(99)	1.517(7)
S(15)-C(71)	1.778(10)
S(15)-C(85)	1.795(11)
S(16)-C(80)	1.748(12)
O(16)-S(21)	1.547(7)
S(17)-C(302)	1.751(11)
S(17)-C(309)	1.756(13)
O(17)-S(25)	1.528(7)
S(18)-C(82)	1.755(10)
S(18)-C(306)	1.775(10)
S(19)-C(308)	1.755(14)
S(19)-C(312)	1.786(13)
S(20)-C(304)	1.754(11)
S(20)-C(307)	1.772(12)
S(21)-C(90)	1.766(11)
S(21)-C(89)	1.799(12)
S(25)-C(84)	1.767(12)
S(25)-C(88)	1.773(11)

S(31)-C(311)	1.752(13)
S(31)-C(313)	1.778(12)
N(41)-C(63)	1.118(15)
C(51)-N(67)	1.158(14)
C(52)-N(52)	1.133(15)
C(56)-N(63)	1.135(14)
C(59)-N(59)	1.132(14)
C(60)-N(65)	1.172(15)
C(61)-N(66)	1.160(14)
N(61)-C(66)	1.137(15)
N(62)-C(65)	1.182(15)
C(62)-N(68)	1.123(15)
C(68)-N(69)	1.221(18)
S(99)-C(317)	1.717(14)
S(99)-C(318)	1.760(16)
N(100)-C(202)	1.147(16)
N(101)-C(201)	1.153(14)
O(2)-Th(1)-O(8)	73.2(2)
O(2)-Th(1)-O(9)	134.4(2)
O(8)-Th(1)-O(9)	81.1(2)
O(2)-Th(1)-O(6)	74.7(2)
O(8)-Th(1)-O(6)	82.2(3)
O(9)-Th(1)-O(6)	138.4(2)
O(2)-Th(1)-O(4)	140.4(2)
O(8)-Th(1)-O(4)	139.0(2)
O(9)-Th(1)-O(4)	81.8(2)
O(6)-Th(1)-O(4)	86.5(3)
O(2)-Th(1)-O(3)	95.7(3)
O(8)-Th(1)-O(3)	136.0(3)
O(9)-Th(1)-O(3)	77.5(2)
O(6)-Th(1)-O(3)	136.9(2)
O(4)-Th(1)-O(3)	74.6(3)
O(2)-Th(1)-O(7)	129.6(3)
O(8)-Th(1)-O(7)	68.6(2)
O(9)-Th(1)-O(7)	69.7(2)
O(6)-Th(1)-O(7)	68.8(2)
O(4)-Th(1)-O(7)	70.5(2)
O(3)-Th(1)-O(7)	134.7(2)
O(2)-Th(1)-O(1)	66.6(2)
O(8)-Th(1)-O(1)	70.4(2)
O(9)-Th(1)-O(1)	69.6(2)
O(6)-Th(1)-O(1)	137.3(2)
O(4)-Th(1)-O(1)	135.3(3)
O(3)-Th(1)-O(1)	66.3(2)
O(7)-Th(1)-O(1)	125.4(2)

O(2)-Th(1)-O(5)	69.7(2)
O(8)-Th(1)-O(5)	137.1(2)
O(9)-Th(1)-O(5)	141.3(3)
O(6)-Th(1)-O(5)	68.1(2)
O(4)-Th(1)-O(5)	71.1(2)
O(3)-Th(1)-O(5)	69.1(2)
O(7)-Th(1)-O(5)	122.8(2)
O(1)-Th(1)-O(5)	111.8(2)
C(65)-Pt(1)-C(67)	88.6(5)
C(65)-Pt(1)-C(66)	178.9(5)
C(67)-Pt(1)-C(66)	92.2(5)
C(65)-Pt(1)-C(59)	89.4(5)
C(67)-Pt(1)-C(59)	176.1(4)
C(66)-Pt(1)-C(59)	89.7(5)
S(14)-O(1)-Th(1)	122.9(4)
O(17)-Th(2)-O(11)	136.4(2)
O(17)-Th(2)-O(16)	73.9(2)
O(11)-Th(2)-O(16)	137.5(2)
O(17)-Th(2)-O(19)	74.1(2)
O(11)-Th(2)-O(19)	80.9(2)
O(16)-Th(2)-O(19)	82.5(2)
O(17)-Th(2)-O(12)	98.0(2)
O(11)-Th(2)-O(12)	76.2(2)
O(16)-Th(2)-O(12)	137.8(2)
O(19)-Th(2)-O(12)	136.2(2)
O(17)-Th(2)-O(14)	138.5(2)
O(11)-Th(2)-O(14)	82.2(2)
O(16)-Th(2)-O(14)	85.2(3)
O(19)-Th(2)-O(14)	138.8(2)
O(12)-Th(2)-O(14)	74.0(2)
O(17)-Th(2)-O(15)	129.4(2)
O(11)-Th(2)-O(15)	68.1(2)
O(16)-Th(2)-O(15)	69.4(2)
O(19)-Th(2)-O(15)	67.7(2)
O(12)-Th(2)-O(15)	132.5(2)
O(14)-Th(2)-O(15)	71.1(2)
O(17)-Th(2)-O(18)	69.6(2)
O(11)-Th(2)-O(18)	140.4(2)
O(16)-Th(2)-O(18)	68.6(2)
O(19)-Th(2)-O(18)	138.4(2)
O(12)-Th(2)-O(18)	69.8(2)
O(14)-Th(2)-O(18)	69.5(2)
O(15)-Th(2)-O(18)	123.6(2)
O(17)-Th(2)-O(13)	66.6(2)
O(11)-Th(2)-O(13)	71.6(2)
O(16)-Th(2)-O(13)	136.5(2)

O(19)-Th(2)-O(13)	70.1(2)
O(12)-Th(2)-O(13)	67.4(2)
O(14)-Th(2)-O(13)	137.3(2)
O(15)-Th(2)-O(13)	124.9(2)
O(18)-Th(2)-O(13)	111.5(2)
C(68)-Pt(2)-C(202)	89.7(5)
C(68)-Pt(2)-C(62)	89.2(5)
C(202)-Pt(2)-C(62)	178.8(6)
C(68)-Pt(2)-C(63)	178.3(5)
C(202)-Pt(2)-C(63)	90.0(5)
C(62)-Pt(2)-C(63)	91.1(5)
S(7)-O(2)-Th(1)	137.1(4)
C(60)-Pt(3)-C(61)	90.9(5)
C(60)-Pt(3)-C(51)	87.6(5)
C(61)-Pt(3)-C(51)	178.1(5)
C(60)-Pt(3)-C(52)	178.6(5)
C(61)-Pt(3)-C(52)	89.9(5)
C(51)-Pt(3)-C(52)	91.6(5)
S(17)-O(3)-Th(1)	132.2(4)
C(201)-Pt(4)-C(56)	179.3(5)
C(201)-Pt(4)-C(55)	89.2(5)
C(56)-Pt(4)-C(55)	91.2(5)
C(201)-Pt(4)-C(64)	90.0(5)
C(56)-Pt(4)-C(64)	89.6(5)
C(55)-Pt(4)-C(64)	177.3(5)
S(11)-O(4)-Th(1)	138.8(4)
S(8)-O(5)-Th(1)	128.8(4)
S(18)-O(6)-Th(1)	135.5(4)
O(2)-S(7)-C(11)	102.3(5)
O(2)-S(7)-C(10)	103.1(5)
C(11)-S(7)-C(10)	99.2(6)
S(16)-O(7)-Th(1)	129.1(4)
O(5)-S(8)-C(301)	105.2(5)
O(5)-S(8)-C(501)	104.4(5)
C(301)-S(8)-C(501)	95.8(7)
S(9)-O(8)-Th(1)	129.2(4)
O(8)-S(9)-C(13)	102.6(5)
O(8)-S(9)-C(81)	103.8(5)
C(13)-S(9)-C(81)	98.5(6)
S(19)-O(9)-Th(1)	136.6(4)
O(15)-S(10)-C(86)	103.9(5)
O(15)-S(10)-C(70)	104.6(4)
C(86)-S(10)-C(70)	98.7(6)
O(4)-S(11)-C(315)	105.5(7)
O(4)-S(11)-C(316)	103.2(6)
C(315)-S(11)-C(316)	97.9(8)

S(31)-O(11)-Th(2)	135.3(4)
O(19)-S(12)-C(319)	102.3(5)
O(19)-S(12)-C(305)	102.9(5)
C(319)-S(12)-C(305)	100.1(6)
S(20)-O(12)-Th(2)	134.5(4)
O(18)-S(13)-C(310)	105.4(6)
O(18)-S(13)-C(87)	104.6(6)
C(310)-S(13)-C(87)	97.0(6)
S(15)-O(13)-Th(2)	122.6(4)
O(1)-S(14)-C(303)	104.9(5)
O(1)-S(14)-C(314)	103.7(6)
C(303)-S(14)-C(314)	98.6(6)
S(99)-O(14)-Th(2)	141.3(4)
O(13)-S(15)-C(71)	103.8(5)
O(13)-S(15)-C(85)	103.7(5)
C(71)-S(15)-C(85)	98.5(6)
S(10)-O(15)-Th(2)	129.6(4)
O(7)-S(16)-C(80)	104.7(5)
O(7)-S(16)-C(12)	103.7(5)
C(80)-S(16)-C(12)	96.8(5)
S(21)-O(16)-Th(2)	133.3(4)
O(3)-S(17)-C(302)	104.6(5)
O(3)-S(17)-C(309)	103.8(5)
C(302)-S(17)-C(309)	98.7(7)
S(25)-O(17)-Th(2)	138.6(4)
O(6)-S(18)-C(82)	104.2(5)
O(6)-S(18)-C(306)	102.7(5)
C(82)-S(18)-C(306)	99.1(6)
S(13)-O(18)-Th(2)	128.8(4)
O(9)-S(19)-C(308)	103.9(6)
O(9)-S(19)-C(312)	103.7(6)
C(308)-S(19)-C(312)	98.9(7)
S(12)-O(19)-Th(2)	128.1(4)
O(12)-S(20)-C(304)	103.2(5)
O(12)-S(20)-C(307)	104.6(5)
C(304)-S(20)-C(307)	99.2(6)
O(16)-S(21)-C(90)	103.7(5)
O(16)-S(21)-C(89)	104.9(5)
C(90)-S(21)-C(89)	98.9(6)
O(17)-S(25)-C(84)	102.7(5)
O(17)-S(25)-C(88)	103.9(5)
C(84)-S(25)-C(88)	98.8(6)
O(11)-S(31)-C(311)	105.1(6)
O(11)-S(31)-C(313)	104.5(5)
C(311)-S(31)-C(313)	99.9(7)
N(67)-C(51)-Pt(3)	177.5(11)

N(52)-C(52)-Pt(3)	176.7(12)
N(2)-C(55)-Pt(4)	178.5(12)
N(63)-C(56)-Pt(4)	178.2(12)
N(59)-C(59)-Pt(1)	175.6(11)
N(65)-C(60)-Pt(3)	178.2(12)
N(66)-C(61)-Pt(3)	174.8(10)
N(68)-C(62)-Pt(2)	178.4(13)
N(41)-C(63)-Pt(2)	175.9(13)
N(1)-C(64)-Pt(4)	176.5(15)
N(62)-C(65)-Pt(1)	175.6(11)
N(61)-C(66)-Pt(1)	177.7(13)
N(3)-C(67)-Pt(1)	177.7(12)
N(69)-C(68)-Pt(2)	177.5(12)
O(14)-S(99)-C(317)	105.8(6)
O(14)-S(99)-C(318)	103.9(6)
C(317)-S(99)-C(318)	97.2(8)
N(101)-C(201)-Pt(4)	175.6(12)
N(100)-C(202)-Pt(2)	177.7(13)

---

**Crystallographic Table 35.** Anisotropic displacement parameters ( $\text{\AA}^2 \times 10^3$ ) for  $[\text{Th}(\text{C}_2\text{H}_6\text{SO})_9][\text{Pt}(\text{CN})_4]_2 \cdot 4\text{H}_2\text{O}$ . The anisotropic displacement factor exponent takes the form:  $-2 \pi^2 [ h^2 a^{*2} U_{11} + \dots + 2 h k a^* b^* U_{12} ]$

	U11	U22	U33	U23	U13	U12
Th(1)	27(1)	24(1)	21(1)	4(1)	7(1)	8(1)
Pt(1)	37(1)	32(1)	28(1)	5(1)	8(1)	9(1)
O(1)	30(4)	35(4)	32(4)	10(4)	10(3)	4(3)
N(1)	69(9)	51(8)	86(10)	28(8)	1(7)	18(7)
O(1W)	77(11)	129(17)	91(14)	5(12)	10(9)	-11(10)
Th(2)	23(1)	23(1)	21(1)	3(1)	5(1)	7(1)
Pt(2)	38(1)	40(1)	36(1)	9(1)	11(1)	18(1)
O(2)	42(4)	42(5)	24(4)	15(4)	13(3)	18(4)
N(2)	67(8)	53(8)	85(10)	25(8)	20(7)	9(6)
O(2W)	158(19)	86(15)	150(20)	46(14)	-7(14)	32(12)
Pt(3)	34(1)	34(1)	26(1)	3(1)	7(1)	7(1)
O(3)	25(4)	35(5)	39(5)	1(4)	8(3)	-6(3)
N(3)	69(8)	64(9)	63(9)	33(7)	1(7)	6(6)
O(3W)	110(30)	170(40)	120(30)	90(30)	-10(20)	10(20)
Pt(4)	36(1)	39(1)	29(1)	6(1)	7(1)	14(1)
O(4)	36(4)	47(5)	35(5)	5(4)	6(4)	3(4)
O(4W)	100(30)	50(20)	80(30)	22(19)	10(20)	4(17)
O(5)	34(4)	52(5)	15(4)	-2(4)	15(3)	17(4)
O(6)	49(5)	31(4)	22(4)	0(4)	14(4)	10(4)
S(7)	37(2)	33(2)	22(1)	4(1)	3(1)	11(1)
O(7)	28(4)	31(4)	21(4)	0(3)	6(3)	10(3)
S(8)	30(2)	49(2)	48(2)	-5(2)	6(1)	12(1)
O(8)	35(4)	52(5)	17(4)	9(4)	14(3)	2(4)
S(9)	31(1)	36(2)	28(2)	8(1)	9(1)	4(1)
O(9)	47(4)	32(4)	17(4)	3(3)	15(3)	19(3)
S(10)	29(1)	27(2)	28(2)	2(1)	4(1)	10(1)
C(10)	58(8)	41(8)	23(6)	-10(6)	-21(6)	-2(6)
S(11)	39(2)	48(2)	28(2)	11(2)	8(1)	-3(1)
O(11)	29(4)	44(5)	20(4)	2(4)	9(3)	11(3)
C(11)	60(8)	48(8)	23(6)	15(6)	23(6)	24(6)
S(12)	33(1)	25(1)	32(2)	3(1)	1(1)	4(1)
O(12)	39(4)	27(4)	23(4)	10(3)	14(3)	11(3)
C(12)	44(7)	35(7)	25(6)	8(5)	8(5)	11(5)
S(13)	42(2)	41(2)	36(2)	14(2)	16(1)	25(1)

O(13)	25(4)	35(4)	23(4)	6(3)	10(3)	12(3)
C(13)	39(6)	31(6)	36(7)	10(6)	11(5)	11(5)
S(14)	45(2)	38(2)	32(2)	4(1)	5(1)	20(1)
O(14)	45(4)	29(4)	20(4)	-9(3)	3(3)	11(3)
S(15)	31(1)	35(2)	28(2)	9(1)	7(1)	12(1)
O(15)	32(4)	35(4)	13(4)	5(3)	12(3)	14(3)
S(16)	33(1)	31(2)	27(2)	9(1)	5(1)	7(1)
O(16)	29(4)	43(5)	23(4)	7(4)	11(3)	16(3)
S(17)	35(2)	38(2)	33(2)	-5(1)	14(1)	0(1)
O(17)	24(4)	40(5)	33(5)	0(4)	2(3)	8(3)
S(18)	39(2)	29(2)	32(2)	3(1)	13(1)	10(1)
O(18)	38(4)	34(4)	19(4)	1(3)	19(3)	19(3)
S(19)	64(2)	46(2)	30(2)	13(2)	23(2)	34(2)
O(19)	44(4)	27(4)	28(4)	8(4)	8(3)	10(3)
S(20)	45(2)	25(2)	34(2)	8(1)	17(1)	8(1)
S(21)	37(2)	37(2)	39(2)	13(2)	21(1)	11(1)
S(25)	24(1)	37(2)	31(2)	10(1)	4(1)	9(1)
S(31)	25(1)	54(2)	35(2)	-8(2)	3(1)	8(1)
N(41)	48(7)	71(9)	67(9)	24(8)	-4(6)	1(6)
C(51)	46(7)	31(6)	24(6)	-12(5)	24(5)	2(5)
C(52)	52(7)	42(8)	17(6)	-4(6)	20(5)	18(6)
N(52)	77(9)	54(8)	49(8)	18(7)	-4(6)	-8(7)
C(55)	45(7)	51(8)	26(6)	8(6)	28(5)	21(6)
C(56)	44(7)	39(8)	48(8)	10(7)	15(6)	12(6)
C(59)	40(6)	37(7)	23(6)	-11(5)	5(5)	12(5)
N(59)	45(6)	52(7)	66(9)	-12(6)	0(6)	22(5)
C(60)	29(6)	50(8)	37(7)	14(6)	6(5)	10(6)
C(61)	37(6)	43(7)	28(6)	3(6)	24(5)	6(5)
N(61)	58(7)	37(7)	83(10)	12(7)	23(7)	18(6)
N(62)	91(9)	42(7)	38(7)	14(6)	10(6)	10(6)
C(62)	39(7)	51(8)	56(9)	25(7)	-4(6)	13(6)
N(63)	60(7)	56(7)	21(5)	5(5)	4(5)	24(6)
C(63)	37(7)	55(9)	35(7)	11(7)	11(6)	20(6)
C(64)	39(7)	70(11)	66(10)	32(9)	9(7)	32(7)
N(65)	44(6)	57(8)	77(9)	32(7)	13(6)	3(6)
C(65)	49(7)	55(9)	23(6)	26(6)	10(5)	17(6)
N(66)	49(6)	53(7)	36(6)	12(6)	8(5)	13(5)
C(66)	36(7)	48(9)	44(8)	-7(7)	4(6)	-3(6)
N(67)	67(8)	72(9)	41(7)	19(7)	4(6)	37(7)
C(67)	40(6)	38(7)	26(6)	6(6)	21(5)	10(5)
C(68)	49(8)	84(11)	22(7)	1(7)	17(6)	40(8)
N(68)	52(7)	81(9)	33(7)	-4(6)	4(5)	20(6)
N(69)	56(8)	56(9)	118(13)	29(9)	15(8)	19(7)
C(70)	50(7)	41(8)	45(8)	15(7)	15(6)	20(6)
C(71)	29(6)	69(9)	40(8)	15(7)	25(5)	12(6)
C(80)	55(8)	46(8)	22(6)	6(6)	24(6)	3(6)

C(81)	40(7)	47(8)	64(9)	23(7)	31(6)	23(6)
C(82)	61(8)	54(8)	14(6)	-2(6)	27(5)	19(6)
C(84)	33(6)	35(7)	53(8)	12(6)	-5(6)	2(5)
C(85)	55(8)	35(7)	33(7)	-7(6)	-9(6)	4(6)
C(86)	53(7)	44(8)	28(7)	7(6)	-1(6)	11(6)
C(87)	24(6)	62(10)	85(12)	9(9)	7(7)	16(6)
C(88)	45(7)	49(8)	46(8)	22(7)	0(6)	14(6)
C(89)	75(9)	57(9)	12(6)	-10(6)	31(6)	9(7)
C(90)	46(7)	74(10)	37(8)	3(7)	33(6)	16(7)
S(99)	52(2)	35(2)	23(2)	2(1)	4(1)	2(1)
N(100)	64(8)	77(9)	53(8)	32(7)	12(6)	26(7)
N(101)	64(8)	71(9)	50(8)	9(7)	-11(6)	13(7)
C(201)	45(7)	38(7)	33(7)	-4(6)	4(6)	18(6)
C(202)	52(8)	48(9)	65(10)	15(8)	13(7)	27(7)
C(301)	55(8)	57(9)	42(8)	-9(7)	29(7)	9(7)
C(302)	42(7)	69(10)	27(7)	1(7)	16(6)	19(6)
C(303)	67(9)	43(8)	31(7)	0(6)	22(6)	19(6)
C(304)	35(6)	42(8)	59(9)	8(7)	11(6)	-5(5)
C(305)	45(7)	40(8)	62(9)	8(7)	10(6)	21(6)
C(306)	69(9)	13(6)	81(11)	13(7)	22(8)	20(6)
C(307)	67(9)	47(8)	45(8)	22(7)	11(7)	20(7)
C(308)	118(13)	38(8)	31(8)	-11(7)	15(8)	30(8)
C(309)	52(8)	42(8)	66(10)	15(8)	5(7)	-9(6)
C(310)	67(9)	33(8)	77(11)	14(8)	12(8)	26(7)
C(311)	57(8)	79(11)	33(8)	-8(8)	31(7)	-7(7)
C(312)	42(8)	77(11)	75(11)	4(9)	0(7)	33(7)
C(313)	50(8)	65(10)	46(8)	1(7)	24(6)	32(7)
C(314)	122(13)	34(8)	47(9)	23(7)	16(9)	26(8)
C(315)	105(13)	53(10)	98(14)	37(11)	26(11)	25(9)
C(316)	163(18)	132(18)	32(9)	23(11)	67(11)	70(14)
C(317)	50(9)	105(15)	68(12)	5(11)	-4(8)	-9(9)
C(318)	55(10)	139(18)	91(14)	-68(13)	-12(9)	33(10)
C(319)	59(8)	41(8)	24(6)	1(6)	6(6)	7(6)
C(501)	102(12)	90(12)	38(8)	18(8)	62(8)	58(10)

**Crystallographic Table 36.** Hydrogen coordinates ( $\times 10^4$ ) and isotropic displacement parameters ( $\text{\AA}^2 \times 10^3$ ) for  $[\text{Th}(\text{C}_2\text{H}_6\text{SO})_9][\text{Pt}(\text{CN})_4]_2 \cdot 4\text{H}_2\text{O}$ .

	x	y	z	U(eq)
H(10A)	7603	7136	4189	70
H(10B)	7509	6591	4613	70
H(10C)	6796	7181	4698	70
H(11A)	4636	5689	3992	59
H(11B)	5015	6342	4563	59
H(11C)	5707	5741	4505	59
H(12A)	2609	7567	729	51
H(12B)	1608	6997	393	51
H(12C)	2808	6869	317	51
H(13A)	2836	5456	3169	52
H(13B)	1786	5614	2754	52
H(13C)	1826	5632	3504	52
H(70A)	9445	660	3612	64
H(70B)	9722	1225	4267	64
H(70C)	10441	641	4152	64
H(71A)	12091	2602	800	65
H(71B)	11574	2302	58	65
H(71C)	11985	1819	500	65
H(80A)	2019	5629	1255	60
H(80B)	2486	5750	631	60
H(80C)	1275	5858	700	60
H(81A)	1718	7434	3441	68
H(81B)	1164	6814	3675	68
H(81C)	1116	6779	2922	68
H(82A)	4804	5999	784	62
H(82B)	4955	5231	630	62
H(82C)	5934	5787	1033	62
H(84A)	6782	734	1054	62
H(84B)	7178	979	458	62
H(84C)	5972	1026	582	62
H(85A)	8987	1206	127	68
H(85B)	10155	984	129	68
H(85C)	9747	1441	-342	68
H(86A)	12420	2173	4179	63
H(86B)	12212	1546	4492	63
H(86C)	11486	2127	4602	63
H(87A)	6452	3045	2309	87

H(87B)	6694	3561	1871	87
H(87C)	6350	3815	2555	87
H(88A)	7185	2839	877	68
H(88B)	6227	2274	466	68
H(88C)	7441	2231	358	68
H(89A)	9020	2440	4251	73
H(89B)	7869	2213	4425	73
H(89C)	8029	2822	4082	73
H(90A)	6077	1503	2798	76
H(90B)	6257	2249	3226	76
H(90C)	6133	1631	3561	76
H(30V)	9261	7289	2158	78
H(30W)	9160	7645	2877	78
H(30X)	8555	7880	2278	78
H(30Y)	7945	8491	3982	69
H(30Z)	7368	9129	4191	69
H(31D)	8498	9212	3945	69
H(30A)	5199	9352	4175	69
H(30B)	5128	9311	4902	69
H(30C)	4055	9154	4370	69
H(30D)	12666	4297	2245	70
H(30E)	12189	4692	1733	70
H(30F)	12415	3945	1494	70
H(30G)	11095	485	1387	72
H(30H)	10368	-235	1191	72
H(30I)	10808	112	1935	72
H(30J)	5299	4812	2262	78
H(30K)	6237	5087	1919	78
H(30L)	5269	4527	1509	78
H(30M)	9376	3778	1078	75
H(30N)	10439	3616	793	75
H(30O)	10261	4373	1031	75
H(30P)	4055	9467	2990	95
H(30Q)	2870	9634	2787	95
H(30R)	3558	9372	2245	95
H(30S)	6610	9660	2647	82
H(30T)	7717	9902	3148	82
H(30U)	6598	9825	3405	82
H(31E)	9185	4705	2794	86
H(31F)	7948	4784	2811	86
H(31G)	8324	4512	2139	86
H(31H)	13403	2955	2096	88
H(31I)	14325	2507	2215	88
H(31J)	13837	2884	2810	88
H(31K)	1274	7948	1911	98
H(31L)	1920	8478	1606	98

H(31M)	1200	8724	2136	98
H(31N)	12909	1056	2738	77
H(31O)	13599	1733	3180	77
H(31P)	14023	1350	2561	77
H(31Q)	4251	7483	4804	97
H(31R)	3492	8042	4759	97
H(31S)	4579	8206	5279	97
H(31T)	5202	8881	1345	121
H(31U)	5639	8736	677	121
H(31V)	6444	8808	1340	121
H(31W)	6377	7027	526	149
H(31X)	7155	7692	926	149
H(31Y)	6439	7686	249	149
H(31Z)	12731	3774	3807	120
H(32A)	12566	4275	4447	120
H(32B)	12118	4397	3754	120
H(32C)	9596	4053	4354	166
H(32D)	10300	4553	4045	166
H(32E)	10722	4462	4753	166
H(31A)	7758	85	1799	64
H(31B)	8785	-150	2164	64
H(31C)	8351	-471	1415	64
H(50A)	7776	6049	2920	102
H(50B)	8598	6702	3303	102
H(50C)	8872	6244	2669	102

---

**Crystallographic Table 37** Crystal data and structure refinement for **Usalzine**.

Identification code	Usalzine
Empirical formula	C <sub>25</sub> H <sub>26</sub> N <sub>4</sub> O <sub>7</sub> S <sub>2</sub> U
Formula weight	796.65
Temperature	182(2) K
Wavelength	0.71073 Å
Crystal system, space group	Monoclinic, P2(1)/n
Unit cell dimensions	a = 8.6053(18) Å α = 90 ° b = 20.457(4) Å β = 101.532(3) ° c = 16.111(3) Å γ = 90 °
Volume	2778.9(10) Å <sup>3</sup>
Z, Calculated density	4, 1.904 Mg/m <sup>3</sup>
Absorption coefficient	6.042 mm <sup>-1</sup>
F(000)	1536
Crystal size	0.17 x 0.13 x 0.10 mm
Theta range for data collection	1.63 to 24.75 deg.
Limiting indices	-10<=h<=9, -24<=k<=24, -18<=l<=18
Reflections collected / unique	40617 / 4727 [R(int) = 0.0754]
Completeness to theta = 24.75	99.5 %
Absorption correction	None
Max. and min. transmission	0.5918 and 0.4178
Refinement method	Full-matrix least-squares on F <sup>2</sup>
Data / restraints / parameters	4727 / 12 / 351
Goodness-of-fit on F <sup>2</sup>	1.105
Final R indices [I>2sigma(I)]	R1 = 0.0441, wR2 = 0.1111
R indices (all data)	R1 = 0.0590, wR2 = 0.1234
Largest diff. peak and hole	3.058 and -0.927 e. Å <sup>-3</sup>

**Crystallographic Table 38** Atomic coordinates ( $\times 10^4$ ) and equivalent isotropic displacement parameters ( $\text{\AA}^2 \times 10^3$ ) for **Usalzine**. U(eq) is defined as one third of the trace of the orthogonalized  $U_{ij}$  tensor.

	x	y	z	U(eq)
U(1)	964(1)	2095(1)	1341(1)	26(1)
S(1)	-914(3)	2546(1)	-778(1)	30(1)
S(2)	3331(3)	9518(1)	8542(2)	46(1)
O(5)	1250(9)	988(3)	1909(4)	50(2)
O(6)	881(8)	1063(3)	533(4)	42(2)
N(2)	306(8)	4236(3)	2254(4)	28(2)
O(3)	1245(7)	2270(3)	2723(4)	32(1)
O(2)	3001(9)	2151(3)	1422(4)	41(2)
O(4)	535(6)	2467(3)	-55(3)	27(1)
O(7)	4764(10)	9916(4)	8485(5)	60(2)
C(8)	1264(9)	3841(4)	1186(5)	23(1)
C(3)	-1058(11)	2585(5)	4323(6)	39(2)
N(4)	2225(8)	5690(3)	276(4)	29(2)
N(3)	2990(7)	4522(3)	-519(4)	26(1)
C(20)	1120(11)	724(4)	1192(6)	40(2)
C(21)	1212(14)	-5(5)	1144(7)	53(3)
N(1)	846(7)	3324(3)	1623(4)	26(2)
C(19)	939(9)	4448(4)	1564(5)	23(1)
C(7)	292(10)	3576(4)	2254(5)	28(2)
C(6)	-263(9)	3217(4)	2937(5)	28(2)
C(5)	-1217(10)	3526(4)	3429(5)	33(2)
C(4)	-1606(11)	3214(5)	4124(6)	39(2)
C(2)	-151(11)	2262(5)	3845(6)	37(2)
C(1)	265(10)	2570(4)	3145(5)	27(2)
C(18)	1258(10)	5056(4)	1303(5)	29(2)
C(17)	1935(10)	5090(4)	569(5)	28(2)
C(16)	2910(10)	5707(4)	-405(5)	30(2)
C(15)	3243(10)	6321(4)	-753(5)	32(2)
C(14)	3951(11)	6350(5)	-1413(6)	39(2)
C(13)	4404(11)	5779(4)	-1792(6)	37(2)
C(12)	4089(10)	5173(4)	-1504(5)	33(2)
C(11)	3324(10)	5125(4)	-801(5)	28(2)
C(10)	2314(9)	4503(4)	160(5)	24(2)
C(9)	1964(10)	3882(4)	474(5)	26(2)
O(1)	-1084(9)	2068(3)	1242(4)	43(2)
C(22)	-229(14)	3124(5)	-1430(6)	52(3)
C(23)	-854(12)	1825(5)	-1396(6)	50(3)

C(24)	3329(14)	8875(5)	7814(7)	55(3)
C(25)	3888(17)	9068(6)	9494(7)	74(4)

---

**Crystallographic Table 39** Bond lengths [ $\text{\AA}$ ] and angles [ $^\circ$ ] for Usalzine.

---

U(1)-O(2)	1.735(8)
U(1)-O(1)	1.739(8)
U(1)-O(3)	2.221(6)
U(1)-O(4)	2.333(5)
U(1)-O(5)	2.437(6)
U(1)-O(6)	2.474(6)
U(1)-N(1)	2.559(7)
U(1)-C(20)	2.822(9)
S(1)-O(4)	1.535(6)
S(1)-C(22)	1.759(10)
S(1)-C(23)	1.788(10)
S(2)-O(7)	1.496(8)
S(2)-C(24)	1.762(11)
S(2)-C(25)	1.771(11)
O(5)-C(20)	1.259(12)
O(6)-C(20)	1.252(11)
N(2)-C(7)	1.350(10)
N(2)-C(19)	1.400(11)
N(2)-H(2)	0.8800
O(3)-C(1)	1.334(10)
C(8)-N(1)	1.358(11)
C(8)-C(9)	1.402(11)
C(8)-C(19)	1.435(10)
C(3)-C(2)	1.370(13)
C(3)-C(4)	1.386(14)
C(3)-H(3)	0.9500
N(4)-C(16)	1.345(11)
N(4)-C(17)	1.357(10)
N(3)-C(10)	1.339(10)
N(3)-C(11)	1.365(10)
C(20)-C(21)	1.495(13)
C(21)-H(21A)	0.9800
C(21)-H(21B)	0.9800
C(21)-H(21C)	0.9800
N(1)-C(7)	1.313(10)
C(19)-C(18)	1.358(12)
C(7)-C(6)	1.478(11)
C(6)-C(5)	1.401(12)
C(6)-C(1)	1.418(12)
C(5)-C(4)	1.387(12)
C(5)-H(5)	0.9500
C(4)-H(4)	0.9500

C(2)-C(1)	1.400(12)
C(2)-H(2A)	0.9500
C(18)-C(17)	1.421(12)
C(18)-H(18)	0.9500
C(17)-C(10)	1.438(11)
C(16)-C(15)	1.429(11)
C(16)-C(11)	1.429(12)
C(15)-C(14)	1.328(12)
C(15)-H(15)	0.9500
C(14)-C(13)	1.409(14)
C(14)-H(14)	0.9500
C(13)-C(12)	1.369(12)
C(13)-H(13)	0.9500
C(12)-C(11)	1.423(12)
C(12)-H(12)	0.9500
C(10)-C(9)	1.420(11)
C(9)-H(9)	0.9500
C(22)-H(22A)	0.9800
C(22)-H(22B)	0.9800
C(22)-H(22C)	0.9800
C(23)-H(23A)	0.9800
C(23)-H(23B)	0.9800
C(23)-H(23C)	0.9800
C(24)-H	0.9800
C(24)-HA	0.9800
C(24)-HB	0.9800
C(25)-HC	0.9800
C(25)-HD	0.9800
C(25)-HE	0.9800
O(2)-U(1)-O(1)	177.9(3)
O(2)-U(1)-O(3)	90.5(2)
O(1)-U(1)-O(3)	90.1(3)
O(2)-U(1)-O(4)	90.8(2)
O(1)-U(1)-O(4)	87.7(2)
O(3)-U(1)-O(4)	151.6(2)
O(2)-U(1)-O(5)	90.4(3)
O(1)-U(1)-O(5)	91.7(3)
O(3)-U(1)-O(5)	77.9(2)
O(4)-U(1)-O(5)	130.5(2)
O(2)-U(1)-O(6)	91.0(2)
O(1)-U(1)-O(6)	90.2(2)
O(3)-U(1)-O(6)	130.6(2)
O(4)-U(1)-O(6)	77.80(19)
O(5)-U(1)-O(6)	52.7(2)
O(2)-U(1)-N(1)	89.9(2)

O(1)-U(1)-N(1)	88.4(2)
O(3)-U(1)-N(1)	70.4(2)
O(4)-U(1)-N(1)	81.2(2)
O(5)-U(1)-N(1)	148.3(2)
O(6)-U(1)-N(1)	159.0(2)
O(2)-U(1)-C(20)	90.4(3)
O(1)-U(1)-C(20)	91.4(3)
O(3)-U(1)-C(20)	104.3(2)
O(4)-U(1)-C(20)	104.1(2)
O(5)-U(1)-C(20)	26.4(2)
O(6)-U(1)-C(20)	26.3(2)
N(1)-U(1)-C(20)	174.7(2)
O(4)-S(1)-C(22)	101.9(4)
O(4)-S(1)-C(23)	103.1(4)
C(22)-S(1)-C(23)	99.9(6)
O(7)-S(2)-C(24)	104.9(5)
O(7)-S(2)-C(25)	104.6(5)
C(24)-S(2)-C(25)	98.7(6)
C(20)-O(5)-U(1)	94.1(5)
C(20)-O(6)-U(1)	92.6(5)
C(7)-N(2)-C(19)	108.3(6)
C(7)-N(2)-H(2)	125.9
C(19)-N(2)-H(2)	125.9
C(1)-O(3)-U(1)	129.2(5)
S(1)-O(4)-U(1)	135.5(3)
N(1)-C(8)-C(9)	132.3(7)
N(1)-C(8)-C(19)	111.1(7)
C(9)-C(8)-C(19)	116.6(7)
C(2)-C(3)-C(4)	121.6(8)
C(2)-C(3)-H(3)	119.2
C(4)-C(3)-H(3)	119.2
C(16)-N(4)-C(17)	116.7(7)
C(10)-N(3)-C(11)	116.9(7)
O(6)-C(20)-O(5)	120.6(8)
O(6)-C(20)-C(21)	120.7(9)
O(5)-C(20)-C(21)	118.7(9)
O(6)-C(20)-U(1)	61.1(5)
O(5)-C(20)-U(1)	59.5(4)
C(21)-C(20)-U(1)	178.2(8)
C(20)-C(21)-H(21A)	109.5
C(20)-C(21)-H(21B)	109.5
H(21A)-C(21)-H(21B)	109.5
C(20)-C(21)-H(21C)	109.5
H(21A)-C(21)-H(21C)	109.5
H(21B)-C(21)-H(21C)	109.5
C(7)-N(1)-C(8)	105.7(7)

C(7)-N(1)-U(1)	123.9(5)
C(8)-N(1)-U(1)	130.4(5)
C(18)-C(19)-N(2)	131.5(7)
C(18)-C(19)-C(8)	126.3(8)
N(2)-C(19)-C(8)	102.1(7)
N(1)-C(7)-N(2)	112.9(7)
N(1)-C(7)-C(6)	127.0(8)
N(2)-C(7)-C(6)	120.1(7)
C(5)-C(6)-C(1)	118.9(7)
C(5)-C(6)-C(7)	120.7(8)
C(1)-C(6)-C(7)	120.3(7)
C(4)-C(5)-C(6)	120.8(9)
C(4)-C(5)-H(5)	119.6
C(6)-C(5)-H(5)	119.6
C(3)-C(4)-C(5)	119.3(8)
C(3)-C(4)-H(4)	120.4
C(5)-C(4)-H(4)	120.4
C(3)-C(2)-C(1)	120.1(9)
C(3)-C(2)-H(2A)	120.0
C(1)-C(2)-H(2A)	120.0
O(3)-C(1)-C(2)	119.5(8)
O(3)-C(1)-C(6)	121.0(7)
C(2)-C(1)-C(6)	119.3(8)
C(19)-C(18)-C(17)	116.4(7)
C(19)-C(18)-H(18)	121.8
C(17)-C(18)-H(18)	121.8
N(4)-C(17)-C(18)	118.0(7)
N(4)-C(17)-C(10)	121.4(7)
C(18)-C(17)-C(10)	120.6(7)
N(4)-C(16)-C(15)	119.9(8)
N(4)-C(16)-C(11)	122.1(7)
C(15)-C(16)-C(11)	118.0(8)
C(14)-C(15)-C(16)	120.9(9)
C(14)-C(15)-H(15)	119.6
C(16)-C(15)-H(15)	119.6
C(15)-C(14)-C(13)	121.5(8)
C(15)-C(14)-H(14)	119.2
C(13)-C(14)-H(14)	119.2
C(12)-C(13)-C(14)	120.8(8)
C(12)-C(13)-H(13)	119.6
C(14)-C(13)-H(13)	119.6
C(13)-C(12)-C(11)	119.1(8)
C(13)-C(12)-H(12)	120.4
C(11)-C(12)-H(12)	120.4
N(3)-C(11)-C(12)	119.3(7)
N(3)-C(11)-C(16)	121.1(7)

C(12)-C(11)-C(16)	119.6(8)
N(3)-C(10)-C(9)	118.3(7)
N(3)-C(10)-C(17)	121.7(7)
C(9)-C(10)-C(17)	120.0(7)
C(8)-C(9)-C(10)	120.1(7)
C(8)-C(9)-H(9)	119.9
C(10)-C(9)-H(9)	119.9
S(1)-C(22)-H(22A)	109.5
S(1)-C(22)-H(22B)	109.5
H(22A)-C(22)-H(22B)	109.5
S(1)-C(22)-H(22C)	109.5
H(22A)-C(22)-H(22C)	109.5
H(22B)-C(22)-H(22C)	109.5
S(1)-C(23)-H(23A)	109.5
S(1)-C(23)-H(23B)	109.5
H(23A)-C(23)-H(23B)	109.5
S(1)-C(23)-H(23C)	109.5
H(23A)-C(23)-H(23C)	109.5
H(23B)-C(23)-H(23C)	109.5
S(2)-C(24)-H	109.5
S(2)-C(24)-HA	109.5
H-C(24)-HA	109.5
S(2)-C(24)-HB	109.5
H-C(24)-HB	109.5
HA-C(24)-HB	109.5
S(2)-C(25)-HC	109.5
S(2)-C(25)-HD	109.5
HC-C(25)-HD	109.5
S(2)-C(25)-HE	109.5
HC-C(25)-HE	109.5
HD-C(25)-HE	109.5

---

**Crystallographic Table 40** Anisotropic displacement parameters ( $\text{\AA}^2 \times 10^3$ ) for **Usalzine**. The anisotropic displacement factor exponent takes the form:  
 $-2\pi^2 [ h^2 a^{*2} U_{11} + \dots + 2 h k a^{*} b^{*} U_{12} ]$

---

	U11	U22	U33	U23	U13	U12
U(1)	35(1)	19(1)	25(1)	1(1)	7(1)	-1(1)
S(1)	33(1)	25(1)	31(1)	0(1)	4(1)	1(1)
S(2)	49(2)	47(1)	43(1)	6(1)	14(1)	4(1)
O(5)	89(6)	22(3)	40(4)	8(3)	16(4)	2(3)
O(6)	69(5)	21(3)	35(3)	-1(3)	9(3)	-1(3)
N(2)	40(4)	23(3)	25(4)	-2(3)	14(3)	5(3)
O(3)	40(4)	28(3)	30(3)	0(2)	8(3)	3(3)
O(2)	74(5)	29(3)	14(3)	-2(2)	-7(3)	10(3)
O(4)	30(3)	25(3)	26(3)	0(2)	5(2)	-3(2)
O(7)	78(6)	48(4)	55(5)	16(4)	17(4)	-19(4)
C(8)	24(3)	21(3)	20(3)	-7(2)	-9(2)	6(2)
C(3)	38(5)	46(5)	35(5)	6(4)	12(4)	-12(4)
N(4)	34(4)	19(3)	34(4)	3(3)	6(3)	-2(3)
N(3)	24(4)	28(4)	24(4)	0(3)	2(3)	-2(3)
C(20)	49(6)	22(4)	50(6)	7(4)	16(5)	-6(4)
C(21)	65(7)	27(5)	65(7)	6(5)	8(6)	1(5)
N(1)	23(3)	29(4)	27(4)	-6(3)	6(3)	-5(3)
C(19)	24(3)	21(3)	20(3)	-7(2)	-9(2)	6(2)
C(7)	26(4)	31(5)	24(4)	-1(3)	-3(3)	2(3)
C(6)	24(4)	33(4)	28(4)	2(4)	9(3)	0(3)
C(5)	33(5)	35(5)	33(5)	-1(4)	10(4)	0(4)
C(4)	38(5)	45(5)	40(5)	-7(4)	20(4)	-9(4)
C(2)	38(5)	36(5)	36(5)	5(4)	4(4)	-9(4)
C(1)	28(4)	27(4)	25(4)	0(3)	1(3)	-8(3)
C(18)	44(5)	21(4)	23(4)	-3(3)	11(4)	1(3)
C(17)	34(5)	22(4)	22(4)	-1(3)	-5(3)	1(3)
C(16)	31(5)	27(4)	29(5)	1(3)	3(4)	-4(3)
C(15)	34(5)	26(4)	34(5)	6(4)	-1(4)	-8(4)
C(14)	44(6)	33(5)	36(5)	13(4)	3(4)	-7(4)
C(13)	43(5)	38(5)	34(5)	9(4)	13(4)	-9(4)
C(12)	31(5)	35(5)	31(5)	0(4)	5(4)	-1(4)
C(11)	28(5)	29(4)	26(4)	0(3)	3(3)	2(3)
C(10)	27(4)	22(4)	23(4)	2(3)	6(3)	2(3)
C(9)	39(5)	17(4)	21(4)	0(3)	6(3)	0(3)

---

O(1)	84(5)	21(3)	23(3)	0(2)	6(3)	-2(3)
C(22)	68(7)	48(6)	32(5)	12(5)	-11(5)	-18(5)
C(23)	58(7)	33(5)	52(6)	-15(5)	-5(5)	6(5)
C(24)	75(8)	49(6)	44(6)	8(5)	18(5)	-6(5)
C(25)	114(11)	64(8)	40(6)	16(6)	8(7)	-40(8)

---

**Crystallographic Table 41** Hydrogen coordinates ( $\times 10^4$ ) and isotropic displacement parameters ( $\text{\AA}^2 \times 10^3$ ) for **Usalzine**.

	x	y	z	U(eq)
H(2)	-25	4490	2624	34
H(3)	-1316	2373	4802	47
H(21A)	175	-179	871	80
H(21B)	1515	-185	1717	80
H(21C)	2006	-128	813	80
H(5)	-1604	3955	3285	40
H(4)	-2240	3429	4460	47
H(2A)	195	1828	3989	44
H(18)	1040	5438	1596	34
H(15)	2953	6715	-510	39
H(14)	4157	6764	-1634	46
H(13)	4935	5815	-2253	45
H(12)	4378	4790	-1770	39
H(9)	2206	3495	200	31
H(22A)	-102	3549	-1144	78
H(22B)	-999	3164	-1966	78
H(22C)	794	2981	-1545	78
H(23A)	171	1798	-1571	75
H(23B)	-1708	1841	-1900	75
H(23C)	-993	1439	-1057	75
H	3117	9050	7237	83
HA	2503	8558	7874	83
HB	4365	8658	7929	83
HC	4889	8840	9493	111
HD	3060	8748	9537	111
HE	4024	9367	9978	111

**Crystallographic Table 42** Torsion angles [°] for Usalzine

---

O(2)-U(1)-O(5)-C(20)	-90.0(6)
O(1)-U(1)-O(5)-C(20)	89.8(6)
O(3)-U(1)-O(5)-C(20)	179.6(6)
O(4)-U(1)-O(5)-C(20)	1.4(7)
O(6)-U(1)-O(5)-C(20)	0.9(5)
N(1)-U(1)-O(5)-C(20)	179.5(5)
O(2)-U(1)-O(6)-C(20)	88.9(6)
O(1)-U(1)-O(6)-C(20)	-92.9(6)
O(3)-U(1)-O(6)-C(20)	-2.6(7)
O(4)-U(1)-O(6)-C(20)	179.5(6)
O(5)-U(1)-O(6)-C(20)	-0.9(5)
N(1)-U(1)-O(6)-C(20)	-178.9(6)
O(2)-U(1)-O(3)-C(1)	148.1(6)
O(1)-U(1)-O(3)-C(1)	-29.9(6)
O(4)-U(1)-O(3)-C(1)	55.5(8)
O(5)-U(1)-O(3)-C(1)	-121.6(7)
O(6)-U(1)-O(3)-C(1)	-120.2(6)
N(1)-U(1)-O(3)-C(1)	58.4(6)
C(20)-U(1)-O(3)-C(1)	-121.4(6)
C(22)-S(1)-O(4)-U(1)	159.2(6)
C(23)-S(1)-O(4)-U(1)	-97.6(6)
O(2)-U(1)-O(4)-S(1)	173.2(5)
O(1)-U(1)-O(4)-S(1)	-8.4(5)
O(3)-U(1)-O(4)-S(1)	-94.4(6)
O(5)-U(1)-O(4)-S(1)	81.9(5)
O(6)-U(1)-O(4)-S(1)	82.3(5)
N(1)-U(1)-O(4)-S(1)	-97.1(5)
C(20)-U(1)-O(4)-S(1)	82.5(5)
U(1)-O(6)-C(20)-O(5)	1.7(10)
U(1)-O(6)-C(20)-C(21)	-180.0(8)
U(1)-O(5)-C(20)-O(6)	-1.7(10)
U(1)-O(5)-C(20)-C(21)	179.9(8)
O(2)-U(1)-C(20)-O(6)	-91.5(6)
O(1)-U(1)-C(20)-O(6)	87.5(6)
O(3)-U(1)-C(20)-O(6)	177.9(5)
O(4)-U(1)-C(20)-O(6)	-0.5(6)
O(5)-U(1)-C(20)-O(6)	178.3(10)
N(1)-U(1)-C(20)-O(6)	176(2)
O(2)-U(1)-C(20)-O(5)	90.2(6)
O(1)-U(1)-C(20)-O(5)	-90.9(6)
O(3)-U(1)-C(20)-O(5)	-0.4(6)
O(4)-U(1)-C(20)-O(5)	-178.9(6)

O(6)-U(1)-C(20)-O(5)	-178.3(10)
N(1)-U(1)-C(20)-O(5)	-3(3)
O(2)-U(1)-C(20)-C(21)	88(22)
O(1)-U(1)-C(20)-C(21)	-93(22)
O(3)-U(1)-C(20)-C(21)	-3(22)
O(4)-U(1)-C(20)-C(21)	179(100)
O(5)-U(1)-C(20)-C(21)	-2(22)
O(6)-U(1)-C(20)-C(21)	179(100)
N(1)-U(1)-C(20)-C(21)	-5(24)
C(9)-C(8)-N(1)-C(7)	177.7(8)
C(19)-C(8)-N(1)-C(7)	-0.4(8)
C(9)-C(8)-N(1)-U(1)	-3.9(12)
C(19)-C(8)-N(1)-U(1)	178.0(5)
O(2)-U(1)-N(1)-C(7)	-121.6(6)
O(1)-U(1)-N(1)-C(7)	59.6(6)
O(3)-U(1)-N(1)-C(7)	-31.1(6)
O(4)-U(1)-N(1)-C(7)	147.5(6)
O(5)-U(1)-N(1)-C(7)	-31.0(8)
O(6)-U(1)-N(1)-C(7)	145.9(7)
C(20)-U(1)-N(1)-C(7)	-29(3)
O(2)-U(1)-N(1)-C(8)	60.2(6)
O(1)-U(1)-N(1)-C(8)	-118.6(7)
O(3)-U(1)-N(1)-C(8)	150.7(7)
O(4)-U(1)-N(1)-C(8)	-30.6(6)
O(5)-U(1)-N(1)-C(8)	150.8(6)
O(6)-U(1)-N(1)-C(8)	-32.3(10)
C(20)-U(1)-N(1)-C(8)	153(2)
C(7)-N(2)-C(19)-C(18)	-177.3(8)
C(7)-N(2)-C(19)-C(8)	0.2(8)
N(1)-C(8)-C(19)-C(18)	177.8(7)
C(9)-C(8)-C(19)-C(18)	-0.6(11)
N(1)-C(8)-C(19)-N(2)	0.1(8)
C(9)-C(8)-C(19)-N(2)	-178.3(6)
C(8)-N(1)-C(7)-N(2)	0.6(9)
U(1)-N(1)-C(7)-N(2)	-178.0(5)
C(8)-N(1)-C(7)-C(6)	-177.4(7)
U(1)-N(1)-C(7)-C(6)	4.0(11)
C(19)-N(2)-C(7)-N(1)	-0.5(9)
C(19)-N(2)-C(7)-C(6)	177.6(7)
N(1)-C(7)-C(6)-C(5)	-162.2(8)
N(2)-C(7)-C(6)-C(5)	19.9(12)
N(1)-C(7)-C(6)-C(1)	22.7(12)
N(2)-C(7)-C(6)-C(1)	-155.2(8)
C(1)-C(6)-C(5)-C(4)	1.9(13)
C(7)-C(6)-C(5)-C(4)	-173.3(8)
C(2)-C(3)-C(4)-C(5)	-0.5(14)

C(6)-C(5)-C(4)-C(3)	-1.0(13)
C(4)-C(3)-C(2)-C(1)	1.1(14)
U(1)-O(3)-C(1)-C(2)	129.6(7)
U(1)-O(3)-C(1)-C(6)	-55.2(10)
C(3)-C(2)-C(1)-O(3)	175.0(8)
C(3)-C(2)-C(1)-C(6)	-0.2(13)
C(5)-C(6)-C(1)-O(3)	-176.4(8)
C(7)-C(6)-C(1)-O(3)	-1.2(12)
C(5)-C(6)-C(1)-C(2)	-1.3(12)
C(7)-C(6)-C(1)-C(2)	173.9(8)
N(2)-C(19)-C(18)-C(17)	179.0(8)
C(8)-C(19)-C(18)-C(17)	2.0(12)
C(16)-N(4)-C(17)-C(18)	178.1(7)
C(16)-N(4)-C(17)-C(10)	-1.3(11)
C(19)-C(18)-C(17)-N(4)	178.0(7)
C(19)-C(18)-C(17)-C(10)	-2.6(12)
C(17)-N(4)-C(16)-C(15)	179.6(7)
C(17)-N(4)-C(16)-C(11)	-0.3(12)
N(4)-C(16)-C(15)-C(14)	178.5(8)
C(11)-C(16)-C(15)-C(14)	-1.6(12)
C(16)-C(15)-C(14)-C(13)	-0.2(13)
C(15)-C(14)-C(13)-C(12)	1.7(14)
C(14)-C(13)-C(12)-C(11)	-1.4(13)
C(10)-N(3)-C(11)-C(12)	178.0(7)
C(10)-N(3)-C(11)-C(16)	-2.4(11)
C(13)-C(12)-C(11)-N(3)	179.1(8)
C(13)-C(12)-C(11)-C(16)	-0.5(12)
N(4)-C(16)-C(11)-N(3)	2.2(12)
C(15)-C(16)-C(11)-N(3)	-177.7(7)
N(4)-C(16)-C(11)-C(12)	-178.2(8)
C(15)-C(16)-C(11)-C(12)	1.9(12)
C(11)-N(3)-C(10)-C(9)	-179.4(7)
C(11)-N(3)-C(10)-C(17)	0.8(11)
N(4)-C(17)-C(10)-N(3)	1.1(12)
C(18)-C(17)-C(10)-N(3)	-178.3(7)
N(4)-C(17)-C(10)-C(9)	-178.7(7)
C(18)-C(17)-C(10)-C(9)	2.0(12)
N(1)-C(8)-C(9)-C(10)	-178.2(8)
C(19)-C(8)-C(9)-C(10)	-0.1(11)
N(3)-C(10)-C(9)-C(8)	179.7(7)
C(17)-C(10)-C(9)-C(8)	-0.6(12)

---

**Crystallographic Table 43** Crystal data and structure refinement for **salzine**.

Identification code	salzine		
Empirical formula	$C_{19} H_{12} N_4 O$		
Formula weight	312.33		
Temperature	296(2) K		
Wavelength	0.71073 Å		
Crystal system, space group	Monoclinic, $P2_1/n$		
Unit cell dimensions	$a = 6.692(3)$ Å	$\alpha = 90^\circ$	
	$b = 26.911(14)$ Å	$\beta = 104.413(9)^\circ$	
	$c = 8.086(4)$ Å	$\gamma = 90^\circ$	
Volume	$1410.3(12)$ Å <sup>3</sup>		
Z, Calculated density	4, 1.471 Mg/m <sup>3</sup>		
Absorption coefficient	0.096 mm <sup>-1</sup>		
F(000)	648		
Crystal size	0.1 x 0.1 x 0.1 mm		
Theta range for data collection	2.71 to 26.47 deg.		
Limiting indices	$-8 \leq h \leq 8, -33 \leq k \leq 33, -10 \leq l \leq 10$		
Reflections collected / unique	13099 / 2924 [R(int) = 0.0581]		
Completeness to theta = 26.47	99.8 %		
Refinement method	Full-matrix least-squares on F <sup>2</sup>		
Data / restraints / parameters	2924 / 0 / 220		
Goodness-of-fit on F <sup>2</sup>	1.032		
Final R indices [I>2sigma(I)]	R1 = 0.0428, wR2 = 0.0895		
R indices (all data)	R1 = 0.0700, wR2 = 0.1013		
Largest diff. peak and hole	0.189 and -0.199 e. Å <sup>-3</sup>		

**Crystallographic Table 44 Salzine** Atomic coordinates ( $\times 10^4$ ) and equivalent isotropic displacement parameters ( $\text{\AA}^2 \times 10^3$ ) for salzine. U(eq) is defined as one third of the trace of the orthogonalized  $U_{ij}$  tensor.

	x	y	z	U(eq)
O(1)	-62(2)	10442(1)	6163(2)	27(1)
N(1)	10015(2)	8799(1)	10557(2)	24(1)
N(2)	6342(2)	10188(1)	7286(2)	23(1)
N(3)	6069(2)	8472(1)	10852(2)	22(1)
N(4)	3228(2)	9937(1)	7518(2)	22(1)
C(1)	11363(3)	7668(1)	13040(2)	32(1)
C(2)	11565(3)	8089(1)	12166(2)	30(1)
C(3)	9789(3)	8380(1)	11399(2)	23(1)
C(4)	8290(2)	9061(1)	9855(2)	21(1)
C(5)	8478(3)	9502(1)	8948(2)	22(1)
C(6)	6705(2)	9756(1)	8239(2)	20(1)
C(7)	4265(2)	10279(1)	6889(2)	21(1)
C(8)	3293(3)	10703(1)	5882(2)	21(1)
C(9)	4441(3)	11055(1)	5243(2)	27(1)
C(10)	3513(3)	11451(1)	4280(2)	31(1)
C(11)	1379(3)	11501(1)	3917(2)	30(1)
C(12)	9389(3)	7504(1)	13192(2)	31(1)
C(13)	7665(3)	7770(1)	12468(2)	28(1)
C(14)	7801(3)	8215(1)	11555(2)	22(1)
C(15)	6274(3)	8894(1)	10003(2)	20(1)
C(16)	4477(2)	9171(1)	9249(2)	21(1)
C(17)	4699(2)	9595(1)	8380(2)	20(1)
C(18)	1135(3)	10763(1)	5535(2)	22(1)
C(19)	198(3)	11160(1)	4532(2)	27(1)

**Crystallographic Table 45** Bond lengths [ $\text{\AA}$ ] and angles [ $^\circ$ ] for **salzine**.

---

O(1)-C(18)	1.360(2)
O(1)-H(9)	0.98(2)
N(1)-C(3)	1.345(2)
N(1)-C(4)	1.351(2)
N(2)-C(7)	1.369(2)
N(2)-C(6)	1.383(2)
N(2)-H(3)	0.8600
N(3)-C(14)	1.347(2)
N(3)-C(15)	1.353(2)
N(4)-C(7)	1.328(2)
N(4)-C(17)	1.399(2)
C(1)-C(2)	1.360(3)
C(1)-C(12)	1.427(3)
C(1)-H(1)	0.9300
C(2)-C(3)	1.428(2)
C(2)-H(7)	0.9300
C(3)-C(14)	1.438(2)
C(4)-C(5)	1.417(2)
C(4)-C(15)	1.454(2)
C(5)-C(6)	1.366(2)
C(5)-H(8)	0.9300
C(6)-C(17)	1.442(2)
C(7)-C(8)	1.457(2)
C(8)-C(9)	1.398(2)
C(8)-C(18)	1.410(2)
C(9)-C(10)	1.375(2)
C(9)-H(11)	0.9300
C(10)-C(11)	1.390(3)
C(10)-H(12)	0.9300
C(11)-C(19)	1.381(3)
C(11)-H(2)	0.9300
C(12)-C(13)	1.360(3)
C(12)-H(4)	0.9300
C(13)-C(14)	1.422(2)
C(13)-H(5)	0.9300
C(15)-C(16)	1.417(2)
C(16)-C(17)	1.368(2)
C(16)-H(6)	0.9300
C(18)-C(19)	1.393(2)
C(19)-H(10)	0.9300
C(18)-O(1)-H(9)	106.7(12)

C(3)-N(1)-C(4)	117.26(15)
C(7)-N(2)-C(6)	108.00(13)
C(7)-N(2)-H(3)	126.0
C(6)-N(2)-H(3)	126.0
C(14)-N(3)-C(15)	117.35(15)
C(7)-N(4)-C(17)	106.06(14)
C(2)-C(1)-C(12)	121.10(17)
C(2)-C(1)-H(1)	119.5
C(12)-C(1)-H(1)	119.5
C(1)-C(2)-C(3)	120.15(17)
C(1)-C(2)-H(7)	119.9
C(3)-C(2)-H(7)	119.9
N(1)-C(3)-C(2)	119.51(16)
N(1)-C(3)-C(14)	121.75(15)
C(2)-C(3)-C(14)	118.74(16)
N(1)-C(4)-C(5)	118.53(15)
N(1)-C(4)-C(15)	121.19(15)
C(5)-C(4)-C(15)	120.28(15)
C(6)-C(5)-C(4)	117.18(15)
C(6)-C(5)-H(8)	121.4
C(4)-C(5)-H(8)	121.4
C(5)-C(6)-N(2)	131.98(15)
C(5)-C(6)-C(17)	123.10(15)
N(2)-C(6)-C(17)	104.92(14)
N(4)-C(7)-N(2)	112.50(14)
N(4)-C(7)-C(8)	123.61(15)
N(2)-C(7)-C(8)	123.89(14)
C(9)-C(8)-C(18)	118.55(16)
C(9)-C(8)-C(7)	121.83(16)
C(18)-C(8)-C(7)	119.63(14)
C(10)-C(9)-C(8)	121.54(17)
C(10)-C(9)-H(11)	119.2
C(8)-C(9)-H(11)	119.2
C(9)-C(10)-C(11)	119.32(17)
C(9)-C(10)-H(12)	120.3
C(11)-C(10)-H(12)	120.3
C(19)-C(11)-C(10)	120.65(17)
C(19)-C(11)-H(2)	119.7
C(10)-C(11)-H(2)	119.7
C(13)-C(12)-C(1)	120.32(17)
C(13)-C(12)-H(4)	119.8
C(1)-C(12)-H(4)	119.8
C(12)-C(13)-C(14)	120.63(17)
C(12)-C(13)-H(5)	119.7
C(14)-C(13)-H(5)	119.7
N(3)-C(14)-C(13)	119.44(16)

N(3)-C(14)-C(3)	121.50(15)
C(13)-C(14)-C(3)	119.06(15)
N(3)-C(15)-C(16)	118.52(15)
N(3)-C(15)-C(4)	120.94(15)
C(16)-C(15)-C(4)	120.54(15)
C(17)-C(16)-C(15)	118.07(15)
C(17)-C(16)-H(6)	121.0
C(15)-C(16)-H(6)	121.0
C(16)-C(17)-N(4)	130.66(15)
C(16)-C(17)-C(6)	120.83(15)
N(4)-C(17)-C(6)	108.51(14)
O(1)-C(18)-C(19)	118.96(16)
O(1)-C(18)-C(8)	121.40(15)
C(19)-C(18)-C(8)	119.64(15)
C(11)-C(19)-C(18)	120.27(17)
C(11)-C(19)-H(10)	119.9
C(18)-C(19)-H(10)	119.9

---

**Crystallographic Table 46** Anisotropic displacement parameters ( $\text{\AA}^2 \times 10^3$ ) for **salzine**. The anisotropic displacement factor exponent takes the form:  
 $-2 \pi^2 [ h^2 a^{*2} U_{11} + \dots + 2 h k a^{*} b^{*} U_{12} ]$

---

	U11	U22	U33	U23	U13	U12
O(1)	20(1)	28(1)	33(1)	4(1)	8(1)	1(1)
N(1)	21(1)	24(1)	28(1)	-1(1)	6(1)	1(1)
N(2)	19(1)	22(1)	28(1)	3(1)	8(1)	-1(1)
N(3)	23(1)	20(1)	24(1)	-2(1)	5(1)	0(1)
N(4)	20(1)	22(1)	23(1)	2(1)	4(1)	0(1)
C(1)	31(1)	30(1)	35(1)	5(1)	6(1)	10(1)
C(2)	24(1)	31(1)	35(1)	1(1)	8(1)	4(1)
C(3)	25(1)	21(1)	22(1)	-2(1)	6(1)	1(1)
C(4)	19(1)	21(1)	22(1)	-3(1)	5(1)	1(1)
C(5)	17(1)	23(1)	26(1)	-2(1)	8(1)	-2(1)
C(6)	22(1)	19(1)	21(1)	-2(1)	7(1)	-1(1)
C(7)	20(1)	21(1)	21(1)	-3(1)	6(1)	0(1)
C(8)	25(1)	20(1)	20(1)	-3(1)	6(1)	0(1)
C(9)	26(1)	27(1)	30(1)	1(1)	9(1)	-1(1)
C(10)	36(1)	26(1)	33(1)	5(1)	14(1)	-3(1)
C(11)	39(1)	26(1)	27(1)	5(1)	9(1)	7(1)
C(12)	38(1)	23(1)	34(1)	5(1)	9(1)	3(1)
C(13)	28(1)	23(1)	32(1)	1(1)	8(1)	-1(1)
C(14)	23(1)	21(1)	21(1)	-3(1)	4(1)	1(1)
C(15)	22(1)	19(1)	19(1)	-4(1)	6(1)	-1(1)
C(16)	15(1)	24(1)	24(1)	-1(1)	5(1)	-3(1)
C(17)	20(1)	20(1)	20(1)	-3(1)	5(1)	-1(1)
C(18)	25(1)	22(1)	21(1)	-4(1)	9(1)	-2(1)
C(19)	25(1)	29(1)	27(1)	0(1)	6(1)	7(1)

---

**Crystallographic Table 47** Hydrogen coordinates ( x 10<sup>4</sup>) and isotropic displacement parameters (Å<sup>2</sup> x 10<sup>3</sup>) for **salzine**.

---

	x	y	z	U(eq)
H(9)	860(30)	10182(7)	6780(20)	40
H(3)	7260	10368	6995	27
H(1)	12531	7484	13548	39
H(7)	12861	8188	12067	36
H(8)	9755	9613	8840	26
H(11)	5867	11020	5475	33
H(12)	4303	11684	3876	37
H(2)	742	11766	3253	37
H(4)	9281	7214	13790	38
H(5)	6384	7659	12570	33
H(6)	3184	9067	9343	25
H(10)	-1228	11197	4275	33

---

**Crystallographic Table 48 Salzine Torsion angles [°] for salzine.**

---

C(12)-C(1)-C(2)-C(3)	0.9(3)
C(4)-N(1)-C(3)-C(2)	-179.99(15)
C(4)-N(1)-C(3)-C(14)	-0.1(2)
C(1)-C(2)-C(3)-N(1)	179.15(16)
C(1)-C(2)-C(3)-C(14)	-0.7(2)
C(3)-N(1)-C(4)-C(5)	-179.51(14)
C(3)-N(1)-C(4)-C(15)	-0.2(2)
N(1)-C(4)-C(5)-C(6)	179.41(15)
C(15)-C(4)-C(5)-C(6)	0.1(2)
C(4)-C(5)-C(6)-N(2)	-179.63(16)
C(4)-C(5)-C(6)-C(17)	0.1(2)
C(7)-N(2)-C(6)-C(5)	179.80(17)
C(7)-N(2)-C(6)-C(17)	0.03(17)
C(17)-N(4)-C(7)-N(2)	-0.31(18)
C(17)-N(4)-C(7)-C(8)	179.50(14)
C(6)-N(2)-C(7)-N(4)	0.18(18)
C(6)-N(2)-C(7)-C(8)	-179.63(15)
N(4)-C(7)-C(8)-C(9)	179.96(16)
N(2)-C(7)-C(8)-C(9)	-0.3(2)
N(4)-C(7)-C(8)-C(18)	0.0(2)
N(2)-C(7)-C(8)-C(18)	179.80(15)
C(18)-C(8)-C(9)-C(10)	-0.7(2)
C(7)-C(8)-C(9)-C(10)	179.36(16)
C(8)-C(9)-C(10)-C(11)	-0.7(3)
C(9)-C(10)-C(11)-C(19)	0.9(3)
C(2)-C(1)-C(12)-C(13)	-0.4(3)
C(1)-C(12)-C(13)-C(14)	-0.3(3)
C(15)-N(3)-C(14)-C(13)	179.70(14)
C(15)-N(3)-C(14)-C(3)	-0.6(2)
C(12)-C(13)-C(14)-N(3)	-179.91(16)
C(12)-C(13)-C(14)-C(3)	0.4(2)
N(1)-C(3)-C(14)-N(3)	0.5(2)
C(2)-C(3)-C(14)-N(3)	-179.61(15)
N(1)-C(3)-C(14)-C(13)	-179.77(15)
C(2)-C(3)-C(14)-C(13)	0.1(2)
C(14)-N(3)-C(15)-C(16)	179.96(14)
C(14)-N(3)-C(15)-C(4)	0.3(2)
N(1)-C(4)-C(15)-N(3)	0.1(2)
C(5)-C(4)-C(15)-N(3)	179.41(14)
N(1)-C(4)-C(15)-C(16)	-179.57(15)
C(5)-C(4)-C(15)-C(16)	-0.2(2)
N(3)-C(15)-C(16)-C(17)	-179.42(14)

C(4)-C(15)-C(16)-C(17)	0.2(2)
C(15)-C(16)-C(17)-N(4)	179.82(15)
C(15)-C(16)-C(17)-C(6)	-0.1(2)
C(7)-N(4)-C(17)-C(16)	-179.57(17)
C(7)-N(4)-C(17)-C(6)	0.32(17)
C(5)-C(6)-C(17)-C(16)	-0.1(2)
N(2)-C(6)-C(17)-C(16)	179.69(15)
C(5)-C(6)-C(17)-N(4)	179.99(15)
N(2)-C(6)-C(17)-N(4)	-0.22(17)
C(9)-C(8)-C(18)-O(1)	-178.03(15)
C(7)-C(8)-C(18)-O(1)	1.9(2)
C(9)-C(8)-C(18)-C(19)	1.9(2)
C(7)-C(8)-C(18)-C(19)	-178.16(15)
C(10)-C(11)-C(19)-C(18)	0.4(3)
O(1)-C(18)-C(19)-C(11)	178.18(15)
C(8)-C(18)-C(19)-C(11)	-1.7(2)

---

**Crystallographic Table 49** Crystal data and structure refinement for **t-butylsalzine**.

Identification code	bam137_0m
Empirical formula	C <sub>32</sub> H <sub>38</sub> N <sub>4</sub> O <sub>2</sub>
Formula weight	510.66
Temperature	183(2) K
Wavelength	0.71073 Å
Crystal system, space group	Triclinic, P-1
Unit cell dimensions	a = 9.0785(5) Å      α = 103.4900(10) ° b = 9.9896(6) Å      β = 103.2300(10) ° c = 16.3768(9) Å      γ = 99.4810(10) °
Volume	1368.08(13) Å <sup>3</sup>
Z, Calculated density	2, 1.240 Mg/m <sup>3</sup>
Absorption coefficient	0.078 mm <sup>-1</sup>
F(000)	548
Crystal size	0.1 x 0.1 x 0.1 mm
Theta range for data collection	1.33 to 30.75 °
Limiting indices	-13<=h<=13, -14<=k<=14, -23<=l<=23
Reflections collected / unique	37120 / 8315 [R( <sub>int</sub> ) = 0.0313]
Completeness to theta = 30.75	97.5 %
Absorption correction	Numerical
Refinement method	Full-matrix least-squares on F <sup>2</sup>
Data / restraints / parameters	8315 / 3 / 358
Goodness-of-fit on F <sup>2</sup>	1.646
Final R indices [I>2sigma(I)]	R1 = 0.0576, wR2 = 0.2008
R indices (all data)	R1 = 0.0659, wR2 = 0.2135
Largest diff. peak and hole	0.716 and -0.386 e.Å <sup>-3</sup>

**Crystallographic Table 50** Atomic coordinates ( $\times 10^4$ ) and equivalent isotropic displacement parameters ( $\text{\AA}^2 \times 10^3$ ) for **t-butylsalazine**. U(eq) is defined as one third of the trace of the orthogonalized  $U_{ij}$  tensor.

	x	y	z	U(eq)
O(1)	-1590(1)	6661(1)	7088(1)	31(1)
O(2)	7143(1)	7150(1)	4385(1)	34(1)
O(3)	3166(2)	9372(1)	8977(1)	58(1)
N(2)	365(1)	6953(1)	6203(1)	23(1)
N(3)	1721(1)	5305(1)	5876(1)	21(1)
N(4)	4074(1)	7677(1)	4043(1)	22(1)
C(1)	2863(3)	7116(2)	9179(2)	67(1)
C(2)	3054(3)	8179(2)	10042(1)	56(1)
C(3)	2838(3)	9496(2)	9790(2)	63(1)
C(4)	2694(5)	7954(2)	8529(2)	107(1)
C(5)	-82(2)	1332(2)	8466(1)	36(1)
C(6)	848(1)	2095(1)	7972(1)	23(1)
C(7)	130(1)	3262(1)	7692(1)	21(1)
C(8)	653(1)	3906(1)	7112(1)	21(1)
C(9)	91(1)	5045(1)	6900(1)	20(1)
C(10)	707(1)	5752(1)	6324(1)	20(1)
C(11)	1215(1)	7336(1)	5658(1)	20(1)
C(12)	1318(1)	8500(1)	5347(1)	22(1)
C(13)	2312(1)	8644(1)	4805(1)	20(1)
N(1)	2472(1)	9808(1)	4521(1)	22(1)
C(15)	3358(1)	9885(1)	3972(1)	22(1)
C(16)	3505(2)	11064(1)	3620(1)	28(1)
C(17)	4347(2)	11124(1)	3037(1)	32(1)
C(18)	943(2)	980(1)	7175(1)	28(1)
C(19)	-991(1)	3798(1)	8051(1)	22(1)
C(20)	-1592(1)	4927(1)	7868(1)	22(1)
C(21)	-2788(1)	5489(1)	8301(1)	26(1)
C(22)	-4314(2)	5333(2)	7602(1)	31(1)
C(23)	-3187(2)	4669(2)	8937(1)	34(1)
C(24)	-2134(2)	7055(2)	8828(1)	38(1)
C(25)	-1037(1)	5557(1)	7280(1)	22(1)
C(26)	2085(1)	6286(1)	5442(1)	19(1)
C(27)	3031(1)	6366(1)	4905(1)	20(1)
C(28)	3155(1)	7562(1)	4573(1)	19(1)
C(29)	4148(1)	8796(1)	3716(1)	21(1)
C(30)	5118(2)	10037(2)	2775(1)	32(1)

C(31)	5030(2)	8910(1)	3115(1)	29(1)
C(32)	2510(2)	2777(2)	8572(1)	34(1)

---

**Crystallographic Table 51** Bond lengths [ $\text{\AA}$ ] and angles [ $^\circ$ ] for **t-butylsalzine**.

---

O(1)-C(25)	1.3554(13)
O(1)-H(20)	0.97(2)
O(2)-H(37)	0.829(9)
O(2)-H(38)	0.835(9)
O(3)-C(4)	1.378(3)
O(3)-C(3)	1.412(3)
N(2)-C(10)	1.3344(13)
N(2)-C(11)	1.3846(15)
N(3)-C(10)	1.3700(14)
N(3)-C(26)	1.3787(13)
N(3)-H(21)	0.8600
N(4)-C(28)	1.3454(15)
N(4)-C(29)	1.3450(14)
C(1)-C(4)	1.496(3)
C(1)-C(2)	1.510(3)
C(1)-H(1)	0.9700
C(1)-H(4)	0.9700
C(2)-C(3)	1.497(3)
C(2)-H(6)	0.9700
C(2)-H(5)	0.9700
C(3)-H(2)	0.9700
C(3)-H(7)	0.9700
C(5)-C(6)	1.5283(17)
C(5)-H(31)	0.9600
C(5)-H(8)	0.9600
C(5)-H(30)	0.9600
C(6)-C(7)	1.5357(15)
C(6)-C(18)	1.5358(17)
C(6)-C(32)	1.5408(18)
C(7)-C(8)	1.3888(15)
C(7)-C(19)	1.4050(16)
C(8)-C(9)	1.4040(14)
C(8)-H(28)	0.9300
C(9)-C(25)	1.4183(16)
C(9)-C(10)	1.4571(15)
C(11)-C(12)	1.3716(14)
C(11)-C(26)	1.4415(15)
C(12)-C(13)	1.4163(16)
C(12)-H(22)	0.9300
C(13)-N(1)	1.3486(13)
C(13)-C(28)	1.4527(15)
N(1)-C(15)	1.3428(16)

C(15)-C(16)	1.4278(15)
C(15)-C(29)	1.4345(16)
C(16)-C(17)	1.3585(19)
C(16)-H(26)	0.9300
C(17)-C(30)	1.423(2)
C(17)-H(9)	0.9300
C(18)-H(35)	0.9600
C(18)-H(36)	0.9600
C(18)-H(10)	0.9600
C(19)-C(20)	1.3948(15)
C(19)-H(29)	0.9300
C(20)-C(25)	1.4072(16)
C(20)-C(21)	1.5378(16)
C(21)-C(23)	1.5364(18)
C(21)-C(22)	1.5402(18)
C(21)-C(24)	1.5411(19)
C(22)-H(13)	0.9600
C(22)-H(11)	0.9600
C(22)-H(12)	0.9600
C(23)-H(14)	0.9600
C(23)-H(16)	0.9600
C(23)-H(15)	0.9600
C(24)-H(18)	0.9600
C(24)-H(17)	0.9600
C(24)-H(19)	0.9600
C(26)-C(27)	1.3691(15)
C(27)-C(28)	1.4227(14)
C(27)-H(27)	0.9300
C(29)-C(31)	1.4170(17)
C(30)-C(31)	1.3664(17)
C(30)-H(24)	0.9300
C(31)-H(25)	0.9300
C(32)-H(33)	0.9600
C(32)-H(34)	0.9600
C(32)-H(32)	0.9600
C(25)-O(1)-H(20)	105.4(12)
H(37)-O(2)-H(38)	102.8(16)
C(4)-O(3)-C(3)	106.18(16)
C(10)-N(2)-C(11)	105.79(9)
C(10)-N(3)-C(26)	107.37(9)
C(10)-N(3)-H(21)	126.3
C(26)-N(3)-H(21)	126.3
C(28)-N(4)-C(29)	118.00(10)
C(4)-C(1)-C(2)	104.31(16)
C(4)-C(1)-H(1)	110.9

C(2)-C(1)-H(1)	110.9
C(4)-C(1)-H(4)	110.9
C(2)-C(1)-H(4)	110.9
H(1)-C(1)-H(4)	108.9
C(3)-C(2)-C(1)	103.44(16)
C(3)-C(2)-H(6)	111.1
C(1)-C(2)-H(6)	111.1
C(3)-C(2)-H(5)	111.1
C(1)-C(2)-H(5)	111.1
H(6)-C(2)-H(5)	109.0
O(3)-C(3)-C(2)	107.16(16)
O(3)-C(3)-H(2)	110.3
C(2)-C(3)-H(2)	110.3
O(3)-C(3)-H(7)	110.3
C(2)-C(3)-H(7)	110.3
H(2)-C(3)-H(7)	108.5
O(3)-C(4)-C(1)	108.52(19)
C(6)-C(5)-H(31)	109.5
C(6)-C(5)-H(8)	109.5
H(31)-C(5)-H(8)	109.5
C(6)-C(5)-H(30)	109.5
H(31)-C(5)-H(30)	109.5
H(8)-C(5)-H(30)	109.5
C(5)-C(6)-C(7)	112.51(10)
C(5)-C(6)-C(18)	107.72(10)
C(7)-C(6)-C(18)	110.86(9)
C(5)-C(6)-C(32)	108.80(11)
C(7)-C(6)-C(32)	108.39(10)
C(18)-C(6)-C(32)	108.47(10)
C(8)-C(7)-C(19)	116.97(10)
C(8)-C(7)-C(6)	120.72(10)
C(19)-C(7)-C(6)	122.14(10)
C(7)-C(8)-C(9)	121.39(10)
C(7)-C(8)-H(28)	119.3
C(9)-C(8)-H(28)	119.3
C(8)-C(9)-C(25)	119.85(10)
C(8)-C(9)-C(10)	120.64(10)
C(25)-C(9)-C(10)	119.45(10)
N(2)-C(10)-N(3)	112.73(10)
N(2)-C(10)-C(9)	122.36(10)
N(3)-C(10)-C(9)	124.87(10)
C(12)-C(11)-N(2)	129.75(10)
C(12)-C(11)-C(26)	121.40(11)
N(2)-C(11)-C(26)	108.84(9)
C(11)-C(12)-C(13)	117.92(10)
C(11)-C(12)-H(22)	121.0

C(13)-C(12)-H(22)	121.0
N(1)-C(13)-C(12)	118.67(10)
N(1)-C(13)-C(28)	121.00(11)
C(12)-C(13)-C(28)	120.32(10)
C(15)-N(1)-C(13)	117.50(10)
N(1)-C(15)-C(16)	119.69(11)
N(1)-C(15)-C(29)	121.61(10)
C(16)-C(15)-C(29)	118.69(11)
C(17)-C(16)-C(15)	120.16(12)
C(17)-C(16)-H(26)	119.9
C(15)-C(16)-H(26)	119.9
C(16)-C(17)-C(30)	121.20(11)
C(16)-C(17)-H(9)	119.4
C(30)-C(17)-H(9)	119.4
C(6)-C(18)-H(35)	109.5
C(6)-C(18)-H(36)	109.5
H(35)-C(18)-H(36)	109.5
C(6)-C(18)-H(10)	109.5
H(35)-C(18)-H(10)	109.5
H(36)-C(18)-H(10)	109.5
C(20)-C(19)-C(7)	124.40(10)
C(20)-C(19)-H(29)	117.8
C(7)-C(19)-H(29)	117.8
C(19)-C(20)-C(25)	117.22(11)
C(19)-C(20)-C(21)	121.90(10)
C(25)-C(20)-C(21)	120.87(10)
C(23)-C(21)-C(20)	111.74(10)
C(23)-C(21)-C(22)	107.34(11)
C(20)-C(21)-C(22)	110.25(10)
C(23)-C(21)-C(24)	107.41(11)
C(20)-C(21)-C(24)	110.19(11)
C(22)-C(21)-C(24)	109.83(11)
C(21)-C(22)-H(13)	109.5
C(21)-C(22)-H(11)	109.5
H(13)-C(22)-H(11)	109.5
C(21)-C(22)-H(12)	109.5
H(13)-C(22)-H(12)	109.5
H(11)-C(22)-H(12)	109.5
C(21)-C(23)-H(14)	109.5
C(21)-C(23)-H(16)	109.5
H(14)-C(23)-H(16)	109.5
C(21)-C(23)-H(15)	109.5
H(14)-C(23)-H(15)	109.5
H(16)-C(23)-H(15)	109.5
C(21)-C(24)-H(18)	109.5
C(21)-C(24)-H(17)	109.5

H(18)-C(24)-H(17)	109.5
C(21)-C(24)-H(19)	109.5
H(18)-C(24)-H(19)	109.5
H(17)-C(24)-H(19)	109.5
O(1)-C(25)-C(20)	118.96(10)
O(1)-C(25)-C(9)	120.87(10)
C(20)-C(25)-C(9)	120.17(10)
C(27)-C(26)-N(3)	132.10(10)
C(27)-C(26)-C(11)	122.63(10)
N(3)-C(26)-C(11)	105.26(9)
C(26)-C(27)-C(28)	116.98(10)
C(26)-C(27)-H(27)	121.5
C(28)-C(27)-H(27)	121.5
N(4)-C(28)-C(27)	118.67(10)
N(4)-C(28)-C(13)	120.62(10)
C(27)-C(28)-C(13)	120.71(10)
N(4)-C(29)-C(31)	119.67(11)
N(4)-C(29)-C(15)	121.07(11)
C(31)-C(29)-C(15)	119.25(10)
C(31)-C(30)-C(17)	120.14(12)
C(31)-C(30)-H(24)	119.9
C(17)-C(30)-H(24)	119.9
C(30)-C(31)-C(29)	120.53(12)
C(30)-C(31)-H(25)	119.7
C(29)-C(31)-H(25)	119.7
C(6)-C(32)-H(33)	109.5
C(6)-C(32)-H(34)	109.5
H(33)-C(32)-H(34)	109.5
C(6)-C(32)-H(32)	109.5
H(33)-C(32)-H(32)	109.5
H(34)-C(32)-H(32)	109.5

---

**Crystallographic Table 52** Anisotropic displacement parameters ( $\text{\AA}^2 \times 10^3$ ) for **t-butylsalzine**. The anisotropic displacement factor exponent takes the form:  $-2 \pi^2 [ h^2 a^{*2} U_{11} + \dots + 2 h k a^{*} b^{*} U_{12} ]$

---

	U11	U22	U33	U23	U13	U12
O(1)	40(1)	30(1)	42(1)	22(1)	24(1)	22(1)
O(2)	32(1)	27(1)	44(1)	7(1)	12(1)	15(1)
O(3)	75(1)	42(1)	58(1)	26(1)	16(1)	9(1)
N(2)	30(1)	21(1)	25(1)	10(1)	13(1)	11(1)
N(3)	26(1)	18(1)	24(1)	10(1)	12(1)	9(1)
N(4)	25(1)	20(1)	26(1)	11(1)	11(1)	7(1)
C(1)	107(2)	35(1)	71(1)	21(1)	41(1)	19(1)
C(2)	74(1)	56(1)	52(1)	28(1)	26(1)	27(1)
C(3)	88(2)	51(1)	60(1)	18(1)	24(1)	34(1)
C(4)	221(4)	39(1)	51(1)	10(1)	48(2)	-9(2)
C(5)	43(1)	37(1)	44(1)	27(1)	24(1)	20(1)
C(6)	27(1)	24(1)	24(1)	12(1)	10(1)	10(1)
C(7)	24(1)	21(1)	21(1)	8(1)	8(1)	8(1)
C(8)	25(1)	21(1)	22(1)	9(1)	11(1)	10(1)
C(9)	24(1)	20(1)	20(1)	8(1)	9(1)	8(1)
C(10)	24(1)	19(1)	20(1)	7(1)	8(1)	8(1)
C(11)	25(1)	18(1)	20(1)	7(1)	8(1)	7(1)
C(12)	28(1)	18(1)	25(1)	8(1)	11(1)	10(1)
C(13)	23(1)	15(1)	20(1)	6(1)	6(1)	6(1)
N(1)	28(1)	18(1)	25(1)	9(1)	8(1)	7(1)
C(15)	24(1)	18(1)	24(1)	8(1)	6(1)	5(1)
C(16)	35(1)	22(1)	33(1)	14(1)	11(1)	9(1)
C(17)	39(1)	27(1)	37(1)	19(1)	14(1)	8(1)
C(18)	34(1)	24(1)	30(1)	8(1)	10(1)	12(1)
C(19)	27(1)	22(1)	22(1)	8(1)	11(1)	8(1)
C(20)	25(1)	23(1)	23(1)	7(1)	10(1)	9(1)
C(21)	31(1)	25(1)	28(1)	8(1)	16(1)	12(1)
C(22)	31(1)	32(1)	38(1)	13(1)	16(1)	15(1)
C(23)	40(1)	39(1)	35(1)	16(1)	24(1)	18(1)
C(24)	48(1)	28(1)	37(1)	1(1)	21(1)	10(1)
C(25)	27(1)	21(1)	25(1)	8(1)	11(1)	12(1)
C(26)	22(1)	17(1)	20(1)	7(1)	6(1)	6(1)
C(27)	24(1)	17(1)	25(1)	9(1)	9(1)	8(1)
C(28)	21(1)	17(1)	21(1)	7(1)	6(1)	6(1)

---

C(29)	22(1)	20(1)	24(1)	9(1)	7(1)	5(1)
C(30)	36(1)	32(1)	38(1)	20(1)	18(1)	8(1)
C(31)	31(1)	28(1)	36(1)	17(1)	18(1)	10(1)
C(32)	34(1)	34(1)	32(1)	10(1)	1(1)	11(1)

---

**Crystallographic Table 53** Hydrogen coordinates ( $\times 10^4$ ) and isotropic displacement parameters ( $\text{\AA}^2 \times 10^3$ ) for **t-butylsalzine**.

	x	y	z	U(eq)
H(20)	-940(20)	7030(20)	6758(13)	47
H(37)	7530(20)	7914(14)	4768(10)	50
H(38)	6198(11)	7140(20)	4246(12)	50
H(21)	2068	4552	5868	25
H(1)	3767	6713	9194	80
H(4)	1947	6359	9038	80
H(6)	2275	7874	10319	67
H(5)	4080	8325	10436	67
H(2)	1778	9594	9740	76
H(7)	3537	10321	10228	76
H(31)	-1158	1031	8136	53
H(8)	16	1964	9026	53
H(30)	310	523	8546	53
H(28)	1391	3575	6860	25
H(22)	753	9174	5488	26
H(26)	3024	11793	3791	34
H(9)	4420	11890	2804	38
H(35)	1419	276	7366	42
H(36)	1553	1427	6863	42
H(10)	-86	540	6797	42
H(29)	-1356	3371	8436	26
H(13)	-4795	4348	7334	47
H(11)	-4092	5765	7164	47
H(12)	-5004	5789	7871	47
H(14)	-3585	3684	8629	51
H(16)	-3958	5028	9181	51
H(15)	-2267	4783	9399	51
H(18)	-2850	7372	9137	57
H(17)	-1991	7615	8437	57
H(19)	-1153	7154	9240	57
H(27)	3569	5669	4763	24
H(24)	5683	10094	2372	39
H(25)	5553	8211	2949	34
H(33)	2473	3501	9064	52
H(34)	3131	3187	8251	52
H(32)	2960	2068	8774	52

**Crystallographic Table 54** Torsion angles [°] for **t-butylsalzine**.

---

C(4)-C(1)-C(2)-C(3)	4.7(3)
C(4)-O(3)-C(3)-C(2)	33.2(3)
C(1)-C(2)-C(3)-O(3)	-22.7(2)
C(3)-O(3)-C(4)-C(1)	-30.1(3)
C(2)-C(1)-C(4)-O(3)	15.2(4)
C(5)-C(6)-C(7)-C(8)	-169.03(11)
C(18)-C(6)-C(7)-C(8)	-48.33(14)
C(32)-C(6)-C(7)-C(8)	70.62(14)
C(5)-C(6)-C(7)-C(19)	15.73(16)
C(18)-C(6)-C(7)-C(19)	136.43(12)
C(32)-C(6)-C(7)-C(19)	-104.62(13)
C(19)-C(7)-C(8)-C(9)	0.34(17)
C(6)-C(7)-C(8)-C(9)	-175.14(10)
C(7)-C(8)-C(9)-C(25)	-0.16(17)
C(7)-C(8)-C(9)-C(10)	177.06(10)
C(11)-N(2)-C(10)-N(3)	-0.93(13)
C(11)-N(2)-C(10)-C(9)	176.96(10)
C(26)-N(3)-C(10)-N(2)	0.76(13)
C(26)-N(3)-C(10)-C(9)	-177.07(10)
C(8)-C(9)-C(10)-N(2)	-170.48(11)
C(25)-C(9)-C(10)-N(2)	6.75(17)
C(8)-C(9)-C(10)-N(3)	7.15(17)
C(25)-C(9)-C(10)-N(3)	-175.62(11)
C(10)-N(2)-C(11)-C(12)	-178.25(12)
C(10)-N(2)-C(11)-C(26)	0.73(12)
N(2)-C(11)-C(12)-C(13)	178.79(11)
C(26)-C(11)-C(12)-C(13)	-0.08(17)
C(11)-C(12)-C(13)-N(1)	-177.59(10)
C(11)-C(12)-C(13)-C(28)	1.65(17)
C(12)-C(13)-N(1)-C(15)	-176.68(10)
C(28)-C(13)-N(1)-C(15)	4.08(16)
C(13)-N(1)-C(15)-C(16)	177.11(10)
C(13)-N(1)-C(15)-C(29)	-1.89(17)
N(1)-C(15)-C(16)-C(17)	-177.29(12)
C(29)-C(15)-C(16)-C(17)	1.73(18)
C(15)-C(16)-C(17)-C(30)	-1.1(2)
C(8)-C(7)-C(19)-C(20)	-0.48(17)
C(6)-C(7)-C(19)-C(20)	174.93(11)
C(7)-C(19)-C(20)-C(25)	0.40(18)
C(7)-C(19)-C(20)-C(21)	-178.39(11)
C(19)-C(20)-C(21)-C(23)	0.45(17)

C(25)-C(20)-C(21)-C(23)	-178.30(11)
C(19)-C(20)-C(21)-C(22)	-118.83(12)
C(25)-C(20)-C(21)-C(22)	62.42(15)
C(25)-C(20)-C(21)-C(24)	-58.97(15)
C(19)-C(20)-C(25)-O(1)	-179.75(10)
C(21)-C(20)-C(25)-O(1)	-0.95(17)
C(19)-C(20)-C(25)-C(9)	-0.19(17)
C(21)-C(20)-C(25)-C(9)	178.61(11)
C(8)-C(9)-C(25)-O(1)	179.63(10)
C(10)-C(9)-C(25)-O(1)	2.38(17)
C(8)-C(9)-C(25)-C(20)	0.08(17)
C(10)-C(9)-C(25)-C(20)	-177.17(10)
C(10)-N(3)-C(26)-C(27)	180.00(12)
C(10)-N(3)-C(26)-C(11)	-0.25(12)
C(12)-C(11)-C(26)-C(27)	-1.43(17)
N(2)-C(11)-C(26)-C(27)	179.48(10)
C(12)-C(11)-C(26)-N(3)	178.79(10)
N(2)-C(11)-C(26)-N(3)	-0.30(12)
N(3)-C(26)-C(27)-C(28)	-179.07(11)
C(11)-C(26)-C(27)-C(28)	1.22(16)
C(29)-N(4)-C(28)-C(27)	178.34(10)
C(29)-N(4)-C(28)-C(13)	-2.05(16)
C(26)-C(27)-C(28)-N(4)	179.99(10)
C(26)-C(27)-C(28)-C(13)	0.38(16)
N(1)-C(13)-C(28)-N(4)	-2.23(17)
C(12)-C(13)-C(28)-N(4)	178.55(10)
N(1)-C(13)-C(28)-C(27)	177.37(10)
C(12)-C(13)-C(28)-C(27)	-1.85(16)
C(28)-N(4)-C(29)-C(31)	-176.22(10)
C(28)-N(4)-C(29)-C(15)	4.26(17)
N(1)-C(15)-C(29)-N(4)	-2.40(18)
C(16)-C(15)-C(29)-N(4)	178.60(11)
N(1)-C(15)-C(29)-C(31)	178.08(11)
C(16)-C(15)-C(29)-C(31)	-0.92(17)
C(16)-C(17)-C(30)-C(31)	-0.4(2)
C(17)-C(30)-C(31)-C(29)	1.2(2)
N(4)-C(29)-C(31)-C(30)	179.94(12)
C(15)-C(29)-C(31)-C(30)	-0.53(19)

---